Finite volume methods in the quantum sinh-Gordon theory

Márton Kálmán Lájer

2020

A dissertation submitted in partial fulfillment

of the requirements for the degree of

Doctor of Philosophy

with the supervision of

Dr. Zoltán Bajnok

DSc., scientific advisor (Wigner Research Centre for Physics)

Doctoral School of Physics, Eötvös Loránd University

Head: Prof. Jenő Gubicza

Particle Physics and Astronomy Program

Head: Prof. Sándor Katz

Acknowledgments

I would like to express my sincere gratitude and deep appreciation to my supervisor, Zoltán Bajnok, for guiding me through the path culminating in the present thesis. His personality motivated me to become a theoretical physicist, and his wisdom drove me towards reaching the scientific maturity expected from a PhD in Physics.

During the second half of my doctoral studies, I have been honoured by the privilege of working in collaboration with Robert Konik and Giuseppe Mussardo. Our discussions on the sinh-Gordon model and related topics shaped my understanding and viewpoint in an imperishable way. I am also indebted to Giuseppe for the opportunity to visit SISSA in November 2018, and to Robert for his invitation to Brookhaven National Laboratory in November 2019.

I am grateful to my collaborators, without whom this thesis could not take its present form: Zoltán Bajnok, János Balog, Robert Konik, Giuseppe Mussardo, Bálint Szépfalvi, István Vona, and Chao Wu.

I am thankful to the Wigner Research Centre for Physics, Eötvös Loránd University, and especially, Bolyai College for creating an ideal environment to pursue scientific research. In particular, I thank Director Jenő Kürti for his benevolent attitude during the COVID-19 pandemic.

Furthermore, I would like to take the occasion to acknowledge my mentors from previous stages of my career. The work on this thesis could not be started without the pillars laid by the lecturers at Eötvös Loránd University, and especially by my BSc thesis supervisors: József Cserti, Gyöngyi Pergerné Klupp and Katalin Kamarás. I think with utmost respect and gratitude to József Jaloveczki, whose training originally motivated me to apply to the BSc program in Physics, and Gyula Dávid, whose lectures subsequently lead me to attempt to become an actual physicist.

I am grateful, even after so many years, to Katalin Havasi, my first math teacher, who provided the initial foundations to all of the above, and to Mária Serege, for helping me overcome the language barrier.

Finally, I would like to thank my parents and Irén for staying beside me. They provided me with the opportunity to aim for the stars, and I am giving my best effort.

Contents

Nomenclature

AdS Anti-de Sitter (space)

BPZ Belavin-Polyakov-Zamolodchikov (framework)

BYE Bethe-Yang equations

CFT Conformal field theory

FF Form factor

FLZZ Fateev-Lukyanov-Zamolodchikov-Zamolodchikov (formula)

FV Finite volume

IFT Integrable (quantum) field theory

IR Infrared

LSZ Lehmann-Symanzik-Zimmermann (formula)

QFT Quantum field theory

RG Renormalisation group

ShG sinh-Gordon model

TBA Thermodynamic Bethe Ansatz

TSM Truncated spectrum method

UV Ultraviolet

WZNW Wess-Zumino-Novikov-Witten model

Chapter 1

Introduction

A large part of our current understanding about the nature of our Universe is framed in the language of quantum field theories (QFTs). On the one hand, they provide the general framework in which we describe at least three of the four known fundamental interactions of Nature: electromagnetic, weak, and strong interactions. On the other hand, they are frequently used in effective models appearing in particle, solid-state and statistical physics.

Quantum field theories are the fruit of combining quantum mechanics and special relativity. They inherit locality from classical field theory, together with fluctuations from quantum mechanics and Poincaré invariance from relativity.

The fundamental excitations of QFTs are particles. In some exotic cases, particles carry a topological charge, making them appear as discrete lumps already on a classical level. In this case, quantum fluctuations usually produce corrections to the physical properties of their classical counterparts. Apart from these, particles are themselves thought of as quantised fluctuations of the field. They can arise either as perturbative elementary excitations or nonperturbative bound states. In general, particles can decay into one or more other particles. They also scatter on each other, acquiring phase shifts and creating or destroying particles. In some circumstances, particles arrange themselves into ever more complex and weakly bound structures, like atoms and molecules, building up all matter we perceive around us, including ourselves.

Due to their extraordinary phenomenological richness, QFTs are not expected to be exactly solvable, except for a number of special cases. The typical observables of a QFT (with massive excitations) are the mass spectrum, the scattering matrix, matrix elements of local operators (i.e., form factors), and the correlation functions of these operators. We use solvability here as a rather vague concept. We may conclude that a model is solved if there is a sufficient method available (e.g., an algorithm running in polynomial time with respect to the desired accuracy) to obtain all physical quantities, including correlators.

Potentially solvable models are distinguished by the presence of a vast amount of

symmetries. These exceptional cases include free theories and integrable models. They are essential as they function as the starting points of approximate methods to reach other QFTs in their neighbourhood. Approximate methods vary from analytic expansions in a small parameter (i.e., perturbation theory and resummations) to numerical methods like lattice Monte Carlo and variational methods.

A particular class of QFTs possesses conformal symmetry. Along with the usual Poincaré invariance, correlation functions of these models are also invariant under rescaling the spacetime coordinates and the so-called special conformal transformations [1]. These are called conformal field theories (CFT).

Models without scaling invariance are described by a set of coupling constants and at least one dimensionful scale. A rescaling effectively modifies these coupling constants. Hence one can imagine a trajectory in the infinite-dimensional space of coupling constants, starting from a particular model, and subsequently applying small scaling transformations. The collection of these trajectories is called the renormalisation group (RG) flow. Scale-invariant theories are fixed points in this flow. One can trace back renormalisation group trajectories to the vicinity of a fixed point. The term „perturbing a conformal field theory" means providing the direction in which the RG trajectory departs from the fixed point. A trajectory then either leads to another fixed point („massless perturbation") or a massive limit.

The renormalisation group flow can be generated in several ways. In the conventional Wilsonian approach [2], one starts by defining a theory with a momentum cutoff Λ. The rescaling is implemented by integrating out degrees of freedom of momenta between $\Lambda - \delta\Lambda$ and Λ, inducing effective couplings, and then redefining the length scale such that the value of the momentum cutoff is again Λ. Another approach [3] is to consider the model with periodic boundary conditions with extension L in each spacelike direction. Rescaling then amounts to tracking the variation of physical quantities upon changing the volume of the world. The starting, ultraviolet (UV) fixed point is approached in the $L \to 0$ limit. The terminating fixed point is instead called infrared (IR) and is approached in the $L \to \infty$ limit. Both viewpoints will take a role in different parts of our study.

In most applications, the concrete physical system under examination has a finite size. Scattering experiments are performed in a finite accelerator/detector; solid-state systems are analysed in laboratories, even the lattice simulations of gauge theories are performed on finite lattices. The understanding of finite size effects is therefore unavoidable, and it is natural to extend the concept of solvability to include finite volume physical quantities. Fortunately, there are profound reasons to believe that finite-size corrections can be formulated purely in terms of the infinite volume characteristics of the theory [4–7].

The behaviour of QFTs depends crucially on the dimensionality of the spacetime

they are embedded. In our spacetime consisting of 3 space and one time directions, the cluster decomposition principle ensures [8] there are precisely two possibilities a wavefunction can behave under the interchange of two identical particles. Either it remains unaffected if the swapped particles are bosons, or it changes sign if the particles are fermions. The same picture persists in any space dimensionality above 3. In two spacelike dimensions, anyons can appear [9,10], the interchange of which causes a more general phase shift. In one space dimension, the phase shift due to particle interchange is indistinguishable from scattering. This ambiguity sets the stage for further exotic phenomena such as equivalences between certain bosonic and fermionic systems [11–15].

Low dimensional systems are interesting to study, not only for their exotic properties [16,17], but also because they appear naturally in the description and the quantisation of (super)strings.

In the following, we will work exclusively in $1+1$ dimensions. This dimensionality offers a unique opportunity to study strongly interacting and strongly correlated systems as highly anisotropic condensed matter systems [18]. This line of research lead to invaluable insights and unexpected discoveries in various experimentally relevant areas throughout the past century. Relevant areas include magnetic systems [19] and their phase transitions [20]; conductors, like carbon nanotubes and quantum wires [21–24]; metal-insulator phase transitions [25, 26]; and quantum gases in atomic traps [27–29]. On the other hand, they take an important role in the quantization of (super)strings and, through the AdS/CFT correspondence [30–32], they are key to solving certain four-dimensional gauge theories[1] [35–41].

The extreme speciality of two dimensions is twofold. On the one hand, the symmetry algebra of conformal transformations automatically extends to an infinite-dimensional symmetry algebra [42]. In many cases, this allows a complete solution of conformal field theories. On the other hand, in $1+1$ dimensions, the presence of higher spin geometric charges do not entirely prevent the possibility of interactions even if the spectrum is completely characterized by a finite set of massive particles (contrary to the usual scenario in higher dimensions due to the Coleman-Mandula theorem [43]). Purely elastic scattering is allowed, though particle production or decay is not. In this case, the scattering amplitudes factorise and satisfy the Yang-Baxter equations [44–46]. Therefore models with higher spin conserved charges are called integrable field theories (IFT) .

Both CFTs and IFTs have been studied extensively and zealously in the past decades. In particular, so-called rational CFTs (where the ratio of any two energy levels is always rational [47]) are understood well in terms of the Belavin-Polyakov-Zamolodchikov (BPZ) framework [42]. They include important subclasses as the min-

[1] Some aspects of integrability were observed in the context of QCD even before the advent of AdS/CFT [33, 34].

imal models and compact Wess-Zumino-Novikov-Witten (WZNW) theories [48]. A huge class of rational CFTs can be constructed as a coset reduction [49] of compact WZNW models[2]. On the other hand, the landscape of non-rational CFTs is far richer, and much less is known about them in general. They include noncompact WZNW theories [53] and the Toda hierarchy[3] [56–58]. They are of principal significance to the quantisation of sting theories and, in particular, in the AdS_3/CFT_2 correspondence [59–61], and therefore are subject of active study [62]. A particularly important and reasonably well-understood example is the simplest instance of the Toda hierarchy, Liouville field theory [63, 64]. It describes two-dimensional quantum gravity and is of principal importance for string theory as well [63, 65, 66]. Liouville field theory actually fits in the BPZ scheme with minimal modifications [67]. In particular, the exact expression for the three-point functions is known [68, 69]. Let us point out that Liouville field theory exhibits a mysterious self-duality property, which will be under some scrutiny in the present dissertation.

Integrable quantum field theories are hoped to be solvable. However, this very ambitious project is far from over. Nevertheless, integrability has offered us systematic methods to attack these models. In infinite volume, analyticity and crossing symmetry are powerful tools to derive restrictive functional relations for the scattering matrix and form factors. These are called the S-matrix and form factor (FF) bootstraps [70–73]. The first step of a systematic solution is thus to produce exact expressions for the S-matrices and form factors of the theory in infinite volume.

The set of two-dimensional integrable models is an adequate testing ground to study finite-size effects. In particular, the finite size energy spectrum can be calculated systematically in integrable theories. The most striking finite-size corrections are polynomial in the inverse volume and originate from momentum quantisation [5]. Periodicity of the wave function requires that the scattering phase cancels the translational phase when a particle is moved around the cylinder and scattered through all other particles. For the finite volume energy levels, the so-called Bethe-Yang equations (BYE) [5, 74, 75] provide the quantisation conditions for momenta. They sum up all polynomial corrections. In this approximation, the energy of a multiparticle state is simply the sum of infinite volume energies but with the appropriately quantised momenta depending on the infinite volume scattering matrix.

However, this is not the end of the story. There are also exponentially small corrections related to virtual processes. If bound states are present, the leading exponential corrections for bound states (called μ-terms) are related to the fact that in a finite volume bound states can virtually decay into their constituents. The next exponential

[2]In fact, there was a hope that all RCFTs may be classified through this particular construction. Recent developments [50–52] indicate that the situation is more complicated.

[3]Toda field theories can be viewed as the gauge invariant part of certain gauged WZNW models [54, 55]

corrections (F-terms) are caused by the polarisation of the non-trivial finite volume vacuum [4]. A pair of virtual particles can appear from the vacuum. These travel around the world and scatter on the physical particles, then annihilate each other. The next exponential correction contains two virtual particle pairs and a single pair which wraps twice around the cylinder [76]. The total energy gets a contribution from the sea of virtual particles. Leading exponential corrections for standing one-particle states were identified in [4] and were extended for a single moving particle in [77, 78]. The contribution of a single pair of virtual particles was generalised for multiparticle states in [38]. The similar contribution with two pairs of virtual particles was analysed for the vacuum in [79], and multiparticle states in [76]. For an exact description, one has to sum up all these virtual processes, which is provided by the Thermodynamic Bethe Ansatz (TBA) equations [75]. TBA equations can be derived (for the ground state) by evaluating the Euclidean torus partition function in the limit when one of the sizes goes to infinity. If we interpret this size as Euclidean time, then only the lowest energy state, namely the finite volume ground state contributes. If, however, we interpret it as a very large volume, then the partition function is dominated by the contribution of finite density states. Since the volume eventually goes to infinity the BY equations are almost exact and can be used to derive (nonlinear) TBA integral equations to determine the density of the particles, which minimise the partition function in the saddle point approximation. By careful analytical continuations, this exact TBA integral equation can be extended for excited states [80, 81].

The similar program to determine the finite volume form factors is still in its infancy. Since there is a sharp difference between diagonal and non-diagonal form factors, they have to be analysed separately. For non-diagonal form factors the polynomial finite size corrections, besides the already explained momentum quantisation, also involve the renormalisation of states, to conform with the finite volume Kronecker delta normalisation [6]. The polynomial corrections for diagonal form factors are much more complicated, as they contain disconnected terms. They were conjectured in [7, 82] and confirmed in [83]. For exponential corrections, the situation is the opposite. Exact expressions for the finite volume one-point function can be obtained in terms of the infinite volume form factors by evaluating the one-point function on a Euclidean torus where one of the sizes is sent to infinity [82, 84]. This result was extended by analytic continuation for diagonal matrix elements in diagonally scattering theories [85–87]. The expansion of these formulae provides the leading exponential corrections for diagonal form factors. In the case of bound states, the leading exponential volume correction is also called μ-term by analogy to the energy corrections. It originates from a process in which the particle can virtually decay in a finite volume into its constituents. This idea was used to calculate the leading μ-term explicitly for the simplest non-diagonal form factor in [88]. One of the aims of the present thesis is to go beyond these results

in simple diagonally scattering theories.

In this thesis, we will extensively study a particularly important example of IFTs: the sinh-Gordon model (ShG) . We are going to take as a starting point the Lagrangian formulation of the model given by

$$\mathcal{L}_{\mathrm{ShG}} = \frac{1}{16\pi} \left(\partial_\nu \varphi\right)^2 - 2\mu \cosh\left(b\varphi\right) \tag{1.1}$$

Here $\varphi\left(x,t\right)$ is a real noncompact scalar field, μ is some dimensionful mass scale, and b is a dimensionless coupling constant. Upon quantisation, μ is replaced by a renormalised coupling constant depending on the chosen quantisation scheme. The spectrum of the model is exceedingly simple, consisting of a single massive particle of mass M_{ShG}. ShG is thus the simplest of interacting integrable field theories. Much is known about its properties. Its elastic S-matrix was found in [89]. The infinite volume form factors of local operators were obtained in [90, 91], while the vacuum expectation values of exponential operators were found in [92]. The exact relationship between the physical mass M_{ShG} and the renormalised coupling in the perturbed gaussian CFT scheme, here denoted later as μ_{ShG}, as a function of the coupling b, was derived in [93]. Its thermodynamic Bethe ansatz for the ground state and the excited states was studied in [94, 95], while the thermal correlation functions of the model were discussed in [84, 96, 97]. A suggestive connection between the ShG model and roaming renormalisation group trajectories among the minimal models of CFT was studied in [98]. A mapping between the ShG and the Ising model was established in [99]. The ShG model finds applications in a wide range of areas of physics running from toy models of quantum gravity [100], to cold atomic gases [101, 102], studies of thermalisation in classical field theories [103, 104], and lattice models with noncompact quantum group symmetries [105].

One of the most striking but mysterious aspects of the ShG model[4] is its weak-strong duality:

$$b \leftrightarrow b^{-1}. \tag{1.2}$$

In the presence of such symmetry, the self-dual point $b = 1$ becomes a unique instance of the ShG model, for it divides the weak-coupling regime, $b < 1$, from the strong-coupling regime, $b > 1$. It is important to underline that this duality is not at all manifest in the Lagrangian of the theory but is apparent, as discussed later, in its S-matrix formulation.

It is also worth stressing that the ShG model is the simplest example of affine Toda field theories, a large class of models with exponential interactions based on root systems of Lie algebras, see for instance [106] and references therein. The main difference between the ShG model and the rest of the affine Toda field theories is that

[4]The Toda field theories have a similar duality.

the ShG does not have bound states.

We have now reached the position to proclaim the main goals of the present thesis:

- Provide a formula for the leading finite volume corrections to nondiagonal form factors in diagonally scattering theories due to vacuum polarisation (the F-terms). These provide the leading exponential corrections in theories without bound states, in particular in the sinh-Gordon model. We will develop analytical and numerical methods to verify this formula.

- Establish numerical truncated spectrum methods (TSM) to study the sinh-Gordon model and related theories. Apart from being related to the previous point, this is also useful to gain a better understanding on the nature of self-duality.

For reasons which will become clear later, the obvious regime in which truncated spectrum methods can be implemented is the weak-coupling regime $b < 1$, but we can extend them to approach the $b = 1$ self-dual point. As we shall see, at $b = 1$ the physical mass vanishes and the theory appears to be (at least naively) critical. Ultimately we aim to explore the ShG at $b = 1$ and understand what theory is described by the Lagrangian given in eq. (1.1). The theory's duality, as expressed in eq. (1.2), is built on results established at $b < 1$ which are then subsequently analytically continued to regimes beyond their nominal validity. It is then an important question to understand whether the Lagrangian corresponding to these analytic continuations is the same as given in eq. (1.1) with $b > 1$.

As we explore in this thesis, the development of TSM for the ShG nearby the self-dual point $b = 1$ proves to be surprisingly challenging. Truncated spectrum methods treat a model by first defining it on a finite volume (typically an infinitely long cylinder of width L) and then, secondly, introducing a hard UV cutoff, E_c, in the number of energy levels which are included in the computation [107–117]. Under these two conditions, numerics can be performed (either exact diagonalisation or Lánczos-based approaches) and the low lying energy spectrum, together with vacuum expectation values and matrix elements of several operators, can be computed. Of course, in this treatment, it is crucial to understand the effect of E_c on the computed results. For certain models, even small values of E_c lead to results that are, in effect, independent of the cutoff (the $c = \frac{1}{2}$ Ising model perturbed by the presence of a magnetic field being a classic example [108]). In other cases, for instance those analysed in Refs. [109, 118–123], the results are instead noticeably affected by E_c. In order to ameliorate truncation effects, renormalisation group strategies (both analytic and numerical) have been employed [110, 111, 114–117, 124–126].

The premise of all these RG strategies is that cutoff dependent effects are in some sense small. However, in the case of the ShG model, we shall see that such cutoff effects

near $b = 1$ can be on the contrary extremely large, and therefore the traditional RG strategies do not work. In order to deal with this new situation, we will consider a number of different approaches to tackle the problem.

We first consider the conventional RG improvement techniques and point out why they are problematic in the present case. We will trace back the problem to the ill-defined nature of expansions in the coupling μ, which also arises in the small-volume expansion of energy levels. In particular, we will see that without a cutoff, the perturbative series is divergent term-by-term for any fixed $b > 0$.

In contrast, as we will show, TSM provides a faithful reproduction of the small-volume spectrum, efficiently resumming the problematic μ-perturbative energy series. This is an important and nontrivial result in the case of ShG.

The singular μ-series is then analysed in more detail. We point out that it is possible to motivate the power-law fits to the cutoff dependence of TSM data by performing a "supra-Borel" resummation as the function of the TSM cutoff and considering the large-cutoff asymptotics.

As an alternative, we will also consider different basis choices, including the massive Fock basis and a novel TSM approach based on the form factors of sinh-Gordon theory itself.

Armed with the above experiences, we then turn to finite volume corrections to form factors. As a first step, we present a Lagrangian-based analytical framework which provides direct access to excited states' energy levels and finite volume form factors at the same time [127]. The idea is to calculate the Euclidean torus two-point function in the limit when one of the sizes is sent to infinity. The exact finite volume two-point function then can be used, similarly to the Lehmann-Symanzik-Zimmermann (LSZ) formula, to extract the information needed. The momentum space two-point function, when continued analytically to imaginary values, has poles exactly at the finite volume energy levels whose residues are the products of finite volume form factors. Of course, the exact determination of the finite-volume two-point function is hopeless in interacting theories, but developing any systematic expansion leads to a systematic expansion of both the energy levels and the form factors. We analyse two such expansions in this thesis. In the first, we expand the two-point function in the volume, which leads to the leading exponential corrections. We perform the calculation for a moving one-particle state. In the second expansion, we calculate the same quantities perturbatively in the coupling in the sinh-Gordon theory. By comparing the two approaches in their overlapping domain, we find complete agreement.

As a next step, we extend these analyses for generic non-diagonal matrix elements in diagonally scattering theories [128]. Although the F-term calculation was based on the form factor expansion of the torus two-point function, this method is complicated to generalise, even considering exciting developments detailed in [129, 130]. We thus

focus on a formal and direct derivation of the cylinder one-point function in the crossed channel. Our results provide the leading exponential corrections for form factors, which contribute to the leading exponential correction to correlation functions, too. We test the conjectured results by comparing them to numerical data obtained from the Truncated Spectrum Approach developed for the sinh-Gordon theory.

The dissertation is organised as follows.

In Chapter 2, we introduce the quantum field theories relevant for the thesis. We begin with the free massless boson, the free massive boson and Liouville field theory. We then discuss the sinh-Gordon model in more detail, presenting two alternative definitions (based on the Lagrangian and the S-matrix, respectively), and pointing out its relation to the sine-Gordon model. The chapter is essentially an overview of relevant results already known in the literature. The discussion follows mostly along the lines of our paper [151] with some rearrangements.

Chapter 3 is devoted to the development of truncated spectrum methods to the sinh-Gordon theory. The results presented are based on [151] with some results already published in [128]. We first consider the massless scheme with zero mode separation and explore the numerical accuracy of the technique for various physical quantities. The problems of analytical improvement will be discussed as well. We will also examine the massive basis (both with zero-mode separation and the pure case) built using the conventional Fock oscillators, and provide the connection between the different schemes. After these, a detailed examination of the small-volume spectrum follows. We then discuss the cutoff-dependence of the energy eigenvalues in more detail and provide an explanation for the observed power-law cutoff dependence. We close the chapter by presenting the results of using the basis of sinh-Gordon eigenstates to reproduce the spectrum of ShG at a different coupling.

In Chapter 4, we examine the leading exponential finite volume corrections to non-diagonal form factors in the sinh-Gordon theory. After a short overview of the necessary concepts and notations. we outline a direct method based on the two-point function to systematically obtain the exponential finite volume corrections of nondiagonal form factors. We then present for the leading exponential correction of the result for the vacuum-one particle form factor. We derive the volume-exact, perturbatively expanded vacuum-one particle form factor. The obtained perturbative formula is compared to the formal Lüscher correction, and they are shown to agree in their overlapping domain of relevance. This is based on [127]. After recalling the formal derivation of the leading exponential corrections in the general nondiagonal case, we confirm the form of these corrections numerically, using our newly developed truncated spectrum methods. This is based on [128].

Finally, we present our conclusions in Chapter 5.

This dissertation contains a number of appendices as well. In Appendix A, we

collect a number of essential facts on conformal field theories. Appendix B details the way the small-volume limit of the energy spectrum is obtained from TBA. Appendix C is contains the derivation of useful integral representations of sums. In Appendix D, we provide the details of obtaining the general coefficients and cutoff-dependence of the ill-defined μ-series. Appendix E, in turn, contains the perturbative expansion of TBA equations with respect to the semi-classical coupling b. Likewise, Appendix F discusses the technicalities involved in calculating the perturbative expansion of the vacuum-one particle matrix element. Lastly, Appendix G explains the trick through which the lowest eigenvalues of the ShG Hamiltonian can be found in a reasonable time for large cutoffs corresponding to millions of kept basis states.

Chapter 2

Relevant models

In this chapter, we introduce the quantum field theories that will be relevant in the present thesis. We begin with free massless and massive bosons in Section 2.1. In Section 2.2, we briefly review the essential properties of Liouville field theory, an interacting, noncompact conformal field theory. Afterwards, we discuss the sinh-Gordon model in more detail. We start with the conventional Lagrangian quantization in Section 2.3. Following this, it will be advantageous to compare ShG to its famous sister, the sine-Gordon model. This comparison is presented in Section 2.4. The bootstrap approach, covered in Section 2.5, provides an entirely independent way of defining the sinh-Gordon model, starting from the S-matrix instead of the Lagrangian. This point of view provides a systematic way to describe finite volume corrections to the spectrum. The connections between the parameters appearing in the two schemes are conjectured but so far they have only been partially checked. The corresponding UV-IR relations will be discussed in Section 2.6, along with the introduction of inherently mixed UV-IR objects as vacuum expectation values and form factors. This chapter is mostly an overview of relevant results known in the literature. With the exception of Section 2.2, The discussion follows along the lines of our paper [151] with certain rearrangements.

2.1 The free boson

2.1.1 $c = 1$ massless boson: Gaussian CFT

The theory of the massless (noncompact) free boson on the plane is arguably the simplest non-rational CFT. The classical action is given by

$$S = \frac{g}{2} \int d^2x \partial_\mu \varphi \partial^\mu \varphi \tag{2.1}$$

In later sections we will generally fix $g = \frac{1}{8\pi}$. Some sections of Chapter 4 use the $g = 1$ convention as well. In the following, we will rely on the nomenclature of

conformal field theories. A useful reference is provided by the "yellow book" of di Francesco et al. [131]. We collected the most essential facts in Appendix A.

To define the quantum theory, it is sufficient to fix the stress-energy tensor on the plane, given by

$$T_{\mu\nu}(z,\bar{z}) = g\left(:\partial_\mu\varphi\partial_\nu\varphi - \frac{1}{2}\eta_{\mu\nu}\partial_\rho\varphi\partial^\rho\varphi:\right) \tag{2.2}$$

where the field φ is given by the mode expansion

$$\varphi(z,\bar{z}) = \varphi_0 - \frac{i}{4\pi g}\Pi_0 \ln z\bar{z} + \frac{i}{\sqrt{4\pi g}}\sum_{n\neq 0}\frac{1}{n}\left(\alpha_n z^{-n} + \bar{\alpha}_n \bar{z}^{-n}\right) \tag{2.3}$$

The mode operators α_n, $\bar{\alpha}_n$ satisfy the commutation relations

$$[\alpha_n,\alpha_m] = n\delta_{n+m}; \quad [\bar{\alpha}_n,\bar{\alpha}_m] = n\delta_{n+m}; \quad [\alpha_n,\bar{\alpha}_m] = 0 \tag{2.4}$$

while the zero mode operators satisfy $[\varphi_0,\Pi_0] = i$. Normal ordering (::) means that in a product, the mode operators $\alpha_n,\bar{\alpha}_n$ with $n<0$ are to be written to the left of those with $n>0$.

The generator of dilatations is given in terms of the stress-energy tensor as

$$D^{(0)} = \frac{1}{2\pi i}\left[\int_C dz\, zT(z) + \int_C d\bar{z}\,\bar{z}\bar{T}(\bar{z})\right] = L_0 + \bar{L}_0 \tag{2.5}$$

where the contour C may be chosen as the positively directed unit circle around the origin.

Vertex operators (of charge b) are defined as normal ordered exponentials of the field (2.3)

$$\mathcal{V}_b^{(pl)}(z,\bar{z}) \equiv :e^{\pm b\varphi(z,\bar{z})}: \tag{2.6}$$

The OPE of the vertex operator with the holomorphic and antiholomorphic components of the stress-energy tensor shows that $\mathcal{V}_b$ is a primary operator with chiral dimensions $h = \bar{h} = -\frac{b^2}{8\pi g}$.

We are most interested in QFTs on a cylinder of circumference L. The mapping is given by the transformation

$$z = e^{\frac{2\pi}{L}w}, \quad w \equiv \tau + ix \tag{2.7}$$

where τ is (Euclidean) time and x is the space coordinate around the circumference. Under the mapping, the generator $D^{(0)}$ of (2.5) becomes the generator of (euclidean) time translations. Both T, $\bar{T}$ and the integration measure is transformed such that the

Hamiltonian on the cylinder reads

$$H_{\text{cyl}}^{(0)} = \frac{2\pi}{L}\left(L_0 + \bar{L}_0 - \frac{c}{12}\right), \quad c = 1 \tag{2.8}$$

Instead of the convention emphasizing holomorphic and antiholomorphic parts of the field (2.3), it is worthwhile to introduce an equivalent set of mode operators

$$\alpha_n = \begin{cases} -i\sqrt{n}a_n & n > 0 \\ i\sqrt{|n|}a_{|n|}^\dagger & n < 0 \end{cases}; \quad \bar{\alpha}_n = \begin{cases} -i\sqrt{n}a_{-n} & n > 0 \\ i\sqrt{|n|}a_{-|n|}^\dagger & n < 0 \end{cases} \tag{2.9}$$

Written in terms of the new modes, the field takes the form ($k_n = 2\pi n L^{-1}$)

$$\varphi(x,\tau) = \varphi_0 + \frac{\tau\Pi_0}{gR} + \frac{1}{\sqrt{4\pi g}}\sum_{n\neq 0}\frac{1}{\sqrt{|n|}}\left(a_n e^{ik_n x} + a_n^\dagger e^{-ik_n x}\right), \tag{2.10}$$

and the Hamiltonian (2.8) can be written as

$$H_{\text{cyl}}^{(0)} = \left(\frac{\Pi_0^2}{2gL} - \frac{\pi}{6L}\right) + \sum_{n\neq 0}\frac{2\pi|n|}{L}a_n^\dagger a_n \tag{2.11}$$

The Hilbert space on which $H_{\text{cyl}}^{(0)}$ acts is a tensor product of a zero mode with the Fock space of the „non-minimal" modes

$$\mathcal{H} = L_2(\mathbb{R}) \otimes \text{span}\left\{a_{n_1}^\dagger \ldots a_{n_k}^\dagger |0\rangle : \; k \geq 0, n_j \in \mathbb{Z}\right\} \tag{2.12}$$

such that the mode operators with negative indices are interpreted as creation operators of particles.

Note that the relation between fields and elements to the Hilbert space is not one-to-one. Vertex operators with imaginary parameter create plane-wave normalizable states. Plane-wave normalizable states are referred to as macroscopic states. However, objects obtained by acting vertex operators with real charge on the vacuum are not normalizable. These are only meaningful inside an inner product with appropriate superpositions of macroscopic states. These non-normalizable states are called microscopic states.

Finally, we note that under the mapping (2.7), vertex operators transform as

$$\mathcal{V}_b^{(cyl)}(w,\bar{w}) = \left(\frac{L}{2\pi}\right)^{\frac{b^2}{4\pi g}}\mathcal{V}_b^{(pl)}(z(w), \bar{z}(\bar{w})) \tag{2.13}$$

2.1.2 Massive boson

We now consider the massive boson as a perturbation of the massless one. To this end we define the perturbed dilatation on the plane as

$$D^{(m)} = L_0 + \bar{L}_0 + \lim_{b\to 0} \frac{gm^{2+\frac{b^2}{4\pi g}}}{2b^2} \int_C dz \left(\mathcal{V}_b^{(pl)}(z,z^*) + \mathcal{V}_{-b}^{(pl)}(z,z^*) \right). \tag{2.14}$$

By mapping this operator to the cylinder, and expanding in b, we obtain the following Hamiltonian for the free massive boson:

$$H_{\text{cyl}}^{(m)} = H_{\text{cyl}}^{(0)} + \frac{gm^2}{2} \int_0^L :\varphi^2(x,0): dx + \frac{m^2 L}{4\pi} \ln\left(\frac{mL}{2\pi}\right) + \frac{gm^2}{b^2}. \tag{2.15}$$

It is customary to subtract the singular $\frac{gm^2}{b^2}$ term. On the other hand, notice the other, volume-dependent c-number term, a result of applying eq. (2.13) in the $b \to 0$ limit. This term will be important for making contact with energies as determined by the thermodynamic Bethe ansatz (TBA).

Using the mode expansion of eq. (2.10), we can write our Hamiltonian as

$$\begin{aligned} H_{\text{cyl}}^{(m)} &= H_{\text{ZM}}^{(m)} + H_{\text{osc}}^{(m)}; \\ H_{\text{ZM}}^{(m)} &= \left(\frac{1}{2gL}\Pi_0^2 + \frac{gm^2 L}{2}\varphi_0^2 - \frac{\pi}{6L} + \frac{m^2 L}{4\pi}\ln\left(\frac{mL}{2\pi}\right)\right); \\ H_{\text{osc}}^{(m)} &= \sum_{n\neq 0} \left[\frac{2\pi|n|}{L} a_n^\dagger a_n + \frac{m^2 L}{8\pi|n|}\left(2a_n^\dagger a_n + a_n^\dagger a_{-n}^\dagger + a_n a_{-n}\right)\right]. \end{aligned} \tag{2.16}$$

We now rewrite this Hamiltonian in term of a massive oscillator basis.

We begin here with the zero mode Hamiltonian. It is a harmonic oscillator of frequency m and 'mass' gL. Introducing massive zero mode operators a_0 and $a_0^\dagger$, we can write:

$$\varphi_0 = \frac{1}{\sqrt{2gmL}}\left(a_0 + a_0^\dagger\right); \quad \Pi_0 = i\sqrt{\frac{gmL}{2}}\left(a_0^\dagger - a\right). \tag{2.17}$$

In terms of the creation operators the zero mode Hamiltonian takes the form

$$H_{\text{ZM}}^{(m)} = m a_0^\dagger a_0 + \frac{m}{2} - \frac{\pi}{6L} + \frac{m^2 L}{4\pi}\ln\left(\frac{Lm}{2\pi}\right). \tag{2.18}$$

We now turn to the oscillator part, $H_{\text{osc}}^{(m)}$, of the Hamiltonian. This can be diago-

nalized by means of a Bogoliubov transformation implemented by the unitary operator

$$U = \exp\left\{ -\sum_{m>0} \chi_m \left(a_m a_{-m} - a_m^\dagger a_{-m}^\dagger \right) \right\}, \tag{2.19}$$

where

$$e^{\chi_n} = \left(\frac{\omega_n}{|k_n|} \right)^{\frac{1}{2}}, \quad \omega_n = \sqrt{k_n^2 + m^2}. \tag{2.20}$$

This acts on the mode operators a_n as

$$\begin{aligned} U^\dagger a_n U &= a_n \cosh \chi_{|n|} - a_{-n}^\dagger \sinh \chi_{|n|}; \\ U^\dagger a_{-n}^\dagger U &= a_{-n}^\dagger \cosh \chi_{|n|} - a_n \sinh \chi_{|n|}. \end{aligned} \tag{2.21}$$

Applying the Bogoliubov transformation to the Hamiltonian we obtain

$$\begin{aligned} H_{\text{cyl}}^{(m)} &= \sum_{n=-\infty}^{\infty} \omega_n a_n^\dagger a_n + \frac{m}{2} - \frac{\pi}{6L} + \frac{m^2 L}{4\pi} \ln\left(\frac{Lm}{2\pi} \right) + S_2(m, L); \\ S_2(m, L) &= \sum_{n \neq 0} \frac{\omega_n}{2} - \frac{|k_n|}{2} - \frac{m^2}{4\,|k_n|}. \end{aligned} \tag{2.22}$$

The factor $S_2(m, L)$ arises from normal ordering the massive oscillator basis after the Bogoliubov transformation is performed. In Appendix C we show that it admits an integral representation,

$$S_2(m, L) = \frac{\pi}{6L} - \frac{m}{2} + \frac{m^2 L}{4\pi} \left(\frac{1}{2} + \ln \frac{2}{m} - \gamma_E \right) + \frac{m^2 L}{4\pi} \ln \frac{2\pi}{L} + E_0^{(m)}(m, L), \tag{2.23}$$

where $E_0^{(m)}(m, L)$ is defined as

$$E_0^{(m)}(m, L) = m \int_{-\infty}^{\infty} \frac{du}{2\pi} \cosh u \ln\left(1 - e^{-mL \cosh u} \right). \tag{2.24}$$

Our final result for the Hamiltonian is

$$\begin{aligned} H_{\text{cyl}}^{(m)} &= \sum_{n=-\infty}^{\infty} \omega_n a_n^\dagger a_n + \mathcal{E}_0 L + E_0^m(m, L); \\ \mathcal{E}_0^{(m)} &= \frac{m^2}{4\pi} \left(\frac{1}{2} + \ln 2 - \gamma_E \right). \end{aligned} \tag{2.25}$$

The ground state energy of this Hamiltonian agrees with the energy $E_0^{(m)}(m, L)$ associated with a free massive boson computed in TBA [106]. Here we are able to pin down the bulk energy density, $\mathcal{E}_0$, that would be observed in a TSM computation.

We also remark in advance that substituting $\mu = \frac{gm^{2+\frac{b^2}{4\pi g}}}{2b^2}$ into the exact sinh-Gordon bulk energy formula eq. (2.77) and expanding in b results in the $O\left(b^0\right)$ term precisely coinciding with vacuum energy density of eq. (2.25).

2.2 Liouville CFT

An extensive review of Liouville CFT is provided[1] in [67]. Let us recall some important properties.

Classical Liouville field theory [132] is a classical field theory with action

$$S_{cl} = \int d^2x \frac{1}{16\pi} \left(\partial_\mu \varphi_c\left(x\right)\right)^2 - \mu_c e^{\varphi_c(x)} \tag{2.26}$$

The model described by the action (2.26) enjoys local conformal symmetry. Upon quantization, we want to calculate path integrals involving the weight

$$e^{\frac{i}{\hbar}S_{cl}} = e^{i\int d^2x \frac{1}{16\pi}\left(\partial_\mu \frac{\varphi_c(x)}{\sqrt{\hbar}}\right)^2 - \frac{\mu_c}{\hbar}e^{\varphi_c(x)}} \tag{2.27}$$

Let's introduce $\varphi\left(x\right) = \frac{1}{\sqrt{\hbar}}\varphi_c\left(x\right)$. In the following, we rename $\hbar = b^2$, $\mu_L = \mu_c b^{-2}$. We yield the equivalent action

$$S = \int d^2x \frac{1}{16\pi} \left(\partial_\mu \varphi\right)^2 - \mu_L e^{b\varphi} \tag{2.28}$$

It is clear that $b \to 0$ constitutes a classical limit, and the expansion in b is a semiclassical expansion.

The model provided by employing canonical quantization to the classical action (2.28) on a cylinder of circumference L is conformally invariant [64] with central charge

$$c = 1 + 6Q^2, \quad Q = b + b^{-1}. \tag{2.29}$$

In order to ensure the correct asymptotics of the field [69], we need to introduce a large-time regularization as we map the action from the cylinder to the plane, $\tau \leq \frac{R}{2\pi}\ln z$, $R \to \infty$. Mapping the regularized action to the plane, we yield additional boundary terms

$$S = \frac{1}{16\pi}\int\limits_{\Gamma} d^2z \left[\left(\partial_a\varphi\right)^2 + 16\pi\mu_L e^{b\varphi}\right] + \frac{Q}{2\pi L}\int\limits_{\partial\Gamma} \varphi dl + 2Q^2 \ln R \tag{2.30}$$

where Γ is a large disk of radius R. The boundary terms can be interpreted as a background charge $-Q$ at infinity.

[1] see also [66] for a string theory-oriented review.

Vertex operators $V_\alpha = e^{a\varphi}$ are again primaries with chiral dimensions [133]

$$h_\alpha = \bar{h}_\alpha = \alpha(Q-\alpha) \tag{2.31}$$

In particular the field $V_{Q-\alpha}$ has the same dimensions as V_α.

Similarly to the Gaussian case, the set of primaries is continuous. (Plane-wave) normalizable states with momentum P correspond to the subset of vertex operators V_α with $\alpha = \frac{Q}{2} + iP$, $Q = b + \frac{1}{b}$ [134]. Other vertex operators correspond to non-normalizable (microscopic) states [135]. Global conformal symmetry restricts the spacetime dependence of three-point functions to be of the form [1]

$$G(\alpha_1,\alpha_2,\alpha_3) = |x_{12}|^{2h_{12}}|x_{23}|^{2h_{23}}|x_{31}|^{2h_{31}} C\left(\alpha_1,\alpha_2,\alpha_3\right) \tag{2.32}$$

where $h_{23} = h_{\alpha_1} - h_{\alpha_2} - h_{\alpha_3}$, $h_{31} = h_{\alpha_2} - h_{\alpha_3} - h_{\alpha_1}$, $h_{12} = h_{\alpha_3} - h_{\alpha_1} - h_{\alpha_2}$ and $x_{ij} = x_i - x_j$.

To obtain the amplitudes C, one may start by considering the path integral representation

$$G(\alpha_1,\alpha_2,\alpha_3) = \int [\mathcal{D}\varphi] e^{-S[\varphi]} \prod_{i=1}^{3} e^{\alpha_i \varphi(w_i,\bar{w}_i)} \tag{2.33}$$

In the following, we will assume that the measure $[\mathcal{D}\varphi]e^{-S[\varphi]}$ factorises as

$$[\mathcal{D}\varphi]e^{-S[\varphi]} = d\varphi_0 [\mathcal{D}\tilde{\varphi}]_{\varphi_0} \tag{2.34}$$

and that the measure over the zero mode $d\varphi_0$ is translationally invariant. The vanishing of the Liouville interaction as $\varphi_0 \to -\infty$ indicates that $[\mathcal{D}\tilde{\varphi}]$ approximates the Gaussian measure $[\mathcal{D}\tilde{\varphi}]_Q$ of the free field theory with background charge $-Q$, with corrections given by the interaction term

$$[\mathcal{D}\tilde{\varphi}] \sim [\mathcal{D}\tilde{\varphi}]_Q \sum_{n=0}^{\infty} \frac{(-\mu_L)^n e^{bn\varphi_0}}{n!} \left(\int d^2 z e^{b\tilde{\varphi}} \right)^n, \quad \varphi_0 \to -\infty \tag{2.35}$$

After separating the zero mode dependence as

$$G(\alpha_1,\alpha_2,\alpha_3) = \lim_{q_0 \to -\infty} \int_{q_0}^{\infty} d\varphi_0 e^{-sb\varphi_0} \int [\mathcal{D}\tilde{\varphi}] \prod_{i=1}^{3} e^{\alpha_i \tilde{\varphi}(w_i,\bar{w}_i)}, \quad s = \frac{1}{b}\left(Q - \sum_{i=1}^{3} \alpha_i \right) \tag{2.36}$$

and substituting the expanded measure (2.35) into eq. (2.36), the integral over the zero mode φ_0 may be taken, yielding the pole structure

$$G(\alpha_1,\alpha_2,\alpha_3) \simeq \sum_{n=0}^{\infty} \frac{e^{-(s-n)bq_0}}{s-n} \mathcal{G}^{(n)}_{\alpha_1,\alpha_2,\alpha_3} \tag{2.37}$$

with residues given by

$$\mathcal{G}^{(n)}_{\alpha_1,\alpha_2,\alpha_3} = \frac{(-\mu_L)^n}{bn!}\int [\mathcal{D}\tilde{\varphi}]_Q \prod_{i=1}^{3} e^{\alpha_i \tilde{\varphi}(z_i,\bar{z}_i)} \left(\int d^2z e^{b\tilde{\varphi}}\right)^n \tag{2.38}$$

The quantities $\mathcal{G}^{(n)}_{\alpha_1,\alpha_2,\alpha_3}$ were calculated explicitly by Dotsenko and Fateev [136] and result in

$$\mathcal{G}^{(n)}_{\alpha_1,\alpha_2,\alpha_3}(z_1,z_2,z_3) = |z_{12}|^{2h_{12}}|z_{13}|^{2h_{13}}|z_{23}|^{2h_{23}} I_n(\alpha_1,\alpha_2,\alpha_3) \tag{2.39}$$

where α_i are subject to the kinematical condition $\sum_{i=1}^{3}\alpha_i = Q - nb$ and

$$I_n(\alpha_1,\alpha_2,\alpha_3) = \left(\frac{-\pi\mu_L}{\gamma(-b^2)}\right)^n \frac{\prod_{j=1}^{n}\gamma(-jb^2)}{\prod_{k=0}^{n-1}[\gamma(2\alpha_1 b + kb^2)\gamma(2\alpha_2 b + kb^2)\gamma(2\alpha_3 b + kb^2)]} \tag{2.40}$$

where $\gamma(x) = \Gamma(x)/\Gamma(1-x)$.

One way to conjecture the exact form of the three-point correlator (2.32) is to look for a meromorphic function with poles and residues corresponding to (2.38) and the required coordinate dependence. The exact three-point function was conjectured independently by Dorn and Otto [68] and by Zamolodchikov and Zamolodchikov [69]. It is called accordingly the DOZZ formula. The amplitude C of (2.32) reads explicitly

$$C(\alpha_1,\alpha_2,\alpha_3) = \left[\pi\mu_L\gamma(b^2)b^{2-2b^2}\right]^s \cdot \frac{\Upsilon_0\Upsilon(2\alpha_1)\Upsilon(2\alpha_2)\Upsilon(2\alpha_3)}{\Upsilon(\alpha_1+\alpha_2+\alpha_3-Q)\Upsilon(\alpha_1+\alpha_2-\alpha_3)\Upsilon(\alpha_2+\alpha_3-\alpha_1)\Upsilon(\alpha_3+\alpha_1-\alpha_2)} \tag{2.41}$$

where $\Upsilon(x)$ is defined as the analytic continuation of the integral representation

$$\log\Upsilon(x) = \int_0^\infty \frac{dt}{t}\left[\left(\frac{Q}{2}-x\right)^2 e^{-t} - \frac{\sinh^2\left(\frac{Q}{2}-x\right)\frac{t}{2}}{\sinh\frac{bt}{2}\sinh\frac{t}{2b}}\right] \tag{2.42}$$

and $\Upsilon_0 = \partial_x\Upsilon(x=0)$.

This formula passed a large number of checks and was subsequently obtained through conformal bootstrap as well [137]. Recently, it was rigorously derived using a probabilistic definition of the path integral [138].

However, formula (2.41) has more poles than predicted by (2.37). Quite confusingly, all extra poles would be nicely explained by the addition of an extra term $\tilde{\mu}_L e^{b^{-1}\varphi}$ to the action (2.28). where $\tilde{\mu}_L$ is defined as

$$\tilde{\mu}_L = \frac{\left(\pi\mu_L\gamma(b^2)\right)^{b^{-2}}}{\pi\gamma(b^{-2})} \tag{2.43}$$

This observation naturally raises the question whether the above term should actually be written into the action to yield the correct quantum Liouville model. This interpretation seems problematic as in many cases the resulting potential is not bounded below, at least classically. Some results of the present dissertation, especially those of Section 3.5, may be considered as indirect analytical and numerical evidence that the explicit addition of such term is *not* necessary. On the contrary, all extra poles are generated by nonperturbative effects from the naive action on the cylinder, in agreement with [138].

The amplitudes $C(\alpha_1, \alpha_2, \alpha_3)$ of eq. (2.41) admit a remarkable reflection property $C(\alpha_1, \alpha_2, \alpha_3) = R(\alpha_1) C(Q - \alpha_1, \alpha_2, \alpha_3)$ [69]. The quantity $R(\alpha)$ is defined as

$$R\left(\frac{Q}{2} + iP\right) = S_L(P) = -\left(\frac{\pi\mu_L\Gamma(b^2)}{\Gamma(1-b^2)}\right)^{-2iP/b} \frac{\Gamma(1+2iP/b)\,\Gamma(1+2iPb)}{\Gamma(1-2iP/b)\,\Gamma(1-2iPb)} \quad . \tag{2.44}$$

where $S_L(P)$ is conventionally called the Liouville reflection amplitude. The reflection amplitude is self-dual, in the sense that it is invariant under

$$\mu_L \to \tilde{\mu_L}$$
$$b \to \frac{1}{b}$$

Under any correlator, we are thus forced to make the identification

$$V_\alpha = R(\alpha)\, V_{Q-\alpha}. \tag{2.45}$$

This has grave consequences. If we are to distinguish operators by their $\varphi \to -\infty$ asymptotics, we have to conclude that V_α with $\mathrm{Re}(\alpha) > \frac{Q}{2}$ don't exist. In fact it can be shown that any vertex operator that asymptotes to $: e^{b\varphi} :$ as $\varphi \to -\infty$ and $b > Q/2$ would have zero matrix element between any normalizable wavepackets. The DOZZ formula is then to be interpreted using (2.45) as always containing operators satisfying the bound

$$\mathrm{Re}(\alpha) \leq \frac{Q}{2}.$$

up to reflection factors. This is called the Seiberg bound [135].

2.3 Sinh-Gordon model I. UV definition

In this section we briefly review the basic properties of the ShG model.

The sinh-Gordon model (ShG) is a quantum integrable field theory. In this subsection we are going to take as a starting point the Lagrangian formulation of the model

given by

$$\mathcal{L}_{ShG} = \frac{1}{16\pi}\left(\partial_\mu\phi\right)^2 - 2\mu\cosh(b\phi) \ . \tag{2.46}$$

Here $\phi(x,t)$ is a real non-compact scalar field, μ is some dimensionful mass scale and b is a dimensionless coupling constant.

The scale dimension of the renormalized counterpart of the coupling μ appearing in the ShG Lagrangian depends on the quantization scheme of the model. Hereafter we are going to discuss three such schemes: (i) a perturbative scheme based on Feynman diagrams; (ii) treating the theory on the same grounds as its analytically continued cousin, the sine-Gordon model, namely as a perturbed Gaussian CFT; and (iii) as a perturbation of a Liouville quantum field theory. The model's self-duality is often encoded in the parameter

$$Q = b + b^{-1}, \tag{2.47}$$

inherited from Liouville field theory.

2.3.1 Feynman diagrammatic analysis

In the first scheme, the ShG model is considered by employing perturbation theory in the coupling constant b and evaluating all quantities in terms of Feynman diagrams. This can be done by introducing a momentum cutoff Λ and expanding the potential of the theory in terms of b:

$$2\mu\,\cosh(b\phi) = 2\mu(\bar{\mu},\Lambda,b)\left(1+\frac{b^2}{2}\phi^2+\frac{b^4}{4!}\phi^4+\cdots+\frac{b^{2n}}{(2n)!}\phi^{2n}+\cdots\right). \tag{2.48}$$

Here $\mu(\bar{\mu},\Lambda,b)$ is a bare parameter of dimension mass squared. Let us immediately remark that in two ($1+1$, space+time) dimensions, all Landau-Ginzburg interactions (ϕ^n, $n\in\mathbb{Z}_{\geq 0}$) are super-renormalisable with engineering dimension 0. Using the cutoff Λ, we have introduced a renormalized coupling $\bar{\mu}$, which we aim to keep fixed as we tune μ such that the physical quantities are finite:

$$\mu(\bar{\mu},\Lambda,b) = \bar{\mu} + O(b^2\log(\Lambda)) \tag{2.49}$$

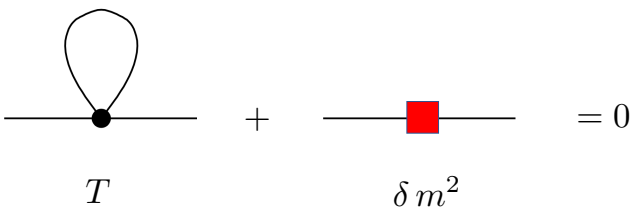

Figure 2.1: Diagrams for the first order tadpole diagram T and the corresponding relative mass counterterm $\delta m^2 = -T(m_0)$.

Above the unique ground state of the theory, there is a massive excitation, whose mass at the lowest order in b is m_0 given by

$$m_0^2 \;=\; 16\pi\, b^2\, \bar{\mu} \;\; . \tag{2.50}$$

Of course the actual mass of the particle will get corrections by all the higher order interactions. However, the perturbative series contains divergences. Fortunately, in 1+1d theories with local interactions all divergences come from the tadpole diagrams. These divergences can be cured by introducing a mass counter-term δm^2 and imposing that, order by order, δm^2 cancels the infinities coming from the tadpole diagrams. At the lowest order in b^2, for instance, we have the condition expressed in Fig. 2.1, where the tadpole is regularized in terms of the momentum cutoff Λ as

$$T(m_0) \;=\; (8\pi)^2 b^4 \bar{\mu} \int_{-\Lambda}^{\Lambda} \frac{dk_1}{2\pi} \int_{-\infty}^{\infty} \frac{dk_0}{(2\pi)} \frac{1}{k^2+m_0^2} \;=\; (8\pi)^2 b^4 \bar{\mu} \frac{1}{2\pi} \log\left(\frac{\Lambda}{m_0} + \sqrt{1+\frac{\Lambda^2}{m_0^2}} \right). \tag{2.51}$$

The counterterm $\delta m^2 = -T(m_{IR})$, involving in general an arbitrary mass scale m_{IR}, is absorbed by the bare parameter μ such that

$$\mu(\bar{\mu}, \Lambda, b) = \bar{\mu} + \frac{\delta m^2}{16\pi b^2} + O(b^4 \log^2 \Lambda). \tag{2.52}$$

This prescription is equivalent to defining a normal ordering for the Lagrangian (eq. (2.46)). The quantization scheme is fixed by the choice of m_{IR}. In particular, setting $m_{IR} = m_0$ leads to the usual scheme of a perturbed massive boson, where normal ordering is with respect to the free mass m_0, eliminating altogether the tadpole diagrams at each order. The exact relation between μ and $\bar{\mu}$ in the normal ordering scheme m_{IR} is easily obtained by means of the Baker-Campbell-Hausdorff formula. It reads

$$\mu(\bar{\mu}, \Lambda, b) = \bar{\mu} \left(\frac{\Lambda}{m_{IR}} + \sqrt{1+\frac{\Lambda^2}{m_{IR}^2}} \right)^{-2b^2} \;\; . \tag{2.53}$$

In this way, all n-point correlation functions of the theory are finite to all orders in perturbation theory. In particular, one can compute the physical mass M_{ShG} of the theory, as a function of m_0 and b^2, by looking at the pole of the 2-point correlation function. In the scheme $m_{IR} = m_0 \equiv m$, we obtain

$$M_{ShG}^2 \;=\; m^2 \left(1 - \frac{b^4}{384 g^2} + \frac{b^6}{g^3} \left(\frac{1}{1536\pi} + \frac{7\,\zeta(3)}{3072\pi^3} - \frac{14\,\zeta(3)}{3072\pi^3} \right) \right) + \mathcal{O}\left(\frac{b^8}{g^4} \right), \tag{2.54}$$

where $g = \frac{1}{8\pi}$ and each term comes from the Feynman diagrams of Fig. 2.2. We will point out later that this perturbative analysis is consistent with an exact formula for

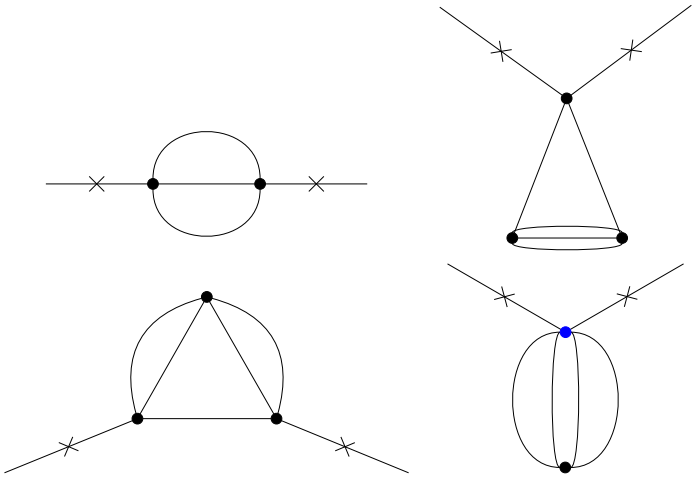

Figure 2.2: Feynman diagrams up to order b^6 entering the expansion of M^2_{ShG}. The ϕ^6 vertex is distinguished by a blue dot.

the mass that we present in Section 2.6.

We note that at $\mathcal{O}(b^4)$, the ShG coincides with a ϕ^4 Landau-Ginzburg model. Given the repulsive nature of this latter theory, the ShG is expected to have no bound states, its spectrum consisting of multi-particle states of the same particle. As we will see shortly, this conclusion is in agreement with the exact S-matrix of the model.

2.4 Sine-Gordon model

Many properties of the ShG model are conventionally extracted from a closely related and more famous model, the sine-Gordon (SG) theory. The SG model has a Lagrangian given by

$$\mathcal{L}_{SG} = \frac{1}{16\pi}\left(\partial_\mu\phi\right)^2 + 2\mu\,\cos(b\phi) \ . \tag{2.55}$$

This can be obtained from the ShG Lagrangian (2.46) by making the substitutions

$$\begin{aligned} b &\to ib \ , \\ \mu &\to -\mu \ . \end{aligned} \tag{2.56}$$

It is important to stress that, although the two theories are related by this simple transformation, their underlying nature is rather different and there are indeed a series of hidden subtleties behind the innocent looking analytic continuation (2.56), some of which are discussed below.

2.4.1 SG and ShG models as deformations of a Gaussian theory

Both sine-Gordon and sinh-Gordon theories may be regarded as deformations of the Gaussian fixed point action given by (2.1)

$$\mathcal{A}_0 \,=\, \int \frac{1}{16\pi}(\partial_\mu\phi)^2\, d^2x \ . \tag{2.57}$$

In fact, the sine-Gordon model is usually considered as the perturbation of the *compactified* $c = 1$ boson, by requiring the additional identification $\varphi \equiv \varphi + \frac{2\pi}{b}$. This makes the spectrum of the CFT discrete, thus enabling a more straightforward application of truncated space methods. In contrast, the sinh-Gordon potential is not periodic, so we will have to deal with the noncompact boson.

With respect to this CFT of central charge $c = 1$, the chiral conformal dimension of a vertex operator, $V(a) = e^{ia\phi}$, is $h_a = a^2$. The sine-Gordon model involves the vertex operators $V(\pm b) = e^{\pm i\, b\phi}$ which are compact and bounded, while the sinh-Gordon model employs the vertex operators $V(\mp ib) = e^{\pm b\phi}$ which are instead non-compact and unbounded. Moreover, while in the sine-Gordon model the conformal dimensions of the vertex operators are positive and given by

$$h_{\pm b} \,=\, b^2 \ , \tag{2.58}$$

in the sinh-Gordon model they are instead *negative* and given by

$$h_{\pm ib} \,=\, -b^2 \ . \tag{2.59}$$

How the sinh-Gordon model turns out to be a unitary quantum field theory, despite the negative conformal dimension of its basic vertex operators, is one of the remarkable aspects of this model. The way the theory restores its unitarity is through the existence of non-zero vacuum expectation values (VEV), whose exact values are provided in eq. (2.92) below. With $x_{12} = x_1 - x_2$, consider for instance the operator product expansion (OPE) with respect to the Gaussian fixed point:

$$\cosh(b\phi(x_1))\,\cosh(b\phi(x_2)) \,=\, \frac{1}{|x_{12}|^{4b^2}}\,\cosh(2b\phi(x_2)) + |x_{12}|^{4b^2}\mathbb{1} + \cdots \,, \tag{2.60}$$

and taking the vacuum expectation value of both terms of this equation, we have

$$\langle\cosh(b\phi(x_1))\,\cosh(b\phi(x_2))\rangle \simeq \frac{\langle\cosh(2b\phi(0))\rangle}{|x_{12}|^{4b^2}} + |x_{12}|^{4b^2} + \cdots \,. \tag{2.61}$$

Hence, if $\langle\cosh(2b\phi(0))\rangle \neq 0$, we see that the two-point function of the vertex operators $e^{\pm b\phi}$ has effectively the *same* leading short-distance singularity as it would have in the

case of a *positive* $h = b^2$ conformal dimension.

2.4.2 Coleman bound in SG and its formal absence in ShG

From a renormalization group point of view, the vertex operators which give rise to the sine-Gordon model are relevant operators for $b^2 \leq 1$, where the upper value $b^2 = 1$ is known in the literature as Coleman's bound [12]. The values $0 \leq b^2 \leq 1$ are those for which the SG is ultraviolet stable (i.e. we do not need extra non-trivial counter-terms in its Lagrangian to cure its ultraviolet divergencies). As we already know, the only divergences come from the tadpoles, which can be absorbed by a normal ordering prescription under which the vertex operators get renormalized multiplicatively. Defining m_{IR} as the mass scale by which normal ordering is defined and using a^{-1} as the UV cutoff, the multiplicative renormalization appears as

$$e^{\pm ib\phi} \;=\; \left[\left(\frac{m_{IR}a}{2}\right)^{2b^2} + O(a^2)\right] \;:\; e^{\pm ib\phi} \;:_{m_{IR}} . \tag{2.62}$$

When $b^2 > 1$, the vertex operators are irrelevant: hence the SG model becomes essentially a massless theory [139].

In the ShG model, the renormalization of the operators (or the coupling) occurs with the *inverse factor* of the SG model

$$e^{\pm b\phi} \;=\; \left[\left(\frac{2}{m_{IR}a}\right)^{2b^2} + O(a^2)\right] \;:\; e^{\pm b\phi} \;:_{m_{IR}} . \tag{2.63}$$

Typically in this multiplicative renormalization the power of a that arises is absorbed into the bare coupling μ so defining a renormalized dimensionful parameter $\mu_{SG/ShG}$:

$$\mu_{SG/ShG} = \mu a^{\pm 2b^2}, \tag{2.64}$$

where $+$ is for the SG theory and $-$ is for the ShG model. $\mu_{SG/ShG}$ then has scaling dimension in the two theories of $2 \mp 2b^2$. The scale m_{IR} that appears in this multiplicative renormalization is then typically absorbed into the definition of the normal ordered vertex operator so that the OPE has the conventions expressed in eq. (2.60). Henceforth it is understood as part of the definition of $\mu_{SG/ShG}$ that m_{IR} is chosen this way. The relation between the free mass m appearing in eq. (2.54) and the coupling μ_{ShG} is [128]

$$\mu_{ShG} \;=\; \frac{m^{2+2b^2}}{2^{4+2b^2}\pi b^2}\, e^{2b^2\gamma_E} \;\;, \tag{2.65}$$

as derived in Section 3.4.

Because of the negative conformal dimension of its vertex operators (which makes them relevant operators), at least formally the ShG model does not have a Coleman

bound. However, according to the argument given above, the singularity structure of the OPE for the ShG interaction eq. (2.61) is the same as for the SG model. One thus may suspect that there is in fact a Coleman bound for the ShG model, namely that the theory is properly defined only for $b^2 < 1$, has a singularity at $b^2 = 1$ and a massless phase for $b^2 > 1$. This is the scenario we will actually present later in the thesis.

2.4.3 The spectrum of SG model

Let us now turn our attention to the spectrum of the SG model. This quantity is key as the spectrum and S-matrix of the SG model will be connected to that of the ShG model by analytic continuation. Reproducing this spectrum will be one of the major targets of our TSM studies.

We note that this analytic continuation is subtle. While the sinh-Gordon model has only one vacuum state, the sine-Gordon model has instead an infinite number of vacuum states, $|n\rangle$, which are associated to the minima of the potential, $\phi_n = 2\pi n/b$. These multiple vacua give rise to solitons and anti-solitons, excitation which interpolate between two neighboring vacua, $|n\rangle$ and $|n \pm 1\rangle$. For the integrability of the theory, scattering among solitons and anti-solitons is elastic and the relative amplitudes can be computed exactly [70]. Here it is sufficient to remind the reader of the main results of this analysis. It is convenient to define

$$\xi = \frac{b^2}{1 - b^2} \ , \tag{2.66}$$

as this parameter controls the spectrum of the SG theory. The number of neutral soliton-anti-soliton bound states (breathers) is given by

$$N \ = \ \left\lfloor \frac{1}{\xi} \right\rfloor , \tag{2.67}$$

where $\lfloor x \rfloor$ denotes the integer part of x. Denoting by M_s the mass of the soliton, the breather masses are given by

$$m_n \ = \ 2M_s \sin\left(n\frac{\pi\xi}{2}\right), \quad n = 1, 2, \ldots < \frac{1}{\xi}. \tag{2.68}$$

Hence, the first breather exists provided $\xi \leq 1$, namely only in the range $b^2 \leq 1/2$. Ignoring this restriction, we plot $m_1(b)$ vs b for the entire interval $(0, 1)$ (see Fig. 2.3.b). Notice that even though the breather does not exist for $b^2 > 1/2$, its mass remains positive until $b^2 = 2/3$. After this, its value turns negative and begins to rapidly oscillate, reflecting its possession of an essential singularity at $b^2 = 1$.

The mass scale M_s can be related to the renormalized coupling of the theory μ_{SG}

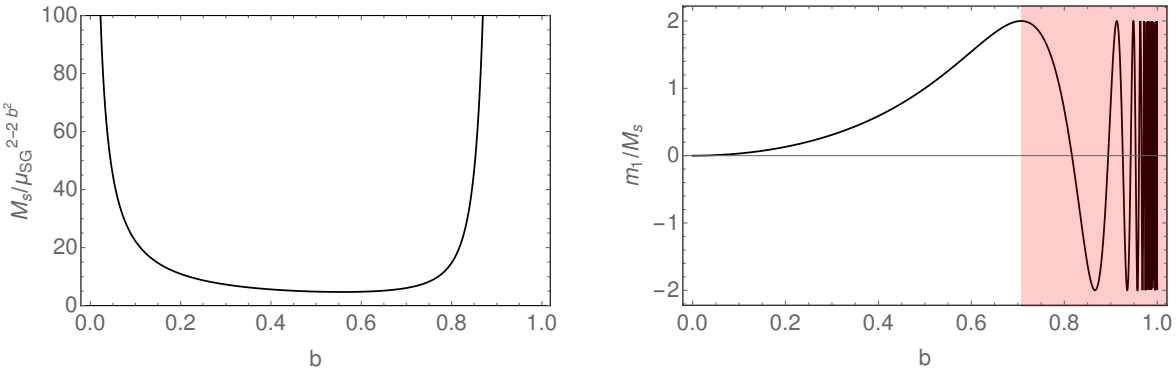

(a) Mass of the sine-Gordon soliton as a function of b.

(b) Mass of first SG breather vs b. The non-physical region is highlighted in red.

Figure 2.3: Masses in the sine-Gordon model.

(as defined in eq. (2.64)). In the SG model the ground state energy in finite volume and in the presence of an external field coupled to the topological charge of the model can be computed in two different ways: using the thermodynamic Bethe ansatz (TBA) and using conformal perturbation theory. The former approach employs the physical mass M_s while the latter, the renormalized mass scale μ_{SG}. Comparing the results coming from the two different approaches, Al. Zamolodchikov [93] was able to obtain an exact formula encoding the $\mu_{SG} - M_s$ relation:

$$M_s = \frac{2\Gamma\left(\frac{\xi}{2}\right)}{\sqrt{\pi}\Gamma\left(\frac{1}{2}+\frac{\xi}{2}\right)}\left(\mu_{SG}\frac{\pi\Gamma(1-b^2)}{\Gamma(b^2)}\right)^{\frac{1}{2-2b^2}} . \tag{2.69}$$

We see that this formula is consistent with μ_{SG} in the SG model having dimension $2-2b^2$. It is also important to stress that this formula assumes the vertex operators are normalized with the convention of eq. (2.60).

This formula is physical in the interval $0 \leq b^2 \leq 1$. It has an essential singularity when $b^2 \to 1$ (i.e. $\xi \to \infty$)

$$M_s \simeq 2\sqrt{2}e^{\frac{1}{2}-\gamma_E}\mu_{SG}^{\frac{\xi+1}{2}}(\pi\xi)^{\frac{\xi}{2}}e^{\frac{1}{4\xi}}, \quad b^2 \to 1. \tag{2.70}$$

It also diverges when $b^2 \to 0$ as

$$M_s \simeq 4\sqrt{\frac{\mu_{SG}}{\pi}}\frac{1}{b}, \quad b^2 \to 0. \tag{2.71}$$

Its behaviour in the interval $0 \leq b^2 \leq 1$ is shown on Fig. 2.3a.

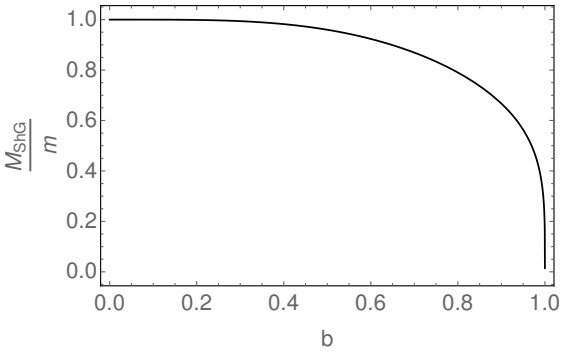

(a) Mass of the ShG normalized to m, the renormalized mass appearing in perturbation theory.

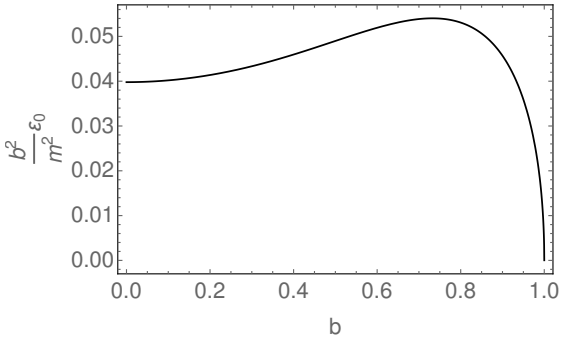

(b) Ground state energy density (bulk energy), normalized with respect to $\frac{m^2}{b^2}$.

Figure 2.4: Mass and ground state energy of the ShG model.

2.5 Sinh-Gordon model II. Bootstrap definition

2.5.1 S-matrix

There is an alternative way to define a consistent quantum field theory: by providing all S-matrix elements. This way one can avoid ever referring to a Lagrangian.

In a general QFT this is usually impractical. However, for *integrable* field theories, there is only elastic scattering. Moreover, multiparticle scattering factorises according to the Yang-Baxter equation. Let us point out Dorey's lecture notes for the 1996 Eötvos Graduate School [72] and two particularly useful textbooks, [17, 106] for an introduction on the nomenclature.

For an integrable theory with (generally multiple) particle types, one seeks to find a consistent set of elastic S-matrices at once. This procedure is referred to as S-matrix bootstrap. The fact that the bootstrap quantisation never refers to the Lagrangian is also a caveat. When there is a Lagrangian available for an integrable theory, the claim that scattering in the UV theory is described in terms of the exact S-matrix obtained through the bootstrap is usually a conjecture with perturbative checks available up to the first few orders.

For reasons that will become clear later, one chooses the sinh-Gordon S-matrix to be the analytically continued SG breather-breather S-matrix, $S_{B_1B_1}(\theta)$, the latter given by [44, 45]

$$S_{B_1B_1}(\theta) \;=\; \frac{\sinh\theta + i\sin\pi\xi}{\sinh\theta - i\sin\pi\xi} \;, \tag{2.72}$$

Here $\theta = \theta_1 - \theta_2$ and θ_i $(i = 1, 2)$ is the rapidity of each of the breathers involved in the scattering, with energy and momentum given by $E_i = m_1 \cosh\theta_i$ and $p_i = m_1 \sinh\theta_i$.

This amplitude has a pole at $\theta = i\pi\xi$,

$$S(\theta) \simeq i\,\frac{2\tan(\pi\xi)}{\theta - i\pi\xi} \ , \tag{2.73}$$

and, for $\xi < 1$, its residue is positive, i.e. this pole signals a further bound state, while for $\xi > 1$ the residue changes sign, which can be interpreted as another signal of the absence in the spectrum of the first breather for $\xi > 1$.

If we now continue this expression analytically by substituting $-b^2$ for b^2 in eq. (2.72), we obtain the exact 2-body S-matrix of the ShG model

$$S(\theta) = \frac{\sinh\theta - i\sin\pi B}{\sinh\theta + i\sin\pi B} \ , \tag{2.74}$$

where

$$B = \frac{\bar{b}^2}{1+\bar{b}^2} \ . \tag{2.75}$$

This expression is the S-matrix of the ShG model proposed in [89]. In eq. (2.75) we emphasize with bars that the relation between B (thus, $\bar{b}$) and b appearing in the Lagrangian is not a priori obvious. If the conjecture holds, then $\bar{b} = b$. Although the analytical continuation argument is amazingly simple, the final result is nonetheless surprising because a duality has appeared. The S-matrix now is invariant under the weak/strong duality $\bar{b} \leftrightarrow 1/\bar{b}$ or $B \leftrightarrow 1 - B$. However this duality is nowhere apparent in the Lagrangian (2.46) of the model.

2.5.2 Finite volume energy levels

The exact ground state energy, $E_0(L)$ at a finite volume L is obtained through the Thermodynamical Bethe Ansatz (TBA), based on the 'finite volume-finite temperature' equivalence of the partition function Z:

$$E_0\,(L) = L\,\mathcal{E}_0 - M_{ShG}\int_{-\infty}^{\infty}\frac{du}{2\pi}\,\cosh\theta\,\log(1+e^{-\epsilon(u)}) \ , \tag{2.76}$$

where $\mathcal{E}_0 = -\lim_{L\to\infty}\frac{1}{L}\ln Z\,(L)$ is the 'vacuum' energy density equal to the VEV of Eqn. (2.92):

$$\mathcal{E}_0 = \frac{M_{ShG}^2}{8\sin\pi B} \ . \tag{2.77}$$

The pseudo-energy $\epsilon\,(\theta)$ in Eqn. (2.76) is defined as the solution of the nonlinear integral equation

$$\epsilon(\theta) = M_{ShG}L\cosh\theta - \int_{-\infty}^{\infty}\frac{dv}{2\pi}\phi(\theta - v)\log(1+e^{-\epsilon(v)}) \ , \tag{2.78}$$

where the kernel is related to the S-matrix as

$$\phi\left(\theta\right) \;=\; -i\frac{d}{d\theta}\log S(\theta) \;\;. \tag{2.79}$$

For excited states, the exact finite volume energies can be obtained either by careful analytic continuations of the ground state TBA (following [80]), or by examining the continuum limit of an integrable lattice regularization [95]. A finite volume n-particle state can thus be described by the *multiparticle* pseudo energy $\epsilon(\theta|\{\vartheta_j\}_{j=1}^n) \equiv \epsilon(\theta|\{\vartheta\})$ and a set of quantization numbers $\{I_j\}_{j=1}^n$ satisfying the non-linear integral equation

$$\epsilon(\theta|\{\vartheta\}) = M_{ShG}L\cosh\theta + \sum_j \log S(\theta-\vartheta_j-\frac{i\pi}{2}) - \int_{-\infty}^{\infty}\frac{dv}{2\pi}\phi(\theta-v)\log(1+e^{-\epsilon(v|\{\vartheta\})}), \tag{2.80}$$

together with the additional quantization conditions

$$Q_j(\{\vartheta\}) = 2\pi I_j, \quad Q_j(\{\vartheta\}) = -i\epsilon(\vartheta_j+\frac{i\pi}{2}|\{\vartheta\}) - \pi, \quad j=1,\ldots,n. \tag{2.81}$$

Finite energy eigenstates can be described by a finite number n of particles with momenta $p_j = M\sinh\theta_j$. Given quantization numbers I_j, the rapidities $\{\vartheta\}$ and the pseudo energy $\epsilon(\theta|\{\vartheta\})$ can be determined self-consistently by efficient numerical methods. In turn, these provide the finite volume energy of the multiparticle state as

$$E_{\{I_j\}}(L) \;=\; L\,\mathcal{E}_0 + M_{ShG}\sum_j \cosh\vartheta_j - M_{ShG}\int_{-\infty}^{\infty}\frac{du}{2\pi}\,\cosh u\,\log(1+e^{-\epsilon(u|\{\vartheta\})}) \;\;. \tag{2.82}$$

Large-volume asymptotics. The well-known asymptotic Bethe Ansatz equations [5, 74, 75] arise from (2.80)-(2.81)-(2.82), by neglecting all terms exponentially suppressed in $M_{ShG}L$. We note that because the mass M_{ShG} is a parameter in these equations, they are invariant under the duality $b \leftrightarrow 1/b$. The Bethe-Yang equations essentially impose the one-valuedness of the quantum mechanical multi-particle wavefunction in presence of the purely elastic two-particle scattering $S\left(\theta\right) = e^{i\delta(\theta)}$

$$Q_j^0\left(\{\theta\}\right) \equiv p_j L + \sum_{k\neq j}^{n}\delta\left(\theta_j-\theta_k\right) = 2\pi I_j, \quad j\in\{1,\ldots,n\} \tag{2.83}$$

$$\delta(\theta) = 2\tan^{-1}\left(\frac{\sinh(\theta)}{\sin(\pi B)}\right). \tag{2.84}$$

where the sum in (2.83) is over k.

The system (2.83) is solved for the set of rapidities θ_j. The energy and total

momentum of the state is then given by the formulae

$$E = \sum_{j=1}^{n} M_{ShG} \cosh\theta_j, \quad P_{tot} = \sum_{j=1}^{n} M_{ShG} \sinh\theta_j$$

Small-volume asymptotics In the small-volume limit a quantization condition for the exact energy levels can be obtained from the TBA system [95]. We sketch the line of argument in Appendix B. In the zero mode sector the UV behaviour of the energy levels is as follows

$$E_n = \frac{2\pi}{L}\left(2P_n^2 - \frac{1}{12}\right) \ , \tag{2.85}$$

where the quantity P (not to be confused with P_{tot} above) is subject to the quantization condition

$$2\,\Theta(P) = n\pi, \quad n \in \mathbb{Z}_{\geq 0} \ . \tag{2.86}$$

The phase $\Theta(P)$ is given by

$$e^{2i\Theta(P)} \ = \ -\bar{b}^{\frac{8iP}{b}} \rho^{-4iPQ(\bar{b})} \frac{\Gamma\left(1+2iP\bar{b}\right)\Gamma\left(1+2iP\bar{b}^{-1}\right)}{\Gamma\left(1+2iP\bar{b}\right)\Gamma\left(1+2iP\bar{b}^{-1}\right)} \ , \tag{2.87}$$

where

$$\rho \ = \ \frac{L}{2\pi}\frac{M}{4\sqrt{\pi}}\Gamma\left(\frac{1-B}{2}\right)\Gamma\left(\frac{2+B}{2}\right) \ . \tag{2.88}$$

2.6 Sinh-Gordon model III. UV-IR relation and form factors

2.6.1 Mass-coupling relation from analytic continuation

As we have stated, the ShG model can be thought of as the analytic continuation of the SG. How then to connect the rich spectrum of SG containing topological excitations and their bound states to the much simpler spectrum of ShG consisting of a single parity odd excitation? The choice typically made is to identify the first breather of the SG model with the massive excitation of ShG.

To obtain the mass, M_{ShG}, of the fundamental excitation in ShG, we then take $M_{ShG}(b) = m_1(ib)$. Using eqns. (2.69) and (2.68) we arrive at [92]

$$M_{ShG} \ = \ \frac{4\sqrt{\pi}}{\Gamma\left(\frac{1}{2+2b^2}\right)\Gamma\left(1+\frac{b^2}{2+2b^2}\right)}\left[-\mu_{ShG}\frac{\pi\Gamma(1+b^2)}{\Gamma(-b^2)}\right]^{\frac{1}{2+2b^2}} \ , \tag{2.89}$$

where we have replaced μ_{SG} with $-\mu_{ShG}$ - necessary as only μ_{ShG} has the correct dimension. The plot of this quantity can be found on Fig. 2.4. A few remarks are in

order:

1. Keeping μ_{ShG} fixed, the mass formula (eq. 2.89) is *not* invariant under the weak-strong duality $b \to 1/b$ of the ShG model. Moreover, its analytic continuation for $b^2 > 1$ gives generally complex values for M_{ShG}.

2. For any finite value of μ_{ShG}, the mass M_{ShG} vanishes both at $b^2 = 0$ and $b^2 = 1$. The nature of these zeros is however very different. Indeed, the zero at $b^2 = 0$ disappears if we rescale $\mu_{ShG} \to \mu_{ShG}/(8\pi b^2)$ adopting the more conventional definition of the coupling constant of the model used in the Feynman diagram expansion. However on the approach to $b^2 = 1$, we instead find a singular point:

$$M_{ShG} \simeq (1 - b^2)^{1/4}, \quad b^2 \to 1. \tag{2.90}$$

3. In order to compare with the perturbative expansion (eq. 2.54), it is necessary to connect the renormalization scheme used to define μ_{ShG} with that used to define m (eq. (2.46)). Substituting eq. (2.65) into (eq. 2.89) and expanding in b^2, we have

$$M_{ShG} \;=\; m\,\left(1 - \frac{\pi^2}{12}b^4 + \frac{2\pi^2 - 7\zeta(3)}{12}b^6\right) + \mathcal{O}\left(b^8\right), \tag{2.91}$$

agreeing with the series expansion of the square root of expression eq. (2.54).

2.6.2 Vacuum expectation values in the ShG model

Similar to the mass and S-matrix, the vacuum expectation values (VEVs) of the vertex operators of the ShG model can be obtained as analytic continuations from the corresponding expressions (the Lukyanov-Zamolodchikov formula) for the SG model, leading to the Fateev-Lukyanov-Zamolodchikov-Zamolodchikov (FLZZ) formula [92, 140]:

$$\begin{aligned} G(\alpha) \;=\; \langle e^{\alpha\phi}\rangle \quad \equiv \quad M_{ShG}^{-2\alpha^2}\,\mathcal{G}(\alpha) \;=\; M_{ShG}^{-2\alpha^2}\left[\frac{\Gamma\left(\frac{1}{2+2b^2}\right)\Gamma\left(1+\frac{b^2}{2+2b^2}\right)}{4\sqrt{\pi}}\right]^{-2\alpha^2} \\ \times \exp\left\{\int_0^\infty \frac{dt}{t}\left[-\frac{\sinh^2(2\alpha b t)}{2\sinh(b^2 t)\sinh t\,\cosh((1+b^2)t)} + 2\alpha^2\, e^{-2t}\right]\right\}, \end{aligned} \tag{2.92}$$

with $G(\alpha) = G(-\alpha)$. Notice that the integral above converges for

$$|\alpha| \;<\; \frac{1}{2}\,Q, \tag{2.93}$$

a bound conceived for physical operators by N. Seiberg in his study of the allied Liouville problem [135]. For values of α beyond the Seiberg bound, one can exploit

an analytic continuation of $\mathcal{G}(\alpha)$. Obtaining this continuation is facilitated by the expression [141]:

$$\begin{aligned}\mathcal{G}(\alpha) &= e^{-2\gamma_E\alpha^2}\cos\frac{\pi\alpha}{Q} \\ &\times \prod_{k=1}^{\infty}\frac{e^{\frac{2\alpha^2}{k}}\,\Gamma^2\left(\frac{1}{2}+\frac{kB}{2}\right)\,\Gamma^2\left(\frac{1}{2}+\frac{k(1-B)}{2}\right)}{\Gamma\left(\frac{1}{2}-\frac{\alpha}{Q}+\frac{kB}{2}\right)\,\Gamma\left(\frac{1}{2}+\frac{\alpha}{Q}+\frac{kB}{2}\right)\,\Gamma\left(\frac{1}{2}-\frac{\alpha}{Q}+\frac{k(1-B)}{2}\right)\,\Gamma\left(\frac{1}{2}+\frac{\alpha}{Q}+\frac{k(1-B)}{2}\right)}.\end{aligned} \tag{2.94}$$

From it one can see that the VEV, as a function of α, does not have poles but only zeros. Besides the zero at $\alpha = Q/2$, there is an infinite set of generically simple zeros located at:

$$\begin{aligned}&\alpha = \pm\alpha_{n,m} = \pm\frac{Q}{2}\mp\left(\frac{m}{2}\,b^{-1}+\frac{n}{2}\,b\right), \\ &\text{with } m\geq n\geq 2 \quad n\in 2\,\mathbb{Z} \qquad \text{or} \qquad n>m\geq 2 \quad m\in 2\,\mathbb{Z}.\end{aligned} \tag{2.95}$$

Formula (2.94) is positive for $-\frac{Q}{2} < \alpha < \frac{Q}{2}$, but it changes sign at its zeroes. The vertex operators, being the exponentials of Hermitian operators, are positive (semi-)definite. This means that, outside the above domain, the analytic continuation cannot directly correspond to the expectation value. We will therefore consider these values "unphysical". The function $\mathcal{G}(\alpha)$ itself is self-dual, i.e. invariant under $b \to 1/b$ but the VEV is not itself self-dual because of the presence of $M_{ShG}^{-2\alpha^2}$. From the dependence on α of this term, we can infer that the scaling dimension of the vertex operator $V(\alpha)$ is $h_\alpha = -\alpha^2$, a value which coincides with its conformal dimension with respect to the Gaussian fixed point.

Using the VEV (2.92) we can also compute the expectation value of the trace of the stress-energy tensor, an operator that, on general terms, is defined as

$$\hat{\Theta}(x) = 2\pi\beta(\mu_{ShG})\,\mathcal{O}\ , \tag{2.96}$$

where $\beta(\mu_{ShG})$ is the β-function of the coupling μ_{ShG} which perturbs a critical point and $\mathcal{O}$ its conjugate field. For the case at hand, we have

$$\hat{\Theta}(x) = 8\pi(1+b^2)\,\mu_{ShG}\cosh b\phi(x). \tag{2.97}$$

Using the mass formula (eq. 2.89) and the simplified expression of the VEV at $\alpha = b$

$$\langle e^{\pm b\phi}\rangle = -M_{ShG}^{-2b^2}\,\frac{\pi}{16(1+b^2)}\,\frac{1}{\sin\pi B}\,\frac{\Gamma(1+b^2)}{\Gamma(-b^2)}\left[\frac{\Gamma\left(\frac{1}{2+2b^2}\right)\Gamma\left(1+\frac{b^2}{2+2b^2}\right)}{4\sqrt{\pi}}\right]^{-(2+2b^2)}, \tag{2.98}$$

we end up with

$$\langle\hat{\Theta}\rangle \;=\; \frac{\pi M_{ShG}^2}{2\sin\pi B}\;. \tag{2.99}$$

2.6.3 Questions arising from the analytic continuation $b \leftrightarrow ib$

In the previous two subsections we presented a number of results for the ShG model (its spectrum, its S-matrix, and the VEVs of its exponential operators) that are arrived at by analytically continuing results from SG. The question of the validity of these analytic continuations has to be raised. While the S-matrix of the ShG model is physically sensible for all b, the expressions for the mass and VEVs are not. Given that the fundamental excitation of the ShG is identified with the breather of SG and the SG breather ceases to exist for $b < 1/\sqrt{2}$, what exactly can be said for $b > 1/\sqrt{2}$ is not entirely clear. And certainly the mass formula for M_{ShG} for $b > 1$ breaks down entirely giving complex-valued results.

That we are able to match perturbative computations of the mass formula with the exact expression is thus important. This gives us some confidence that the results for M_{ShG} are valid for $b < 1$. However the validity and interpretation of formulae at $b > 1$ including the S-matrix arising from the analytic continuation remains, in our opinion, an open question.

2.6.4 Vacuum expectation values from perturbed Liouville point of view

The ShG model can be obtained as a perturbation of the Liouville action:

$$S_{ShG} = S_{Liouville} + \mu_L d^{-4-4b^2}\int d^2x\,\rho(x)^{2+2b^2}\,:e^{-b\phi}:\,. \tag{2.100}$$

In order to ensure the theory is IR finite, the theory can be placed on a Riemann sphere (of area A) with a metric

$$g_{\mu\nu}(x) = \rho(x)\delta_{\mu\nu};\quad \rho(x) \;=\; (1+\pi|x|^2/A)^{-2}. \tag{2.101}$$

Note that we have made a scale d that comes from normal ordering the vertex operator explicit instead of absorbing it into μ_L. We use d here to distinguish this scale from the scale a previously introduced in normal ordering vertex operators in the Gaussian scheme. The parameter μ_L here is the same dimensionless constant that appears in the original Liouville action, eq. (2.28).

A key property of the Liouville field theory is that the exponential operators are pairwise identified as [69]

$$e^{\alpha\phi(x)} \;=\; R(\alpha)\,e^{(Q-\alpha)\phi(x)}\;, \tag{2.102}$$

where $R(\alpha)$ is related to the Liouville reflection amplitude $S_L(P)$ according to (2.44). This identification of the operators implies that their VEV must satisfy the reflection relations

$$\begin{aligned} G_L(\alpha) &= R(\alpha)\, G_L(Q-\alpha), \\ G_L(-\alpha) &= R(\alpha)\, G_L(-Q+\alpha). \end{aligned} \tag{2.103}$$

Here the L-subscripts indicate that we are taking these VEVs as defined in the perturbed Liouville formulation of ShG and are not assuming these relations are the same as in eq. (2.94). A solution of these equations can be obtained by an infinite iteration

$$G_L(\alpha) \propto \prod_{n=0}^{\infty} R(\alpha - nQ). \tag{2.104}$$

With the further assumption of minimality, we can find a result equivalent to combining (2.89) and (2.92). This provides below an alternate way of understanding these formulae without resorting to analytic continuation from results derived for SG.

In order to present this argument, we need to trace carefully the dimensions of the quantities involved [2] This is an issue because in the Liouville approach the exponential operator, $e^{a\phi}$, has dimension (2.31) whereas the dimension of this operator in the perturbed Gaussian formulation of the ShG model is instead $-\alpha^2$. To understand this dimensional transmutation, we follow along with Ref. [92] and interpret properly the results.

To begin, we use the action (eq. (2.100) to write the following perturbative expansion of the VEV of $e^{a\phi}$:

$$G_L(\alpha) = Z^{-1} \sum_{n=2}^{\infty} \frac{(-\mu_L)^n}{n!} \int d^2y_1 \dots d^2y_n \, \langle e^{\alpha\phi}(x)\, e^{-b\phi}(y_1) \dots e^{-b\phi}(y_n) \rangle_{\mathrm{L}} \ . \tag{2.105}$$

Since in Liouville field theory the coupling μ_L can be absorbed into the field ϕ via a redefinition of this field by an additive shift, it is easy to obtain the explicit μ_L dependence of all correlators appearing in eq. (2.105). With the IR regulator A of eq. (2.101) in place, this expression can be written as the following series:

$$G_L(\alpha) = \mu_L^{-\alpha/b}\, A^{\alpha(\alpha-Q)} \sum_{n=2}^{\infty} \left[\mu_L^2 \left(\frac{A}{d^2} \right)^{2(1+b^2)} \right]^n \tilde{G}_{Ln}(\alpha) \ , \tag{2.106}$$

where $\tilde{G}_{Ln}(\alpha)$ is independent of μ_L. The prefactor $\mu_L^{-\alpha/b}$ also ensures the satisfiability of the reflection relations (2.103), given the dependence on μ_L of the refection amplitude $R(\alpha)$, see eq. (2.44). We see that our IR regulator appears in a dimensionless combination with the scale d in this perturbative expansion. If we assume that this

[2] I gratefully acknowledge Giuseppe Mussardo for the clarification and resolution of this issue.

expression has a sensible large A limit, the above series must behave asymptotically as

$$\tilde{G}_L(\alpha,t) \equiv \sum_{n=2}^{\infty} t^n \, \tilde{G}_{Ln}(\alpha) \to \tilde{G}_L(\alpha)\, t^{-\frac{\alpha(\alpha-Q)}{2(1+b^2)}}, \quad t = \mu_L^2 \left(\frac{A}{d^2}\right)^{2(1+b^2)} . \tag{2.107}$$

Thus in the large A limit, we obtain

$$G_L(\alpha) = d^{2\alpha(\alpha-Q)}\, \mu_L^{-2\alpha^2/(2+2b^2)} \tilde{G}_L(\alpha). \tag{2.108}$$

We thus see the VEV has dimension $-2\alpha(\alpha-Q)$ as set by the UV cutoff d - the dimension set by the Liouville CFT. At the same time its dependence upon μ_L is exactly what would be expected from thinking of the ShG model as a perturbation of a free non-compact boson.

Using eq. (2.103), we obtain [92] for the function $\tilde{G}_L(\alpha)$:

$$\begin{aligned} \tilde{G}_L(\alpha) &= \left(\frac{\pi\Gamma(1+b^2)}{\Gamma(-b^2)}\right)^{-\alpha^2/(1+b^2)} \\ &\quad \times \exp\left\{\int_0^\infty \frac{dt}{t}\left[-\frac{\sinh^2(2\alpha b t)}{2\sinh(b^2 t)\sinh t\,\cosh((1+b^2)t)} + 2\alpha^2\, e^{-2t}\right]\right\} \end{aligned} \tag{2.109}$$

If we compare $\tilde{G}_L(\alpha)$ with the expression for $G(\alpha)$ presented in eq. (2.92) and eq. (2.89), we see that they are consistent, i.e.

$$\frac{G(\alpha)}{\mu_{SG}^{-2\alpha^2}} = \tilde{G}_L(\alpha) \ . \tag{2.110}$$

If we identify the couplings in the Gaussian and Liouvillean formulations via

$$\mu_{ShG} = \mu_L d^{-2-2b^2} \ ,$$

we can identify the expressions for the VEVs in the two formulations via

$$G_L(\alpha) = d^{-2\alpha Q} G(\alpha) \ . \tag{2.111}$$

It is reassuring that we obtain the same (nontrivial) formulas either by analytic continuation and by solving the Liouville reflection functional equations. The appearance of the factor d in this expression is a reflection of the different normal ordering schemes in the Gaussian vs Liouville pictures.

2.6.5 Exact form factors

Using the S-matrix (2.74) and the integrability of the model, one can compute the exact form factors of the local operators $\mathcal{O}$ on the multi-particle states of the theory [90, 91]

$$\langle 0|\mathcal{O}(0)|\theta_1,\dots,\theta_n\rangle \equiv F_n^{\mathcal{O}}(\theta_1,\dots,\theta_n) \ , \tag{2.112}$$

that are understood as functions of $n \geq 0$ complex variables.

Note that we fix the normalization of the infinite volume one-particle states as

$$\langle\theta|\theta'\rangle = 2\pi\delta(\theta-\theta'). \tag{2.113}$$

These infinite volume form factors satisfy the monodromy axioms:

$$F_N^{\mathcal{O}}(\theta_1,\dots,\theta_N) = F_N(\theta_2,\dots,\theta_N,\theta_1-2i\pi) = S(\theta_{i,i+1})F_N(\theta_1,\dots,\theta_{i+1},\theta_i,\dots,\theta_N) \tag{2.114}$$

which together with their known analytic properties allows one to find the relevant physical solutions.

Form factors have pole singularities, with either kinematical or dynamical origin. The kinematical pole is related to disconnected diagrams and appear whenever an outgoing particle coincides with an incoming one. At the level of the elementary form factor this implies that

$$F^{\mathcal{O}}_{N+2}(\theta+i\pi+\frac{\epsilon}{2},\theta-\frac{\epsilon}{2},\{\theta\}) = \frac{i}{\epsilon}(1-\prod_j S(\theta-\theta_j))F_N(\{\theta\})+F^r_{N+2}(\theta+i\pi,\theta,\{\theta\})+O(\epsilon) \tag{2.115}$$

where we introduced a specific symmetric evaluation, since the $O(1)$ piece defined this way, that we call the *regulated* form factor, will be relevant in the further discussions. The notation $\{\theta\}$ abbreviates the ordered set $\{\theta_1,\dots,\theta_N\}$. Dynamical poles are related to bound states and are absent in the sinh-Gordon model.

Introducing the notation

$$[k] \ = \ \frac{\sin k\,\pi B}{\sin \pi B} \tag{2.116}$$

where the function $B(\bar{b})$ is given in eq. (2.75), the form factors of the exponential fields in the ShG model can be written as

$$\langle 0|e^{kb\phi(0)}|\theta_1,\dots,\theta_n\rangle \ = \ \langle e^{kb\phi}\rangle\, F_n^{(k)}(\theta_1,\dots,\theta_n) \tag{2.117}$$

where $\langle e^{kb\phi}\rangle$ is the VEV given in eq. (2.92) below. For the remaining term we have

$$F_n^{(k)}(\theta_1,\dots,\theta_n) \ = \ H_n^{(k)}\, Q_n^{(k)}(x_1,\dots,x_n)\prod_{i<j}^{n}\frac{F_{min}(\theta_{ij})}{x_i+x_j}\,, \tag{2.118}$$

where

$$F_{min}(\theta) \;=\; \exp\left\{-2\int_0^\infty \frac{dt}{t}\,\frac{\sinh\left(\frac{tB}{2}\right)\sinh\left(\frac{t(1-B)}{2}\right)}{\sinh(t)\cosh\left(\frac{t}{2}\right)}\,\cos\left(\frac{t(i\pi-\theta)}{\pi}\right)\right\}\,, \tag{2.119}$$

$$H_n^{(k)} \;=\; \left(\frac{4\sin\pi B}{F_{min}(i\pi)}\right)^{\frac{n}{2}}\,[k] \quad , \quad x_i = e^{\theta_i} \tag{2.120}$$

and $Q_n^{(k)}(x_1,\ldots,x_n)$ are symmetric polynomials in x_i given by

$$Q_n^{(k)}(x_1,\ldots,x_n) \;=\; \det M \qquad M_{i,j} \;=\; [i-j+k]\,\sigma_{2i-j}^{(n)} \tag{2.121}$$

with $\sigma_s^{(n)}$ the elementary symmetric polynomials in n variables of total degree s. Form factors of the ShG model were also studied in [142, 143].

What concerns the form factors of the elementary field itself, they admit the same structure of eq. (2.118), $k = 0$, but with a different normalization constant. The normalization for the field is given by $H_{2n+1}^{\varphi} = \sqrt{\frac{Z(b)}{2}}\left(\frac{4\sin\pi B}{F_{min}(i\pi)}\right)^n$, where $Z(b)$ is the wavefunction renormalization constant [156]

$$Z(b) = \frac{8\pi^2 B^2 g}{b^2\sin(\pi B)\,F_{min}(i\pi)} \tag{2.122}$$

with $g = \frac{1}{8\pi}$.

2.6.6 Finite volume matrix elements

What concerns the matrix elements, the Pozsgay-Takács formulae [6] [7] come to our help. For completely non-diagonal form factors, where all rapidities are pairwise different between the bra and the ket states, the formula reads

$$\left\langle \{I_i\}_{i=1}^k \left|\mathcal{O}(x,0)\right| \left\{\tilde{I}_j\right\}_{j=1}^l \right\rangle_L = \frac{e^{iM\left(\sum_{j=1}^l \sinh\vartheta_j - \sum_{i=1}^k \sinh\theta_i\right)x}\left\langle \{\theta_i\}_{i=1}^k \left|\mathcal{O}(0,0)\right| \{\vartheta_j\}_{j=1}^l \right\rangle}{\sqrt{\rho_k(\{\theta_i\})\,\rho_l(\{\vartheta_j\})}\mathcal{N}_k^*(\{\theta_i\})\,\mathcal{N}_l(\{\vartheta_j\})} \tag{2.123}$$

$$+\,O\left(e^{-ML}\right)$$

with

$$\mathcal{N}_k(\{\theta_i\}) = \sqrt{\prod_{r=1}^k\prod_{s=r+1}^k S(\theta_r-\theta_s)} \tag{2.124}$$

and ρ_k is the Gaudin determinant

$$\rho_k\left(\{\theta_i\}_{i=1}\right) = \det R_{pq}, \quad R_{pq} = \frac{\partial Q_q^{(0)}}{\partial \theta_p} \tag{2.125}$$

The normalization coefficients of (2.124) make all matrix elements (2.123) real. When at least one pair of rapidities coincide between the bra and the ket vector, significantly more complicated formulas take the role of eq. (2.123). This happens in two circumstances. It is obviously the case when the bra and the ket is the same state (diagonal form factor). The other possibility is that two different states have an odd number of particles $2n+1$ and $2m+1$, respectively, with quantization number set $\{I_j\}_{j=1}^n \cup \{0\} \cup \{-I_j\}_{j=1}^n$ and $\left\{\tilde{I}_j\right\}_{j=1}^m \cup \{0\} \cup \left\{-\tilde{I}_j\right\}_{j=1}^m$. In the latter case, a particle of exactly zero momentum is present in both states.

In the case of the VEV and diagonal form factors, all exponential finite volume corrections can be written as a series in $e^{-M_{ShG}L}$. The finite volume corrections for the VEV are given by the Leclair-Mussardo formula [84]

$$\mathcal{G}(a,L) = \mathcal{G}(a)\left(1 + \sum_{n=1}^{\infty} \frac{1}{n!(2\pi)^n} \int \prod_{i=1}^{n} \frac{d\theta_i}{1+e^{\epsilon(\theta_i)}} C_n^a(\{\theta_i\})\right) \tag{2.126}$$

where C_n^a is the *connected* evaluation of the n-particle diagonal form factor for the operator $e^{a\varphi}$

$$\lim_{\forall \epsilon_j \to 0} F_{2n}^a(\theta_n + i\pi + \epsilon_n, \ldots, \theta_1 + i\pi + \epsilon_1, \theta_1, \ldots, \theta_n) = C_n^a(\{\theta_i\}) + O(\epsilon^{-1}) \tag{2.127}$$

such that C_n^a is independent of ϵ_i. Exponential corrections for diagonal states admit a similar series representation is available [87].

Finally, let us remark that a TBA-like integral representation is known for certain ratios of VEVs [97] and diagonal form factors [144].

Chapter 3

Truncated spectrum approach to the sinh-Gordon model and related theories

In this chapter, we develop the truncated spectrum approach to the sinh-Gordon model. The results presented are based on [151] which is itself partially built on our earlier work in [128]. Following a general overview of the method in Section 3.1, we first consider the so-called massless scheme with zero mode separation in Section 3.2. We then explore the numerical accuracy of the technique for various physical quantities in Section 3.3. We provide the connection between the massless scheme and the purely massive basis built using the conventional Fock oscillators in Section 3.4. We provide a detailed examination of the small-volume spectrum in Section 3.5, yielding one of the most spectacular successes of the truncated spectrum method. In the following two sections, we initiate progress in improving the accuracy of the numerical method. We discuss the cutoff-dependence of the energy eigenvalues in Section 3.6 and provide an explanation for the observed power-law cutoff dependence. In Section 3.7 we explore the idea of using the basis of sinh-Gordon eigenstates to reproduce the spectrum of ShG at a different coupling. This line of thought leads to useful arguments regarding the Lagrangian theory beyond the self-dual point.

3.1 Truncated spectrum methods

The purpose of this section is to give the reader an overview of truncated spectrum methods (TSMs) and their application to the sinh-Gordon model. TSMs were introduced by Yurov and Zamolodchikov [107] to study the low-energy spectrum of 2D perturbed conformal field theories. However the method is able to study the spectrum and matrix elements of any theory whose Hamiltonian can be conveniently written as

a sum of two terms

$$H \;=\; H_0 + \int_0^L dx\, V_{\rm pert}(x)\ , \tag{3.1}$$

where H_0 is a base theory of which we assume to have a complete control of its energy eigenvalues and eigenstates $|E_n\rangle_0$. In particular, we assume that we are able to write down the matrix elements of the second term in the full Hamiltonian, $V_{\rm pert}(x)$, in the basis $\{|E_n\rangle_0\}$ of eigenvectors of H_0. From a computational point of view, the actual implementation of the method requires both a denumerable set of energy states and finite-dimensional subspaces of the Hilbert space of the model: the former condition is typically achieved by putting the model onto a cylinder of finite circumference L in the spatial direction; the latter condition is satisfied by restricting the set of eigenstates of H_0 to those whose energies fall below a cutoff E_c. Once a finite basis is obtained in this way, the truncated Hamiltonian is constructed. This operator possesses the same matrix elements as the original Hamiltonian in the truncated subspace, but acts trivially in the orthogonal subspace. Having this in hand, one then solves, numerically, the eigenproblem of the truncated Hamiltonian. Assuming for the moment that the dependence of the data on the cutoff E_c is under control (e.g. extrapolated), once the truncated Hamiltonian is diagonalized for different volumes, the infinite volume quantities can be obtained via Lüscher's principle [4, 5, 77, 118].

TSMs were first applied to the scaling Lee-Yang model [107] and the Ising model [108]. In both cases the reported numerical results were strongly convergent in E_c. In the study of the perturbed tri-critical Ising theory, though, it was argued that the convergence in E_c of the TSM results depends on the scaling dimension of the perturbing operator [109, 118]. Various renormalization group approaches have been advocated to treat cases where convergence in E_c is not fast enough. These strategies are both numerical [110] and analytical [124–126, 145] (For a comprehensive review of such strategies see [111].) We will demonstrate later that these strategies require modification (at the very least) for the case of the ShG.

The performance of TSMs depends on the choice of the computational basis used to perform the calculations (or, in other words, how we split the Hamiltonian H into H_0 and $\int dx V_{\rm pert}$). As with any variational method, we want to use a computational basis that captures at the start features of the physics of the model at hand. In this thesis we study the ShG model by means of three different choices of H_0 or computational bases:

1. In the first, discussed in the Section 3.2, we consider the ShG model as a deformation of a Gaussian CFT and the corresponding non compact bosonic field expanded in terms of an infinite number of oscillators and a single zero mode. When H_0 is a compact CFT on a cylinder and V is a relevant operator, one typically has control of the magnitude of the interaction between different energy scales in the theory. The ShG model is,

however, different, and the low and high energy scales in the problem become strongly coupled on the approach towards $b = 1$.

2. In the second, we switch to the massive oscillator Fock basis. In Section 3.4 we first consider the case when the zero mode is kept separated. It is expected that the massive basis catches more correlations among the oscillators. Then we assimilate the zero mode into the massive oscillator framework. This paves the way and functions as a reference point to our third method:

3. Our final basis choice, outlined in Section 3.7, uses the eigenstates of the ShG model itself as the computational basis. In particular, we use the basis of the ShG model at one value of $b = b_0$ to compute the properties of the model at a different value of $b = b_1$. In this scheme, $V_{\rm pert}$ is the difference between two hyperbolic cosines. This approach does immediately raise questions of circularity. We are, after all, using conjectured information about the model at a point b_0 as input, to obtain results at point $b_1 \neq b_0$. We will address this question in Section 3.7, and attempt to ameliorate this concern.

3.2 Massless scheme: separation of the zero mode

In our first attempt to study the ShG model using TSMs, we employ a computational basis based on a non-compact massless basis. In this section we review the details surrounding this choice of basis.

3.2.1 Non-compact massless boson

In describing this basis the starting point is the mode expansion of the massless non-compact bosonic field on an infinite cylinder of radius R:

$$\varphi\left(x,t\right) = \varphi_0 + 8\pi\frac{\Pi_0}{L}t + \sum_{n\neq 0}\sqrt{\frac{2}{|n|}}\left(a_n e^{i(k_n x - |k_n|t)} + a_n^\dagger e^{-i(k_n x - |k_n|t)}\right); \quad k_n = \frac{2\pi n}{L}, \tag{3.2}$$

where the oscillators are subject to the usual Fock commutator relations,

$$\left[a_n, a_m^\dagger\right] \;=\; \delta_{nm}\;, \tag{3.3}$$

while the zero mode defines an effective 1D quantum mechanical system with the canonical commutator $[\varphi_0, \Pi_0] = i$.

The computational basis of states follows from the specification of H_0 in eq. (3.1). Here we will divide H_0 into a zero mode H_{ZM} and non-zero mode H_{NZM} part:

$$H_0 \;=\; H_{ZM} + H_{NZM}\;;$$

$$
\begin{aligned}
H_{ZM} &= \frac{4\pi}{L}\Pi_0^2 + \mu_{ShG} L \left(\frac{L}{2\pi}\right)^{2b^2} \left[: e^{b\varphi_0} : + : e^{-b\varphi_0} :\right] \ ; \\
H_{NZM} &= \frac{2\pi}{L}\left(L_0 + \bar{L}_0 - \frac{1}{12}\right) \ , \qquad (3.4)
\end{aligned}
$$

where the Virasoro generators L_0 and $\bar{L}_0$ appearing in H_{NZM} are related to the Fock mode operators as

$$
L_0 = \sum_{n>0} n a_n^\dagger a_n \quad , \quad \bar{L}_0 = \sum_{n<0} |n|\, a_n^\dagger a_n \ .
$$

Notice that H_{ZM}, unlike H_{NZM}, is an interacting Hamiltonian. With this writing of H_0, our computational eigen-basis has a tensor product structure composed of a zero mode and an oscillator sector:

$$
\mathcal{H} = \mathcal{H}_{ZM} \otimes \mathcal{H}_{osc} \equiv \mathcal{H}_{ZM} \otimes \mathcal{H}_R \otimes \mathcal{H}_L \ . \qquad (3.5)
$$

Here $\mathcal{H}_{osc}$ is decomposed into a chiral subspace, $\mathcal{H}_R$, is spanned by right-moving particles

$$
\mathcal{H}_R = \left\{ a_{n_1}^\dagger \dots a_{n_k}^\dagger \left|0\right\rangle, n_i > 0 \right\} \ ,
$$

and an anti-chiral subspace, $\mathcal{H}_L$, is spanned by left-moving particles

$$
\mathcal{H}_L = \left\{ a_{-n_1}^\dagger \dots a_{-n_k}^\dagger \left|0\right\rangle, n_i > 0 \right\} \ .
$$

3.2.2 Zero modes

Unlike the non-interacting H_{NZM}, we have chosen a form for H_{ZM} that is non-trivial. We do so following [113, 115, 128] so that $\mathcal{H}_{ZM}$ consists of a countable (i.e. discrete) basis of states. We will denote this basis of states as follows

$$
\mathcal{H}_{ZM} = \{ |m\rangle \ , \ H_{ZM}|m\rangle = E_{ZM,m}|m\rangle \}. \qquad (3.6)
$$

Unlike the states in $\mathcal{H}_{NZM}$, in our implementation of the TSM the eigenstates $|m\rangle$ will be found numerically. To do so, we need to choose a computational basis to represent H_{ZM} in eq. (3.4) and, for this aim, we choose the particle-in-a-box basis in the zero mode coordinate with box width D

$$
\mathcal{H}_{ZM,computational} = \{ |\phi_0\rangle, \phi_0 = \sqrt{\frac{2}{D}} \sin\left(\frac{2n\pi\left(x + \frac{D}{2}\right)}{D}\right), n = 1, \cdots, N_{ZM,max} \} \ , \qquad (3.7)
$$

In performing our computations here, we have always taken D and $N_{ZM,max}$ large enough so that the eigenvalues and eigenstates (or at least their matrix elements) of H_{ZM} have converged completely. Experience shows that the convergence rate is fast in these parameters. Practically we worked with $N_{ZM,max} = 800$ and D was chosen such that the "infinite walls" are placed where the zero-mode quantum mechanical potential takes the numerical value $V_{ZM}(x_0) = 3000$.

3.2.3 Truncated Hilbert spaces

Having determined $\mathcal{H}_{ZM}$, we are now in a position to define the truncated basis, $\mathcal{H}_T$, for the problem as a whole. We truncate each part of the Hilbert space separately. In particular we write

$$\begin{aligned}
\mathcal{H}_T &= \mathcal{H}_{ZM,T} \otimes \mathcal{H}_{R,T} \otimes \mathcal{H}_{L,T}; \\
\mathcal{H}_{R,T} &= \left\{ a^\dagger_{n_1} \dots a^\dagger_{n_k} |0\rangle , n_i > 0, \sum_{i=1}^{k} n_i \leq N_c \right\}; \\
\mathcal{H}_{L,T} &= \left\{ a^\dagger_{-m_1} \dots a^\dagger_{-m_l} |0\rangle , m_i > 0, \sum_{i=1}^{l} m_i \leq N_c \right\}; \\
\mathcal{H}_{ZM,T} &= \{ |m\rangle, m = 1, \cdots, N_{ZM}, E_{ZM,1} \leq \cdots \leq E_{ZM,N_{ZM}} \} . \qquad (3.8)
\end{aligned}$$

The cutoff is then implemented in terms of two separate parameters, N_c, the level of which we cut off the chiral oscillator mode part of the Hilbert space, and N_{ZM}, the number of zero mode eigenstates of smallest energy (w.r.t. to H_{ZM}) that we keep. We typically work not in this full space, but its zero-momentum counterpart composed of tensored states from $\mathcal{H}_{R,T}$ and $\mathcal{H}_{L,T}$ that satisfy

$$\sum_{i=1}^{k} n_i = \sum_{i=1}^{l} m_i.$$

The last step of forming the Hamiltonian matrix consists of specifying the interaction part of the Hamiltonian and its corresponding matrix elements. In the zero-momentum subspace, $P = 0$, we can write

$$\int_0^L dx\, V_{pert}(x) = \delta_{P,0} \mu_{ShG} \left(\frac{L}{2\pi} \right)^{2b^2} L \left[e^{b\varphi_0} \left(: e^{b\tilde{\varphi}(0)} : -1 \right) + e^{-b\varphi_0} \left(: e^{-b\tilde{\varphi}(0)} : -1 \right) \right], \qquad (3.9)$$

where $\delta_{P,0}$ reflects the projection onto the zero momentum subspace and we have separated out the zero mode from the field:

$$\varphi(x,\tau) = \varphi_0(\tau) + \tilde{\varphi}(x,\tau) \equiv \varphi_0(\tau) + \varphi_R(x,\tau) + \varphi_L(x,\tau) + \varphi_R^\dagger(x,\tau) + \varphi_L^\dagger(x,\tau);$$

$$\varphi_0(\tau) \;=\; \phi_0 - i\frac{8\pi\tau}{L}\Pi_0. \tag{3.10}$$

In the above, normal ordering is defined as

$$: e^{b\varphi(x,\tau)} :\equiv\; e^{b\phi_0(\tau)} e^{b\varphi_R^\dagger(x,\tau)} e^{b\varphi_R(x,\tau)} e^{b\varphi_L^\dagger(x,\tau)} e^{b\varphi_L(x,\tau)} \;\;, \tag{3.11}$$

where

$$\varphi_R(x,\tau) = \sum_{n>0} \sqrt{\frac{2}{|n|}} a_n e^{ik_n x - k_n \tau}, \quad \varphi_L(x,\tau) = \sum_{n<0} \sqrt{\frac{2}{|n|}} a_n e^{ik_n x - |k_n|\tau} \;\;. \tag{3.12}$$

The matrix elements of the chiral parts of $: e^{b\tilde{\varphi}(x)} :$ admit a closed analytic expression

$$\begin{aligned} \left\langle n_1, \ldots, n_k \left| e^{b\varphi_R^\dagger} e^{b\varphi_R} \right| m_1, \ldots, m_k \right\rangle \;\; &= \\ = \prod_{q=1}^{k} \frac{1}{\sqrt{n_q! m_q!}} &\left\{ \sum_{n_{1q}=0}^{\min(n_q,m_q)} n_{1q}! \binom{n_q}{n_{1q}} \binom{m_q}{n_{1q}} \left(b\sqrt{\frac{2}{q}}\right)^{n_q+m_q-2n_{1q}} \right\} \end{aligned} \tag{3.13}$$

where the chiral state vector $|n_1, \ldots, n_k\rangle$ is a normalized state having n_q right-moving particles with momentum $\frac{2\pi q}{L}$ for each $q \in \{1, \ldots, k\}$. Using this expression together with the knowledge of the (numerical) zero mode matrix elements

$$\langle m | e^{b\varphi_0} | n \rangle \;\;,$$

we can construct the full matrix elements of H_{int}.

3.2.4 Methods of diagonalization

Once we have collected all the matrix elements of both H_0 and H_{int}, for any truncated space we have a finite dimensional matrix to diagonalise. To find its eigenstates and eigenvalues we can proceed in two ways:

- We can use exact diagonalization perhaps augmented with a numerical renormalization group. This latter procedure will be discussed further in Section 3.3.4.
- We can also use iterative methods that, thanks to their reverse communication protocols, do not require us to store the full Hamiltonian in memory. The only cost that we need to pay is that we are restricted here to computing the low-lying eigenvalues. However for our purposes here this is not a limitation. Using the Jacobi-Davidson method and exploiting the tensor product structure (i.e. eq. (3.5)) of the Hilbert space, we can treat matrices arising from truncation

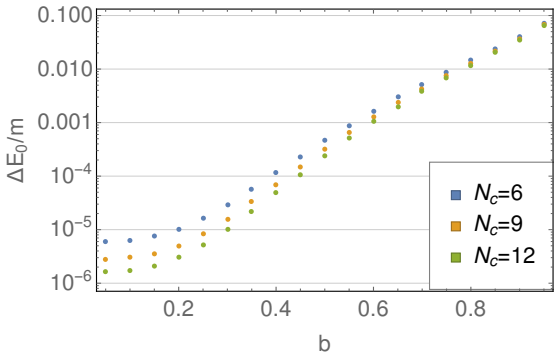

(a) E_{gs} at different b's.

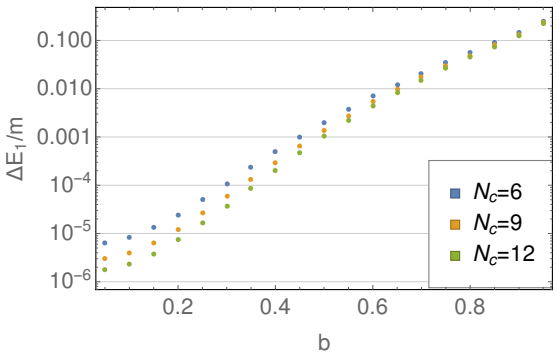

(b) $E_{1,exc}$ at different b's.

Figure 3.1: Here we present results on the behavior of the ground state energy (a) and first excited state (b) as a function of b at fixed $M_{ShG}L = 1$. We present results for 3 different values of the cutoff ($N_c = 6, 9, 12, N_{ZM}$=24). The energies are normalized with respect to the free mass m. We have plotted the results as differences between the numerical values and the expected exact values from TBA.

parameters of up to ($N_c = 20, N_{ZM} = 24$), corresponding to a truncated Hilbert space of size approximately 2.4×10^7. We elaborate on the usage of the tensor product structure in Appendix G. We specifically use the JDQMR_ETOL algorithm provided in the package PRIMME [146, 147].

3.3 Measurement of finite volume spectrum and mass relation

We present our numerical results with the aim to answer the following specific questions:

1. What is the performance of the TSM applied to the ShG model? What level of precision can be achieved below the self-dual point (compared directly to finite volume theoretical quantities), and how does it depend on the coupling b and the volume L?

2. Is there a simple extrapolation that robustly improves the accuracy of the numerics? How much does it improve?

3. Not assuming any special properties of the ShG model (in other words, relying only on standard TSM analysis), to what extent can the conjectured infinite volume parameters (mass, vacuum energy density, S-matrix) be reproduced?

4. How effectively does TSM reproduce the one-point functions of vertex operators? In particular, what happens when we probe them outside the region of validity of the FLZZ formula, eq. (2.92)?

The following results are organized according to the four points listed above.

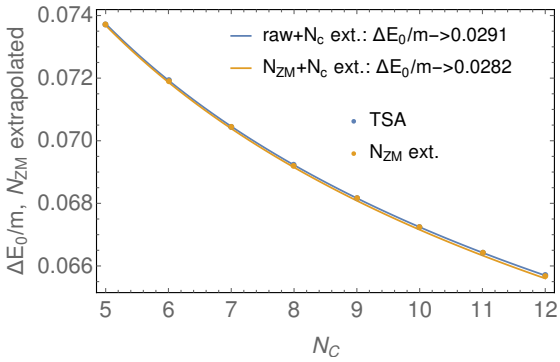

(a) Raw TSM ($N_{zm} = 42$) and N_{zm}-extrapolated values of E_{gs} as a function of N_c.

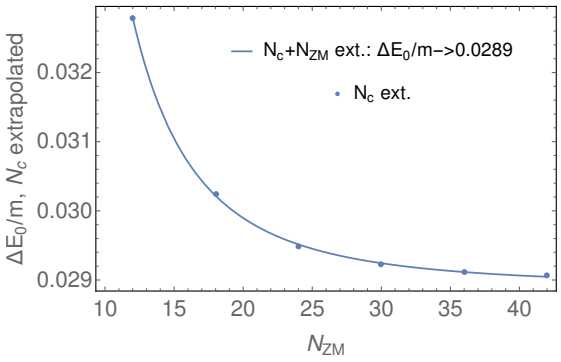

(b) Values of E_{gs} after extrapolation in N_c, as a function of N_{zm}.

Figure 3.2: Here we present the two extrapolation schemes for the cutoffs N_c and N_{ZM}. We perform the extrapolation for data of the ground state energy at $b = 0.95$, $M_{ShG}L = 1$). In a) we first extrapolate in N_{ZM}, plotting the results at each N_c, then performing a further extrapolation in N_c. The results of this extrapolation is shown in the legend. In b) we reverse the order of extrapolations. Note that the data has a much stronger dependence on N_c than on N_{ZM}.

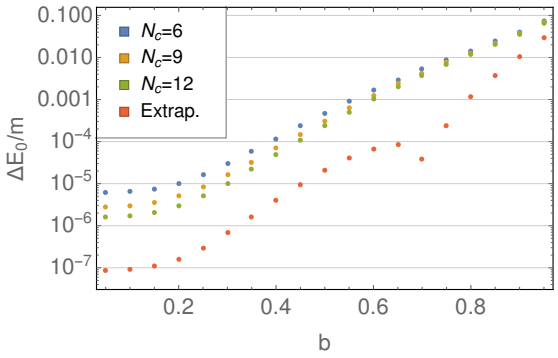

(a) Raw TSM data together with extrapolation in N_c for E_{gs} at different b's.

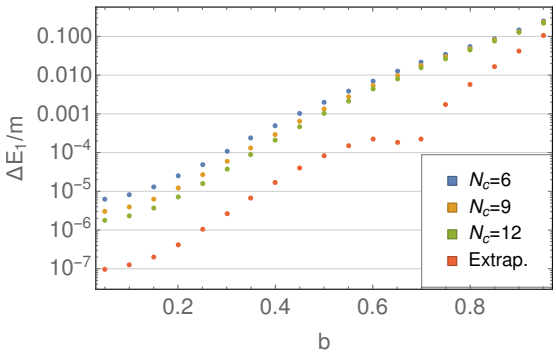

(b) Raw TSM data together with extrapolation in N_c for E_{exc} at different b's.

Figure 3.3: The behaviour of the N_c-extrapolated TSM data as a function of b.

3.3.1 Finite volume spectrum

Let us begin with the finite volume spectrum. In Fig. 3.1 we present results for the ground state energy and the first excited state energy for different values of b at fixed volume $M_{ShG}L = 1$, where M_{ShG} is the physical mass. The computations were done using different chiral cut-offs N_c, at a fixed zero mode cutoff N_{ZM}. On the other hand, we have also calculated the corresponding quantities by numerically integrating the (excited state) TBA equations eq. (2.82). We consider the difference between TSM and TBA (taking into account the vacuum energy density (2.77)) to be the error of the former. The energy levels are normalized with respect to the free mass m defined in eq. (2.65) and we plot the differences between the TBA computations and the TSM data

on a log scale. The largest cutoff, $N_c = 12$, $N_{ZM} = 24$, at which data are presented has been obtained using a truncated Hilbert space of size 3×10^5.

It is apparent that the errors are slightly different for the ground state and the excited state, but the overall pattern is very similar: for small b, even a raw cutoff can produce precise results, and a reasonable increase in the cutoff N_c actually has a strong positive effect on the precision. On the other hand, the error increases exponentially in increasing the coupling constant b and, at the same time, the precision becomes less sensitive to the cutoff. In the immediate vicinity of the self-dual point, the error essentially becomes $O(1)$, indicating that the naive TSM is limited to a region below the self-dual point. As a first step to improve the results, we propose an (at this point 'empirical') extrapolation scheme, which involves fitting the numerical results with power laws in N_c and N_{ZM}.

In Fig. 3.2, we present two implementations of this power law fitting at $b = 0.95$, $M_{ShG}L = 1$. In the first, presented in Fig. 3.2(a), we first extrapolate in zero mode number N_{ZM} and then perform a further extrapolation in N_c. Fig. 3.2(a) then shows the result of this first extrapolation in N_{ZM} at each N_c. We see that the results of this extrapolation differ little from the raw data determined at $N_{ZM} = 42$. Having done this, we then perform a separate extrapolation with respect to the chiral cutoff N_c. The result, reported in the legend of Fig. 3.2(a) is about a 3% error in units of the free mass m. We also perform the same extrapolation in N_c for the raw data obtained at $N_{ZM} = 42$. The result is essentially identical. In Fig. 3.2(b), we consider the second implementation. This is obtained by performing the two extrapolations in the opposite order but for the same set of input data. Shown in Fig. 3.2(b) is the result of the first extrapolation in N_c at fixed N_{ZM}. The second extrapolation in N_{ZM} leads to results essentially the same as the results reported with the first scheme.

We now consider TSM data over a range of values of b. Having seen that the data is essentially converged at N_{ZM} sufficiently large, we work at fixed N_{ZM} and only consider extrapolations in N_c. In particular we use the following simple choice for the fitting

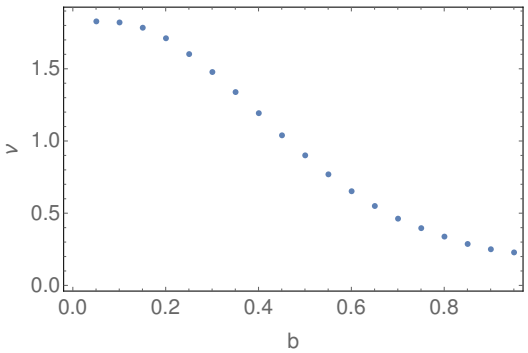

Figure 3.4: Power law exponents as a function of b for the extrapolation in N_c given in eq. (3.14).

function:

$$E(N_c) \;=\; E_{\text{extrap}} + d \cdot N_c^{-\nu} \;\; . \tag{3.14}$$

In Fig. 3.3 we report our results for the ground state and first excited state energies at $M_{ShG}L = 1$. We show the raw TSM data at different N_c together with the extrapolated values (red dots). In most cases, the extrapolation improves the numerical data by at least an order of magnitude. We note that the cusp-like feature appearing in the extrapolated data is due to a sign change of the extrapolated error, of which we take the absolute value to produce the log-scale plot. The precise position of the cusp is also volume-dependent. In Fig. 3.4 we present the fitting exponent $\nu(b)$ (see eq. (3.14)) coming from these extrapolations. We see that at small b the exponent is large indicating that the data is rapidly converging in N_c while at values of b approaching the self-dual point, the exponent becomes much smaller. We will provide a partial explanation for the behavior of the power law in Section 3.6.

Having presented results as a function of b, we now consider the spectrum as a function of L. In Fig. 3.5 we present data for the low-lying finite volume spectrum (after extrapolation in N_c) after subtraction of the exact vacuum energy density (2.77) for two different couplings, $b = 0.4$ and $b = 0.8$. The TSM data is plotted against the numerical solution of the exact TBA equations (shown in the plots with continuous curves). It is apparent that TSM follows very closely the theoretical excited-TBA data for $b = 0.4$, while small discrepancies become visible at $b = 0.8$, especially at larger volumes. Contrary to the previous plots, here we opted for normalizing the energies with respect to the physical mass M_{ShG}, owing to the emphasis of finite volume corrections presented in these plots.

We close the first part of this subsection with a contour plot (Figure 3.6), which shows the order of magnitude of errors as a function of both b and the dimensionless volume $M_{ShG}L$ at the same time. The error can be smaller than 10^{-8} in the small-L region of the perturbative sector, and remains below 10^{-4} over a wide range of couplings and volumes. On the other hand, the error increases exponentially as either the volume or the coupling is increased. We note that the apparent 'islands' on the top and the 'valley' around $M_{ShG}L = 9$ are due to the same sign-changing phenomenon that causes the cusps in Fig. 3.3.

3.3.2 Determination of mass, bulk energy and S-matrix

In this subsection, we present and discuss the TSM numerical results for the particle mass, M_{ShG}, the bulk energy density, and the S-matrix of the ShG model.

Physical Mass: We have measured the physical mass M_{ShG} of the ShG model through taking the difference of the two lowest energy levels. Ideally, this difference converges to

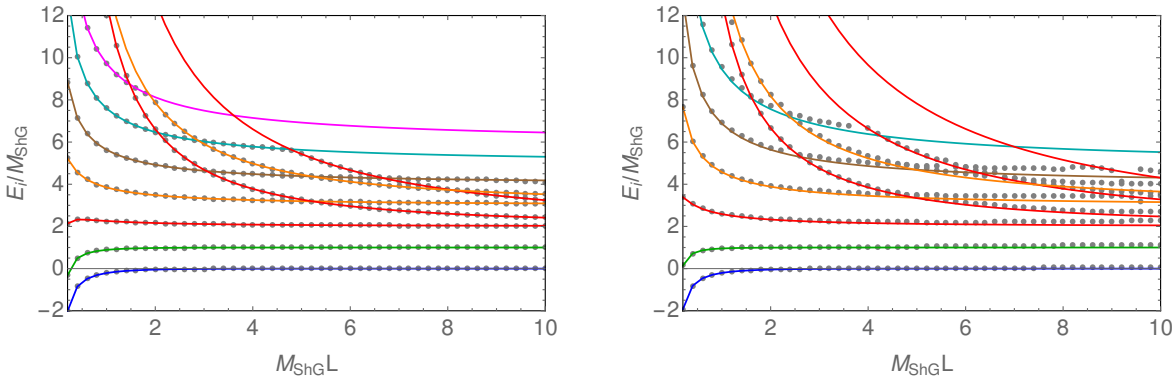

(a) Energy levels at $b = 0.4$.

(b) Energy levels at $b = 0.8$.

Figure 3.5: Here we present TSM data (dots) for the first 8 energy levels after N_c extrapolation as functions of the dimensionless volume $M_{ShG}L$ in the zero momentum sector. The vacuum energy $\mathcal{E}_0$ is subtracted and energies are normalized with respect to the mass M_{ShG}. The color coding of the TBA (solid) curves is as follows: the ground state is depicted in blue, the one-particle state in green, two-particle states in red, three-particle states in orange, four-particle states in brown, five-particle states in teal, and six-particle states in pink.

the physical mass in the $L \to \infty$ limit. In practice, for large volumes, truncation effects produce an overestimate for the mass. On the other hand, small-volume effects also produce an overestimate. As a consequence, we determine the mass as the minimum of the volume-dependent energy difference.

The results are shown as the function of b in Fig. 3.7(a) and (c). In (a) we plot the TSM data (extrapolated) against the theoretical curve expected from eq. (2.89). In (c) we plot, on a logarithm scale, the absolute value of the differences between the measured mass and the same theoretical value. For comparison here, we show the differences of the perturbative expansions of the exact mass formula, truncated at various orders with their exact counterpart. This gives an idea of the relative precision of TSM with respect to a perturbative expansion. We see that for intermediate couplings, the TSM outperforms a 5-loop (up to and including $O(b^{10})$) perturbative expansion of the mass, coming close to 6-loop accuracy. Approaching the self-dual point, the region of viable TSM data shrinks to a region in $M_{ShG}L$ where the exponential corrections become relevant and therefore the standard TSM methods are not available. (Of course, in the sinh-Gordon model everything is supposedly known about these exponential corrections, but for now we intentionally opt for neglecting any *a priori* knowledge on the integrability of the model.)

Vacuum energy density: Let us now turn our attention to the vacuum or bulk energy density, $\mathcal{E}_0$. The measurement of this quantity proceeds by measuring the slope of the ground state energy $E_0(L) \approx \mathcal{E}_0 L$. For small L, this function enjoys a conformal L^{-1} dependence up to logarithms, and is monotonically increasing. For intermediate

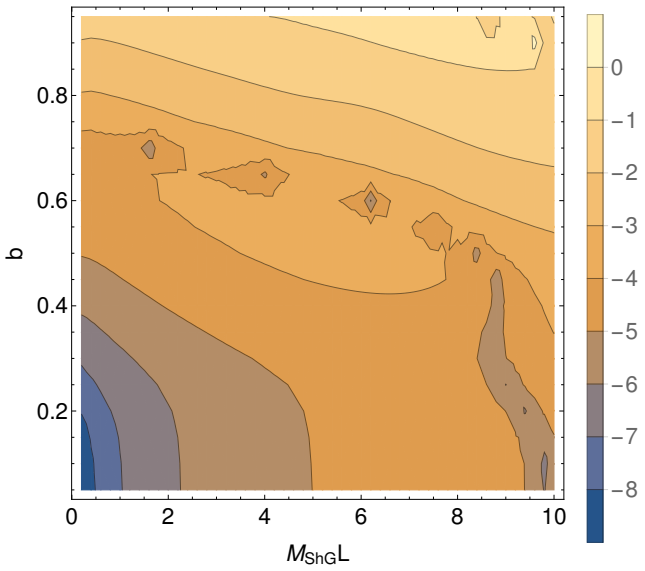

Figure 3.6: Base 10 logarithm of the normalized differences between the TSM ground state energies and their TBA counterparts for different couplings and volumes.

volumes, it is essentially linear. The bulk energy needs to be measured in this linear region since for larger volumes, truncation errors are expected to dominate. Therefore the best first approximation to $\mathcal{E}_0$ is the minimum of the numerical derivative of $E_0(L)$. In a general field theory, the leading exponential (Lüscher) correction to the ground state energy is of the form

$$E_0(L) \;=\; L\mathcal{E}_0 - M \int_{-\infty}^{\infty} \frac{du}{2\pi} \cosh u \, e^{-ML\cosh u} \quad . \tag{3.15}$$

Substituting the mass measured previously and subtracting this correction from the numerical ground state energy improves the precision. The results as a function of b are shown in Fig. 3.7(b) and (d) in the same fashion as presented in (a) and (c) of this same figure for the physical mass. Like with Fig. 3.7(c), we show the differences between a finite order Feynman perturbative computation and the exact value for orders b^4 through b^{14}. Note that the convergence radius of the series for $\mathcal{E}_0$ is only $b_{\max} = 1/\sqrt{2}$ as opposed to 1 for the mass, M_{ShG}.[1] We thus only show the perturbative curves up to this point in b. Conventional TSM is able to measure the bulk energy with an error of 10^{-3} even in this strongly coupled region.

***S*-matrix:** Finally, let us consider the measurement of the S-matrix from TSM data. For asymptotically large volumes, two-particle states with zero overall momentum (each particle having rapidity $\pm\theta$) are quantized by the requirement that the multi-particle

[1] This can be seen from the analytic structure of eq. (2.77).

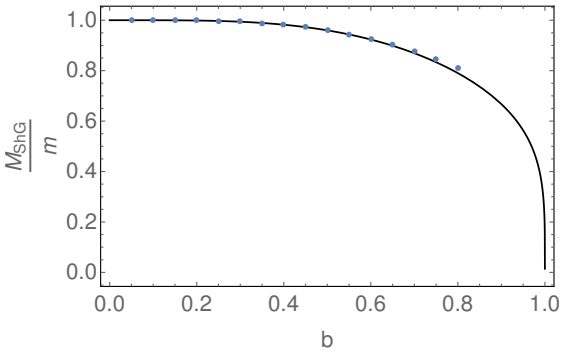

(a) Measured versus theoretical masses, normalized with respect to m.

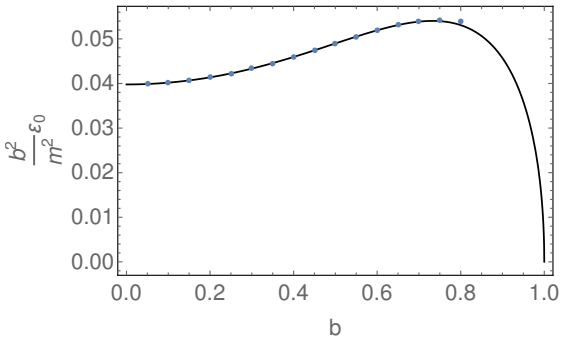

(b) Measured versus theoretical vacuum energies, normalized with respect to $\frac{m^2}{b^2}$.

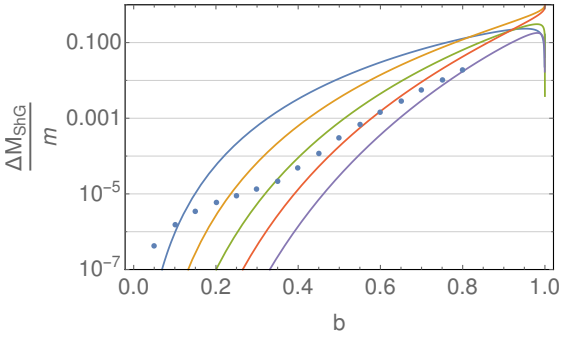

(c) Error in TSM determination of normalized masses.

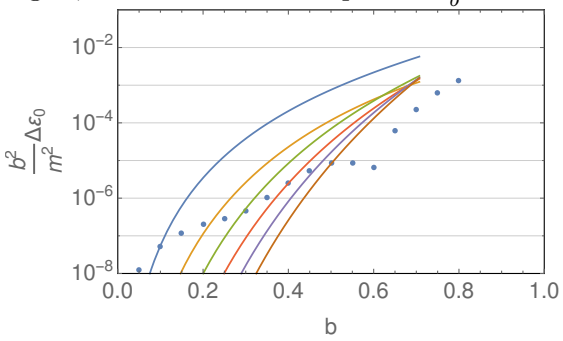

(d) Error in TSM determination of normalized vacuum energies.

Figure 3.7: Measured mass (a) and vacuum energy (b) from TSM (blue dots) plotted against the solid theoretical curve. In panels (c) and (d), the error in the TSM results (i.e. the normalized difference between the TSM results and the theoretical values) are presented. We also present the differences between a Feynman perturbative expansion in b with the exact formula. Shown are differences for orders b^4 (blue), b^6 (orange), b^8 (green), b^{10} (red), b^{12} (purple), and b^{14} (brown).

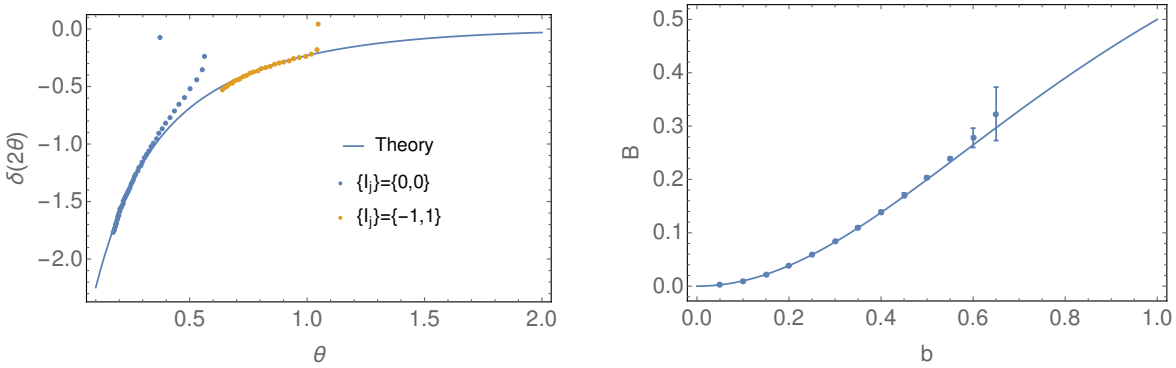

(a) Measured versus theoretical phase shifts obtained from the $n = 0$ and $n = 1$ two-particle states at $b = 0.4$.

(b) Measurement of the parameter B of the S-matrix as a function of b.

Figure 3.8: Measurement of the S-matrix.

wave-function be one-valued on the cylinder

$$e^{iM_{ShG}L\sinh\theta}\,S(2\theta) \;=\; 1 \;\;, \tag{3.16}$$

which, after taking the logarithm, provides the Bethe-Yang quantization condition

$$\delta(2\theta) + M_{ShG}L\,\sinh(\theta) \;=\; 2\pi n, \quad n \geq 0, \tag{3.17}$$

where we have introduced the phase shift $S(\theta) = e^{i\delta(\theta)}$. Eq. (3.17) is a quantization condition which determines the rapidity θ. In fact, it is the large-volume limit of the TBA quantization condition (2.81) for the state $\{I_1 = -n, I_2 = n\}$. Once this quantity is known, we have access to the energy of the two-particle state since, up to exponential corrections, the energy is a sum of one-particle terms

$$E_{\text{largeL}} \;=\; L\mathcal{E} + M_{ShG}\sum_{j=1}^{k}\cosh(\theta_j) \;\;. \tag{3.18}$$

We focus on the lowest energy two-particle states in the zero-momentum sector by taking $n = 0, 1$ in (3.17). Numerically, for large enough volumes, this corresponds to the fourth lowest energy level. In this domain, we express the rapidity θ in terms of the energy difference between the two-particle state and the vacuum:

$$\theta \;=\; \text{Arcosh}\left(\frac{E - E_0}{2M_{ShG}}\right) \;\;. \tag{3.19}$$

Thus we can directly measure the phase shift appearing in eq. (3.17). The result extracted from the $n = 0$ and $n = 1$ two-particle states is shown on Fig. 3.8(a).

In the following, we have assumed that the S-matrix indeed consists of a single

CDD-like factor, namely

$$S(\theta) = \frac{\sinh\theta - i\,\sin\pi B}{\sinh\theta + i\,\sin\pi B} \ , \tag{3.20}$$

but we have treated the quantity B in the S-matrix amplitude as a parameter to be fitted to the numerical data. To perform this fitting, we have only utilized our $n = 1$ TSM data in region of L where no level crossings occur. The numerical phase shift obtained in this way is more robust than that coming from the $n = 0$ state. We estimate the phase shift by two methods. In the first method, we increase the parameter B until one of the numerically determined phases coincide with the theoretical curve. The value of B at this point is the estimate. In the second method, we instead look at the two largest rapidities available from the $n = 1$ data. We then find the value of B for which eq. (3.20) best approximates the values of $\delta(\theta)$ at these rapidities. The difference of the results of the two methods is considered to be the error of the measurement.

We will return to the measurement of the above quantities by an alternative method in Section 3.5.5.

3.3.3 One-point functions

TSMs can be used to measure one-point functions (either on the vacuum or on exited states) by sandwiching Schrödinger-picture operators between the numerically obtained eigenstates. Since the method directly uses the eigenvectors, the resulting precision is inevitably more limited as compared to the energy spectrum. Nevertheless, it is possible to compare the numerical estimate of the VEVs of the exponential operators to their theoretical FLZZ formula eq. (2.92) in a wide region.

Beyond the usual b and L-dependence, the convergence of the VEV of the exponential operators, $\langle e^{a\varphi}\rangle$, heavily depends on the exponent a of the operator. We have again tried to control the cutoff dependence of the one-point functions by power-law fits on the chiral cutoff N_c. The functional form eq. (3.21) is helpful as long as b is small enough. Generally the cutoff extrapolation becomes less stable as the coupling or the volume is increased. For larger couplings, we have found it advantageous to use a sum of two power laws as a fitting function:

$$E(N_c) = E_{\text{extrap}} + d_1 \cdot N_c^{-\nu_1} + d_2 \cdot N_c^{-\nu_2}. \tag{3.21}$$

We show the dimensionless quantity $\mathcal{G}(a)$ as a function of a in Fig. 3.9, for two different couplings and at $L = 6$. For small to moderate a, the extrapolated numerics agrees with the FLZZ formula to at least to 1%. Regardless of the coupling, the error (and the cutoff dependence) always becomes significant before reaching the first pair of zeros (located at the Seiberg bounds $\pm Q/2$) of the analytic VEV formula. For larger couplings, it is possible to achieve higher precision by performing the computations at

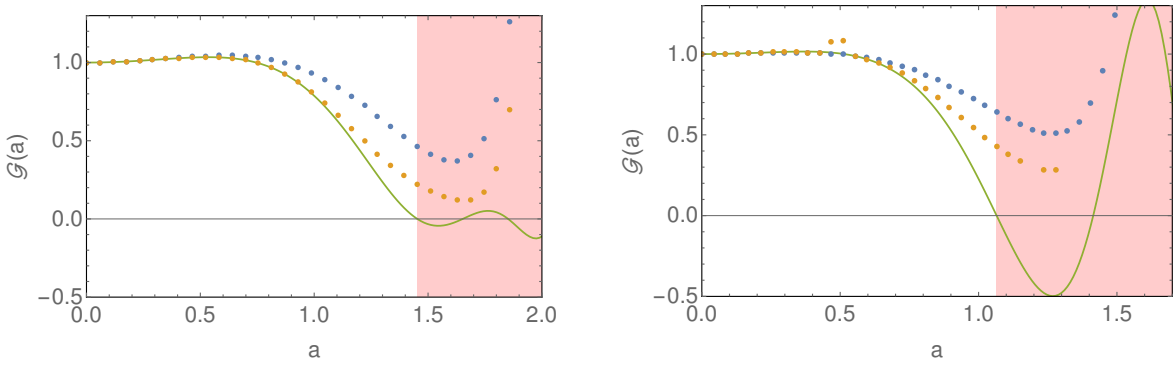

(a) Expectation values for $b = \frac{2}{\sqrt{8\pi}} \approx 0.4$.

(b) Expectation values for $b = \frac{4}{\sqrt{8\pi}} \approx 0.8$.

Figure 3.9: Vacuum expectation values for $\mu_{ShG} = 0.1, L = 6$. The solid green curve is predicted by the FLZZ formula. Raw TSM results are shown with blue dots, while their power-extrapolated counterparts are shown orange. The $a > Q/2$ (unphysical) domain is highlighted with red.

a small volume. However, in this case one needs to take into account the finite volume corrections of the VEV, which are available through the LeClair-Mussardo formula [84] in the form of an infinite series, as recalled in eq. (2.126)

$$\mathcal{G}(a, L) = \mathcal{G}(a) \left(1 + \sum_{n=1}^{\infty} \frac{1}{n!(2\pi)^n} \int \prod_{i=1}^{n} \frac{d\theta_i}{1 + e^{\epsilon(\theta_i)}} C_n^a(\{\theta_i\}) \right), \tag{3.22}$$

where C_n^a is the connected evaluation of the n-particle diagonal form factor for the operator $e^{a\varphi}$, defined in eq. (2.127).

In Fig. 3.10, we show the numerical results for $L = 2$. Exploiting finite volume corrections extends the availability of TSM estimates of $\mathcal{G}(a)$ up to $b \approx 0.8$, as long as $a \ll Q/2$.

3.3.4 The problem of analytical improvement

In the previous section, we presented a series of results for various quantities in the ShG model as measured with TSM. We showed in general that as one moves towards the self-dual point, the quality of the results found using TSM deteriorates in comparison to the available exact predictions. This deterioration is largely due to the presence of finite cutoff effects. There are a standard set of renormalization group-like techniques that are employed in ameliorating the effects of a finite cutoff. We show in this section that these strategies are not practical for the sinh-Gordon model close to the self-dual point. However this failure is instructional and point the way to a better understanding of some of the peculiarities of the model and new strategies to tackle them. The strategies take two forms: analytical and numerical. We discuss the analytic form first.

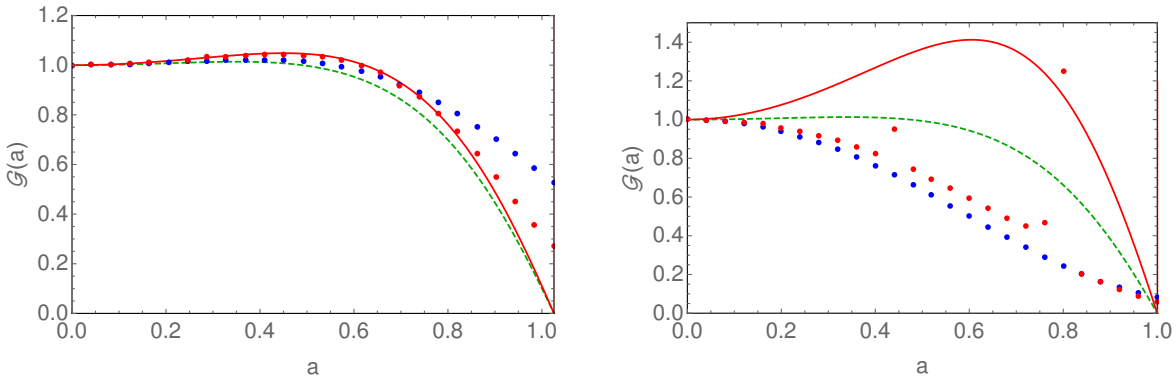

(a) Expectation values for $b = \frac{4}{\sqrt{8\pi}} \approx 0.8$.

(b) Expectation values for $b = \frac{5}{\sqrt{8\pi}} \approx 0.99$.

Figure 3.10: Vacuum expectation values for $\mu_{ShG} = 0.1, L = 2$. Raw TSM results are shown with blue dots, while their power-extrapolated counterparts are depicted with red dots. The $L \to \infty$ theoretical value of the VEV is plotted as a dashed green line. The finite volume corrected version involving up to 2nd order terms in the Leclair-Mussardo series is shown as a red solid curve.

3.3.4.1 Analytic renormalization group

In presenting how one can analytically take into account the effects of states above the cutoff, we follow the discussion in Ref. [145]. The first step is to divide the Hilbert space, $\mathcal{H}$ into two parts: $\mathcal{H} = \mathcal{H}_l \oplus \mathcal{H}_h$. Here $\mathcal{H}_l$, the low energy Hilbert space, consists of all states of the form

$$\mathcal{H}_l = \Big\{ a^\dagger_{n_1} \dots a^\dagger_{n_k} |0\rangle \otimes a^\dagger_{-m_1} \dots a^\dagger_{-m_l} |0\rangle \otimes |s\rangle; \sum_{i=1}^{k} n_k \leq N_c, \quad \sum_{m=1}^{l} n_l \leq N_c; \quad s = 1, \cdots, N_{ZM} \Big\}, \tag{3.23}$$

while $\mathcal{H}_h$, the high energy part of the Hilbert space consists of states where

$$\mathcal{H}_h = \Big\{ a^\dagger_{n_1} \dots a^\dagger_{n_k} |0\rangle \otimes a^\dagger_{-m_1} \dots a^\dagger_{-m_l} |0\rangle \otimes |s\rangle \; ; \sum_{i=1}^{k} n_k > N_c \;\; \text{or} \;\; \sum_{m=1}^{l} n_l > N_c; \quad s = 1, \cdots, N_{ZM} \Big\}. \tag{3.24}$$

Here note we have expressed $\mathcal{H}_l$ and $\mathcal{H}_h$ in a way reflective of the tensor nature of the computational Hilbert space (at least as conceived as that of a free massless non-compact boson). We are also working at a fixed number of zero mode states, N_{ZM}, assuming in effect, that this number of zero mode states leads to completely convergent results (an assumption born from our numerics reported in the previous section). In particular the high and low energy parts of the Hilbert space have the same zero mode content.

We can thus write our Hamiltonian in the following manner:

$$H = \begin{bmatrix} H_{ll} & H_{lh} \\ H_{hl} & H_{hh} \end{bmatrix}, \tag{3.25}$$

where H_{ij} $(i, j = h, l)$ corresponds to the Hamiltonian matrix restricted to the two subdivisions of the Hilbert space. If we have an eigenstate

$$\begin{bmatrix} c_l \\ c_h \end{bmatrix}, \tag{3.26}$$

with energy E_*, we can write the Schrödinger equation as

$$\begin{aligned} H_{ll}c_l + H_{lh}c_h &= E_*c_l, \\ H_{hl}c_l + H_{hh}c_h &= E_*c_h. \end{aligned} \tag{3.27}$$

By eliminating c_h from the above set of equations, we have

$$\left(H_{ll} + H_{lh}\frac{1}{E_* - H_{hh}}H_{hl}\right)c_l = (H_{ll} + \delta H)c_l = E_*c_l. \tag{3.28}$$

In doing so, we have reformulated the eigenvalue problem in terms of coefficients of states that live in the low energy Hilbert space alone.

Now we are studying a Hamiltonian of the form $H = H_0 + \mu_{ShG}V$ with V given by

$$V = 2\left(\frac{L}{2\pi}\right)^{2b^2}\int_0^L dx\,[:\cosh b\phi(x):-\cosh(b\phi_0)]\,. \tag{3.29}$$

We can then expand δH in powers of μ_{ShG}, giving

$$\begin{aligned} \delta H &= -\mu_{ShG}^2 V_{lh}\frac{1}{H_0 - E_*}V_{hl} \\ &\quad +\mu_{ShG}^3 V_{lh}\frac{1}{H_0 - E_*}V_{hh}\frac{1}{H_0 - E_*}V_{hl} + O(\mu_{ShG}^4). \end{aligned} \tag{3.30}$$

Introducing the (imaginary) time dependence of operators in the interaction picture,

$$\mathcal{O}(\tau) = e^{H_0\tau}\mathcal{O}(0)e^{-H_0\tau}, \tag{3.31}$$

we can rewrite eq. (3.30) as

$$\delta H = -\mu_{ShG}^2\sum_{c\in\mathcal{H}_h}\int_0^\infty \mathrm{d}\tau\, e^{(E_*-H_0)\tau}V(\tau)|c\rangle\langle c|V(0) + O(\mu_{ShG}^3)$$

$$\equiv \quad \delta H_2 + O(\mu_{ShG}^3). \tag{3.32}$$

This correction turns out to be singular for $b \geq \frac{1}{\sqrt{2}}$. From here on we introduce *another* chiral cutoff $\Lambda > N_c$. We are going to focus upon the most singular (in Λ) contribution to δH_2 and so drop from V in eq. (3.29) the term proportional to $\cosh(b\phi_0)$. Of course if we were interested in using δH_2 in a quantitative fashion, we would need to include this term.

We can readily analyze δH_2 by rewriting the partial resolution of the identity as an Euclidean correlator and exploiting the local approximation (performing a series expansion in τ and the space coordinate difference around 0 and keeping the leading order). This is equivalent to approximating the product $V(\tau)V(0)$ with the leading order of the corresponding OPE. that involves only the states from the high energy part of Hilbert space, $\mathcal{H}_h$. δH_2 satisfies

$$\delta H_2^{(\text{local})} \approx -\mu_{ShG}^2 L^2 \left(\frac{L}{2\pi}\right)^{4b^2} \sum_{n=N_c+1}^{\Lambda} S^2\left(n, 2b^2\right) \delta_P \left(\frac{2}{H_0 + \frac{4\pi n}{L} - E_*} : \cosh 2b\varphi :\right) \tag{3.33}$$

where we have defined

$$S(n,a) \equiv \frac{1}{n!}\frac{\Gamma(a+n)}{\Gamma(a)}. \tag{3.34}$$

and $(\Lambda \to \infty)$.

In eq. (3.33), δ_P enforces momenta conservation. Here the relevant OPE is given by

$$\begin{aligned} &: \cosh(b\phi(x_1,\tau_1)) :: \cosh(b\phi(x_2,\tau_2)) : \quad = \\ &\frac{1}{2}|z_1 - z_2|^{4b^2}\mathbb{1} + \frac{1}{4}|z_1 - z_2|^{-4b^2} : e^{2b\phi(x_2,0)} : + \frac{1}{4}|z_1 - z_2|^{-4b^2} : e^{-2b\phi(x_2,\tau_2)} : \end{aligned} \tag{3.35}$$

where

$$z_{1,2} = e^{-\frac{2\pi}{L}(\tau_{1,2} + i x_{1,2})}, \quad \bar{z}_i = z_i^*. \tag{3.36}$$

We now focus on the part of δH_2 involving the operator $\cosh(2b\phi)$:

$$(\delta H_2)_{ab} = 4\pi^2 \mu_{ShG}^2 \left(\frac{L}{2\pi}\right)^{3+4b^2} \frac{\Lambda^{4b^2-2}}{2-4b^2} (: \cosh(2b\phi) :)_{ab}. \tag{3.37}$$

We can see that this term diverges as $b^2 \to 1/2$ and that furthermore for $b^2 > 1/2$, the correction tends to ∞ as the chiral cutoff, Λ, tends to ∞. This means any strategy to compute corrections to TSM results *perturbatively* due to states coming from above the cutoff fails for values of b close to the self-dual point.

This result is actually worse than the second order result implies. At the third order, we can again use OPEs and find that the most singular third order contribution

to δH_3 goes as

$$(\delta H_3)_{ab} \sim \delta_{P_a,P_b}\mu_{ShG}^3 L^{5+6b^2}\Lambda^{12b^2-4}(:\cosh(3b\phi):)_{ab}. \tag{3.38}$$

Here we see the third order term has a pathological dependence on Λ when $b^2 > 1/3$, even further away from the self-dual point. We can continue this to n-th order, finding

$$(\delta H_n)_{ab} \sim \delta_{P_a,P_b}\mu_{ShG}^n L^{2n-1+2b^2 n}\Lambda^{2(n^2-n)b^2-2n+2}(:\cosh(nb\phi):)_{ab}. \tag{3.39}$$

Here we see that the situation becomes worse and worse as we go to higher and higher perturbative order: at n-th order, the correction diverges as $\Lambda \to \infty$ for $b^2 > 1/n$.

From this analysis we can see that the perturbative series developed here is essentially a small-volume expansion in the parameter L^{2+2b^2}. This implies that the ground state energy does not have a proper expansion in powers of L^{2+2b^2} around the CFT limit $L \to 0$. We also want to remark that the pathologies identified here for the ShG do not apply to its analytically continued cousin, the sine-Gordon model. In the sine-Gordon, this perturbative analysis will give rise to divergences for $b^2 > 1/2$. However these divergences occur in the identity channel in terms of the OPE of eq. (3.35). This means the most singular part of δH_n is proportional to $\mathbb{1}$ and so leads only to corrections to the energies that are state independent, i.e. energies measured relative to the ground state energy are unaffected. Alternatively one can add a single counterterm to the sine-Gordon Hamiltonian to remove this divergent behavior.

As we have stated, in this section we have focused on the leading order singularity at each in perturbative theory as determined by the OPEs. However it is not difficult to determine the subleading divergences. At order n, one can write $(\delta H_n)_{ab}$ as

$$(\delta H_n)_{ab} \sim \delta_{P_a,P_b}\mu_{ShG}^n L^{2n-1+2b^2 n} \sum_{k=n,n-2,n-4,\cdots,n\mathrm{mod}2} c_k(b^2)\Lambda^{2(k^2-n)b^2-2n+2} : \cosh(kb\phi) :_{ab}, \tag{3.40}$$

where $c_k(b^2)$ is some numerical coefficient. There are further singular contributions from descendants. We thus see that not only the leading terms are problematic. We see that the operators $: \cosh(kb\phi) :$ have diverging coefficients (as $\Lambda \to \infty$) once $k^2 > n + (n-1)/b^2$. In Section 3.6 we will consider this problem in further detail and offer a circumvention to the above complications.

3.4 Massive basis

The perturbed dilatation operator defining sinh-Gordon theory on the plane has the form

$$D^{(\mathrm{shG})} = L_0 + \bar{L}_0 + \mu_{ShG} \int_C dz \left(\mathcal{V}_b^{(pl)}(z, z^*) + \mathcal{V}_{-b}^{(pl)}(z, z^*) \right). \tag{3.41}$$

Mapped to the cylinder, this gives rise to the Hamiltonian

$$H^{(\mathrm{shG})} = H_{\mathrm{cyl}}^{(0)} + \mu_{ShG} \left(\frac{L}{2\pi} \right)^{\frac{b^2}{4\pi g}} \int_0^L dx : e^{b\varphi(x,0)} : + : e^{-b\varphi(x,0)} : . \tag{3.42}$$

The spatial integration can easily be carried out at the cost of imposing momentum conservation explicitly, symbolized by the presence of δ_P. Because we are interested in making contact with the analysis of the sinh-Gordon as a massive perturbed boson, we add and subtract at the same time an auxiliary mass term

$$\begin{aligned} H^{(\mathrm{shG})} &= H_{\mathrm{aux}}^{(m)} + \mu_{ShG} L \left(\frac{L}{2\pi} \right)^{\frac{b^2}{4\pi g}} \delta_P \left(: e^{b\varphi(x,0)} : + : e^{-b\varphi(x,0)} : \right) - \frac{gm^2}{2} L \delta_P : \varphi^2(0,0) :; \\ H_{\mathrm{aux}}^{(m)} &\equiv H_{\mathrm{cyl}}^{(0)} + \frac{gm^2}{2} L \delta_P : \varphi^2(0,0) : . \end{aligned} \tag{3.43}$$

$H_{\mathrm{aux}}^{(m)}$ is the same type of Hamiltonian as $H_{\mathrm{cyl}}^{(m)}$ of eq. (2.15). After a Bogoliubov transformation, it can be rewritten as

$$H_{\mathrm{aux}}^{(m)} = \sum_{n=-\infty}^{\infty} \omega_n a_n^\dagger a_n + \mathcal{E}_0^{(m)} L + E_0^{(m)}(m, L) - \frac{m^2 L}{4\pi} \ln \left(\frac{L}{2\pi} \right). \tag{3.44}$$

We now perform the same Bogoliubov transformation on the remaining terms of eq. (3.43):

$$\begin{aligned} U^\dagger \delta_P : \varphi^2(0,0) : U &= \delta_P : \varphi^2(0,0) :_m + \frac{1}{2gmL} + \frac{1}{2Lg} \sum_{n \neq 0} \left(\frac{1}{\omega_n} - \frac{1}{|k_n|} \right); \\ U^\dagger \delta_P : \cosh(b\varphi(0,0) : U &= e^{\frac{b^2}{4gmL}} e^{-\frac{b^2}{4gL} \sum_{q \neq 0} \left(\frac{1}{|k_q|} - \frac{1}{\omega_q} \right)} \delta_P : \cosh(b\varphi(0,0)) :_m . \end{aligned} \tag{3.45}$$

Here the normal ordering $::_m$ indicates the normal ordering is being done w.r.t. the massive oscillator modes. The sum appearing in the above is evaluated in Appendix C.1 to be

$$S_1 \equiv \sum_{n \neq 0} \left(\frac{1}{\omega_n} - \frac{1}{|k_n|} \right) = 2L\rho(mL) - \frac{1}{m} + \frac{L}{\pi} \left(\ln \frac{4\pi}{mL} - \gamma_E \right), \tag{3.46}$$

where $\rho(x)$ is defined as

$$\rho(x) = \int_{-\infty}^{\infty} \frac{du}{2\pi} \frac{1}{(e^{x\cosh u} - 1)}. \tag{3.47}$$

After transformation, our entire Hamiltonian appears as

$$\begin{aligned} H^{(\mathrm{shG})} &= \sum_{n=-\infty}^{\infty} \omega_n a_n^\dagger a_n + \frac{m^2 L}{8\pi} + E_0^{(m)}(m,L) - \frac{m^2 L}{2}\rho(mL) \\ &+\delta_P\left(-\frac{gm^2}{2} L \delta_P : \varphi^2(0,0) :_m + \mu_{ShG} L \left(\frac{2}{m}\right)^{\frac{b^2}{4\pi g}} e^{\frac{b^2}{2g}\rho(mL)} e^{-\frac{b^2\gamma_E}{4\pi g}} : \cosh(b\varphi(0,0)) :_m \right) \end{aligned} \tag{3.48}$$

We are now in a position to establish eq. (2.65). Using the large L limit of ρ, $\lim_{x\to\infty}\rho(x) = 0$, we choose m so that the quadratic term in the second line of eq. (3.48) vanishes, resulting in

$$\mu_{ShG} = \frac{g m^{2+\frac{b^2}{4\pi g}}}{2b^2} \left(\frac{e^{\gamma_E}}{2}\right)^{\frac{b^2}{4\pi g}}. \tag{3.49}$$

It is also possible to perform instead a partial Bogoliubov transformation, affecting the oscillators but keeping the zero mode intact.

$$U_{part}^\dagger \delta_P : e^{b\varphi(0,0)} : U_{part} = e^{-\frac{b^2}{4gL}\sum_{q\neq 0}\left(\frac{1}{|k_q|} - \frac{1}{\omega_q}\right)} \delta_P e^{b\varphi_0} : e^{b\tilde{\varphi}(0,0)} :_m . \tag{3.50}$$

The advantage of this approach is that it essentially retains the double cutoff structure of the chiral basis and is therefore directly comparable to the latter. Using this modification, some improvement can be observed, but the benefit is modest: it is comparable to doubling the dimensions of the chiral oscillator subspace. The results of Section 4.5 are computed this way.

3.5 UV behaviour

In Section 3.3 we argued that a straightforward implementation of analytical RG improvements is hindered because the small volume expansion of energy levels is not perturbative with respect to the parameter $\mu_{ShG} L^{2+2b^2}$. In this section we take a closer look at the small-L UV spectrum. Since the energy of oscillators behave as L^{-1} in the $L \to 0$ limit, one might expect that the UV behaviour of the spectrum is dominated by the quantum mechanics of the zero mode of the field. Using this quantum mechanical picture, a systematic expansion for certain energy levels (more precisely, their corresponding scaling functions) can be developed in terms of $\frac{1}{\ln(\mu_{ShG}L)}$. Alternatively, one can expand the TBA equations, yielding a similar expansion, but involving IR parameters (the physical mass, M_{ShG}, and the S-matrix parameter B). Using the mass-coupling relation and expressing B in terms of the coupling b, we get another

expansion in $\frac{1}{\ln(\mu_{ShG}L)}$, which is however different from the zero mode expansion in subleading orders. As the energies contain an additional $2\pi L^{-1}$ factor relative to the scaling function, the difference between TBA and zero mode energy levels eventually diverge for $L \to 0$ for all $b > 0$.

In Subsection 3.5.3 we derive an effective potential, partially taking into account the effect of oscillators. On one side, we analytically reproduce the exact expansion up to $O(b^{12})$, confirming that the oscillators are able to explain the differences in the log-expansion. On the other side, we show that the TSM numerics significantly outperforms even the numerical solution of the complete effective potential. We then use this fact to provide an alternative measurement of the IR parameters from TSM, combining UV numerics with the small-volume expansion of the TBA.

3.5.1 Semiclassical Reflection Amplitude

In the semiclassical limit $b \to 0$ the small volume behavior of energy levels is dominated by the contribution of the zero mode [69]. For $L \to 0$ the potential walls that the zero mode sees (i.e. the points where the $\mu_{ShG}L^{2+2b^2}\cosh(b\phi_0)$ potential exceeds 1) are far from one another. Then it is sensible to consider first the quantum mechanical problem of a particle reflecting from a single wall:

$$H_{\text{exp}} = \frac{2\pi}{L}\left(2\Pi_0^2 + Me^{b\varphi_0}\right); \quad M = 2\pi\mu_{ShG}\left(\frac{L}{2\pi}\right)^{2+2b^2}. \tag{3.51}$$

Introducing the coordinate representation $\varphi_0 \equiv x$, $\Pi_0 = -i\partial_x$, it is possible to solve the Schrödinger equation

$$H_{\text{exp}}\psi \;=\; E\psi. \tag{3.52}$$

Its general solution is given by modified Bessel functions. Requiring that the wave function vanishes at $x \to \infty$ and evaluating the $x \to -\infty$ asymptotics, we can write the relative phases of the left-moving and right-moving wave as

$$\psi(x) \;\simeq\; e^{iPx} + e^{-iPx}S_{sc}(P); \quad P \;=\; \sqrt{\frac{LE}{4\pi}}\;, \tag{3.53}$$

where the semi-classical reflection amplitude is given as

$$S_{sc}(P) \;=\; \left(-\left(\frac{L}{2\pi}\right)^{-4iPQ}\left(\frac{\pi\mu_{ShG}}{b^2}\right)^{-\frac{2iP}{b}}\frac{\Gamma(1+2iP/b)}{\Gamma(1-2iP/b)}\right); \quad Q = b + \frac{1}{b}. \tag{3.54}$$

This expression is the semi-classical $b \to 0$ limit of the Liouville reflection amplitude (2.44). As the other exponential term is turned on, we can get an approximate quantization condition for the energy levels of the full potential through the quantization

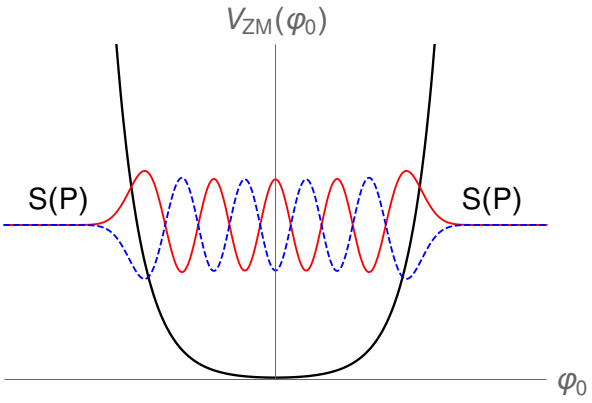

Figure 3.11: Standing waves of the zero mode ruled by the quantization condition eq. (3.55).

condition of the wave number P according to the reflection equation (see Fig. 3.11):

$$S_{sc}\left(P\right)^2 \;=\; 1. \tag{3.55}$$

Denoting $S_{sc}\left(P\right) \;=\; -e^{i\delta(P)}$ and taking the logarithm, the quantization condition (3.55) reads

$$\delta\left(P\right) \;=\; n\,\pi, \quad n \geq 1 \tag{3.56}$$

and the branch cuts of $\delta(P)$ are to be chosen such that it is continuous for real P and $\delta(0) = 0$. The equation for the ground state wave number P_0 is then given by

$$\delta\left(P_0\right) \;=\; \pi \;\;, \tag{3.57}$$

Making a formal expansion of $\delta\left(P\right)$

$$\delta\left(P\right) = \delta_1 P + \delta_3 P^3 + \delta_5 P^5 + \ldots \tag{3.58}$$

we can expand the ground state momentum as a function of $z = \delta_1^{-1}$:

$$P_0 = \pi z - \pi^3 \delta_3 z^4 - \pi^5 \delta_5 z^6 + \ldots, \tag{3.59}$$

where the parameter z reads explicitly

$$z \;=\; -\frac{1}{\frac{4}{b}\gamma_E + \frac{2}{b}\ln\left(\frac{\pi\mu_{ShG}}{b^2}\left(\frac{L}{2\pi}\right)^{2+2b^2}\right)} \;\;. \tag{3.60}$$

Hence, the (semi-classical) ground state energy admits the expansion

$$E_0 \;\;=\;\; \frac{2\pi}{L} b^2\pi^2 \left(\frac{u^2}{2} - \kappa_S u^3 + \frac{3}{2}\kappa_S^2 u^4 - 2\left(\kappa_S^3 - \frac{\pi^2}{3}\zeta\left(3\right)\right)u^5 + \ldots\right);$$

$$\begin{aligned} \kappa_S &= \left(2\gamma_E + \ln\frac{\pi}{b^2}\right); \\ u &= \left[\ln\left(\mu_{ShG}\left(\frac{L}{2\pi}\right)^{2+2b^2}\right)\right]^{-1} . \end{aligned} \tag{3.61}$$

It is important to notice that the terms of this series contain $\log(\mu_{ShG})^{-1}$ factors. Therefore, it is not so surprising if a power expansion in μ_{ShG} around $\mu_{ShG} = 0$ turns out to be pathological.

3.5.2 Quantization condition from the UV limit of TBA

A similar quantization condition exists for the exact energy levels and can be obtained from the small-volume expansion of the TBA system [95]. The derivation of the condition is recalled in Appendix B. In the zero mode sector the UV behaviour of the energy levels is

$$E_n = \frac{2\pi}{L}\left(2P_n^2 - \frac{1}{12}\right) , \tag{3.62}$$

where the quantity P is subject to the quantization condition (2.86):

$$2\,\Theta(P) = n\pi, \quad n \in \mathbb{Z}_{\geq 0} . \tag{3.63}$$

The phase $\Theta(P)$ is given by

$$e^{2i\Theta(P)} = -\bar{b}^{\frac{8iP}{b}}\rho^{-4iPQ(\bar{b})}\frac{\Gamma\left(1+2iP\bar{b}\right)\Gamma\left(1+2iP\bar{b}^{-1}\right)}{\Gamma\left(1+2iP\bar{b}\right)\Gamma\left(1+2iP\bar{b}^{-1}\right)} , \tag{3.64}$$

where

$$\rho = \frac{L}{2\pi}\frac{M}{4\sqrt{\pi}}\Gamma\left(\frac{1-B}{2}\right)\Gamma\left(\frac{2+B}{2}\right) . \tag{3.65}$$

Notice that if we take advantage of the mass-coupling relation and equate $\bar{b} \equiv b$, as it was observed earlier [69, 148], the quantization condition eq. (2.86) can be expressed as

$$S_L^2(P) = 1 , \tag{3.66}$$

where $S_L(P)$ is the Liouville reflection amplitude given in eq. (2.44). This is analogous to the semiclassical formula eq. (3.55) but with the miraculously appearing Liouville reflection amplitude which replaces the quantum mechanical amplitude $S_{sc}(P)$ introduced in Subsection 3.5.1. At the same time, $S_L(P)$ reduces to the semiclassical $S_{sc}(P)$ in the $b \to 0$ limit. Comparing to the quantization condition (3.56) and assuming continuity of energy eigenvalues as functions of b, it is then natural to exclude $n = 0$ from the quantization condition eq. (2.86). Repeating the UV expansion of the energy levels

using the condition eq. (3.66), we get a modified expansion for the ground state energy

$$\begin{aligned} E_0 &= \frac{2\pi}{L} b^2 \pi^2 \left(\frac{u^2}{2} - \kappa_L u^3 + \frac{3}{2}\kappa_L^2 u^4 - 2\left(\kappa_L^3 - \frac{\pi^2}{3}\left(1+b^6\right)\zeta(3) \right) u^5 + \dots \right); \\ \kappa_L &= \left(2\left(1+b^2\right)\gamma_E + \ln \frac{\pi \Gamma\left(b^2\right)}{\Gamma\left(1-b^2\right)} \right); \\ u &= \left[\ln \left(\mu_{ShG} \left(\frac{L}{2\pi} \right)^{2+2b^2} \right) \right]^{-1}. \end{aligned} \tag{3.67}$$

Even though the leading term of this expansion coincides with the semiclassical expansion eq. (3.61), the L^{-1} factor in the front ensures that a difference in any term of the u-expansion leads to a singular discrepancy in the $L \to 0$ limit. This small-volume discrepancy is not trivially accounted for perturbatively. The μ_{ShG}-expansion introduces terms that vanish in the $L \to 0$ limit. On the other hand, in the massive scheme of eq. (3.48), where an expansion in b is natural, the coefficient of the perturbing operator diverges in the $L \to 0$ limit.

In the next subsection, we overcome these obstacles by deriving an effective potential which partially takes into account the corrections appearing in eq. (3.67).

3.5.3 An effective quantum mechanical potential

In the previous subsections, we compared the small-volume expansion of the ground-state energy obtained from the zero mode quantum mechanics to the UV expansion of TBA, and found that they differ by $L^{-1}(\ln L)^{-k}$ type terms. It is then an important question whether the oscillator states neglected in the zero mode calculation can account for these *inverse logarithmic* differences, or is this a sign that we are missing additional terms from the Lagrangian. In any case it is not straightforward to reproduce these terms perturbatively. In the following we derive an effective quantum mechanical potential from the Lagrangian, which provides a more precise description of the UV spectrum of the zero mode subspace, by partially taking into account the effect of oscillators. This is done by means of a Bogoliubov transformation applied to the Hamiltonian, involving the oscillators only (keeping the zero mode intact). Following the notations of Section 3.4, we can start by adding and subtracting an auxiliary quadratic term to the Hamiltonian eq. (3.1),

$$\begin{aligned} H^{(\mathrm{ShG})} = H^{(0)}_{\mathrm{cyl}} &+ \frac{m_{\mathrm{eff}}^2}{16\pi} \int_0^L dx : \tilde{\varphi}^2(x) : \\ &+ 2\mu_{ShG} \left(\frac{L}{2\pi} \right)^{2b^2} \int_0^L dx : \cosh\left(b\varphi(x,0) \right) : - \frac{m_{\mathrm{eff}}^2}{16\pi} \int_0^L dx : \tilde{\varphi}^2(x) :, \end{aligned} \tag{3.68}$$

but considering the zero mode φ_0 as a free parameter with $m_{\text{eff}} \equiv m_{\text{eff}}(\varphi_0)$ a function that depends on it. Upon transforming to the oscillator eigenbasis of the Hamiltonian given by the first two terms of eq. (3.68), the normalization of the cosh term changes

$$\begin{aligned} H^{(\text{ShG})} = & \left(\frac{4\pi}{L}\Pi_0^2 - \frac{\pi}{6L}\right) + \sum_{n\neq 0} \omega\left(m_{\text{eff}}\right) a_n^\dagger a_n \\ & + 2\mu_{ShG} L \delta_P \left(\frac{L}{2\pi}\right)^{2b^2} e^{\frac{2\pi}{L} b^2 S_1(m_{\text{eff}}, L)} : \cosh\left(b\varphi\left(x,0\right)\right) :_{m_{\text{eff}}} \\ & - \frac{m_{\text{eff}}^2}{16\pi} \int_0^L dx : \tilde{\varphi}^2(x) :_{m_{\text{eff}}} dx + \tilde{S}_2\left(m_{\text{eff}}, L\right) \end{aligned}$$

where $S_1(m, L)$ is defined in Subsection C.1 and $\tilde{S}_2(m, L)$ is defined in eq. (C.8). Here $::_{m_{\text{eff}}}$ implies that we are normal ordering w.r.t. to massive (of mass m_{eff}) oscillator modes. The value of m_{eff} is then given by the requirement that the explicit quadratic term precisely cancels that of the cosh function. This leads to the transcendental equation

$$m_{\text{eff}}^2(\varphi_0) \;=\; 16\pi\mu_{ShG} b^2 \left(\frac{L}{2\pi}\right)^{2b^2} e^{\frac{2\pi}{L} b^2 S_1(m_{\text{eff}}, L)} \cosh b\varphi_0, \quad \forall \varphi_0. \tag{3.69}$$

The effective Hamiltonian H_{ZM}^{eff} is then obtained by dropping all higher order oscillator terms of the cosh interaction. This leads to

$$\begin{aligned} H_{ZM}^{\text{eff}} = & \left(\frac{4\pi}{L}\Pi_0^2 - \frac{\pi}{6L}\right) + 2\mu_{ShG} L \left(\frac{L}{2\pi}\right)^{2b^2} e^{\frac{2\pi}{L} b^2 S_1(m_{\text{eff}}(\varphi_0), L)} \cosh\left(b\varphi_0\right) + \\ & + \tilde{S}_2\left(m_{\text{eff}}\left(\varphi_0\right), L\right). \end{aligned} \tag{3.70}$$

consisting of the contribution of a Bogoliubov ground state energy plus a correction due to the change of normalization of the cosh term.

Let us now focus on the small volume limit of the spectrum of H_{ZM}^{eff}. The effective mass of this Hamiltonian is then approximated by

$$m_{\text{eff}}^2(\varphi_0) = \frac{1}{L^2}\left(\mu_{ShG} L^{2+2b^2} \frac{16\pi b^2}{(2\pi)^{2b^2}} \cosh b\varphi_0 + O\left(\mu_{ShG}^2 L^{4+4b^2}\right)\right), \tag{3.71}$$

while the sums S_1 and $\tilde{S}_2$ admit the small-volume behavior

$$\begin{aligned} S_1(m, L) &= -\frac{1}{m}\left[\frac{\zeta(3)}{8\pi^3}(mL)^3 + O\left((mL)^5\right)\right], \\ \tilde{S}_2(m, L) &= m\left[\frac{\zeta(3)}{64\pi^3}(mL)^3 + O\left((mL)^5\right)\right]. \end{aligned} \tag{3.72}$$

Inserting the expansions eq. (3.71) and eq. (3.72) into the effective Hamiltonian eq. (3.70) and using the coordinate representation, we obtain a Schrödinger equation with the asymptotic form

$$-y''(x)+re^{\pm x}y(x)-\epsilon^2e^{\pm 2x}y(x)=c^2y(x),\quad x\to\pm\infty, \tag{3.73}$$

where y is a zero mode wave-function. In writing (3.73) we have introduced the notations

$$\begin{aligned} x &= b\varphi_0+\ln a,\quad a=\mu_{ShG}L\left(\frac{L}{2\pi}\right)^{2b^2},\quad r=\frac{L}{4\pi b^2},\\ \epsilon^2 &= \left(\frac{L}{2\pi}\right)^2 b^2\zeta(3),\quad c^2=\frac{P^2}{b^2}. \end{aligned} \tag{3.74}$$

The potential $V(x\to\pm\infty)=re^{\pm x}-\epsilon^2e^{\pm 2x}$ that we obtain in this way does not possess normalizable eigenfunctions. This is an artefact of expanding the effective mass according to eq. (3.71). However, for small L, the potential builds up a flat plateau around $x=0$, which is bounded by a large peak on either side. WKB analysis predicts that tunneling through the peaks can be neglected as long as $P\ll\frac{1}{4\sqrt{\zeta(3)}b^2}$. In this domain, the amplitude of reflection from the peaks can be approximated as

$$S_2(P)=-\left(\frac{L}{2\pi}\right)^{-4iPQ}\left(4\pi ib\,\mu_{ShG}\sqrt{\zeta(3)}\right)^{-\frac{2iP}{b}}\frac{\Gamma\left(1+\frac{2iP}{b}\right)}{\Gamma\left(1-\frac{2iP}{b}\right)}\frac{\Gamma\left(\frac{1}{2}-\frac{iP}{b}-\frac{i}{4b^3\zeta(3)}\right)}{\Gamma\left(\frac{1}{2}+\frac{iP}{b}-\frac{i}{4b^3\zeta(3)}\right)}. \tag{3.75}$$

For $b\ll 1$, the absolute value of $S_2(P)$ is essentially 1 over a wide interval of P. To now determine the energy levels, we can once more follow the tactic outlined in Subsection 3.5.1, writing a quantization condition for the phase shift $\delta_{\text{eff}}\equiv -i\ln(-S_2(P))=n\pi$. Expanding this in powers of P and using (3.53), we find the small-volume expansion:

$$E_0=\frac{2\pi}{L}b^2\pi^2\left(\frac{u^2}{2}-\kappa_2u^3+\frac{3}{2}\kappa_2^2u^4-2\left(\kappa_2^3-\frac{\pi^2}{3}\left(1+b^6\right)\zeta(3)+4\pi^2\zeta(3)^2b^{12}\right)u^5+\dots\right), \tag{3.76}$$

where

$$\kappa_2=\left(2\gamma_E+\ln\frac{\pi}{b^2}-\frac{2}{3}b^6\zeta(3)\right),\quad u=\left[\ln\left(\mu_{ShG}\left(\frac{L}{2\pi}\right)^{2+2b^2}\right)\right]^{-1}.$$

Notice that while the difference between the zero mode expansion eq. (3.61) and the small-volume expansion eq. (3.67) from the exact UV quantization condition is order $O(b^8)$, the difference between eq. (3.76) and eq. (3.67) is instead only order $O(b^{12})$.

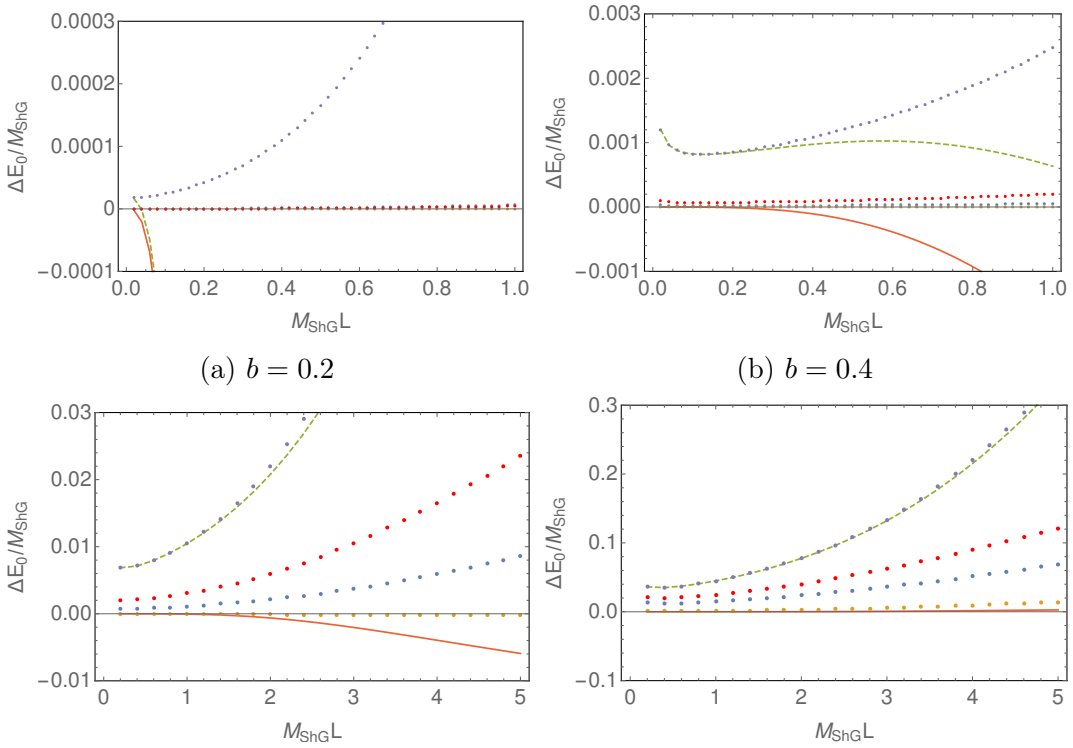

(a) $b = 0.2$ (b) $b = 0.4$

(c) $b = 0.6$ (d) $b = 0.8$

Figure 3.12: Comparison of the six different approaches available to estimate the UV behavior of the ground state energy at four different values of b. All data is presented with the exact TBA values subtracted. Blue dots: Raw ($N_c = 12$) TSM data; orange dots: extrapolated TSM data; purple dots: diagonalization of H_{ZM}; dashed green curve: semi-classical reflection quantization; continuous red curve: Liouville reflection quantization; and red dots: diagonalization of effective zero mode Hamiltonian, H_{ZM}^{eff}.

3.5.4 Numerical performance in the UV

We have now at hand six different ways to estimate the spectrum of the ShG model in the UV small-L limit: i) raw TSM data; ii) extrapolated TSM data; iii) diagonalization of the zero mode Hamiltonian, H_{ZM} (i.e. eq. (3.4)); iv) reflection quantization using the semi-classical reflection amplitude; v) reflection quantization using the full Liouville reflection amplitude; and finally vi) diagonalization of the effective zero mode Hamiltonian, H^{eff}_{ZM}, derived in Section 3.5.3. In this subsection we make an effort to compare the numerical accuracy of these different approaches. We present our results in Fig. 3.12 for four different values of b. Here the ground state energy corresponding to the Hamiltonian in eq. (3.70) was obtained numerically and compared to the raw zero mode potential using a real-space basis of size 16000 – see eq. (3.7). Let us summarise what we learn from these plots.

- The UV limit of TBA is indeed different from that calculated from the zero mode Hamiltonian H_{ZM} alone, apart in the $b \to 0$ limit.
- In precisely the $b \to 0$ limit, the validity of the reflection quantization method shrinks to extremely small volumes. This is intuitive at least in the semiclassical case as the potential increases relatively mildly around the minimum, so neglecting the overlap of the two exponentials in the middle is not well-founded.
- For small couplings, the effective potential eq. (3.70) efficiently accounts for the discrepancy between the eigenvalues of H_{ZM} and the exact TBA energies.
- As the coupling b is increased, higher order oscillator terms in μ_{ShG} not included in eq. (3.70) become significant for arbitrarily small volumes and our expression for the effective potential leads to inaccurate results.
- In this same regime of large b (but always $b < 1$), the accuracy of the ground state energy as obtained from reflection quantization extends to ever larger volumes well into the IR regime of the model.
- However, TSMs (especially after power-law extrapolation) are able to reproduce the TBA result surprisingly well, even for larger b. This provides an important confirmation of the efficiency of TSMs as applied to the sinh-Gordon model.

3.5.5 Extracting M_{ShG}, $\mathcal{E}_0$ and B from UV spectrum

We have shown that the TSM is able to reproduce the UV limit of TBA equations remarkably well. It is thus reasonable to take advantage of this fact and to try to extract infinite volume parameters combining TSM numerics with the quantization

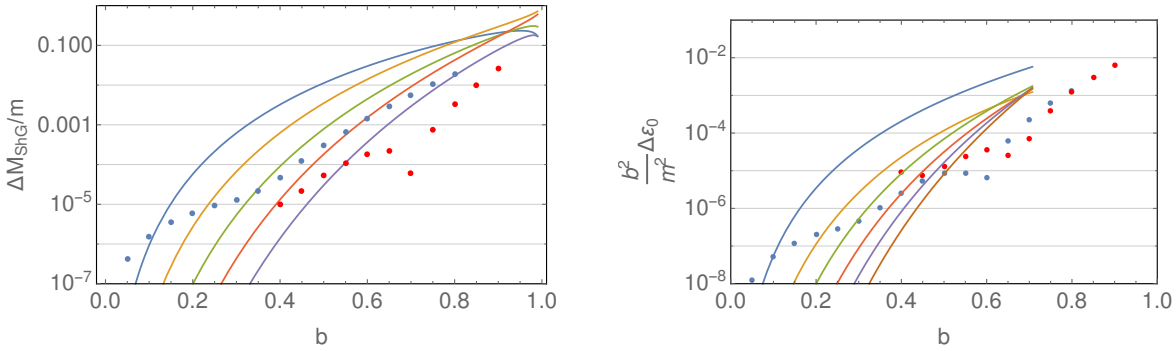

(a) Physical mass, M_{ShG}.

(b) Bulk energy, $\mathcal{E}_0$.

Figure 3.13: a) Presentation of M_{ShG} as computed in Section 3.5.5 (red dots) vs. its determination from extrapolated TSM data (blue dots). b) The same but for the bulk ground state energy density, $\mathcal{E}_0$. Solid curves shown are the same as in Fig. 3.7c-d. Results are presented as differences with the numerically exact TBA values.

condition eq. (2.86). As the exact quantization condition is expressed in terms of the IR parameters, M_{ShG}, $\mathcal{E}_0$, and B, it is possible to fit these parameters using TSM data. To do so we use the lowest two energy levels (the vacuum and the one-particle state) and two values of the volume ($mL = 0.1$ and $mL = 0.2$), and then we minimize the function

$$\sum_{i,j=1}^{2} \left(E_i^{\mathrm{TBA}}(L_j) - E_i^{\mathrm{TSM}}(L_j)\right)^2, \tag{3.77}$$

as function of M_{ShG}, $\mathcal{E}_0$ and B. In Fig. 3.13 we compare the mass and bulk energy obtained in this way to the standard TSM methods discussed in Section 3.3. It is worth stressing that this method produces an estimate for the mass that is an order of magnitude better than the extrapolated TSM data reported in Fig. 3.7 (see panel (a) of Fig. 3.13). The determination of $\mathcal{E}_0$ in provides a precision comparable to the previous analysis. The real power of the UV method is revealed when we consider the measurement of the S-matrix parameter B. Here the improvement of the error generally exceeds two orders of magnitude (see Fig. 3.14).

3.5.6 What have we learned?

In this section we have put the UV behavior of sinh-Gordon theory under scrutiny. After pointing out the incompleteness of the zero mode in describing the small-volume limit of the ground state energy for any finite b, we have derived an effective quantum mechanical potential. This effective potential accounts for the above discrepancies up to an $O(b^{12})$ error, by partially taking into account the oscillators neglected from the zero mode.

Comparing the zero mode, the effective zero mode, and the TBA-Liouville reflection quantization results to TSM and exact TBA numerics, we realized that the effective

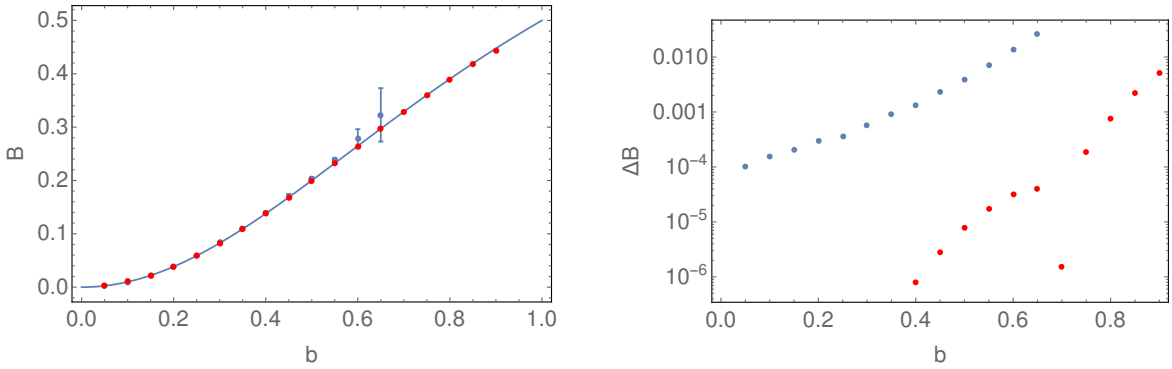

(a) S-matrix parameter B (b) Difference ΔB

Figure 3.14: Determination of S-matrix parameter B. a) Absolute values of B. Blue dots (TSM - see Fig. 3.8b), red dots (method described in Section 3.5.5), solid curve (exact). b) Differences of determined values of B with exact value.

potential significantly outperforms the zero mode. On the other hand, numerical TSM (especially after extrapolation) significantly outperforms the effective potential, providing an even more effective incorporation of the oscillators.

At the same time we noticed that the validity of the reflection quantization approximation extends to larger volumes as the coupling b is increased. This lead to a more precise, UV-based measurement of the mass and the S-matrix parameter B, and even provided a consistency check for the energy density $\mathcal{E}_0$.

We emphasize that both the S-matrix parameter B and (up to the mass scale) the Liouville reflection amplitude are self-dual quantities, which are successfully reproduced directly from the Lagrangian, which is not in any sense manifestly self-dual. In this sense, the 'self-duality' of the Lagrangian ShG model (i.e. the dependence of the model on coupling constant as encoded in the expression as $b^2/(1+b^2)$) is confirmed up to the precision of TSM. This result, together with the partial analytical reproduction of the reflection amplitude, indicate that the discrepancy in the ground state energy as derived in the UV expansion coming from the semi-classical and Liouville quantizations is solely due to the effect of oscillators. Importantly, as anticipated in Section 2.2, no extra terms (like $\cosh(b^{-1}\phi)$) in the Lagrangian are necessary to account for it.

However, note that all the above measurements were done below the self-dual point. As the self-dual point is traversed, the problems arising from the mass-coupling relation are inherited by the Liouville quantization condition as well. In the next section, we develop a supra-Borel resummation technique to motivate the power-law fit and to reach a better understanding of the cutoff dependence in applying TSMs to the ShG model. In Section 3.7, we actually provide an argument that if the Lagrangian with a finite positive μ_{ShG} parameter defines a meaningful theory at all for $b > 1$, this theory should actually be massless.

3.6 Supra-Borel resummation

In Section 3.3.4.1 we demonstrated pathologies in the corrections to the TSM results coming from taking into account perturbatively states above the cutoff. In particular we demonstrated that at n-th order in perturbation theory in μ_{ShG}, the states above the cutoff, N_c, and below an auxiliary cutoff Λ, contributed a factor behaving as

$$\delta E_n \sim \Lambda^{2(n^2-n)b^2-2n+2}\mu_{ShG}^n. \tag{3.78}$$

In the following, we will take a slightly different point of view, starting from the μ_{ShG}-perturbative expansion of energy levels of the TSM Hamiltonian. Details of this perturbative approach are discussed in Appendix D. We will formally consider TSM hamiltonians with their cutoff $N_c \to \infty$. An important nuance is that the singularities will now appear in the function of N_c instead of Λ.

That perturbation theory in μ_{ShG} is pathological should come as no surprise. Because the $\mu_{ShG}\cosh(b\phi)$ potential is (strongly) unbounded from below if $\mu_{ShG} < 0$, the radius of convergence of any perturbation theory in μ_{ShG} is 0. This is also reflected in the TBA energy in μ_{ShG} being a series, not in μ_{ShG} but in $\frac{1}{\log \mu_{ShG}}$. It is thus not surprising to find an ill-defined perturbative series around $\mu_{ShG} = 0$, even though the TBA energies are finite. Thus for any N_c, this series must be treated as asymptotic. The question then becomes whether it can be resummed. We know $E(N_c)$ itself is finite. But can we resum the series and explicitly demonstrate this?[2]

Quite remarkably, this series is not Borel resummable in the standard sense, namely the coefficients at order n are diverging more quickly than $n!$. We show in this section that nonetheless it is possible to resum this series in a meaningful way. From this resummation we will obtain some understanding of the slow convergence of TSM results in N_c as well as a partial justification of the power law scaling that we observed in Section 3.3.

Before doing so, let us reiterate an important point. In quantum field theory, one is used to facing divergences. Starting from finite bare parameters in an action and some regulator, it often happens that one gets divergent answers to physical quantities as the regulator is taken away. The issue is solved by tuning the *bare* parameters such that the physical parameters are fixed, finite quantities (thus hiding the infinities into the bare parameters through, e.g., introduing counterterms). In rough terms, this is the usual renormalization procedure employed in QFTs.

Let us point out in advance that in the μ_{ShG} expansion of sinh-Gordon theory, something different happens. ShG (defined through its exact S-matrix) is a particularly

[2] A priori it is possible that not only the leading divergences, but also all the subleading ones (see eq. 3.40) must be taken into account to obtain a finite resummation. We assume that this is not the case, and that the leading order differences separately sum up to a finite correction.

striking example to the class of theories where the UV behavior of energy levels is not "healthy" in the sense that absent a cutoff, no power expansion exists around $\mu_{ShG} = 0$. We saw this in the previous section, where we actually obtained an UV series in $\log(\mu_{ShG})^{-1}$ from TBA to certain energy levels in eq. (3.67). The apparent UV divergences are not automatically related to any "true" infinity needing to be accounted for. The series is pathological term by term because the corresponding power expansion does not exist.

To illustrate this, let us consider a toy example. The example we discuss in the next subsection shows that there are simple functions which are finite, but whose perturbative expansions suffer from the same behavior in the presence of a cutoff as our quantity of interest, $E(N_c)$.

3.6.1 Toy Example

Here we show that it is easy to find functions for which when one performs a perturbative expansion about a non-analytic point, one can obtain pathological behavior in a cutoff used to regulate each term in the expansion. Consider the function, $f(\mu, \epsilon)$, defined as

$$f(\mu, \epsilon) = \int_{\epsilon}^{1} dx (x + \mu)^{\frac{1}{b^2} - 1} dx. \tag{3.79}$$

Here ϵ is a regulator which if set to zero (analogous to taking $N_c \to \infty$), leaves f finite, i.e.

$$f(\mu, 0) = b^2((1 + \mu)^{\frac{1}{b^2}} - \mu^{\frac{1}{b^2}}). \tag{3.80}$$

This function is clearly well behaved for any $\mu \geq 0$, $b > 0$. However if we now naively expand about $\mu = 0$, we have

$$f(\mu, \epsilon) = \sum_{k=0}^{\infty} \mu^k \binom{b^{-2} - 1}{k} \int_{\epsilon}^{1} x^{b^{-2} - 1 - k} = \sum_{k=0}^{\infty} \mu^k \binom{b^{-2} - 1}{k} \frac{1}{k - b^{-2}} (\epsilon^{b^{-2} - k} - 1). \tag{3.81}$$

We see that while the original form of the function $f(\mu, \epsilon)$ was finite as $\epsilon \to 0$, the expansion in the coupling μ leads to a series where terms beyond a certain order in k are all divergent as the cutoff ϵ goes to 0. This series is thus asymptotic. The k-th order term here goes as $e^{k \log(1/\epsilon)}$ (so more slowly than $k!$) and here at least the series at any fixed ϵ should be resummable via standard Borel resummation techniques. Now, with this toy example in mind, let us turn to the real problem at hand.

3.6.2 Minimal resummation

To start we are going to assume that a perturbative expansion in μ_{ShG} for the ground state energy has the following form:

$$E(z=\tilde{\mu}_{ShG}N_c^{-2(1+b^2)}) = -\frac{N_c^2}{L}\sum_{n=1}^{\infty} a_n z^n e^{\frac{n^2}{16\gamma}}; \quad \gamma \equiv \frac{1}{16(2b^2\log(N_c)+\log(c))}, \tag{3.82}$$

where $\tilde{\mu}_{ShG} = \mu_{ShG}\left(\frac{2\pi}{L}\right)^{-2-2b^2}$ is the dimensionless ShG coupling and a_n, c are dimensionless constants independent of L, N_c. This form for the energy, under certain approximations, is derived in Appendix D.

Despite this series not being Borel resummable, it admits a supra-Borel resummability[3], something G. Hardy in his classical treatise on divergent series [149], termed resummation via moment constant methods. In this procedure, one supposes that one has the asymptotic series $S(z) = \sum_k a_k z^k$. In order to resum it, one chooses a function ρ and then defines its moments on $\mathbb{R}_+$ as

$$r_k = \int_0^\infty t^k \rho(t) dt. \tag{3.83}$$

The series, $S(z)$, is then said to be $r-\rho$ resummable if

$$B(t) = \sum_k \frac{a_k}{r_k} t^k,$$

converges in some neighbourhood of $t=0$ and $B(t)$ has an analytic continuation to a neighbourhood of the positive real axis. If the integral,

$$g(z) = \int_0^\infty B(zt)\rho(t)dt,$$

is convergent for a $z \neq 0$, then the function $g(z)$ exists, is analytic in some domain $-\infty < Re(\log(z)) < c_0$, and has the asymptotic Taylor series $S(z)$. $S(z)$ can then be identified as the resummation of $S(z)$ in this same domain.

For the case at hand we choose the function $\rho(t)$ as

$$\rho(t) = \frac{1}{t} e^{-4\gamma \log^2(t)}, \tag{3.84}$$

with moments

$$\mu_k = \sqrt{\frac{\pi}{4\gamma}} e^{\frac{k^2}{16\gamma}}. \tag{3.85}$$

As discussed in Ref. [150] this choice arises generically in problems with exponential

[3] I am grateful to Robert Konik for pointing this out.

potentials. Ref. [150] discusses the technical conditions needed for resummation for this choice of $\rho(t)$. Assuming for the moment that they are met, we can resum our expression for the ground state energy and rewrite it in the form:

$$\begin{aligned} E &= \frac{a_1\tilde{\mu}}{L} - \frac{N_c^2}{L\sqrt{4\gamma}}\int_{-\infty}^{\infty} dx e^{-x^2} B(\tilde{\mu} N_c^{-(2+2b^2)} e^{-\frac{x}{2\sqrt{\gamma}}}); \\ B(t) &= \left(\frac{4\gamma}{\pi}\right)^{1/2} \sum_{n=2}^{\infty} a_n t^n. \end{aligned} \tag{3.86}$$

In Appendix D, we show that in fact $a_n = (-\alpha)^n$ with $\alpha > 0$. Assuming this, we can then write $B(t)$ as

$$B(t) = \left(\frac{4\gamma}{\pi}\right)^{1/2} \frac{\alpha^2 t^2}{1+\alpha t}, \tag{3.87}$$

and so is analytic along all of the positive real axis.

Now that we have resummed our asymptotic series, let us investigate its properties as a function of N_c. It is not a priori obvious that this resummation will necessarily lead to a sensible result, i.e. something that converges as $N_c \to \infty$. But nonetheless it does. To investigate the asymptotics, we write the integral expression for E in a suggestive form:

$$\begin{aligned} E &= \frac{a_1\tilde{\mu}_{ShG}}{L} - \frac{\tilde{\mu}_{ShG}\alpha c}{L\sqrt{\pi}}\int_{-\infty}^{\infty} dx \frac{e^{-x^2}}{1+\alpha^{-1}e^{\beta(x-\mu_B)}}; \\ \beta &\equiv \frac{1}{2\sqrt{\gamma}}; \\ \mu_B &\equiv \frac{1}{4\sqrt{\gamma}} + 2\sqrt{\gamma}\log(\tilde{\mu}_{ShG} N_c^{-2-2b^2}). \end{aligned} \tag{3.88}$$

We can now do a Sommerfeld-type expansion and obtain asymptotics in large N_c of the form:

$$\begin{aligned} E &= \frac{a_1\tilde{\mu}_{ShG}}{L} - \frac{\alpha\tilde{\mu}_{ShG}c}{L\sqrt{\pi}}\left[\int_{-\infty}^{\mu_B} dx e^{-x^2} + \frac{1}{\beta}\int_0^{\infty} dy e^{-\mu_B^2}\left(\frac{1}{1+\alpha^{-1}e^y} - \frac{1}{1+\alpha e^y}\right) + \mathcal{O}\left(\frac{e^{-\mu_B^2}}{\beta^2}\right)\right] \\ &= \begin{cases} \frac{a_1\tilde{\mu}_{ShG}}{L} - \frac{\alpha\tilde{\mu}_{ShG}c}{L\sqrt{\pi}} e^{-\mu_B^2}\left(\frac{1}{2|\mu_B|} + \frac{1}{\beta}\log\alpha\right) + C\frac{e^{-\mu_B^2}}{L\beta^2}, & b^2 < 1; \\ \frac{a_1\tilde{\mu}_{ShG}}{L} - \frac{\alpha\tilde{\mu}_{ShG}c}{L\sqrt{\pi}} e^{-\mu_B^2}\left(\sqrt{\pi} - \frac{1}{2|\mu_B|} + \frac{1}{\beta}\log\alpha\right) + C'\frac{e^{-\mu_B^2}}{L\beta^2}, & b^2 > 1, \end{cases} \end{aligned} \tag{3.89}$$

where C, C' are constants. We note that in the large-N_c limit, the Borel 'chemical potential', μ_B, can be written as

$$\mu_B \approx \frac{\sqrt{\log N_c}(b^2-1)}{\sqrt{2}b}, \tag{3.90}$$

and so $|\mu_B|$ in this limit is invariant under $b \to 1/b$. We also note that as $N_c \to \infty$,

the resummed part (i.e. involving terms $n \geq 2$) of E vanishes if $b < 1$, but tends to a finite constant if $b > 1$.

We thus expect that for large N_c that

$$E \sim N_c^{-\nu}, \quad \nu = \frac{(b^2-1)^2}{2b^2}. \tag{3.91}$$

We compare in Fig. 3.15 the exponents predicted by this result to those determined from extrapolating TSM data (see Fig. 8 in Section 3.3). We see that as the self-dual point is approached, the exponent predicted by the asymptotics describes approximately the trend observed from power law fits of the data. It however fails to describe the fitted exponents at small b. Instead these are described well by the exponent coming from the first perturbative correction to the TSM data (see eq. (3.37)).

3.6.3 What have we learned?

We have shown in this section that the divergences observed in the perturbative corrections to the TSM can be made sense of.

We have shown the functional form of the resummed corrections gives us important insights into the large N_c asymptotics of the TSM. It provides a partial explanation at values of b close to the self-dual point for the power law fit that we have observed (see Fig. 20). It also provides a guide to how to extrapolate TSM results to $N_c = \infty$. In our paper [151] we considered two fitting functions suggested by the supra-Borel resummation to use with our TSM data. In the first, we employed only the asymptotic form (valid for large N_c) suggested by the resummation. In the second we used a Padé form for the Borel approximant. Unsurprisingly the Padé form outperformed the asymptotic form. The asymptotic form is likely only really appropriate for values of N_c beyond that we have performed TSM computations. In presenting this resummation, we have really only scratched the surface. We are fairly certain that there are more

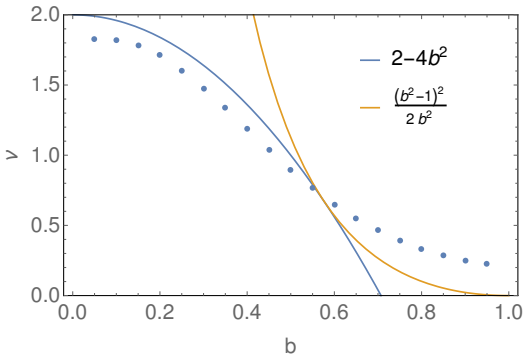

Figure 3.15: Power law exponents as a function of b as determined from TSM extrapolation (blue dots) vs those predicted by eq. (3.91) (solid orange curve) and the exponent of the leading naïve RG correction eq. (3.37).

appropriate Borel approximates than used here that are better tailored to the properties of the ShG model. We view this an important open problem presented by this work.

3.7 Form factor truncated spectrum method

In the previous sections we have focused on numerical TSM data arrived at from a computational basis based on a non-compact free massless boson and its zero mode. We have discussed in detail the strong dependence of the data from the cutoff, E_c, in particular approaching the self-dual point $b = 1$. In light of these results, it is natural to ask the following question:

Is there a starting point H_0 for the TSM much 'closer' to the model of interest?

In this context, 'closer' means having a set of eigenstates such that TSMs is better suited to approximate the spectrum of the perturbed theory. For example, instead of separating the zero mode, we might have started with the Hamiltonian (3.48) and so used a computation basis built on a standard massive Fock basis. Having considered this, a more radical possibility suggests itself. This, however, comes at the cost of abandoning the comfort provided by the *free* nature of H_0.

3.7.1 Using the ShG basis as a computational basis

The main idea is as follows. Our target is a ShG model at coupling b_1 and we choose as our starting point a ShG model at a *different* coupling b_0, setting $H_0 = H_{b_0}^{(\mathrm{shG})}$. While such a starting point does suffer from the critique that we are using as input information that is itself non-trivial and is meant to be, in part, verified by our TSM studies, we believe that there are good reasons to explore this path:

- As we will see soon, this method provides a set of a highly nontrivial self-consistency checks.
- It provides useful insights regarding the validity of the exact VEV formulae in certain domains.
- It is a non-traditional starting point for the application of the TSM to interacting massive field theories[4] and insight gained here will be useful for the study of deformations of other massive integrable field theories.

In the approach taking in here, we write the Hamiltonian as:

$$H = H_{b_0}^{(\mathrm{shG})} + H_1 \ , \tag{3.92}$$

[4]Certainly the TSM has a long history of employing an H_0 that is interacting. However H_0 in such cases is an interacting massless CFT [77, 107, 109, 118, 121, 122, 152–154].

where the solvable piece is given by

$$H_{b_0}^{(\mathrm{shG})} \;=\; H_0 + 2\mu_0 \int_0^L dx \cosh(b_0\phi), \tag{3.93}$$

where H_0 is the Hamiltonian of the non-compact $c = 1$ boson, while the perturbation is given by

$$H_1 = \int_0^L dx \big(2\mu_1 \cosh(b_1\phi(x)) - 2\mu_0 \cosh(b_0\phi(x))\big). \tag{3.94}$$

In order to proceed with the diagonalization of the Hamiltonian (3.92) on a cylinder of finite circumference L we need two highly nontrivial sets of data:

- Finite volume energy levels of $H_{b_0}^{(\mathrm{shG})}$;
- Finite volume matrix elements of H_1 between eigenstates of $H_{b_0}^{(\mathrm{shG})}$.

Fortunately, both pieces of data are available in the ShG model (as well as in a number of other integrable models), at least up to exponentially small corrections in the volume. Indeed, according to Lüscher's principle, all information about finite volume quantities are encoded in infinite volume data, like the physical mass M and the S-matrix. Indeed, the exact energies of all finite volume eigenstates can be computed efficiently from the excited-state thermodynamical Bethe ansatz (see Section 2.5.2). Formulae for the matrix elements, at least up to exponential small corrections [127, 128], are also available. In the special case of diagonal matrix elements, one can use a generalization of the Leclair-Mussardo formula [87] to systematically compute exponential corrections. In the following, we are going work mostly in the regime $5 \leq M_{ShG}L \leq 15$, where exponential corrections should be small and can be neglected.

3.7.1.1 Finite volume energies

We have already discussed in Section 2.5.2 the excited state TBA that provides the finite volume energies of H_0. The finite energy eigenstates can be described by a finite number n of particles with momenta $p_j = M \sinh\theta_j$ quantized due to finite volume L. We can assign an integer quantum number I_j to each momenta. A finite volume state, $|\{I_i\}_{i=1}^k\rangle$, is thus given by the set I_j, $j \in \{1, \ldots, n\}$. The Bethe-Yang system eq. (2.83) is solved for the set of rapidities θ_j giving the total energy and momentum of the state as:

$$E = \sum_{j=1}^{n} M_{ShG} \cosh\theta_j, \quad P = \sum_{j=1}^{n} M_{ShG} \sinh\theta_j \tag{3.95}$$

3.7.1.2 Finite volume matrix elements

We recalled the general formula of finite volume nondiagonal form factors (up to exponential corrections) in Section 2.6.6.

We still need to treat the case of when rapidities in matrix elements happen to coincide. In such a case, the infinite volume form factors have singularities that require regulation. This requires then significantly more complicated formulae than eq. (2.123). As mentioned in Section 2.6.6, coinciding rapidities arise in two different circumstances. In the first the bra and ket states are the same state - so called diagonal form factor). The second possibility is that the two different states have an odd number of particles $2n+1$ and $2m+1$, respectively, with quantization numbers

$$\{I_j\}_{j=1}^n \cup \{0\} \cup \{-I_j\}_{j=1}^n, \text{ and } \{\tilde{I}_j\}_{j=1}^m \cup \{0\} \cup \{-\tilde{I}_j\}_{j=1}^m.$$

In the latter case, a particle of exactly zero momentum is present in both states. There is, however, a simple trick [83] to circumvent the complications in numerical computations by exploiting the factorization property of exponential operators. Introducing an auxiliary particle with rapidity $\theta_\Lambda \to \infty$,

$$\frac{\langle \theta_\Lambda, \{\theta_i\}_{i=1}^k | \mathcal{O} | \{\vartheta_j\}_{j=1}^l \rangle}{\langle \mathcal{O} \rangle} \to \frac{\langle \theta_\Lambda | \mathcal{O} | \text{vac} \rangle \langle \{\theta_i\}_{i=1}^k | \mathcal{O} | \{\vartheta_j\}_{j=1}^l \rangle}{\langle \mathcal{O} \rangle^2} \tag{3.96}$$

and

$$\rho_{k+1}(\theta_\Lambda, \{\theta_i\}) \to \rho_1(\theta_\Lambda)\rho_k(\{\theta_i\}). \tag{3.97}$$

This permits us to isolate the matrix element of interest even if it contains coinciding rapidities. With all $\{I_i\}$ and $\{\tilde{I}_j\}$ finite,

$$\lim_{\Lambda\to\infty} \langle \{I_i\}_{i=1}^k \cup \{\Lambda\} | \mathcal{O}(0,0) | \{\tilde{I}_j\}_{j=1}^l \rangle_L = \frac{\langle \Lambda | \mathcal{O} | \text{vac} \rangle_L}{\langle \mathcal{O} \rangle_L} \langle \{I_i\}_{i=1}^k | \mathcal{O}(0,0) | \{\tilde{I}_j\}_{j=1}^l \rangle_L \tag{3.98}$$

where Λ is the momentum quantization number of the auxiliary particle. Choosing instead a large but finite Λ, the equality is not exact, but the error can be made arbitrarily small by increasing Λ. In practice we need to solve the set of BYE (2.83) twice: once for $k+1$ particles involving the extra quantization number Λ, and once for the quantization number set $\{\tilde{I}_j\}_{j=1}^l$. Thus we obtain rapidities of the form $\theta_i = \vartheta_i + \epsilon_i$, where ϵ_i are small corrections depending on all the I_i and Λ. These are then put back into the left hand side of eq. (3.98), yielding the sought for matrix element.

3.7.2 Sanity checks

The setup of the TSM in the basis of the ShG model itself allows us to make some non-trivial consistency checks. The first such check is offered by an infinitesimal change in the coupling constant $b_1 = b_0 + \delta b$.

3.7.2.1 Comparison with form factor perturbation theory

Denote $\mu_0 = \mu(b)$ and $\mu_1 = \mu(b+\delta b)$. Let us calculate the first order correction of the mass of the particle in form factor perturbation theory [155]. It is convenient to keep the system in a finite (very large) volume L. Here the volume factors from spatial integration and the Hilbert state norms cancel. The first perturbative correction to the mass is then:

$$\delta M_{ShG} = \langle M_{ShG}|H_1|M_{ShG}\rangle - \langle 0|H_1|0\rangle \ , \tag{3.99}$$

where $|M_{ShG}\rangle$ denotes the one-particle state of zero momentum and $|0\rangle$ is the vacuum. The diagonal form factor contains a disconnected term which be cancelled by a similar term arising from the VEV of eq. (3.99):

$$\begin{aligned}\langle M_{ShG}|H_1|M_{ShG}\rangle &= \langle 0|H_1|0\rangle \\ &+\frac{2}{M_{ShG}}(-\mu(b)\langle e^{b\varphi}\rangle F_2^{\exp(b\varphi)}(i\pi,0)+\mu(b+\delta b)\langle e^{(b+\delta b)\varphi}\rangle F_2^{\exp((b+\delta b)\varphi)}(i\pi,0)).\end{aligned}$$

Inserting the explicit form of the two-particle form factor calculated using eq. (2.118), we arrive at the relation:

$$\begin{aligned}M_{ShG}(b)[M_{ShG}(b+\delta b)-M_{ShG}(b)] &= 8(-\mu(b)\langle e^{b\varphi}\rangle \sin(\pi B) \\ &+ \mu(b+\delta b)\langle e^{(b+\delta b)\varphi}\rangle \frac{\sin^2((1+\frac{\delta b}{b})\pi B)}{\sin(\pi B)}) \ ,\end{aligned} \tag{3.100}$$

where the vacuum expectation values are given by the FLZZ formula (2.92). Therefore, for an infinitesimal δb, we can write down a differential equation for the mass shift equation

$$\frac{\partial[M_{ShG}(b)^2]}{\partial b} = 16\mu(b)\langle e^{b\varphi}\rangle(\frac{\delta\langle e^{(b+\delta b)\varphi}\rangle}{\langle e^{b\varphi}\rangle}\sin(\pi B)+\frac{2\pi B}{b}\cos(\pi B)+\frac{\partial(\log\mu)}{\partial b}\sin(\pi B)) \tag{3.101}$$

where

$$\begin{aligned}\frac{\delta\langle e^{(b+\delta b)\varphi}\rangle}{\langle e^{b\varphi}\rangle} &= -2b(1-B)\ln(\frac{-\mu(b)\pi\Gamma(1+b^2)}{\Gamma(-b^2)}) \\ &+\int_0^\infty dt\Big[-b\frac{\sinh(4b^2t)}{\sinh(b^2t)\sinh t\cosh((1+b^2)t)}+\frac{4b}{t}e^{-2t}\Big].\end{aligned} \tag{3.102}$$

The physical mass M_{ShG}, given by the mass-formula (2.89), numerically agrees with the result of integrating equation (3.101). In the special case $\lim_{b\to 0}\mu \propto b^{-2}$, we also have to explicitly specify $M_{ShG}(b=0)$. The integral appearing in the RHS of (3.102)

can be evaluated explicitly in terms of a digamma function $\Psi(z)$:

$$\int_0^\infty dt[-b\frac{\sinh(4b^2t)}{\sinh(b^2t)\sinh t\cosh((1+b^2)t)}+\frac{4b}{t}e^{-2t}] = -2b\Big\{\frac{1}{B}-\Psi(1-b^2)-\Psi(1+b^2) -\frac{1-B}{2}\big(\Psi(\frac{1}{2}-\frac{B}{2})-\Psi(\frac{B}{2})+\Psi(\frac{B-1}{2})-\Psi(1-\frac{B}{2})\big)\Big\} \quad (3.103)$$

A somewhat tedious but straightforward calculation shows that substituting eq. (3.102) into the RHS of eq. (3.101) indeed agrees with the derivative of the exact mass formula (eq. (2.89)), once squared.

3.7.2.2 Massive boson limit

In the second check, we fix $\mu(b_i)=\frac{m^2}{2b_i^2}$ and take the limit $b_0\to 0$. Here we want to show that we then obtain the Hamiltonian in the massive boson basis. In particular in this limit all matrix elements of the perturbation vertex operators need to approach the limit:

$$\langle\{I_i\}_{i=1}^k|:e^{a\varphi}(0,0):|\{\tilde{I}_j\}_{j=1}^l\rangle_L\to \prod_k\frac{1}{\sqrt{n_k!m_k!}}\Big\{\sum_{n_{1k}=0}^{\min(n_k,m_k)}n_{1k}!\binom{n_k}{n_{1k}}\binom{m_k}{n_{1k}}(\frac{a}{\sqrt{2L\omega_k}})^{n_k+m_k-2n_{1k}}\Big\} \quad (3.104)$$

with $a=\pm b_1$ and the quantities on the LHS are understood with respect to theory b_0. In formula eq. (3.104) we denoted the number of particles with quantum number k as n_k in the bra vector and m_k in the ket vector. Furthermore, matrix elements of vertex operators with $a=\pm b_0$ need to approach those of the operator $-\frac{m^2}{2}:\varphi^2:$.

These relations are highly nontrivial, especially for diagonal matrix elements, but we have confirmed numerically their validity on a large number of matrix elements. Note that the $b_0\to 0$ limit of the form factors is numerically unstable and so the precision often needs to be increased from the usual machine (double) precision.

3.7.3 Implementation and results

Due to the high numerical precision needed, especially in taking diagonal limits, we opted for an implementation in Mathematica. The truncated basis was selected with two cutoffs, a momentum cutoff $k_{\max}$ and a limit on the number of particles $N_{\max}$. Fig. 3.16 summarizes the numerical results obtained starting from theories with four different values of b_0.

To facilitate comparison of different bases, we introduce the following double cutoff. We limit the maximum number of particles $N_{\max}$ as well as the sum of Bethe-Yang

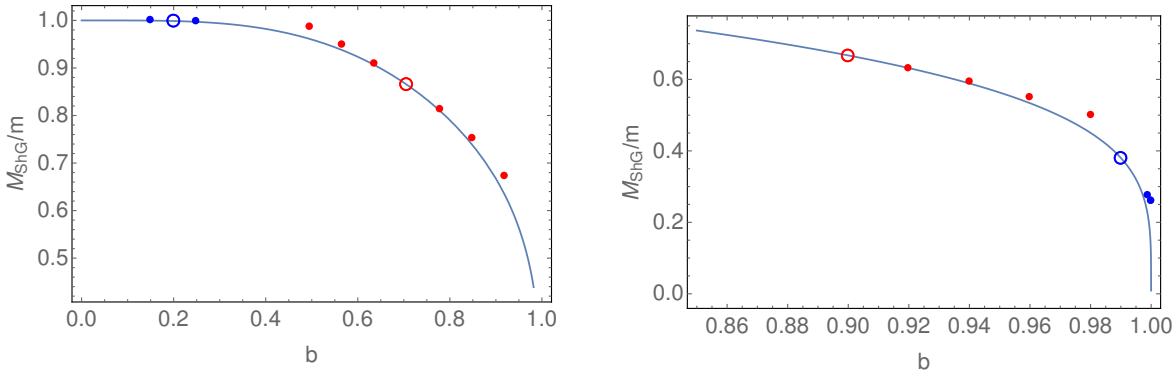

(a) Blue: $b_0 = 0.2$, Red: $b_0 = \frac{1}{\sqrt{2}}$

(b) $b_0 = 0.9$ (red) and $b_0 = 0.99$ (blue)

Figure 3.16: The mass-coupling relation as measured using $H_0 = H_{b_0}^{ShG}$ at four different values of b_0 (two in the left panel and two in the right). The mass of the unperturbed theory at b_0 is plotted as a large unfilled circle while the masses derived at neighbouring values of b_1 are shown as dots of the same color.

quantization numbers of each sign: $\sum_{j:I_j>0} I_j <= k_{\max}$. Let us remark that enlarging the basis size through the increase of $k_{\max}$ only is computationally easier than increasing $N_{\max}$. This is because the latter results in having to evaluate much more complicated expressions for the matrix elements. However, from numerical tests we deduce that the majority of cutoff dependence is found when changing $N_{\max}$ and $k_{\max}$ simultaneously. Therefore in the following we fix $N_{\max} = k_{\max}$.

In Fig. 3.16 we present sample results for the mass gap, starting from four different basis theories (denoted by unfilled circles). Computations were done with a raw cutoff $N_{\max} = 6$. This resulted in Hilbert spaces of dimension 203 in the even particle number sector and 124 in the odd. Numerics were performed at $M_{\rm ShG}L = 6$ with $M_{\rm ShG}$ being the physical mass of the unperturbed (basis) theory.

In Fig. 3.17 we follow the precision of results as the TSM basis is changed from the free massive boson towards the self-dual point. Here we show explicitly the cutoff dependence of the ground state energy at $L = 6$. The $b_0 = 0$ points result from using the free massive Hamiltonian (3.48). The largest cutoff considered for the form factor approach is $N_{\max} = 8$, corresponding to an 1171 dimensional (even sector) truncated Hamiltonian. In the free massive basis, we also show the point corresponding to $N_{\max} = 10, 12$, with basis sizes of 5830 and 25488, respectively. Not surprisingly, the result corresponding to any fixed cutoff improves as we start closer to b_1. However, it is striking that as we approximate b_0 to b_1, the power-law exponent of the cutoff dependence apparently worsens. As we have seen previously, when b_1 is infinitesimally close to b_0, the first order term of the form factor perturbation series dominates. However, as we move b_0 slightly away, corrections from all energy scales play a role.

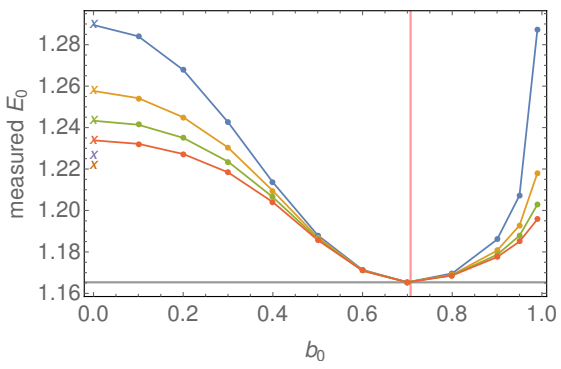

(a) $b_1 = \frac{1}{\sqrt{2}}$. $b_0 = b$ is shown with a red line. Theoretical value is shown with a horizontal line.

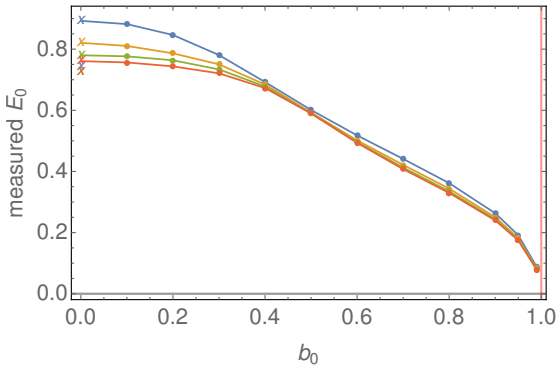

(b) $b_1 = 1$. Theoretical value is zero.

Figure 3.17: Cutoff dependence of ground state energy at coupling b_1, volume $L = 6$, starting from different b_0 couplings. Blue, orange, green, red, purple and brown symbols correspond to cutoffs $N_{\max} = 2, 4, 6, 8, 10, 12$, respectively. Results from the free massive boson basis ($b_0 = 0$) are distinguished with x-marks. $\mu_0 = \frac{1}{2b_0^2}$, $\mu_1 = \frac{1}{2b_1^2}$

3.7.4 What have we learned: massless regime for $b > 1$?

While one can see from the right panel of Fig. 3.17 that it is difficult to obtain accurate results (again because of slow convergence in the cutoff) for b_1 close to the self-dual point (even when b_0 itself is close to $b = 1$), we can use the properties of this massive interacting basis to draw conclusions on the nature of the theory beyond $b > 1$. We begin, as before, with a starting point $b_0 < 1$ and aim to describe the theory for a fixed $b_1 > 1$. We are completely free to choose $b_0 < 1$ and we so chose it such that it satisfies

$$\frac{Q(b_0)}{2} = \frac{1}{2}\left(b_0 + \frac{1}{b_0}\right) = b_1. \tag{3.105}$$

However for this particular choice of b_1, the VEV of the vertex operator $e^{b\varphi}$ (relative to the b_0 theory) is exactly zero! This in turn means that all matrix elements of $e^{b\varphi}$ vanish. Hence according to eq. (3.92), the perturbation consists of simply subtracting the original vertex operators from the original Hamiltonian, which (formally at least) leads to a massless Gaussian model. This argument suggests then that for $b > 1$, the ShG model, like its SG counterpart is trivial.

Because $\frac{Q(b_0)}{2} \geq 1$, $\forall b_0$, this argument only works when the target theory satisfies $b_1 \geq 1$. We note that perturbing a theory with a vertex operator with $b > \frac{Q}{2}$ is meaningless as the vacuum expectation value becomes negative, thus (formally) making the spectrum unbounded. A plausible explanation is that the VEV $\langle e^{a\varphi} \rangle$ in the Lagrangian formulation is only identical to the FFLZ formula in the domain $-\frac{Q}{2} \leq a \leq \frac{Q}{2}$ and vanishes identically outside this interval. We note that this argument then requires us to use the FFLZ formula at the boundary of its validity. These arguments are certainly

heuristic but give nevertheless a hint on the phase of the ShG model in the strong coupling regime $b > 1$.

Chapter 4

Lüscher corrections to matrix elements in the sinh-Gordon model

In this chapter, we investigate the leading exponential finite volume corrections to non-diagonal form factors in the sinh-Gordon theory. In Section 4.1 we introduce the necessary concepts and notations. In Section 4.2, we outline a direct method based on the two-point function to systematically obtain the exponential finite volume corrections of nondiagonal form factors. We explicitly present the leading exponential correction for the vacuum-one particle form factor. We derive the volume-exact, perturbatively expanded vacuum-one particle form factor is Section 4.3. The obtained perturbative formula is compared to the formal Lüscher correction, and they are shown to agree in their overlapping domain of relevance. This discussion follows along the lines of the work [127]. In Section 4.4, we overview a formal derivation of the leading exponential corrections in the case of a general nondiagonal form factor. The formula is confirmed numerically in Section 4.5, using the truncated spectrum approach presented in Section 3.4. The latter results were first presented in our work [128].

4.1 An overview of Lüscher corrections

The finite volume spectrum of the sinh-Gordon model is accessible through the solution of the TBA system (2.80)-(2.81)-(2.82).

The leading exponential correction has two sources [38]. First one has to take into account how the sea of virtual particles changes the quantization condition

$$\epsilon^{(1)}(\theta_j^{(1)} + i\frac{\pi}{2}) = i(2n_j+1)\pi \quad ; \qquad \epsilon^{(1)}(\theta) = \epsilon^{(0)}(\theta) + \delta\epsilon(\theta)$$
$$\delta\epsilon(\theta) = i\int_{-\infty}^{\infty}\frac{d\theta'}{2\pi}\frac{S'(\theta-\theta')}{S(\theta-\theta')}\prod_k S(i\frac{\pi}{2}+\theta_k^{(0)}-\theta')e^{-M_{ShG}L\cosh\theta'} \tag{4.1}$$

where $S'(\theta)$ denotes $\frac{dS(\theta)}{d\theta}$. Here and below the superscripts in parentheses indicate the

highest Lüscher orders involved in the quantities. In particular, in $\theta^{(0)}$ we neglect all exponential corrections, $\theta^{(1)}$ neglects the second Lüscher order, and so on. We then have to add the direct energy contribution of the virtual particles. By expressing all contributions in terms of the leading rapidities, $\theta_j^{(0)}$, we have:

$$\begin{aligned} E_N(L) &= \sum_k M_{ShG}\cosh\theta_k^{(0)} + i\sum_{k,j} M_{ShG}\sinh\theta_k^{(0)}\left(\bar{R}_N^{(0)}\right)^{kj}\delta\epsilon(\theta_j^{(0)}+i\frac{\pi}{2}) \\ &\quad -M_{ShG}\int_{-\infty}^{\infty}\frac{d\theta}{2\pi}\cosh\theta\prod_k S(\frac{i\pi}{2}+\theta-\theta_k^{(0)})e^{-M_{ShG}L\cosh\theta} \end{aligned} \tag{4.2}$$

where $\bar{R}_N^{(0)}$ is the inverse of the matrix $R_N^{(0)}$ with entries $R_{jk}^{(0)} = -i\partial_{\theta_j^{(0)}}\epsilon^{(0)}(\theta_k^{(0)}+i\frac{\pi}{2})$.

In particular, for a moving one-particle state at leading order we obtain

$$-i\epsilon^{(0)}(\theta_1^{(0)}+i\frac{\pi}{2}) = M_{ShG}L\sinh\theta_1^{(0)}+\pi = (2n_1+1)\pi \tag{4.3}$$

and the corresponding energy is

$$E_1(L) = M_{ShG}\cosh\theta_1^{(0)} + O(e^{-M_{ShG}L}) \tag{4.4}$$

The leading exponential correction of the quantization condition contains an extra term of the form

$$\delta\epsilon\left(\theta_1^{(0)}+i\frac{\pi}{2}\right) = i\int_{-\infty}^{\infty}\frac{d\theta'}{2\pi}S'(i\frac{\pi}{2}+\theta_1^{(0)}-\theta')e^{-M_{ShG}L\cosh\theta'} \tag{4.5}$$

The one-particle energy (measured from the finite volume vacuum) is [77, 78]:

$$\begin{aligned} E_1(L)-E_0(L) &= M_{ShG}\cosh\theta_1^{(0)} - \\ &\quad \frac{M_{ShG}}{\cosh\theta_1^{(0)}}\int_{-\infty}^{\infty}\frac{d\theta}{2\pi}\cosh(\theta-\theta_1^{(0)})\,(S(\frac{i\pi}{2}+\theta-\theta_1^{(0)})-1)e^{-M_{ShG}L\cosh\theta} \end{aligned} \tag{4.6}$$

We managed to reproduce this result from the study of the finite volume two-point function in [127].

As discussed in Section 2.6.5, form factors are defined as the matrix elements of local operators sandwiched between finite volume energy eigenstates. The space-time dependence of the form factors can be easily calculated

$$\langle\theta_1',\dots,\theta_M'|\mathcal{O}(x,t)|\theta_1,\dots,\theta_N\rangle_L = e^{i\Delta Et-i\Delta Px}\langle\theta_1',\dots,\theta_M'|\mathcal{O}|\theta_1,\dots,\theta_N\rangle_L \tag{4.7}$$

where $\Delta E = E_M(L)-E_N(L)$ and $\Delta P = P_M(L)-P_N(L)$ with $P_N(L) = \frac{2\pi}{L}\sum_j n_j$, while we simply abbreviated $\mathcal{O}(0,0)$ by $\mathcal{O}$.

The polynomial finite size corrections purely change the normalization of states and

give [6]:

$$\langle\theta'_1,\dots,\theta'_M|\mathcal{O}|\theta_1,\dots,\theta_N\rangle_L = \frac{F^{\mathcal{O}}_{M+N}(\theta'_1+i\pi,\dots,\theta'_M+i\pi,\theta_1,\dots,\theta_N)}{\sqrt{\rho^{(0)}_M\rho^{(0)}_N}} + O(e^{-M_{ShG}L}) \tag{4.8}$$

where $F^{\mathcal{O}}_{M+N}$ denotes the infinite volume form factor

$$F^{\mathcal{O}}_{M+N}(\theta'_1,\dots,\theta'_M,\theta_1,\dots,\theta_N) = \langle 0|\mathcal{O}|\theta'_1,\dots,\theta'_M,\theta_1,\dots,\theta_N\rangle \tag{4.9}$$

and all the rapidities can be taken at the leading order values with superscript (0). Since even the leading exponential correction is not known for these form factors we develop a systematic method based on the two-point function to calculate them.

In particular, for the one-particle form factor the formulae simplify as

$$\langle 0|\mathcal{O}|\theta_1\rangle_L = \frac{F^{\mathcal{O}}_1(\theta^{(0)}_1)}{\sqrt{\rho^{(0)}_1}} + O(e^{-M_{ShG}L}) \tag{4.10}$$

where

$$\rho^{(0)}_1 = -i\partial_{\theta^{(0)}_1}\epsilon^{(0)}(\theta^{(0)}_1 + i\frac{\pi}{2}) = M_{ShG}L\cosh\theta^{(0)}_1 \tag{4.11}$$

and the aim of the next subsections is to calculate the leading exponential corrections to these formulae.

4.2 Finite volume two-point function

Let us focus on the Euclidean finite volume two-point function, which is defined by the path integral[1]

$$\langle\mathcal{O}(x,t)\mathcal{O}\rangle_L = \frac{\int[\mathcal{D}\phi]\mathcal{O}(x,t)\mathcal{O}(0,0)e^{-S[\phi]}}{\int[\mathcal{D}\phi]e^{-S[\phi]}} \tag{4.12}$$

where configurations are periodic in x with L and $t\in\mathbb{R}$. The momentum space form is obtained by its Fourier transform

$$\Gamma(\omega,q) = \frac{1}{L}\int_{-L/2}^{L/2}\mathrm{d}x\int_{-\infty}^{\infty}\mathrm{d}t\,\mathrm{e}^{i(\omega t+qx)}\langle\mathcal{O}(x,t)\mathcal{O}\rangle_L \tag{4.13}$$

where periodicity in x requires that $e^{iqL}=1$. Taking t as Euclidean time the two point function is the vacuum expection value of the time ordered product:

[1]We restrict our attention to the case when the two operators are the same. The generalization for different operators is straightforward.

$$\langle \mathcal{O}(x,t)\mathcal{O}\rangle_L = \langle 0|T(\mathcal{O}(x,t)\mathcal{O})|0\rangle_L = \Theta(t)\langle 0|\mathcal{O}(x,t)\mathcal{O}|0\rangle_L + \Theta(-t)\langle 0|\mathcal{O}\mathcal{O}(x,t)|0\rangle_L \tag{4.14}$$

We can insert a complete system of finite volume energy-momentum eigenstates and use the Euclidean version of the space-time dependence (4.7). By performing the integrals we obtain

$$\Gamma(\omega,q) = \sum_N |\langle 0|\mathcal{O}|\theta_1,\dots,\theta_N\rangle_L|^2 \left\{ \frac{\delta_{q-P_N(L)}}{E_N(L)-i\omega} + \frac{\delta_{q+P_N(L)}}{E_N(L)+i\omega} \right\} \tag{4.15}$$

For a fixed q we can determine the energy levels by searching for poles in the analytically continued ω. For a generic volume and fixed momentum q the energy levels are never degenerate. Thus the poles are located at $\omega = \pm iE_N(L)$ with residue

$$\lim_{\omega\to\pm iE_N(L)} (E_N(L)\pm i\omega)\Gamma(\omega,\pm P_N(L)) = |\langle 0|\mathcal{O}|\theta_1,\dots,\theta_N\rangle_L|^2 \tag{4.16}$$

which is nothing but the square of the finite volume form factor.

In order to obtain the exponential corrections of these form factors we have to expand the two point function on the space-time cylinder in L. The Euclidean version of this cylinder can be thought of as the large size limit of the torus. On the torus we can exchange the role of the Euclidean time and space and represent the two point function as

$$\langle \mathcal{O}(x,t)\mathcal{O}\rangle_L = \Theta(x)\frac{\mathrm{Tr}[\mathcal{O}(0,t)e^{-Hx}\mathcal{O}e^{-H(L-x)}]}{\mathrm{Tr}[e^{-HL}]} + \Theta(-x)\frac{\mathrm{Tr}[\mathcal{O}e^{Hx}\mathcal{O}(0,t)e^{-H(L+x)}]}{\mathrm{Tr}[e^{-HL}]} \tag{4.17}$$

Inserting two complete system of (mirror) states denoted by $|\mu\rangle$ and $|\nu\rangle$ and exploiting the $|\langle\nu|\mathcal{O}|\mu\rangle| = |\langle\mu|\mathcal{O}|\nu\rangle|$ symmetry together with $e^{iqL}=1$ we obtain:

$$Z\Gamma(\omega,q) = \frac{2\pi}{L}\sum_{\mu,\nu} |\langle\nu|\mathcal{O}|\mu\rangle|^2 e^{-E_\nu L}\delta(P_\mu - P_\nu + \omega)\left\{ \frac{1}{E_\mu - E_\nu - iq} + \frac{1}{E_\mu - E_\nu + iq} \right\} \tag{4.18}$$

where $Z = \mathrm{Tr}[e^{-HL}]$. Note that the expansion in ν naturally corresponds to expansions in Lüscher orders. In particular we carried through a systematic expansion related to a moving one-particle state.

For a one-particle state we focus on the one-particle finite volume pole

$$\Gamma(\omega,q) = \frac{\mathcal{F}(q)^2}{E(q)+i\omega} + \dots \quad ; \qquad \mathcal{F}(q) = \langle 0|\mathcal{O}|q\rangle \tag{4.19}$$

where $E(q)$ is the exact finite volume energy with momentum q and $\mathcal{F}(q)$ is the corresponding exact finite volume form factor. We choose the phase of the one-particle

state so that $\mathcal{F}(q)$ is real and positive. We used the momentum variable to label the state, which is related to the rapidity as $q = M_{ShG} \sinh\theta_1$, such that the corresponding energy is $\mathcal{E}(q) = M_{ShG} \cosh\theta_1$. We can expand Γ around the large volume Bethe-Yang pole at $\omega = i\mathcal{E}(q)$. At the leading Lüscher order we have first and second order poles

$$\Gamma(\omega, q) = \frac{F_1^2}{L\mathcal{E}(q)} \frac{-i}{\omega - i\mathcal{E}(q)} + \frac{\mathcal{L}_0(q)}{(\omega - i\mathcal{E}(q))^2} + \frac{\mathcal{L}_1(q)}{\omega - i\mathcal{E}(q)} + \text{regular} \tag{4.20}$$

such that the leading exponential corrections of the energy and form factor can be written as

$$E(q) = \mathcal{E}(q) \left\{ 1 + \frac{L}{F_1^2} \mathcal{L}_0(q) + \dots \right\} \quad ; \quad \mathcal{F}(q) = \frac{F_1}{\sqrt{L\mathcal{E}(q)}} \left\{ 1 + \frac{iL\mathcal{E}(q)}{2F_1^2} \mathcal{L}_1(q) + \dots \right\} \tag{4.21}$$

We calculate Γ in the mirror channel (4.18). The leading order result comes from terms, when $\langle\nu|$ is the vacuum state $\langle 0|$ and $|\mu\rangle$ is a one-particle state. The leading Lüscher corrections, $\mathcal{L}_0$ and $\mathcal{L}_1$, come from terms when $\langle\nu|$ is a one-particle state and $|\mu\rangle$ is either the vacuum or a two-particle state.

Having performed the calculations we could reproduce the Lüscher correction of the 1-particle energy (4.6). For the form factors we obtained the result

$$\mathcal{F}(q) = \frac{1}{\sqrt{\rho_1^{(1)}}} \left\{ F_1 + \int_{-\infty}^{\infty} \frac{d\theta}{2\pi} F_3^{\text{reg}}(\theta + i\pi, \theta, \theta_1^{(0)} - i\frac{\pi}{2}) e^{-M_{ShG} L \cosh\theta} + \dots \right\} \tag{4.22}$$

where the density of states at the leading exponential order is

$$\rho_1^{(1)} = -i\partial_{\theta^{(1)}} \epsilon^{(1)}(\theta^{(1)} + i\frac{\pi}{2}) \tag{4.23}$$

and the regularized form factor is defined to be

$$F_3^{\text{reg}}(\theta, \theta_1, \theta_2) = F_3(\theta, \theta_1, \theta_2) - iF_1 \frac{1 - S(\theta_1 - \theta_2)}{\theta - \theta_1 - i\pi} + \frac{iF_1}{2} S'(\theta_1 - \theta_2) \tag{4.24}$$

In the following sections we derive this result and check it by a second order perturbative calculation in the sinh-Gordon theory.

4.2.1 The $0-1$ finite volume form factor of the fundamental field φ in the sinh-Gordon model

In the bootstrap quantization scheme discussed in Section 2.5, the sinh-Gordon scattering matrix is defined as

$$S(\theta) = \frac{\sinh\theta - i\alpha}{\sinh\theta + i\alpha}, \qquad \alpha = \sin\pi B, \qquad B = \frac{b^2}{1 + b^2}. \tag{4.25}$$

This can also be written as

$$S(\theta) = \exp\left\{-i\int_0^\infty \frac{\mathrm{d}x}{x}\,K(x)\sin\left(\frac{\theta x}{\pi}\right)\right\}, \tag{4.26}$$

where

$$K(x) = 8\,\frac{\sinh\frac{xB}{2}\sinh\frac{x}{2}\,(1-B)\sinh\frac{x}{2}}{\sinh x}. \tag{4.27}$$

We introduce the quantity

$$\Sigma(\Theta) = S\left(\frac{i\pi}{2}+\Theta\right). \tag{4.28}$$

The S-matrix is real analytic and satisfies crossing:

$$[S(\Theta)]^* = S(-\Theta^*), \qquad S(i\pi-\Theta) = S(\Theta), \tag{4.29}$$

from which we conclude that $\Sigma(\Theta)$ is real for real Θ and satisfies

$$\Sigma(\Theta) = \Sigma(-\Theta). \tag{4.30}$$

An important building block of the form factors is the minimal 2-particle form factor [90, 156]:

$$F_{\min}(\beta) = \exp\left\{-\frac{1}{2}\int_0^\infty \frac{\mathrm{d}x}{x}\,K(x)\frac{\cos\frac{x}{\pi}(i\pi-\beta)}{\sinh x}\right\}. \tag{4.31}$$

It is also useful to note the following properties of the minimal form factor:

$$F_{\min}(i\pi-\beta) = F_{\min}(i\pi+\beta), \qquad F_{\min}(\beta) = S(\beta)F_{\min}(-\beta), \tag{4.32}$$

$$F_{\min}(i\pi+\beta)F_{\min}(\beta) = \frac{\sinh\beta}{\sinh\beta+i\alpha}. \tag{4.33}$$

The 3-particle form factor is written as

$$F_3(\beta_1,\beta_2,\beta_3) = \frac{4\alpha F_1}{F_{\min}(i\pi)}\,x_1x_2x_3\frac{F_{\min}(\beta_1-\beta_2)}{x_1+x_2}\frac{F_{\min}(\beta_1-\beta_3)}{x_1+x_3}\frac{F_{\min}(\beta_2-\beta_3)}{x_2+x_3}, \tag{4.34}$$

where $x_j = \mathrm{e}^{\beta_j}$. Removing the singular part we can calculate the subtracted form factor

$$\hat{F}_3(u+i\pi,u,-\frac{i\pi}{2}+\theta) = iF_1[1-\Sigma(w)]\left\{-\frac{1}{2}\,\frac{\mathrm{e}^w-i}{\mathrm{e}^w+i}+\frac{F'_{\min}(\frac{3i\pi}{2}+w)}{F_{\min}(\frac{3i\pi}{2}+w)}\right\}, \tag{4.35}$$

where $w = u-\theta$. Adding the S-matrix derivative contribution and noting that the odd

(in w) terms cancel, we find

$$F_3^{\rm reg}(u+i\pi,u,-\frac{i\pi}{2}+\theta)=-\alpha F_1\frac{1}{\cosh w+\alpha}\left\{\frac{1}{\cosh w}+\frac{1}{2\pi}\int_0^\infty {\rm d}x\,K(x)\frac{\cos\frac{xw}{\pi}}{\cosh\frac{x}{2}}\right\}. \tag{4.36}$$

Using that the gaudin determinant of eq. (4.23) can be written explicitly as

$$\rho_1^{(1)}(q)=M_{ShG}L\cosh\theta\left\{1+\frac{1}{2\pi}\int_{-\infty}^\infty {\rm d}u\,{\rm e}^{-M_{ShG}L\cosh u}\sinh u\left[\frac{\sinh\theta}{\cosh^2\theta}\Sigma(u-\theta)+\frac{\Sigma'(u-\theta)}{\cosh\theta}\right]\right\} \tag{4.37}$$

one can compute the additional terms of the Lüscher correction in eq. (4.22) coming from the normalization:

$$\frac{1}{2\pi}\int_{-\infty}^\infty {\rm d}u\,{\rm e}^{-M_{ShG}L\cosh u}\frac{\alpha}{\cosh^2\theta(\cosh w+\alpha)^2}\left\{\alpha\sinh u\sinh\theta+\cosh^2\theta-\cosh^2 w\right\}. \tag{4.38}$$

We can expand (4.36) and (4.38) in the coupling α:

$$\frac{1}{F_1}F_3^{\rm reg}(u+i\pi,u,-\frac{i\pi}{2}+\theta)=-\alpha\frac{1}{\cosh^2 w}+\alpha^2\left\{\frac{1}{\cosh^3 w}+\frac{2}{\pi}\left[\frac{w\sinh w}{\cosh^3 w}-\frac{1}{\cosh^2 w}\right]\right\}+{\rm O}(\alpha^3), \tag{4.39}$$

and the remaining terms give

$$\alpha\left(\frac{1}{\cosh^2 w}-\frac{1}{\cosh^2\theta}\right)+\alpha^2\left\{\frac{\sinh u\sinh\theta}{\cosh^2\theta\cosh^2 w}+\frac{2}{\cosh^2\theta\cosh w}-\frac{2}{\cosh^3 w}\right\}+{\rm O}(\alpha^3). \tag{4.40}$$

The perturbative expansion of the full Lüscher correction is

$$\begin{aligned}\delta\mathcal{F}(q)=\int_{-\infty}^\infty {\rm d}u\,{\rm e}^{-M_{ShG}L\cosh u}\Bigg\{&-\frac{\alpha}{2\pi\cosh^2\theta}+\frac{\alpha^2}{2\pi}\Bigg(\frac{\sinh u\sinh\theta}{\cosh^2\theta\cosh^2 w}\\&+\frac{2}{\cosh^2\theta\cosh w}-\frac{1}{\cosh^3 w}+\frac{2}{\pi}\left[\frac{w\sinh w}{\cosh^3 w}-\frac{1}{\cosh^2 w}\right]\Bigg)\Bigg\}+{\rm O}(\alpha^3).\end{aligned} \tag{4.41}$$

We have checked the form factor (4.41) by direct second order perturbative calculations. These calculations are presented in Section 4.3 and in Appendix F.

4.3 Hamiltonian perturbation theory for the (exact) volume-dependence of the $0-1$ form factor

In this section, we use time-independent perturbation theory in the finite volume sinh-Gordon theory in order to test the leading Lüscher corrections both to the one-particle energy and form factor.

4.3.1 Finite volume form of the Hamiltonian

In the present section we change our conventions slightly to be consistent with the usual (textbook) normalization of the free massive boson. We will fix $g = 1$ but rescale the coupling b by an explicit $\sqrt{8\pi}$ factor such that the self-dual point still corresponds to $b = 1$.

The sinh-Gordon model in a finite volume L is described by a Hamilton operator H_L of the following form

$$H_L = H_L^0 + V_L \tag{4.42}$$

where $H_L^0 = \int_0^L dx \ : \ \frac{1}{2}\pi^2 + \frac{1}{2}\left(\partial_x\varphi\right)^2 + \frac{1}{2}m^2\varphi^2 \ :_{m,L}$ is a free Hamiltonian, and

$$V_L = \int_0^L dx \ : \ \frac{m^2}{8\pi b^2}\left(\cosh\left(\sqrt{8\pi}b\varphi\right) - 1\right) - \frac{m^2}{2}\varphi^2 \ :_{m,L} + \mathcal{O}\left(e^{-mL}\right) \tag{4.43}$$

contains the interaction. The field operator admits a mode expansion

$$\varphi\left(x,t\right) = \sum_{n\in\mathbb{Z}} \frac{1}{\sqrt{2L\omega_n}}\left(a_n e^{i(k_n x - \omega_n t)} + a_n^\dagger e^{-i(k_n x - \omega_n t)}\right) \tag{4.44}$$

$$\omega_n = \sqrt{m^2 + k_n^2}, \quad k_n = \frac{2\pi n}{L} \tag{4.45}$$

where the ladder operators satisfy the usual bosonic commutation relations $\left[a_n, a_m^\dagger\right] = \delta_{n,m}$ and $\left[a_n, a_m\right] = 0$. The normal ordering $: :_{m,L}$ is understood in the sense that creation operators (creating a particle of mass m in the free theory of volume L) are arranged to the left of the annihilation operators.

The spectrum of H_L^0 is generated by acting with creation operators on the lowest energy state, the vacuum $|0\rangle$:

$$\left|N_{n_1}, N_{n_2}, \ldots, N_{n_k}\right\rangle = \frac{1}{\mathcal{N}\left(\{N_{n_i}\}\right)} \prod_{i=1}^{k} \left(a_{n_i}^\dagger\right)^{N_{n_i}} |0\rangle, \quad n_i \in \mathbb{Z} \tag{4.46}$$

$$H_L^0 \left|N_{n_1}, N_{n_2}, \ldots, N_{n_k}\right\rangle = \sum_i N_{n_i}\omega_{n_i} \tag{4.47}$$

where we have introduced the symbol

$$\mathcal{N}\left(\{N_{n_i}\}\right) = \sqrt{\prod_{i=1}^{k} N_{n_i}!} \tag{4.48}$$

The exponential corrections to V_L indicated in (4.43) are due to the following [114]. In infinite volume, the sinh-Gordon Hamiltonian is naturally expressed in terms of operators normal ordered with respect to the ladder operators of an infinite volume

free theory. As we decrease the volume, we want to keep the UV behaviour of the theory unaffected, which means leaving the coefficients of the *bare* fields unchanged (instead of the normal ordered ones) in the Hamiltonian density. By temporarily introducing a UV regulator Λ, normal ordered powers of the field can be expressed in terms of the bare powers by utilizing Wick's theorem:

$$\varphi^n(x,t) = \sum_{k=0}^{\lfloor n/2 \rfloor} \frac{n!}{2^k k!\,(n-2k)!} \left(\left\langle 0 \left| \varphi^2 \right| 0 \right\rangle_{m,L} \right)^k \; : \; \varphi^{n-2k} \; :_{m,L} \tag{4.49}$$

where $|0\rangle$ is the ground state of H_L^0. Moreover,

$$\left\langle 0 \left| \varphi^2 \right| 0 \right\rangle_{m,L} = [\varphi_+, \varphi_-] = \frac{1}{2L} \sum_{n=-N_\Lambda}^{N_\Lambda} \frac{1}{\omega_n} \tag{4.50}$$

$$\left\langle 0 \left| \varphi^2 \right| 0 \right\rangle_{m,\infty} = [\varphi_+, \varphi_-] = \frac{1}{4\pi} \int_{-\Lambda}^{\Lambda} \frac{dk}{\omega_k}. \tag{4.51}$$

One can use Equation (4.49) together with (4.50) and (4.51) to derive the exponential corrections arising from the different normal ordering prescriptions at finite and infinite volume.

After eliminating the cutoff Λ we arrive at the exact form of the finite volume interaction term

$$V_L = \int_0^L dx \; : \; \frac{m^2 e^{\pi \bar{\rho} b^2}}{8\pi b^2} \left(\cosh\left(\sqrt{8\pi} b \varphi \right) - 1 \right) - \frac{m^2}{2} \varphi^2 \; :_{m,L} + E_0(L) \tag{4.52}$$

where

$$\bar{\rho} = \frac{2}{\pi} \int_{-\infty}^{\infty} du \frac{1}{e^{mL \cosh u} - 1} \tag{4.53}$$

The bar indicates that now the bare Lagrangian parameter m appears in the exponent. Furthermore, E_0 is a (scalar) Casimir term whose value can be calculated exactly but does not affect the masses and form factors, and therefore we now neglect it.

It is possible to expand the interaction term (4.52) in the coupling b to yield

$$V_L = b^2 V_L^{(1)} + b^4 V_L^{(2)} + \mathcal{O}\left(b^6\right) \tag{4.54}$$

$$V_L^{(1)} = 2\pi m^2 \left(\frac{1}{6} O_4 + \frac{\bar{\rho}}{4} O_2 \right) \quad ; \qquad V_L^{(2)} = 4\pi^2 m^2 \left(\frac{1}{45} O_6 + \frac{\bar{\rho}}{12} O_4 + \frac{\bar{\rho}^2}{16} O_2 \right) \tag{4.55}$$

where

$$O_n = \int_0^L : \varphi^n(x) :_{m,L} dx. \tag{4.56}$$

4.3.2 Time-independent perturbation theory

Since H_L has a discrete spectrum, one can treat it as a conventional quantum mechanical Hamilton-operator and attempt to approximate the eigenvalues and eigenvectors employing time-independent perturbation theory. The corrections of the energies (non-degenerate in the free theory) up to $O(b^4)$ can be written in the form

$$E_n = E_n^{(0)} + b^2 E_n^{(1)} + b^4 E_n^{(2)} + \mathcal{O}\left(b^6\right), \tag{4.57}$$

$$E_n^{(1)} = \left\langle n \left| V_L^{(1)} \right| n \right\rangle \equiv V_{nn}^{(1)} \tag{4.58}$$

$$E_n^{(2)} = V_{nn}^{(2)} + {\sum_{|k\rangle\in\mathcal{H}}}' \frac{\left|V_{kn}^{(1)}\right|^2}{E_{nk}^{(0)}} \quad ; \qquad E_{nk}^{(0)} = E_n^{(0)} - E_k^{(0)} \quad ; \qquad V_{kn}^{(i)} = \left\langle k \left| V_L^{(i)} \right| n \right\rangle \tag{4.59}$$

In the above, $E_n^{(0)}$ denotes the energy of the nth lowest energy state in the free theory, the state vectors $|n\rangle, |m\rangle$ are understood to be the eigenvectors of H_L^0, and the sum in (4.59) is for all elements of an eigenbasis of H_L^0, except for $|n\rangle$ itself, which is indicated by $\sum'$. Correspondingly, the expansion of the interacting eigenvectors has the form

$$|n(b)\rangle = |n\rangle + b^2 |n\rangle^{(1)} + b^4 |n\rangle^{(2)} + \mathcal{O}\left(b^6\right), \tag{4.60}$$

$$\left|n^{(1)}\right\rangle = {\sum_{|k\rangle\in\mathcal{H}}}' \frac{V_{kn}^{(1)}}{E_{nk}^{(0)}} |k\rangle \tag{4.61}$$

$$\begin{aligned}\left|n^{(2)}\right\rangle = &{\sum_{|k\rangle\in\mathcal{H}}}' \frac{V_{kn}^{(2)}}{E_{nk}^{(0)}} |k\rangle + {\sum_{|k\rangle,|l\rangle\in\mathcal{H}}}'' \frac{V_{kl}^{(1)} V_{ln}^{(1)}}{E_{nk}^{(0)} E_{nl}^{(0)}} |k\rangle - {\sum_{|k\rangle\in\mathcal{H}}}' \frac{V_{nn}^{(1)} V_{kn}^{(1)}}{(E_{nk}^{(0)})^2} |k\rangle \\ &- \frac{1}{2} {\sum_{|k\rangle\in\mathcal{H}}}' \frac{V_{nk}^{(1)} V_{kn}^{(1)}}{(E_{nk}^{(0)})^2} |n\rangle\end{aligned} \tag{4.62}$$

where we indicated by $\sum''$ that we leave out from the sum the $|k\rangle = |n\rangle$ and $|l\rangle = |n\rangle$ terms. The vector $|n(b)\rangle$ at each order is normalized to 1.

4.3.3 Corrections to the one-particle energy

In the following, we use perturbation theory to calculate the energy corrections to a one-particle state at leading and next to leading orders.

4.3.3.1 $\mathcal{O}(b^2)$ correction

For a one-particle state $|q(b)\rangle$, having momentum $q = 2\pi n_q L^{-1}$ in the free theory, the sole first-order ($\mathcal{O}(b^2)$) contribution to the energy difference $E(q) - E_0$ comes from the expectation value

$$\frac{\pi}{2} m^2 b^2 \bar{\rho} \langle n_q | O_2 | n_q \rangle . \tag{4.63}$$

One can evaluate the matrix element using the mode expansion (4.44), the explicit form of Fock vectors (4.46) and the commutation relations of ladder operators. As a result, one gets

$$E(q) - E_0 = \omega_{n_q} + b^2 \frac{\pi m^2 \bar{\rho}}{2\omega_{n_q}} + \mathcal{O}\left(b^4\right) \tag{4.64}$$

4.3.3.2 $\mathcal{O}(b^4)$ correction

The second corrections can be obtained by a more extended, but mostly straightforward calculation. Let us summarize the general scheme of the computation.

1. First, observe that due to the absolute square appearing in (4.59) and the fact that V_L starts with terms proportional to b^2, only $V_L^{(1)}$ contributes to this order. Besides, O_2 and O_4 will only have nonzero matrix elements between states of equal overall momenta. Furthermore, due to normal ordering, the following restrictions apply to the Hilbert space sum in the above formula:

   (a) $\langle k | O_2 | 0 \rangle$ is only nonzero if $|k\rangle$ is a two-particle state;

   (b) $\langle k | O_4 | 0 \rangle$ is only nonzero if $|k\rangle$ is a four-particle state;

   (c) $\langle k | O_2 | n_q \rangle$ is only nonzero if $|k\rangle$ is a three-particle state (for a one-particle state, $|k\rangle$ should be equal to $|n_q\rangle$ due to momentum conservation. However, this term is excluded from the sum);

   (d) $\langle k | O_4 | n_q \rangle$ is only non-zero for $|k\rangle$ containing either 3 or 5 particles.

2. One then evaluates the relevant matrix elements $\langle k_1, k_2 | O_2 | 0 \rangle$, $\langle k_1, k_2, k_3, k_4 | O_4 | 0 \rangle$, $\langle k_1, k_2, k_3 | O_2 | n_q \rangle$,
   $\langle k_1, k_2, k_3 | O_4 | n_q \rangle$ and $\langle k_1, k_2, k_3, k_4, k_5 | O_4 | n_q \rangle$ by commuting creation-annihilation operators. After collecting the symmetry factors arising from the fact that some subsets of $\{k_i\}$ might be equal, these matrix elements simply turn out to be proportional to the symbol $1/\mathcal{N}(\{k_i\})$ (which comes from normalization) and generally consist of a sum of multiple terms containing a product of momentum-dependent Kronecker-deltas. For example,

$$\langle k_1, k_2, k_3 | O_2 | n_q \rangle = \frac{1}{\mathcal{N}(k_1, k_2, k_3)} \left(\frac{\delta_{k_3, n_q} \delta_{k_1 + k_2, 0}}{\omega_{k_1}} + \frac{\delta_{k_2, n_q} \delta_{k_1 + k_3, 0}}{\omega_{k_1}} + \frac{\delta_{k_1, n_q} \delta_{k_2 + k_3, 0}}{\omega_{k_2}} \right)$$

3. Finally, these matrix elements are substituted back to (4.59), and the Kronecker deltas reduce the appropriately restricted sums. Here another symmetry factor arises because permutations of the ordering of different momenta written inside a Fock vector $|k_1, \ldots, k_i\rangle$ denotes the same vector in the Hilbert space. This symmetry factor cancels the $1/\mathcal{N}$s coming from the matrix elements.

This calculation leads to a linear combination of single, double and triple sums. The triple sums fortunately cancel, and we arrive at the following $\mathcal{O}(b^4)$ result:

$$\begin{aligned} E(q) - E_0 &= \omega_{n_q} + b^2 \frac{\pi}{2} \frac{m^2}{\omega_{n_q}} \bar{\rho} + b^4 \left(\frac{\pi^2}{4} \frac{m^2}{\omega_{n_q}} \bar{\rho}^2 - \frac{\pi^2}{8} \frac{m^4}{\omega_{n_q}^3} \bar{\rho}^2 \right) - b^4 \frac{\pi^2}{2} \frac{m^4}{\omega_{n_q}} \bar{\rho} \frac{1}{L} \sum_{k \in \mathbb{Z}} \frac{1}{\omega_k^3} \\ &\quad - b^4 \frac{2\pi^2}{3} \frac{m^4}{\omega_{n_q}} \frac{1}{L^2} \sum_{k_1, k_2 \in \mathbb{Z}} D_1(k_1, k_2) + \mathcal{O}\left(b^6\right) \end{aligned} \tag{4.65}$$

where

$$\begin{aligned} D_1(k_1, k_2) = \frac{1}{\omega_{k_1} \omega_{k_2} \omega_{k_1+k_2-n_q}} \Bigg(& \frac{1}{\omega_{k_1} + \omega_{k_2} + \omega_{k_1+k_2-n_q} + \omega_{n_q}} \\ & + \frac{1}{\omega_{k_1} + \omega_{k_2} + \omega_{k_1+k_2-n_q} - \omega_{n_q}} \Bigg). \end{aligned} \tag{4.66}$$

4.3.3.3 Extracting Lüscher corrections

The single and double sums appearing in (4.65) can be transformed into integrals by a method well-known from complex analysis. The idea is to introduce a complex function with an infinite number of poles at appropriate positions along the real line, such that one can reproduce a sum through a contour integral. In general, for a sum $\sum_{n \in \mathbb{Z}} f(n)$, one such integral representation is provided by

$$\sum_{n \in \mathbb{Z}} f\left(\frac{2\pi n}{L}\right) = \frac{L}{2\pi} \int_C dz \frac{e^{iLz}}{e^{iLz} - 1} f(z) \tag{4.67}$$

where the closed contour C moves from $-\infty - i\epsilon$ to $+\infty - i\epsilon$ infinitesimally below the real line, then from $\infty + i\epsilon$ to $-\infty + i\epsilon$ just above the real line (additional care is needed when $f(z)$ is not holomorphic in the region enclosed by C). Then the contour C can be blown up assuming $f(z)$ is analytic on the complex plane, except possibly a number of poles and branch cuts. If $f(z)$ decays rapidly enough at complex infinity, then the original sum can be turned into another one containing residual terms and integrals corresponding to different poles and branch cuts of $f(z)$.

For example, the sum $\sum_{n \in \mathbb{Z}} \frac{1}{\omega_n^3}$ does not lead to additional poles in $f(z) = (m^2 + z^2)^{-3/2}$. It has, however, two branch points at $z = \pm im$. The two branch cuts lie along the imaginary axis of the z plane. One connects im and $i\infty$, the other starts at $-im$ and

goes down to $-i\infty$. Upon deforming the contour, the neighbourhood of the branch cut singularities needs careful analysis. The integrals coming from tightening the contour to the lower and upper branch cuts can be mapped onto each other. Then, after a variable change $u \to \cosh u$ and symmetrization in the integration domain, one gets

$$\sum_{k=-\infty}^{\infty} \frac{1}{\omega_k^3} = \frac{L}{\pi m^2} \left(1 + mL \int_{-\infty}^{\infty} du \frac{e^{mL\cosh u}}{\left(e^{mL\cosh u}-1\right)^2} \cosh u \right) \tag{4.68}$$

Transforming the double sum is more complicated. For later purposes it is advantageous to separate the $k_2 = n_q$ part of the sum:

$$\sum_{k_1,k_2\in\mathbb{Z}} D_1(k_1,k_2) = \sum_{k_1\in\mathbb{Z}} \sum_{k_2\neq n_q} D_1(k_1,k_2) + \frac{1}{2\omega_{n_q}} \sum_{k_1\in\mathbb{Z}} \frac{1}{\omega_{k_1}^3} + \frac{1}{2\omega_{n_q}} \sum_{k_1\in\mathbb{Z}} \frac{1}{\omega_{k_1}^2} \frac{1}{\omega_{k_1}+\omega_{n_q}} \tag{4.69}$$

The last term is easily seen to be a particular case of the integral formula

$$\sum_{k_1\in\mathbb{Z}} \frac{1}{\omega_{k_1}^2} \frac{1}{A+\omega_{k_1}} = \frac{L}{2Am} \coth\frac{mL}{2} - \frac{L}{2\pi} \int_{-\infty}^{\infty} du \frac{\coth\left(\frac{mL}{2}\cosh u\right)}{A^2+m^2\sinh^2 u}. \tag{4.70}$$

After a lengthy calculation, which we spell out in Appendix F, we obtain the following representation of the double sum:

$$\sum_{k_1,k_2} D_1(k_1,k_2) = \frac{L^2}{m^2} \left(\frac{1}{8} + 3 \int_{-\infty}^{\infty} \frac{du}{2\pi} \frac{e^{mL\cosh u}}{\left(e^{mL\cosh u}-1\right)^2} \frac{1}{\cosh(u-\theta)} \right) \tag{4.71}$$

where we introduced θ as the rapidity variable $q = m\sinh\theta$.

We can now give an integral representation of the $\mathcal{O}(b^4)$ one-particle energy, from which one can read all the $\mathcal{O}(b^4)$ Luscher corrections directly:

$$\begin{aligned} E(\theta) - E_0 = {} & m\cosh\theta + b^2 \frac{\pi}{2} \frac{m}{\cosh\theta} \bar{\rho} + b^4 \left(\frac{\pi^2}{4} \frac{m}{\cosh\theta} \bar{\rho}^2 - \frac{\pi^2}{8} \frac{m}{\cosh^3\theta} \bar{\rho}^2 \right) \\ & - b^4\pi^2 \frac{m}{\cosh\theta} \bar{\rho} \frac{1}{2\pi} - b^4\pi^2 \frac{m}{\cosh\theta} \bar{\rho} mL \int_{-\infty}^{\infty} \frac{du}{2\pi} \frac{e^{mL\cosh u}}{\left(e^{mL\cosh u}-1\right)^2} \cosh u - b^4 \frac{\pi^2}{12} \frac{m}{\cosh\theta} \\ & - b^4 2\pi^2 \frac{m}{\cosh\theta} \int_{-\infty}^{\infty} \frac{du}{2\pi} \frac{e^{mL\cosh u}}{\left(e^{mL\cosh u}-1\right)^2} \frac{1}{\cosh(u-\theta)} + \mathcal{O}\left(b^6\right) \end{aligned} \tag{4.72}$$

As a final step, we expand this result in the bootstrap parameter α

$$\alpha = \sin\frac{\pi b^2}{1+b^2} \Leftrightarrow b^2 = \frac{\alpha}{\pi} + \frac{\alpha^2}{\pi^2} + \mathcal{O}\left(\alpha^3\right) \tag{4.73}$$

up to $\mathcal{O}(\alpha^2)$. The $\mathcal{O}(\alpha^2)$ term arising from the $\mathcal{O}(b^2)$ correction of the energy cancels with another term in (4.72). Using the trigonometric identity

$$\frac{\cosh u}{\cosh\theta} = \frac{1}{\cosh(u-\theta)} + \frac{\sinh u}{\cosh\theta}\tanh(u-\theta) \tag{4.74}$$

and integrating by parts, we arrive at

$$\begin{aligned} E(\theta) - E_0 = m\cosh\theta + \alpha\frac{m\bar{\rho}}{2\cosh\theta} - \frac{\alpha^2}{12}\frac{m}{\cosh\theta} + \frac{\alpha^2 m}{\cosh\theta}\Bigg[\left(1+\tanh^2\theta\right)\frac{\bar{\rho}^2}{8} \\ - \left(\frac{mL\bar{\rho}}{2}\cosh\theta + 1\right)\bar{\xi}_1(\theta) - \frac{\bar{\rho}}{2}\bar{f}_2(\theta)\Bigg] + \mathcal{O}\left(\alpha^3\right) \end{aligned} \tag{4.75}$$

where we introduced the functions

$$\bar{\xi}_1(\theta) = \int_{-\infty}^{\infty}\frac{du}{\pi}\frac{e^{mL\cosh u}}{\left(e^{mL\cosh u}-1\right)^2}\frac{1}{\cosh(u-\theta)} \tag{4.76}$$

$$\bar{f}_k(\theta) = \int_{-\infty}^{\infty}\frac{du}{\pi}\frac{1}{e^{mL\cosh u}-1}\frac{1}{\cosh^k(u-\theta)} \tag{4.77}$$

However, since the first correction to the physical mass is of order α^2, in an $\mathcal{O}(\alpha^2)$ formula we can omit the bars and arrive at the result from TBA what we calculate in Appendix E.

4.3.4 Corrections to the form factor $\langle 0(b)|\varphi|q(b)\rangle$

By an analogous, albeit more cumbersome calculation, we can obtain the coupling-expanded finite volume form factors and extract their first Lüscher correction. Using the eigenstate expansion (4.62), we can expand the form factor as

$$\langle 0(b)|\varphi|q(b)\rangle = \langle 0|\varphi|q\rangle \qquad \left(\text{order } b^0\right) \tag{4.78}$$

$$+\left\langle 0^{(1)}|\varphi|q\right\rangle + \left\langle 0|\varphi|q^{(1)}\right\rangle \qquad \left(\text{order } b^2\right) \tag{4.79}$$

$$+\left\langle 0^{(2)}|\varphi|q\right\rangle + \left\langle 0^{(1)}|\varphi|q^{(1)}\right\rangle + \left\langle 0|\varphi|q^{(2)}\right\rangle \qquad \left(\text{order } b^4\right) \tag{4.80}$$

$$+\mathcal{O}(b^6). \tag{4.81}$$

Note that since we are effectively working in Schrödinger picture, operators are time-independent, and as a consequence, we can use the free field operator (4.44) in calculating these matrix elements.

4.3.4.1 $\mathcal{O}(b^2)$ correction

The zeroth-order term $\langle 0|\varphi|q\rangle$ is easy to evaluate and in our normalization its value is

$$\langle 0|\varphi|q\rangle = \frac{1}{\sqrt{2L\omega_{n_q}}}. \tag{4.82}$$

The first order contribution comes solely from the $\langle 0|\varphi|q^{(1)}\rangle$ term. It takes the form

$$\langle 0|\varphi|q^{(1)}\rangle = -\frac{1}{\sqrt{2L\omega_{n_q}}}\frac{m^2b^2\pi\bar{\rho}}{4\omega_{n_q}^2} \tag{4.83}$$

4.3.4.2 $\mathcal{O}(b^4)$ correction

Following the steps outlined in subsection 5.3.2, an even lengthier calculation leads us to an explicit (volume-exact) order b^4 correction to the form factor in the form of single, double and triple sums.[2] Again, the triple sums cancel, leading to

$$\begin{aligned}\langle 0(b)|\varphi|q(b)\rangle = \frac{1}{\sqrt{2L\omega_{n_q}}}\Big\{1 - \frac{m^2b^2\pi\bar{\rho}}{4\omega_{n_q}^2} + N_0 + \frac{m^4\pi^2b^4\bar{\rho}}{8L}\sum_k S_1(k) \\ + \frac{m^4\pi^2b^4}{3L^2}\sum_{k_1,k_2}\Big(\frac{D_1(k_1,k_2)}{\omega_{n_q}^2} + \frac{D_2(k_1,k_2)}{\omega_{n_q}}\Big)\Big\}\end{aligned} \tag{4.84}$$

where

$$\begin{aligned} N_0 &= \frac{\pi^2b^4\bar{\rho}^2}{8}\left(\frac{5m^4}{4\omega_{n_q}^4} - \frac{m^2}{\omega_{n_q^2}}\right) \\ S_1(k) &= \frac{1}{\omega_{n_q}^2\omega_k^3} + \frac{1}{\omega_{n_q}^2\omega_k^2\left(\omega_{n_q}+\omega_k\right)} + \frac{1}{\omega_{n_q}\omega_k^3\left(\omega_{n_q}+\omega_k\right)} \\ D_2(k_1,k_2) &= \frac{1}{\omega_{k_1}\omega_{k_2}\omega_{k_1+k_2-n_q}}\Big(\Big(\frac{1}{\omega_{k_1}+\omega_{k_2}+\omega_{k_1+k_2-n_q}+\omega_{n_q}}\Big)^2 \\ &\quad - \Big(\frac{1}{\omega_{k_1}+\omega_{k_2}+\omega_{k_1+k_2-n_q}-\omega_{n_q}}\Big)^2\Big)\end{aligned} \tag{4.85}$$

and $D_1(k_1,k_2)$ was defined in (4.66).

4.3.4.3 Extracting first Lüscher correction

We proceed with the complex analytical method presented previously to transform the sums to integrals from which we will obtain the Lüscher corrections. We have already seen the integral representations of some (parts) of these sums in formulas (4.68), (4.70) and (4.71). The only single sum appearing in $\sum_k S_1(k)$ not covered before is a special

[2]Note that no O_6 matrix element gives a contribution to the result; therefore, the infinite-volume limit of the results obtained here are the same as in the φ^4 theory. The finite-volume behaviour is, however, different from the φ^4 case because V_L gets different corrections.

case of the following sum possessing the integral representation

$$\sum_k \frac{1}{\omega_k^3 (A+\omega_k)} = -\frac{L}{2mA^2}\coth\left(\frac{mL}{2}\right) + \frac{LA}{m^2}\int\limits_{-\infty}^{\infty}\frac{du}{2\pi}\left[\frac{mL\cosh u}{2\sinh^2\left(\frac{mL}{2}\cosh u\right)\left(A^2+m^2\sinh^2 u\right)}\right.$$
$$\left. + \frac{2m^2\cosh^2 u\coth\left(\frac{mL}{2}\cosh u\right)}{\left(A^2+m^2\sinh^2 u\right)^2}\right] \tag{4.86}$$

The transformations of the double sums $\sum_{k_1,k_2} D_2(k_1,k_2)$ into integrals can be done similarly to the case $\sum_{k_1,k_2} D_i(k_1,k_2)$, which one can then expand for large volumes. The detailed calculations are relegated to Appendix F and results in

$$\langle 0(b)|\varphi|q(b)\rangle = \frac{1}{\sqrt{2Lm\cosh\theta}}\left\{1-\alpha\int\frac{du}{2\pi}\left[\frac{e^{-mL\cosh u}}{\cosh^2\theta}\right] + \alpha^2\left(\frac{1}{48}+\frac{1}{24\cosh^2\theta}\right.\right.$$
$$\left. -\frac{1}{4\pi^2}\right) + \alpha^2\int\limits_{-\infty}^{\infty}\frac{du}{2\pi}e^{-mL\cosh u}\left[\frac{\sinh u\sinh\theta}{\cosh^2\theta\cosh^2 w}+\frac{2}{\cosh^2\theta\cosh w}\right.$$
$$\left.\left. -\frac{1}{\cosh^3 w}+\frac{2}{\pi}\left(\frac{w\sinh w}{\cosh^3 w}-\frac{1}{\cosh^2 w}\right)\right]+\dots\right. \tag{4.87}$$

Finally, expressing the right-hand side in terms of the physical mass

$$M_{ShG} = m - \frac{\alpha^2}{12}m + \mathcal{O}\left(\alpha^3\right) \tag{4.88}$$

we obtain our final result:

$$\langle 0(b)|\varphi|q(b)\rangle = \frac{1}{\sqrt{2LM_{ShG}\cosh\theta}}\left\{1-\alpha\int\frac{du}{2\pi}\left[\frac{e^{-M_{ShG}L\cosh u}}{\cosh^2\theta}\right] + \alpha^2\left(\frac{1}{48}-\frac{1}{4\pi^2}\right)\right.$$
$$+\alpha^2\int\limits_{-\infty}^{\infty}\frac{du}{2\pi}e^{-M_{ShG}L\cosh u}\left[\frac{\sinh u\sinh\theta}{\cosh^2\theta\cosh^2 w}+\frac{2}{\cosh^2\theta\cosh w}-\frac{1}{\cosh^3 w}\right.$$
$$\left.\left.+\frac{2}{\pi}\left(\frac{w\sinh w}{\cosh^3 w}-\frac{1}{\cosh^2 w}\right)\right]+\dots\right. \tag{4.89}$$

which entirely agrees with the perturbative expansion of our exact Lüscher correction. We perform an alternative check using Lagrangian perturbation theory in our paper [127].

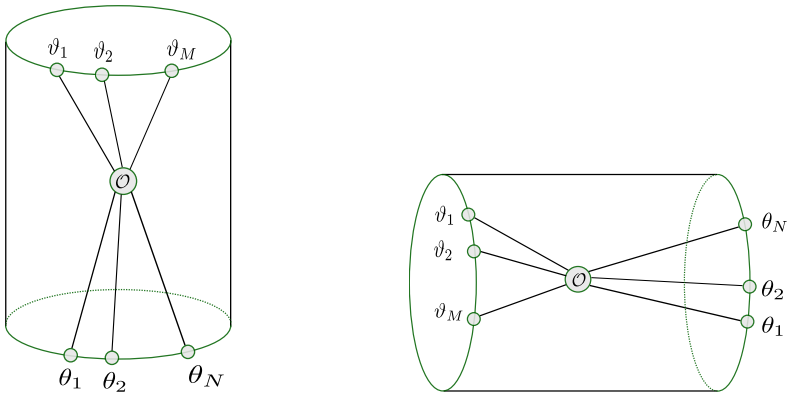

Figure 4.1: On the left: graphical representation of a finite volume form factor with incoming state $|\theta_1, \dots, \theta_N\rangle$ and outgoing state $|\vartheta_1, \dots, \vartheta_M\rangle$. Particles' trajectories are schematically drawn as solid lines and the operator $\mathcal{O}$ is represented as a circle. On the right: the same form factor is represented after double Wick rotation in the thermal channel, i.e. when the Euclidean time is finite and space is infinite.

4.4 Formal derivation for the first Lüscher correction of the general nondiagonal form factor

In this section we give a formal derivation for the F-term of the form factors' finite size correction. In the sinh-Gordon theory this is the leading exponential correction while in theories with bound states it is also intimately related to the μ-term correction [128]. We parametrize the form factor as

$$\langle\{m\}|\mathcal{O}|\{n\}\rangle_L = \frac{F_{N+M}(\{\bar{\vartheta}^{(1)}+i\pi\},\{\bar{\theta}^{(1)}\}) + \delta^{(F)}F_{N+M}(\{\bar{\vartheta}^{(0)}+i\pi\},\{\bar{\theta}^{(0)}\})}{\sqrt{\prod_{i<j}S(\bar{\vartheta}^{(1)}_{j,i})\rho^{(1)}_M(\{\bar{\vartheta}^{(1)}\})\prod_{i<j}S(\bar{\theta}^{(1)}_{i,j})\rho^{(1)}_N(\{\bar{\theta}^{(1)}\})}} \tag{4.90}$$

The quantities denoted with superscript (1) are meant to contain the leading exponential finite volume corrections. The denominator is simply related to the normalization of states. In particular, the Gauden determinant $\rho^{(1)}(\{\bar{\vartheta}\})$ consists of the matrix elements

$$R^{(1)}_{jk} = -i\partial_{\vartheta_j}\epsilon^{(1)}\left(\vartheta_k + \frac{i\pi}{2}\right) \tag{4.91}$$

with $\epsilon^{(1)}$ given in 4.1. The numerator is represented graphically on the left part of Figure 4.1. Exchanging the role of Euclidean space and time leads to the picture on the right of Figure 4.1, where we have to calculate a normalized trace:

$$\frac{\mathrm{Tr}(e^{-LH}\mathcal{O}_{N,M})}{\sqrt{\mathrm{Tr}_N(e^{-LH})\mathrm{Tr}_M(e^{-LH})}} \tag{4.92}$$

In this channel $\mathcal{O}_{N,M}$ is not a local operator as moving a particle with rapidity v around it picks up the phase $\prod_j S(v-\theta_j-\frac{i\pi}{2})\prod_k S(\vartheta_k+i\frac{\pi}{2}-v)$. This is the reason why we cannot apply a finite volume regularization as the system cannot be made

periodic: the past/future or the left/right asymptotics are different. Particularly, in case of diagonal form factors, there is no monodromy and we could impose a periodic boundary condition in a finite volume. Clearly the normalization in this case would be the excited state partition function: $Z_N = \mathrm{Tr}_N(e^{-LH})$ which can be represented graphically as shown on Figure 4.2. A particle with rapidity θ act in this channel as a defect operator with transmission factor $T(v) = S(\frac{i\pi}{2} + \theta - v)$. In the general non-diagonal case, we have the defect operator of the outgoing state on the left half space and that of the incoming excited state on the right half. These half spaces are taken into account by the square roots in the normalization of eq. (4.92). This normalization factor is also understood as the removal of the operator in the trace, with keeping the incoming and outgoing particle lines.

In evaluating the trace we insert two complete systems of states

$$\mathrm{Tr}(e^{-LH}\mathcal{O}_{N,M}) = \sum_{\nu,\mu}\langle\nu|O_{N,M}|\mu\rangle\langle\mu|\nu\rangle e^{-E_\nu L} \tag{4.93}$$

and keep only the vacuum and one-particle states for μ and ν with rapidities u and v. Infinite volume states are normalized as $\langle u|v\rangle = 2\pi\delta(u-v)$ and the matrix element of the defect operator $\mathcal{O}_{N,M}$ can be expressed in terms of the infinite volume form factor as

$$\begin{aligned}\langle v|O_{N,M}|u\rangle \;=\; & F_{N+M+2}(v+i\pi-i\epsilon,\{\vartheta+\frac{i\pi}{2}\},u,\{\theta-\frac{i\pi}{2}\}) + \\ & 2\pi\delta(v-u)\prod_j S(\frac{i\pi}{2}+\vartheta_j-u)F_{N+M}(\{\vartheta+\frac{i\pi}{2}\},\{\theta-\frac{i\pi}{2}\})\end{aligned} \tag{4.94}$$

Therefore, we are faced with the square of the δ-function. Using our experience from evaluating the finite temperature 2-point function [127] we regulate the δ-function as

$$2\pi\delta(u-v) = \frac{i}{u-v+i\epsilon} - \frac{i}{u-v-i\epsilon} \tag{4.95}$$

For the 2-point function this regularization was equivalent to finite volume regularizations [127]. Then, we shift the v contour from the real line to above $i\epsilon$. Taking the $\epsilon \to 0$ limit, in the shifted integral no contribution will survive thus we merely pick up the residue term at $v = u + i\epsilon$. For the excited state partition function this results in

$$\mathrm{Tr}_N(e^{-LH}) = 1 + \int \frac{du}{2\pi}\frac{1}{\epsilon}\prod_j S(\frac{i\pi}{2}+\theta_j-u)e^{-M_{ShG}L\cosh u} + O(\epsilon) \tag{4.96}$$

Note that there is no $O(1)$ term. This is consistent with the usual evaluation of the partition function: if we calculated the contribution via finite volume regularization we would get $M_{ShG}R\cosh u$ instead of $\frac{1}{\epsilon}$. By repeating the same steps for the numerator

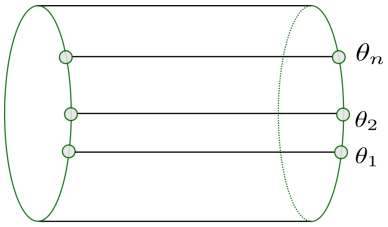

Figure 4.2: Graphical representation of the excited state partition function. A physical particle with rapidity θ_j serves as a defect operator with transmission factor $T(u) = S(\frac{i\pi}{2} + \theta_j - u)$.

we can check that the singular $\frac{1}{\epsilon}$ terms cancel with the square rooted product of the excited state partition functions and we find that the $O(1)$ piece is:

$$\delta^{(F)} F_{N+M}(\{\vartheta + i\pi\}, \{\theta\}) = \int \frac{du}{2\pi} F^r_{N+M+2}(u + i\pi, \{\vartheta + \frac{i\pi}{2}\}, u, \{\theta - \frac{i\pi}{2}\}) e^{-M_{ShG} L \cosh u} \tag{4.97}$$

where the appearing the regulated form factor was introduced in eq. (2.115).

A somewhat more detailed calculation is provided in Appendix B of [128].

4.5 Verification from the truncated spectrum approach

For the following numerical checks, the UV coupling was fixed to $\mu_{ShG} = 0.2$. The mini Hilbert space was chosen to be diagonalized on the particle in a rigid box basis with 800 states per parity sector. It was sufficient to keep only the 6 states of lowest energy out of these [113, 115]. In the Fock subspace, a conformal cutoff at chiral levels up to 9 (in the finite momentum sector, 9 and 10) was used. The dominant cutoff dependence of the results came from this chiral cutoff. This means that the actual computations involved matrices of up to about 12000 dimensions. Since the overall momentum is conserved as well as there is a parity $\mathbb{Z}_2$ symmetry present, it suffices to search the lowest lying eigenpairs of the appropriate sub-Hamiltonians restricted to the different symmetry sectors. The above cutoff should be understood separately in each subsector.

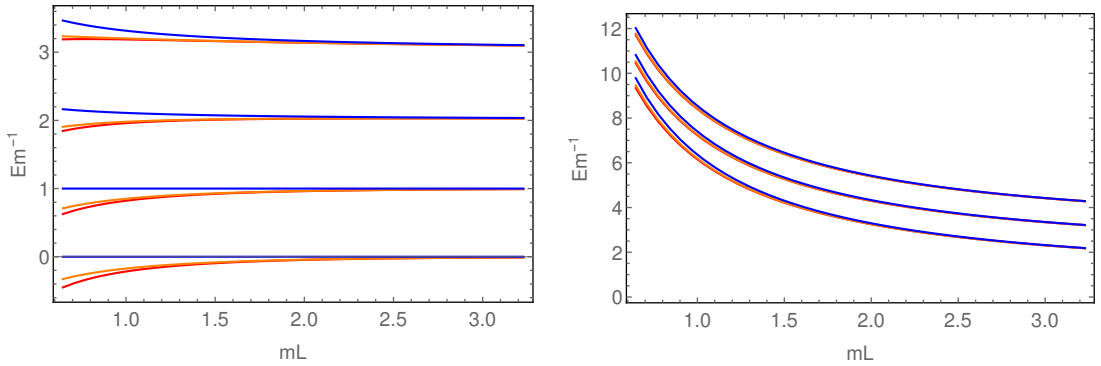

Figure 4.3: Theoretical low-lying energy spectrum of sinh-Gordon model at $b = \frac{1}{\sqrt{8\pi}}$, as the function of the dimensionless volume $M_{ShG}L$. The vacuum energy density is subtracted. Left: states in the sector of overall momentum 0 (from the bottom up: $|\text{vac}\rangle$, $|0\rangle$, $|00\rangle$ and $|000\rangle$). Right: states of overall momentum $1 \cdot 2\pi L^{-1}$ (from the bottom up: $|1\rangle$, $|01\rangle$ and $|001\rangle$). Note that we label the states by the corresponding bosonic Bethe Ansatz quantization numbers. Bethe-Yang lines are drawn with blue curves. The leading Lüscher correction is depicted by orange curves. The exact TBA result is shown with red curves.

The strategy of the computations was to diagonalize the Hamiltonian (3.4-3.9) or (3.48) for a number of volumes, and then plot the volume dependence of the results. A typical spectrum can be seen on Figure 4.3.

Finite volume energies

In order to compare the TSM energies to those obtained by solving the integral equation (2.80)-(2.82), we remark again that the latter is renormalized fixing both the infinite volume energy and energy density to 0. This scheme can be connected to the numerics obtained by TSM by subtracting the (exactly known) vacuum energy density of the sinh-Gordon model eq. (2.77)

We note that the TSM numerics produce reliable results at $b = \frac{1}{\sqrt{8\pi}}$ for both the energy levels and the finite volume form factors. For stronger couplings, e.g. $b = \frac{2}{\sqrt{8\pi}}$, the truncation errors become more significant, see fig. 4.4. Experience suggests the general rule of thumb, using the massive oscillator basis (keeping the same excitation content of the basis) is equivalent to increasing the chiral cutoff of the massless TSM basis by one. Therefore, for the present work, we mostly consider the case $b = \frac{1}{\sqrt{8\pi}}$.

To make the results more transparent, we chose to depict the difference of the quantities of interest from some reference data. In Figs. 4.4-4.5, the results obtained by numerically solving the TBA system (2.80)-(2.82) are subtracted from each other data sets (in the case of the TSM points, the energy density (2.77) is also taken into account). Note that we label the states by the corresponding Bethe Ansatz quantization numbers. The Bethe-Yang lines are calculated via (2.83)-(2.5.2), while the exponential corrections follow from (4.1)-(4.2).

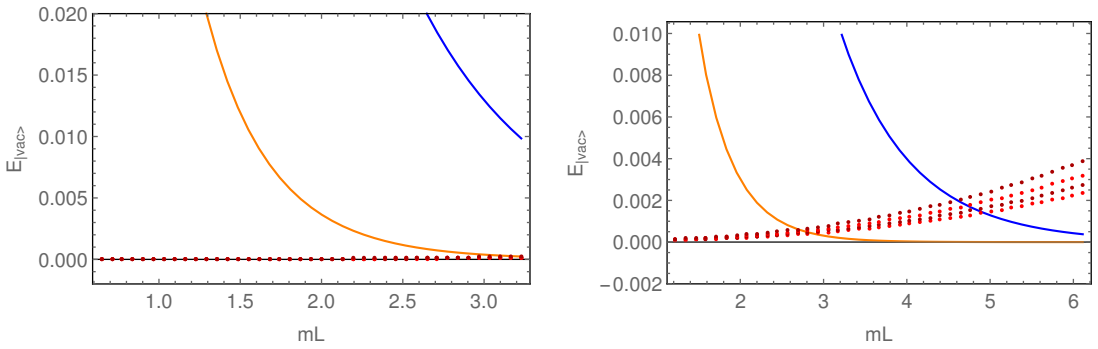

Figure 4.4: Volume ($M_{ShG}L$) dependence of the ground state energy in sinh-Gordon model: comparison of TSM data with BY, Lüscher and TBA predictions for $b = \frac{1}{\sqrt{8\pi}}$ (left) and $b = \frac{2}{\sqrt{8\pi}}$ (right). On these plots, the TBA predictions are subtracted from each data set. TSM measurement points are shown with red and brown dots, corresponding to different chiral cutoffs (from bottom up: $9, 8, 7$ and 6). The difference between the BY lines and TBA (blue) and between BY+leading Lüscher and TBA (orange) are also indicated. For $b = \frac{1}{\sqrt{8\pi}}$, TSM results agree with TBA data to a remarkable precision (the difference is negligible, as well as the cutoff dependence thereof). For $b = \frac{2}{\sqrt{8\pi}}$ truncation errors become more significant.

From these plots it is clear that in the volume range 1-3 the numerical results can be trusted and that adding the leading exponential correction to the Bethe-Yang results considerably improved the precision. We expect similar behaviors for finite volume form factors.

Finite volume form factors

In order to check our results in Section 4.4 we analyze the finite size form factors of the elementary field and the exponential operators $\mathcal{O}_k =: e^{kb\varphi} :$. For both cases the infinite volume form factors have the form of eq. (2.118).

In the plots regarding the finite volume form factors (Figures 4.6 and 4.7), the numerical TSM data is subtracted. Then the "error" of the polynomial (2.123) approximation (more precisely, its difference from TSM numerics), as calculated from (2.118) and (2.123), is shown by dashed lines. Solid curves depict the results of the present thesis ((4.90), (4.97)).

On figure 4.8 we also present some additional checks for the operators $e^{1.5b\varphi}$ and $e^{2b\varphi}$.

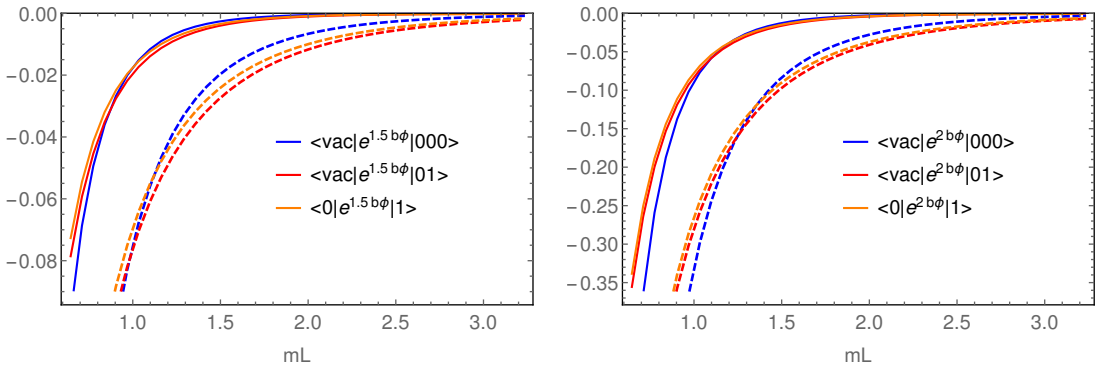

Figure 4.8: Additional checks to some form factors of $e^{1.5b\varphi}$ and $e^{2b\varphi}$ in sinh-Gordon model as the function of $M_{ShG}L$. Polynomial (Pozsgay-Takács) results are depicted by dashed curves, while the results containing the first exponential corrections, conjectured in Section 4.4 and our paper [128], are shown by continuous curves. Again, the TSM results are subtracted from each data set.

As shown on all of the plots including the theoretically predicted leading exponential correction improved the data the same way as the similar corrections improved the energy spectrum. This is a very strong support for our conjectured F-term formulae.

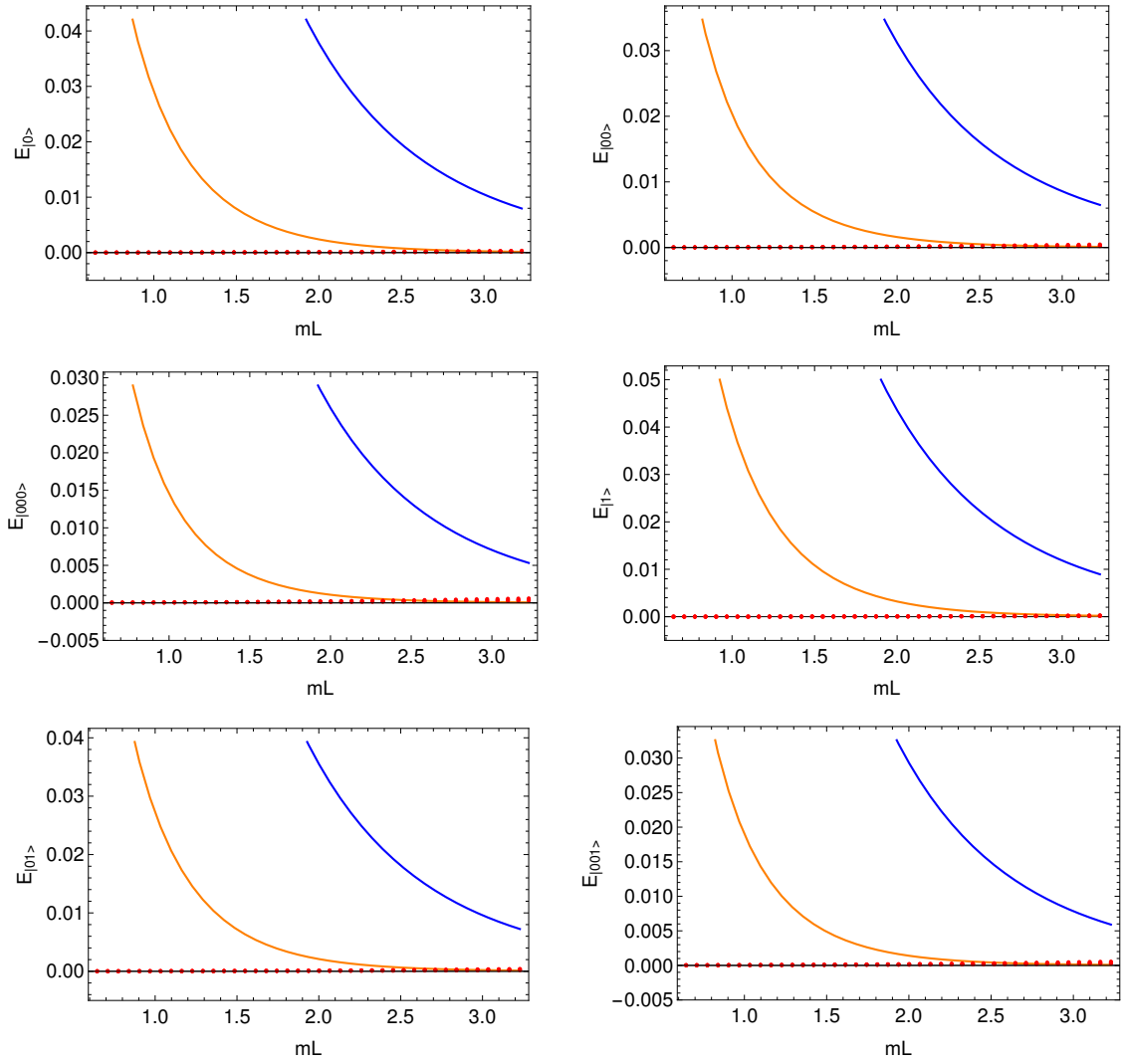

Figure 4.5: Volume ($M_{ShG}L$) dependence of the energy of some relevant low-lying states in sinh-Gordon model at $b = \frac{1}{\sqrt{8\pi}}$. Again, TBA data are subtracted from each data set. TSM data is shown by red dots. The difference between the BY lines and TBA (blue) and between BY+leading Lüscher and TBA (orange) are also indicated. Once again, we see reassuring agreement between the TBA and TSM data (the difference being close to 0, as shown.)

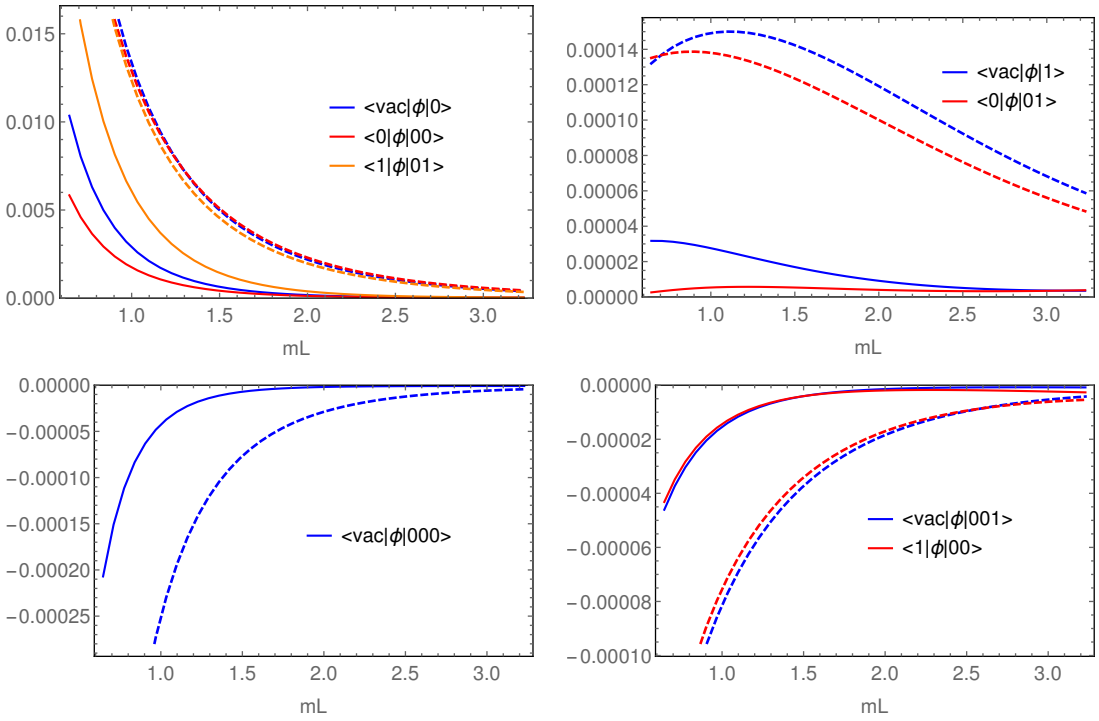

Figure 4.6: Theoretical predictions in sinh-Gordon model for various finite volume form factors of the field ϕ, as compared to numerical TSM data (the latter is subtracted from each data set) at $b = \frac{1}{\sqrt{8\pi}}$, as functions of the dimensionless volume $M_{ShG}L$. Polynomial (Pozsgay-Takács) results are depicted by dashed curves, while the results containing the first exponential corrections, conjectured in Section 4.4 and our paper [128], are shown by continuous curves.

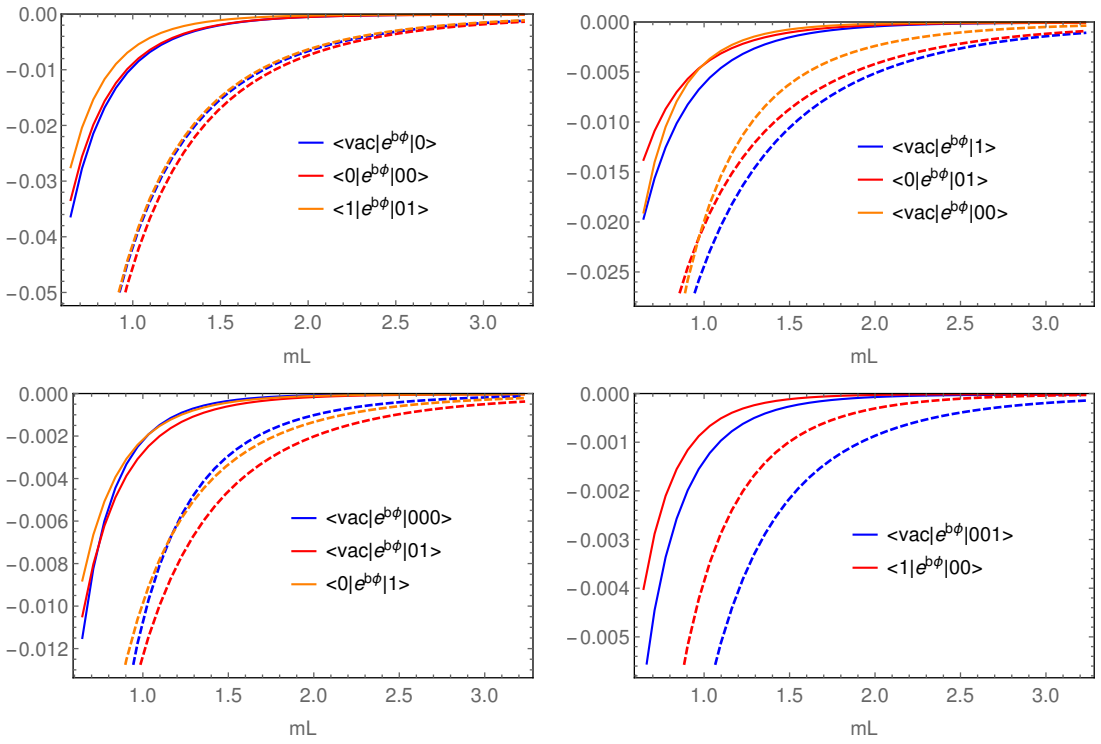

Figure 4.7: Theoretical predictions in sinh-Gordon model for various finite volume form factors of the primary operator $e^{b\varphi}$, as compared to numerical TSM data (the latter is subtracted from each data set) at $b = \frac{1}{\sqrt{8\pi}}$, as the function of the dimensionless volume $M_{ShG}L$. Polynomial (Pozsgay-Takács) results are depicted by dashed curves, while the results containing the first exponential corrections, conjectured in Section 4.4 and our paper [128], are shown by continuous curves.

Chapter 5

Conclusions and discussion

As announced in the Introduction, the main goals of this thesis were to

- Provide a formula for the F-terms of nondiagonal form factors in diagonally scattering theories. Develop analytical and numerical methods to verify this formula;
- Establish TSM methods to study the sinh-Gordon model and reinforce the previous item. Check and study self-duality.

We first set out to study in detail the ShG model in finite volume as a function of its coupling constant b. This analysis has explored several important conceptual and numerical features of this model. At the conceptual level, we have seen that the model admits two different formulations, given in terms of (i) a Lagrangian and (ii) a S-matrix. The S-matrix formulation is inherently an infrared theory, giving rise in particular to a thermodynamic Bethe ansatz equation describing in finite volume the energy of the ground and excited states. Moreover, the S-matrix formulation is ecumenical as to the actual value M_{ShG} of the mass of the physical particle. The Lagrangian formulation, on the other hand, gives us the opportunity to study the theory from several directions. Here the theory can be conceived as a perturbation of a massive free boson or as a perturbation of a conformal field theory, either Gaussian or Liouvillian. While the S-matrix formulation is manifestly invariant under the weak/strong duality transformation, $b \to 1/b$, the Lagrangian formulation has no sign of such a symmetry.

In chapter 3 we used truncated spectrum methods to study in finite volume the ShG model. This proved to be particularly challenging. Indeed, while at small values of the coupling constant b, dynamical quantities of the model – such as physical mass, vacuum expectation values of vertex operators, finite volume energies of the ground state and excited states, the two-body S-matrix – could be accurately determined and were found to coincide with their theoretical predictions, this ceased to be true upon approach to $b = 1$. There we observed that the values of these quantities started to

deviate noticeably from their predicted exact counterparts. Indeed, in the vicinity of the self-dual point $b = 1$, the TSM data showed a marked sensitivity to the cut-off N_c related to the number of states employed by the TSM. This sensitivity is of a different nature from other quantum field theories studied so far by means of TSM, a consequence of the unbounded exponential nature of its interaction.

Understanding and attempting to ameliorate these difficulties have had a series of positive by-products. In Section 3.5, we were able to come to a detailed understanding of the small volume region of the theory through exploring the quantum mechanics of the zero mode of the field. This analysis led us, in particular, to derive an effective potential which took into account the effect of the oscillator modes. This permitted a more precise measurement of the infrared parameters from the TSM through combining UV numerics with the small-volume expansion of the TBA.

In a second happy after effect, we were able to extend the usual RG scheme for improving TSM numerical data. Normally these improvements are perturbative in the coupling of the theory, here μ_{ShG}. This series proved however to be pathological in μ_{ShG} in the sense that its coefficients diverge absent a UV cutoff *and* the coefficients at order n increase more rapidly than $n!$, making the series not even Borel resummable. We were able to overcome these pathologies using generalized resummation techniques for asymptotic series – here dubbed a supra-Borel resummation. In particular we were able to show that summation of this series led to a finite result upon taking the UV cutoff to infinity and that we could partially explain the observed power law dependence in N_c observed in our TSM data. This is the first time that the leading corrections at all orders in this perturbative RG treatment have been explicitly summed. This perhaps might be useful for studies of other theories where partial resummations have been considered [116, 117]. Let us warn, however, that the choice of the optimal functional form of the supra-borel sum remains an interesting open problem, requiring additional insight.

It is important to stress that all results obtained to this point indicate that the Lagrangian of the theory provides a faithful definition of the theory for $b < 1$, even though the Lagrangian does not share the self-duality of the S-matrix. A hint about the ShG model for $b > 1$ may however come from the third spinoff explored in Section 3.7: treating the ShG at a given coupling b_1 as perturbation of a ShG model at another coupling, b_0. As explained in Section 3.7.4, for $b > 1$ there is *always* the possibility of identifying a point b_0 for which the perturbation is given in terms of a vertex operator V_a with $a = (b + b^{-1})/2$. Since the VEV of this operator vanishes, it simultaneously ensures the vanishing of all of the matrix elements involving $\cosh(b\phi)$ and therefore leads to the remarkable conclusion that the ShG model in the strong coupling regime $b > 1$ is a free massless theory!

We have already noted that in the strong coupling regime of the ShG model that

all exact and analytic formulas for the physical mass and vacuum expectation values (see eqs. (2.89) and (2.92)) have a singularity at $b = 1$. If one analytically continues these expressions beyond $b = 1$, they give, in general, complex values which make their physical interpretation challenging. One can take the point of view that for $b > 1$ the Lagrangian should be ignored and one should rely only on the S-matrix (and its explicit duality) to define the theory. In this way one uses explicitly results for $b < 1$ to define the theory for $b > 1$. However this is a tautological way of defining the duality as it leads to no predictions with regards to the mass formula, the VEVs, and the energy levels.

It is worth stressing that the same conclusions may apply as well to all Toda field theories which share with the ShG model all of its basic features, namely an apparent duality of their S-matrix which is absent in their Lagrangian formulation. Using the exact formulae reported in [157] of the Toda field theories for the physical mass, vacuum expectation values, reflection amplitudes of the underlying (generalized) Liouville field theory, one can repeat indeed the analysis done in our paper [151], applying in particular the form factor basis to argue that the Toda field theories for $b > 1$ are massless models. Indeed, establishing whether the ShG model and all Toda field theories are not in fact self-dual models as their S-matrix suggests, but on the contrary are massless, as conjectured in [158], is one of the most interesting and important open problems for the future.

In chapter 4 we initiate a programme to calculate systematically both the finite volume energy levels and the finite volume form factors.

This is done by two methods. Our first method, explained in Section 4.2, can be considered as the finite volume generalization of the LSZ reduction formula as it relates energy levels and form factors to the momentum space finite volume two-point function. We performed two different expansions of this finite volume two-point function: In the first we expanded it in the volume by separating the polynomial and exponential volume corrections in section 4.2.1. In the second we made a perturbative expansion in the coupling in the sinh-Gordon theory in section 4.3. We performed all calculations explicitly for a moving one-particle state. There we could manage to extract the leading exponential volume correction both to the energy level and to the simplest non-diagonal form factor.

We compared the expanded energy correction to the expansion of the TBA equation and found complete agreement. The correction contains both the effect of the modification of the Bethe-Yang equation by virtual particles and also these particles' direct contribution to the energy. In the case of the simplest non-diagonal form factor a local operator is sandwiched between the vacuum and a moving one-particle state. Our result for the Lüscher correction is valid for any local operator and has two types of contributions. The first comes from the normalization of the state. Since virtual

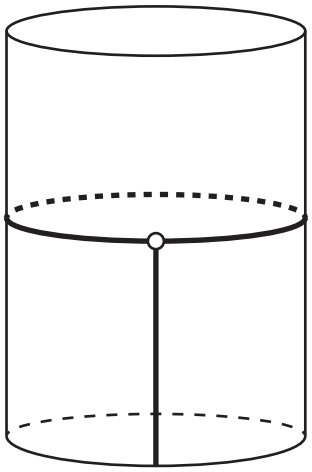

Figure 5.1: Graphical interpretation of the Lüscher correction is shown. Solid thick line represents the physical particle which arrives from the infinite past and is absorbed by the operator represented by a solid circle. The trajectory of a virtual (mirror) particle is represented by a half solid, half dashed ellipse. The operator emits this virtual particle, which travels around the world and is absorbed by the operator again leading to a 3-particle form factor.

particles change the Bethe-Yang equations, they also change the finite volume norm of the moving one-particle state. The other correction can be interpreted as the contribution of a virtual particle traveling around the world as displayed on Figure 5.1. Since the appearing 3-particle form factor is infinite, we had to regularize it by subtracting the kinematical singularity contribution. In addition, a new finite piece appears in our calculation which is related to the derivative of the scattering matrix. We tested all of our results against second order Hamiltonian perturbation theory in the sinh-Gordon theory and we obtained perfect agreement.

The perturbative calculations actually go beyond the Lüscher approximation because they are exact in the volume. Indeed, the volume-exact second order energy formula (4.75) exactly matches (E.22), obtained from the TBA equations. Our perturbative form factor calculations can be used to check any future result (or conjecture) for a volume-exact 1-particle form factor.

In the second approach, we presented a formal derivation of the leading exponentially small volume corrections for non-diagonal form factors. We approached the problem of calculating the partition function through systematic large volume expansions. The F-term is universal in the sense that it is present in theories both with and without bound states, providing the next and leading exponential correction, respectively.

By using TSM to „measure" the finite volume form factors we tested the finite size corrections in the sinh-Gordon model, where we found convincing confirmation of our formulae.

Figure 5.2 visualizes the physical picture behind the F-term: First a virtual particle-

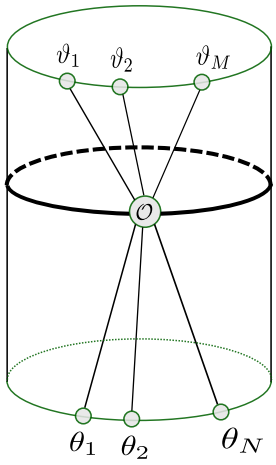

Figure 5.2: Graphical representation of the form factor F-term Lüscher correction. A virtual particle pair appears from the vacuum and after travelling around the world is absorbed by the operator.

anti-particle pair appears from the finite volume vacuum, then one of them travels around the world and finally both are absorbed by the operator. Since the infinite volume form factor with a particle-anti-particle pair is singular we had to regulate the appearing amplitude. The derivation and checks presented in [128] resulted in the proper definition of this *regulated* form factor. In the simplest non-trivial (vacuum-one-particle) form factor it is real and reproduces our earlier results [127], which we review in Section 4.2.

In our paper [128] it is also pointed out that this *regulated* form factor has very nice properties. Its phase is the same as the original form factor's for which we are calculating the correction. In the Lee-Yang theory, where bound states are present, the singularities on the upper and lower half planes are related to each other in such a way that the μ-term corrections are correctly reproduced when the residues are taken .

All the above results can be relevant for various branches of physics, including finite temperature and finite volume correlation functions in statistical and solid-state systems as well as in the AdS/CFT duality.

Understanding the novel properties of the sinh-Gordon TSM can be useful when considering perturbations of other noncompact CFTs. In particular, it sets the stage for a nonperturbative numerical evaluation of the spectrum of strings in noncompact curved backgrounds as well as the string field theory vertex.

Finite volume corrections to form factors can provide exact information for the string vertex in the $AdS_5 \times S^5$ background [159] and also on 3-point function in the maximally supersymmetric 4 dimensional gauge theory [160]. The string vertex describes a process in which a big string splits into two smaller ones. The integrable description decompactifies the strings by cutting the pair of pants worldsheet into sev-

eral parts [161]. Introducing one cut we obtain the decompactified string vertex, two cuts leads to the octagon amplitude, while introducing three cuts splits the worldsheet into two hexagons [162]. To reach an exact description the cut pieces have to be glued back again [163, 164]. These include the introduction of a pair of virtual (mirror) particle states. Unfortunately the amplitude, as it stands, is divergent and one has to figure out how to regulate it [165]. This glueing procedure is analogous to the calculation of finite size effects of form factors and requires a regularisation procedure [165]. Thus, our systematic method, which gives rise to a regulated form factor, could be implemented there as well.

Finite volume form factors are also relevant in lattice gauge theories, where the size of the system is inherently finite, and finite-size effects are unavoidable.

Although the expansion can be useful for practical applications, for obtaining exact results the series has to be summed up. In this respect the integral equation derived recently for diagonal form factors in the sinh-Gordon theory can be useful [144].

Appendix A

Conformal field theory essentials

In this appendix we collect some relevant basic properties of conformal field theories.

A conformal transformation of the coordinates is an invertible mapping $\mathbf{x} \to \mathbf{x}'$, such that the metric tensor remains invariant up to a scale:

$$g'_{\mu\nu}(\mathbf{x}') \equiv \frac{\partial x^\alpha}{\partial x'^\mu}\frac{\partial x^\beta}{\partial x'^\nu} g_{\mu\nu}(\mathbf{x}) = \Lambda(x) g_{\mu\nu}(\mathbf{x}) \tag{A.1}$$

An action S with conformal symmetry is thus invariant under the all geometric transformations preserving the angles, such as translations, rotations, Lorentz boosts, scaling, and special conformal transformations.

In $d = 2$, it is convenient to describe the coordinates by a complex number $z = z^0 + iz^1$. Any transformation described by an (anti)holomorphic function $z \to w(z)$ is a conformal mapping. It is customary to introduce the complex coordinates z and $\bar{z}$ such that

$$z = z^0 + iz^1; \quad \partial_z = \frac{1}{2}\left(\partial_0 - i\partial_1\right) \tag{A.2}$$

$$\bar{z} = z^0 - iz^1; \quad \partial_{\bar{z}} = \frac{1}{2}\left(\partial_0 + i\partial_1\right) \tag{A.3}$$

According to Noether's theorem, the generators of continuous symmetries are conserved charges. The prototypes of these charges are the components of the stress-energy tensor $T^{\mu\nu}$, the conserved current associated to translation invariance. It is defined as

$$\delta S = -\frac{1}{2}\int d^2x T^{\mu\nu}\delta g_{\mu\nu} \tag{A.4}$$

where $\delta g_{\mu\nu}$ is an infinitesimal variation of the metric tensor.

The (anti)holomorphic components of the stress-energy tensor are conventionally defined with an extra normalization factor

$$T(z) \equiv -2\pi T_{zz}(z), \quad \bar{T}(\bar{z}) \equiv -2\pi T_{\bar{z}\bar{z}}(\bar{z}) \tag{A.5}$$

The operator product expansion (OPE) of the holomorphic component of the stress-energy tensor with itself reads

$$T(z)T(w) = \frac{c/2}{(z-w)^4} + \frac{2T(w)}{(z-w)^2} + \frac{\partial T(w)}{z-w} + (\text{regular terms}) \tag{A.6}$$

where c is the central charge. A *primary* field $O(z)$ with chiral dimensions h and $\bar{h}$ is defined as a field having the following singular OPE structure

$$T(z)O(w,\bar{w}) = \frac{h}{(z-w)^2}O(w,\bar{w}) + \frac{1}{z-w}\partial_w O(w,\bar{w}) \tag{A.7}$$

$$\bar{T}(\bar{z})O(w,\bar{w}) = \frac{\bar{h}}{(\bar{z}-\bar{w})^2}O(w,\bar{w}) + \frac{1}{\bar{z}-\bar{w}}\partial_{\bar{w}} O(w,\bar{w}) \tag{A.8}$$

The transformation of any field under conformal transformations is encoded into its OPE with the stress-energy tensor. One can use the conformal Ward identities to obtain the variation of O under an infinitesimal transformation. Then the infinitesimal variations can be integrated into a finite transformation. Under the change of variables $z \to w(z)$, $\bar{z} \to \bar{w}(\bar{z})$, the primary field O transforms as

$$O'(w,\bar{w}) = \left(\frac{dw}{dz}\right)^{-h}\left(\frac{d\bar{w}}{d\bar{z}}\right)^{-\bar{h}} O(z,\bar{z}) \tag{A.9}$$

The components of the stress-energy tensor are not primary fields. In particular, the holomorphic component transforms as

$$T'(w) = \left(\frac{dw}{dz}\right)^{-2}\left[T(z) - \frac{c}{12}\{w;z\}\right] \tag{A.10}$$

where $\{w;z\}$ is the Schwarzian derivative.

In a Euclidean theory, the choice of the time direction is somewhat arbitrary. On the conformal plane, it is customary to consider the origin as the point of infinite past, while the ideal point as the point of infinite future. The equal-time surfaces are concentric circles, and the generator of (Euclidean) time evolution may be identified with the generator of dilatations.

If we assume the existence of a ground state $|\text{vac}\rangle$ (vacuum), it is possible to give an operator interpretation to the fields. The asymptotic state of the system in the infinite past may be specified by inserting a local field at the origin. There is thus mapping between local fields and asymptotic states

$$O(z,\bar{z}) \leftrightarrow |O_{\text{in}}\rangle = \lim_{z,\bar{z}\to 0} O(z,\bar{z})\,|\text{vac}\rangle \tag{A.11}$$

In order to have a well-defined inner product, we introduce the hermitian adjoint field

as

$$O(z,\bar{z})^\dagger = \bar{z}^{-2h} z^{-2\bar{h}} O(1/\bar{z}, 1/z) \tag{A.12}$$

Correlators may be interpreted as radially ordered vacuum expectation values. This interpretation paves the way to calculate commutators between the mode expansion coefficients of fields using contour integrals and OPEs.

Appendix B

UV quantization condition from TBA

In this appendix we recall the quantization condition for the energy levels obtained from the small-volume expansion of the TBA system [95]. In the following we denote the coupling appearing in TBA by $\bar{b}$, to emphasize that this parameter is directly related to the S-matrix parameter $B = \frac{\bar{b}^2}{1+\bar{b}^2}$, and not (immediately) to the parameter b appearing in the Hamiltonian.

In the small-L limit, the TBA equations decouple into a right- and a left-moving part. To obtain these equations, one first performs a shift in the rapidity variables $\{\theta, \vartheta\} \to \{\theta \pm |\ln ML|, \vartheta \pm |\ln ML|\}$, leading to a pair of volume-independent equations up to $O(ML)$ corrections. One then neglects the $O(ML)$ corrections and reverses the previous rapidity shift. Let us introduce the notation $Y_{\pm}(\theta \mid \{\vartheta\}) = e^{-\epsilon_{\pm}(\theta|\{\vartheta\})}$, where the $\pm$ denotes the right- and left-moving solutions. In the following it is advantageous to construct the so-called $\mathcal{Q}$-functions, defined through the pair of functional relations

$$\mathcal{Q}\left(\theta + \frac{i\pi a}{2}\right)\mathcal{Q}\left(\theta - \frac{i\pi a}{2}\right) = Y(\theta \mid \{\vartheta\}) \quad , \tag{B.1}$$

$$\mathcal{Q}\left(\theta + \frac{i\pi}{2}\right)\mathcal{Q}\left(\theta - \frac{i\pi}{2}\right) = 1 + Y(\theta \mid \{\vartheta\}) \quad , \tag{B.2}$$

with $a = 1 - 2B$, where we have suppressed the ϑ-dependence of the $\mathcal{Q}$'s. These functions can be obtained by taking the logarithm of eqs. (B.1)-(B.2) and (carefully) performing a Fourier transform. In the UV limit, corresponding to the decoupling of the TBA equations, we get a pair of functions $\mathcal{Q}_{\pm}$ of the form

$$\ln \mathcal{Q}_{\pm}(\theta) = -\frac{ML}{4\sin \pi B} e^{\pm\theta} + \int \frac{d\theta'}{2\pi} \frac{\ln\left(1 + Y^{\pm}(\theta' \mid \{\vartheta\})\right)}{\cosh(\theta - \theta')} + (\text{source terms}) \,. \tag{B.3}$$

Note that the source terms and quantization conditions of the TBA system can be understood as a prescription for the zeros of the function $1 + Y$. Correspondingly, $\mathcal{Q}_{\pm}$ needs to have an analogous set of zeroes to be compatible with eq. (B.2). It was shown

in [166] that the $\mathcal{Q}$-functions obtained from the decoupled TBA equations possess the asymptotic form

$$\mathcal{Q}_{\pm}(\theta) \underset{\theta\to\mp\infty}{\sim} \frac{\cos\left[2PQ\left(\bar{b}\right)\theta \pm \Theta(P)\right]}{\sqrt{\sinh\left(2\pi\bar{b}P\right)\sinh\left(2\pi\bar{b}^{-1}P\right)}} \ , \tag{B.4}$$

where P is a real parameter and $\Theta(P)$ is an antisymmetric phase (to be obtained below). For small volumes, the asymptotic eq. (B.4) is expected to dominate the θ-dependence over a wide region. The parameter P is quantized by the requirement that $\mathcal{Q}_+$ and $\mathcal{Q}_-$ corresponds to the *same* Y-function $Y_+ = Y_-$, which is nothing else but the UV limit of the $Y(\theta \mid \{\vartheta\}) = e^{-\epsilon(\theta|\{\vartheta\})}$.

Let us focus on the zero mode sector defined by restricting the Bethe quantum numbers to be $I_j = 0$, $\forall j$. Taking into account that $\pm\mathcal{Q}$ leads to the same Y, we arrive at the condition (2.86):

$$2\,\Theta(P) = n\pi, \quad n \in \mathbb{Z} \ . \tag{B.5}$$

Due to the antisymmetry of Θ, it is sufficient to restrict to the cases $n \geq 0$ (subsequently we will see that the ground state corresponds to $n = 1$). In the zero mode sector, energy levels behave in the UV as

$$E_n = \frac{2\pi}{L}\left(2P_n^2 - \frac{1}{12}\right) \ , \tag{B.6}$$

as can be seen by direct integration (for details, see Appendix C of Ref. [95]).

It is hard to extract the phase $\Theta(P)$ directly from eq. (B.3). However, as shown in [167], there exists an ingenious trick to obtain its explicit expression. To this aim, consider the second-order ODE

$$-\psi''(x) + \kappa^2\left(e^{2x} + e^{-\frac{2x}{\bar{b}^2}}\right)\psi(x) \ = \ p^2\psi(x) \ , \tag{B.7}$$

and the pair of solutions defined by their asymptotical behaviour

$$\psi_-(x) \underset{x\to-\infty}{\sim} \frac{1}{\sqrt{2\kappa}}\exp\left(\frac{x}{2\bar{b}^2} - \bar{b}^2\kappa e^{-\frac{x}{\bar{b}^2}}\right) \ , \tag{B.8}$$

$$\psi_+(x) \underset{x\to+\infty}{\sim} \frac{1}{\sqrt{2\kappa}}\exp\left(-\frac{x}{2} - \kappa e^{x}\right) \ . \tag{B.9}$$

Hence, the Wronskian, $W(p)$, constructed in terms of these solutions

$$W(p) \ = \ \psi_+\frac{d}{dx}\psi_- - \psi_-\frac{d}{dx}\psi_+, \tag{B.10}$$

satisfies the same set of functional equations as the $\mathcal{Q}$-system, provided that the parameters κ and p are tuned appropriately. Let us focus on the right-moving part.The

Wronskian $W(p)$ can be evaluated in a small-κ expansion (using the reflection quantization) and a large-κ expansion (by means of the WKB approximation). It is convenient to parametrize κ as $\kappa = c\, e^{\theta}$. Then, comparing the form of the pseudo-energy obtained from the small-κ expansion ($\theta \to -\infty$) to the asymptotic formula eq. (B.4), we can fix

$$p \;=\; \frac{2P}{\bar{b}} \;\;, \tag{B.11}$$

while, from the large-κ expansion, we obtain

$$c \;=\; ML\, \frac{\sqrt{\pi}}{4 \sin \frac{\pi B}{2}} \frac{\Gamma\left(\frac{3-B}{2}\right)}{\Gamma\left(\frac{2-B}{2}\right)} \;\;. \tag{B.12}$$

Finally, the phase $\Theta(P)$ is obtained by comparing the small-κ expansion to eq. (B.4) and is given by

$$e^{2i\Theta(P)} \;=\; -\bar{b}^{\frac{8iP}{b}} \rho^{-4iPQ(\bar{b})} \frac{\Gamma\left(1+2iP\bar{b}\right)\Gamma\left(1+2iP\bar{b}^{-1}\right)}{\Gamma\left(1+2iP\bar{b}\right)\Gamma\left(1+2iP\bar{b}^{-1}\right)} \;\;, \tag{B.13}$$

where

$$\rho \;=\; \frac{L}{2\pi} \frac{M}{4\sqrt{\pi}} \Gamma\left(\frac{1-B}{2}\right) \Gamma\left(\frac{2+B}{2}\right) \;\;. \tag{B.14}$$

Appendix C

Integral representations for S_1 and S_2

In this appendix we provide integral representations for the sums S_1 and S_2 introduced in Section 2.1.2.

C.1 $S_1(m,R) = \sum_{n\neq 0} \frac{1}{\omega_n} - \frac{1}{|k_n|}$

To evaluate this sum, let us first introduce a cutoff $\Lambda = \frac{2\pi N}{R}$, $N \gg 1$, and then add and subtract an auxiliary integral term:

$$S_1 = \lim_{\Lambda\to\infty} \left\{ \left(\sum_{n=-N}^{N} \frac{1}{\omega_n} - \frac{1}{m} - \frac{R}{2\pi} \int_{-\Lambda}^{\Lambda} \frac{dk}{\sqrt{m^2+k^2}} \right) + \left(\frac{R}{2\pi} \int_{-\Lambda}^{\Lambda} \frac{dk}{\sqrt{m^2+k^2}} - 2\frac{R}{2\pi} \sum_{n=1}^{N} \frac{1}{n} \right) \right\}. \tag{C.1}$$

In the first term on the r.h.s. we have rewritten the sum so that it includes the $n = 0$ term. Using the definition of the Euler-Mascheroni constant

$$\gamma_E = \lim_{N\to\infty} \left(\sum_{n=1}^{N} \frac{1}{n} - \ln N \right), \tag{C.2}$$

and the explicit expression of the integral

$$\int_{-\Lambda}^{\Lambda} \frac{dk}{\sqrt{m^2+k^2}} = 2\ln\left(\frac{\Lambda}{m} + \sqrt{1+\frac{\Lambda^2}{m^2}} \right) = 2\ln N + 2\ln\frac{4\pi}{mR} + O\left(\frac{1}{\Lambda^2}\right), \tag{C.3}$$

we can immediately evaluate the second term on the r.h.s. of eq. (C.1):

$$\frac{R}{2\pi} \lim_{\Lambda\to\infty} \left(\int_{-\Lambda}^{\Lambda} \frac{dk}{\sqrt{m^2+k^2}} - 2\sum_{n=1}^{N} \frac{1}{n} \right) = \frac{R}{\pi} \left(\ln\frac{4\pi}{mR} - \gamma_E \right). \tag{C.4}$$

The first term of eq. (C.1) can be evaluated in the same way that Matsubara sums are:

$$\sum_{n=-N}^{N} \frac{1}{\omega_n} = \frac{R}{2\pi} \int\limits_C \frac{e^{ipR}}{e^{ipR}-1} \frac{1}{\sqrt{m^2+p^2}}. \tag{C.5}$$

Here the contour C consists of distinct, small circles around all poles between $p = -\Lambda$ and $p = +\Lambda$ on the real axis. We deform this disjoint contour to form two straight vertical line sections running slightly above and below the real axis. The contour in the lower-half plane is then combined with the first integral in eq. (C.1). At this point the limit $\Lambda \to \infty$ can be taken and the two contours tightened around the branch cuts of the square roots. In this way we obtain the representation,

$$\begin{aligned} \lim_{N\to\infty} \sum_{n=-N}^{N} \frac{1}{\omega_n} - \frac{R}{2\pi} \int\limits_{-\Lambda}^{\Lambda} \frac{dk}{\sqrt{m^2+k^2}} &= \frac{2R}{\pi} \int\limits_{1}^{\infty} \frac{d\tau}{(e^{mR\tau}-1)\sqrt{\tau^2-1}} \\ &= \frac{R}{\pi} \int\limits_{-\infty}^{\infty} \frac{du}{(e^{mR\cosh u}-1)}. \end{aligned} \tag{C.6}$$

Collecting terms, we see that

$$S_1 = \frac{R}{\pi} \int\limits_{-\infty}^{\infty} \frac{du}{(e^{mR\cosh u}-1)} - \frac{1}{m} + \frac{R}{\pi}\left(\ln\frac{4\pi}{mR} - \gamma_E\right). \tag{C.7}$$

C.2 $S_2(m,R) = \sum_{n\neq 0} \frac{\omega_n}{2} - \frac{|k_n|}{2} - \frac{m^2}{4|k_n|}$

Let us begin with adding and subtracting $\sum_{n\neq 0} \frac{m^2}{4\omega_n}$. Then we separate the sum into two convergent parts:

$$\begin{aligned} S_2(m,R) &= \frac{m^2}{4} S_1(m,R) + \tilde{S}_2(m,R) \\ \tilde{S}_2 &= \sum_{n\neq 0} s_2(k_n) = \sum_{n\neq 0} \frac{\omega_n}{2} - \frac{|k_n|}{2} - \frac{m^2}{4\omega_n}, \end{aligned} \tag{C.8}$$

where S_1 is given by eq. (C.7). The sum $\tilde{S}_2$ can again be rewritten as a Matsubara-type contour integral

$$\tilde{S}_2 = \frac{R}{2\pi} \int\limits_C \frac{e^{ipR}}{e^{ipR}-1} s_2(p), \tag{C.9}$$

where now the contour C encloses all poles (in the positive direction) on the real axis except for the one at the origin. The function $s_2(p)$ has two overlapping pairs of branch cuts all along the imaginary axis of the complex p plane. The contour C can

be deformed in the first step into two connected contours at each side of the branch cut, starting and ending at infinity and enclosing all poles lying on one half of the real axis. In the second step, this pair of contours is unbent to form two straight vertical lines aligned in the immediate vicinity of the branch cuts. The contour integrals can then be written as a sum of integrals over the real line:

$$\tilde{S}_2 = I_1 + I_2 \tag{C.10}$$

$$I_1 = -\frac{m^2 R}{2\pi}\left[\int_{-\infty}^{-1} \frac{\tau}{e^{-mR\tau}-1} + \int_{-1}^{\infty} \frac{\tau}{1-e^{mR\tau}}\right] - \frac{m}{4} = \frac{\pi}{6R} + \frac{m^2 R}{4\pi} - \frac{m}{4}, \tag{C.11}$$

$$I_2 = \frac{m^2 R}{4\pi}\left[\int_{1}^{\infty} 2\tau + \frac{1-2\tau^2}{\sqrt{\tau^2-1}} \coth\left(\frac{mR\tau}{2}\right)\right]. \tag{C.12}$$

The explicit term $-m/4$ arises in eq. (C.11) due to the pole at the origin. After a change of variables $\tau = \cosh u$, the integral I_2 becomes

$$I_2 = -\frac{m^2 R}{8\pi} - \frac{m^2 R}{4\pi}\int_0^{\infty} du \left(4\sinh u \frac{\sinh u e^{-mR\cosh u}}{1-e^{-mR\cosh u}} + \frac{2}{e^{mR\cosh u}-1}\right), \tag{C.13}$$

where an explicit integration $\int_0^\infty e^{-2u} du$ was performed. After an integration by parts in the first term of the integral and extending the integration range from $-\infty$ to ∞, we get

$$I_2 = -\frac{m^2 R}{8\pi} - \frac{m^2 R}{4\pi}\int_{-\infty}^{\infty} du \left(-2\cosh u \ln\left(1-e^{-mR\cosh u}\right) + \frac{1}{e^{mR\cosh u}-1}\right). \tag{C.14}$$

Combining all terms, we arrive at

$$\begin{aligned} S_2(m,R) = &-\frac{m}{2} + \frac{m^2 R}{4\pi}\left(\frac{1}{2} + \ln\frac{2}{m} - \gamma_E\right) + \frac{m^2 R}{4\pi}\ln\frac{2\pi}{R} \\ &+ \frac{\pi}{6R} + m\int_{-\infty}^{\infty}\frac{du}{2\pi}\cosh u \ln\left(1-e^{-mR\cosh u}\right). \end{aligned} \tag{C.15}$$

Appendix D

Perturbative expansion of finite volume eigenvalues

In this appendix we will consider the perturbative expansion for the ground state energy. We begin generally and consider a Hamiltonian of the form

$$H \;=\; H_0 + \mu V. \tag{D.1}$$

A convenient representation of the expansion of the ground state energy, E_0, is given by the Brillouin-Wigner series

$$\begin{aligned} E_0 = E_0^0 + \mu V_{00} + \mu^2 \sum_{m_1}{}' \frac{V_{0m_1}V_{m_10}}{E_0 - E^0_{m_1}} + \dots \\ + \mu^n \sum_{m_1}{}' \sum_{m_2}{}' \cdots \sum_{m_{n-1}}{}' \frac{V_{0m_1}V_{m_1m_2}\dots V_{m_{n-1}0}}{(E_0 - E^0_{m_1})\cdots(E_0 - E^0_{m_{n-1}})} + \dots, \end{aligned} \tag{D.2}$$

where the primes indicate that the ground state is to be omitted from the sum. In the above series, the exact value of the energy, E_0, appears on both sides. The disconnected terms of the usual Rayleigh-Schrödinger series are generated by using the formula iteratively and expanding in μ.

Now we are interested in the divergences appearing in the sinh-Gordon model. It can easily seen that these disconnected terms are less divergent. We thus focus on the connected contributions of this series:

$$\begin{aligned} E_0 = E_0^0 + \mu_{ShG} V_{00} + \mu_{ShG}^2 \sum_{m_1}{}' \frac{V_{0m_1}V_{m_10}}{E^0_0 - E^0_{m_1}} + \dots + \\ \mu_{ShG}^n \sum_{m_1}{}' \sum_{m_2}{}' \cdots \sum_{m_{n-1}}{}' \frac{V_{0m_1}V_{m_1m_2}\dots V_{m_{n-1}0}}{(E^0_0 - E^0_{m_1})\cdots(E^0_0 - E^0_{m_{n-1}})} + \dots, \end{aligned} \tag{D.3}$$

where V_{ij} denotes the matrix elements of the perturbation w.r.t. the unperturbed

theory. The n-th order term in the above can be rewritten as

$$\begin{aligned}\delta E_0^{(n)} =&\mu_{ShG}^n \sum_{m_1}{}' \sum_{m_2}{}' \cdots \sum_{m_{n-1}}{}' \frac{V_{0m_1}V_{m_1m_2}\ldots V_{m_{n-1}0}}{(E_0^0-E_{m_1}^0)\cdots(E_0^0-E_{m_{n-1}}^0)}\\ =&(-1)^{n-1}\mu_{ShG}^n \sum_{m_1}{}' \sum_{m_2}{}' \cdots \sum_{m_{n-1}}{}' \int_0^\infty d\tau_1\ldots d\tau_{n-1} e^{E_0^0(\tau_1+\cdots+\tau_{n-1})}\\ &V_{0m_1}e^{-E_{m_1}^{(0)}\tau_1}V_{m_1m_2}e^{-E_{m_2}^{(0)}\tau_2}\ldots e^{-E_{m_{n-1}}^{(0)}\tau_{n-1}}V_{m_{n-1}0}, \end{aligned} \tag{D.4}$$

where, if we introduce $\tau_i = t_i - t_{i+1}$, we can rewrite the nth order term as an integral over an Euclidean correlator of the unperturbed theory:

$$\begin{aligned}\delta E_0^{(n)} &= (-1)^{n-1}\mu_{ShG}^n \langle 0|V(t_1)\ldots V(t_n=0)|0\rangle;\\ V(t) &= e^{H_0 t}Ve^{-H_0 t}. \end{aligned} \tag{D.5}$$

From now on, the time dependence of any operator is understood in the sense of eq. (D.5).

We now turn to the Hamiltonian of direct concern:

$$H = H_0 + \mu_{ShG}(\frac{L}{2\pi})^{2b^2}\int_0^L dx(e^{b\varphi_0}:e^{b\tilde{\varphi}(x)}:+e^{-b\varphi_0}:e^{-b\tilde{\varphi}(x)}:) - \frac{L}{16\pi}\omega_{\varphi_0}^2{\varphi_0}^2, \tag{D.6}$$

with

$$H_0 = \frac{4\pi}{L}\Pi_0^2 + \frac{L}{16\pi}\omega_{\varphi_0}^2{\varphi_0}^2. \tag{D.7}$$

Here we have added and subtracted a term quadratic in the zero mode allowing us to formulate the perturbation theory about a massive zero mode. This choice allows for some additional explicit steps in the following calculations.

Let us begin by evaluating the second order term in this perturbative expansion. The vertex functions of the oscillator part of bosonic field, $\tilde{\varphi}$, can be written as

$$\langle 0|:e^{\alpha\tilde{\varphi}(\tau,\rho)}::e^{\beta\tilde{\varphi}(0,0)}:|0\rangle = \frac{1}{(1-e^{-\frac{2\pi}{L}(\tau+i\rho)})^{2\alpha\beta}(1-e^{-\frac{2\pi}{L}(\tau-i\rho)})^{2\alpha\beta}}. \tag{D.8}$$

This correlator can be expanded into a binomial series

$$\begin{aligned}\langle 0|:e^{b\tilde{\varphi}(t_1,x_1)}::e^{b\tilde{\varphi}(t_2,x_2)}:|0\rangle &= \sum_{p_{12},q_{12}=0}^{\infty}(-1)^{p_{12}+q_{12}}\binom{-2b^2}{p_{12}}\binom{-2b^2}{q_{12}}\\ &e^{-\frac{2\pi}{L}(p_{12}+q_{12})t_1}e^{\frac{2\pi}{L}(p_{12}+q_{12})t_2}e^{-\frac{2\pi i}{L}(p_{12}-q_{12})x_1}e^{-\frac{2\pi i}{L}(q_{12}-p_{12})x_2}, \end{aligned} \tag{D.9}$$

The binomials admit the asymptotic behavior

$$\binom{z}{k} \sim \frac{(-1)^k}{\Gamma(-z)k^{z+1}}, \quad k \gg 1. \tag{D.10}$$

The leading singular part of the second-order perturbative correction has the form

$$\delta E_0^{(2)} = -2\mu_{ShG}^2 \left(\frac{L}{2\pi}\right)^{4b^2} \int_0^\infty dt \int_0^L dx_1 dx_2 \langle 0|e^{b\varphi_0(t)} e^{b\varphi_0(0)}|0\rangle\langle 0| : e^{b\tilde{\varphi}(t,x_1)} :: e^{b\tilde{\varphi}(0,x_2)} : |0\rangle. \tag{D.11}$$

Note that a factor 2 arises due to an analogous term with all exponents negative. The zero mode quantum mechanics (D.7) is that of a harmonic oscillator, so the correlator on the left is easily evaluated. We introduce

$$\varphi_0 = \varphi_{0+} + \varphi_{0-}, \tag{D.12}$$

such that

$$\varphi_{0+} = \left(\frac{4\pi}{L\omega_{\varphi_0}}\right)^{\frac{1}{2}} a_{\varphi_0}; \qquad \varphi_{0-} = \left(\frac{4\pi}{L\omega_{\varphi_0}}\right)^{\frac{1}{2}} a_{\varphi_0}^\dagger$$

$$[a_{\varphi_0}, a_{\varphi_0}^\dagger] = 1. \tag{D.13}$$

The Euclidean correlator takes the form

$$[\varphi_{0+}(t), \varphi_{0-}(0)] = \frac{4\pi}{L\omega_{\varphi_0}} e^{-\omega_{\varphi_0} t}. \tag{D.14}$$

Using eq. (D.9), the x integrals can be performed immediately with the result

$$\delta E_0^{(2)} = -2\mu_{ShG}^2 L^2 \left(\frac{L}{2\pi}\right)^{4b^2} \int_0^\infty dt \langle 0|e^{b\varphi_0(t)} e^{b\varphi_0(0)}|0\rangle \sum_{m=0}^\infty \binom{-2b^2}{m}^2 e^{-\frac{4\pi}{L}mt}. \tag{D.15}$$

For $b < \frac{1}{\sqrt{2}}$, eq. (D.15) evaluates to a finite value. For larger couplings, we need to introduce a chiral cutoff N_c. In this parameter domain, we can approximate the sum by an integral, and using the asymptotic eq. (D.10), we obtain

$$\delta E_0^{(2)} \approx -2\mu_{ShG}^2 \left(\frac{L}{2\pi}\right)^{4b^2} \frac{L^2 e^{b^2 \frac{4\pi}{L\omega_{\varphi_0}}}}{\Gamma(2b^2)^2} \int_0^\infty dt e^{b^2 \frac{4\pi}{L\omega_{\varphi_0}} e^{-\omega_{\varphi_0} t}} \int_0^{N_c} dm m^{4b^2-2} e^{-\frac{4\pi}{L}mt}. \tag{D.16}$$

The $\omega_{\varphi_0}^{-1/2}$ terms make an expansion singular around $\omega_{\varphi_0} = 0$. On the other hand, having in mind $b > \frac{1}{\sqrt{2}}$ and a fixed $\omega_{\varphi_0} > 0$, we argue that the corrections due to the double exponential are subleading for large N_c. Let us expand the outer exponential

into a Taylor series. Then we need to perform simple exponential time integrals, which yield $\frac{1}{m}$-like terms. Rescaling $m \to N_c\tilde{m}$ and factoring out N_c leaves an explicit $k\omega_{\varphi_0}N_c^{-1}$ term in the denominator (k is the order of the Taylor expansion term). Even though k eventually becomes comparable to N_c, the corresponding term is multiplied by an overall $1/k!$ factor, which renders it negligible. What remains is an effective $e^{b^2\frac{4\pi}{L\omega_{\varphi_0}}}$ constant multiplier

$$\delta E_0^{(2)} = -2\mu_{ShG}^2\left(\frac{L}{2\pi}\right)^{4b^2}\frac{L^3 e^{b^2\frac{8\pi}{L\omega_{\varphi_0}}}}{4\pi\Gamma(2b^2)^2}\frac{N_c^{4b^2-2}}{4b^2-2}(1+O(N_c^{-1}))+O(N_c^0). \tag{D.17}$$

Note that the spurious singularity at $b=\frac{1}{\sqrt{2}}$ is due to the asymptotic approximation and is unphysical.

Let us turn to the general case. The relevant correlation function has the form

$$\begin{aligned}\langle 0|:e^{b\tilde{\varphi}(x_1,t_1)}:\cdots:e^{b\tilde{\varphi}(x_n,0)}:|0\rangle &= \prod_{i=1}^{n-1}\prod_{j=i+1}^{n}e^{b^2[\tilde{\varphi}_+(t_i,x_i),\tilde{\varphi}_-(t_j,x_j)]}\\ &= \sum_{\{p_{ij}\}=0}^{\infty}\sum_{\{q_{ij}\}=0}^{\infty}\left\{\prod_{i=1}^{n-1}\prod_{j=i+1}^{n}(-1)^{p_{ij}}\binom{-2b^2}{p_{ij}}(-1)^{q_{ij}}\binom{-2b^2}{q_{ij}}\right\}e^{-\frac{2\pi}{L}\sum_i\sum_{j>i}(p_{ij}+q_{ij})t_i}\\ &\quad\times e^{\frac{2\pi}{L}\sum_j\sum_{i<j}(p_{ij}+q_{ij})t_j}e^{-\frac{2\pi i}{L}\sum_i[\sum_{j>i}(p_{ij}-q_{ij})-\sum_{j<i}(p_{ji}-q_{ji})]x_i}.\end{aligned} \tag{D.18}$$

The spatial integrations yield the relations

$$\sum_{j>i}(p_{ij}-q_{ij})=\sum_{j<i}(p_{ji}-q_{ji}),\quad i=1\cdots n-1, \tag{D.19}$$

which can be used to fix q_{in}, $\forall i$:

$$\sum_{j>i}p_{ij}+\sum_{j<i}q_{ji}-\sum_{j<i}p_{ji}-\sum_{i<j<n}q_{ij}=q_{in}. \tag{D.20}$$

The Euclidean time integrations are to be taken over the simplex $t_1 > t_2 > \cdots > t_{n-1} > 0$. Using the simple formula

$$\int_0^{\infty}dt_{n-1}\ldots\int_{t_3}^{\infty}dt_2\int_{t_2}^{\infty}dt_1 e^{-(\sum_{i=1}^{n-1}m_it_i)}=\frac{1}{m_1(m_1+m_2)\cdots(\sum_{i=1}^{n-1}m_i)}, \tag{D.21}$$

together with eq. (D.20), allows us to write:

$$\int_0^{\infty}dt_{n-1}\ldots\int_{t_3}^{\infty}dt_2\int_{t_2}^{\infty}dt_1\langle 0|V(t_1)\ldots V(t_n=0)|0\rangle = 2(\frac{L}{2\pi})^{2nb^2}\frac{e^{\frac{2\pi b^2}{L\omega_{\varphi_0}}n^2}L^{2n-1}}{(4\pi)^{n-1}\Gamma(2b^2)^{n(n-1)}}$$

$$\times \int_0^{N_c} \frac{\prod_{i=1}^{n-1}\prod_{j=i+1}^{n} dp_{ij} p_{ij}^{\xi}}{\prod_{k=1}^{n-1}(\sum_{j=k+1}^{n}\sum_{i=1}^{k} p_{ij})} \int_0^{N_c} \prod_{i=1}^{n-2}\prod_{j=i+1}^{n-1} dq_{ij} q_{ij}^{\xi}$$
$$\times \prod_{l=1}^{n-1}(\sum_{m>l} p_{lm} + \sum_{m<l} q_{ml} - \sum_{m<l} p_{ml} - \sum_{l<m<n} q_{lm})^{\xi}$$
$$\times \Theta_H(\sum_{m>l} p_{lm} + \sum_{m<l} q_{ml} - \sum_{m<l} p_{ml} - \sum_{l<m<n} q_{lm})$$
$$\times \Theta_H(1 - (\sum_{m>l} p_{lm} + \sum_{m<l} q_{ml} - \sum_{m<l} p_{ml} - \sum_{l<m<n} q_{lm})), \qquad \text{(D.22)}$$

where

$$\xi = 2b^2 - 1.$$

In eq. (D.22) the time dependence of the zero mode correlators were neglected by an analogous argument to that of the $\delta E_0^{(2)}$ case. The cutoff N_c can be scaled out by transforming to new variables $p_{ij} = N_c \tilde{p}_{ij}$, $q_{ij} = N_c \tilde{q}_{ij}$, resulting in the final form of the leading order asymptotic

$$\delta E_0^{n)} \approx (-1)^{n-1} 2\mu_{ShG}^n \left(\frac{L}{2\pi}\right)^{2nb^2} e^{\frac{2\pi b^2}{L\omega\varphi_0} n^2} \frac{L^{2n-1} N_c^{2(1-n)+2b^2(n^2-n)}}{(4\pi)^{n-1}\Gamma(2b^2)^{n(n-1)}} I_n, \qquad \text{(D.23)}$$

with the integral I_n defined as

$$\begin{aligned} I_n \;=\; & \int_0^{1} \frac{\prod_{i=1}^{n-1}\prod_{j=i+1}^{n} dp_{ij} p_{ij}^{\xi}}{\prod_{k=1}^{n-1}(\sum_{j=k+1}^{n}\sum_{i=1}^{k} p_{ij})} \int_0^{1} \prod_{i=1}^{n-2}\prod_{j=i+1}^{n-1} dq_{ij} q_{ij}^{\xi} \\ & \times \prod_{l=1}^{n-1}(\sum_{m>l} p_{lm} + \sum_{m<l} q_{ml} - \sum_{m<l} p_{ml} - \sum_{l<m<n} q_{lm})^{\xi} \\ & \times \Theta_H(\sum_{m>l} p_{lm} + \sum_{m<l} q_{ml} - \sum_{m<l} p_{ml} - \sum_{l<m<n} q_{lm}) \\ & \times \Theta_H(1 - (\sum_{m>l} p_{lm} + \sum_{m<l} q_{ml} - \sum_{m<l} p_{ml} - \sum_{l<m<n} q_{lm})). \end{aligned} \qquad \text{(D.24)}$$

This is the form that we use as a starting point in Section 3.6.2.

Appendix E

Perturbative expansion of the sinh-Gordon TBA equations

In this appendix we expand analytically the sinh-Gordon vacuum and excited state TBA equations in the coupling. As the zeroth order term of the TBA kernel is the Dirac delta function one has to be careful. One can either explicitly subtract this term and then make the expansion, or alternatively it is also possible to shift the integration contour, to take additionally into account the pole of the kernel and expand the shifted equations with the new source term. We performed both calculations and got the same result, which we present now.

The vacuum TBA is an integral equation for the unknown function $Y^{(0)}(u)$ and is of the form

$$Y^{(0)}(u) = \mathrm{e}^{-M_{ShG}L\cosh u} \exp\left\{\frac{1}{2\pi}\int_{-\infty}^{\infty} \mathrm{d}v\, \sigma(u-v)L^{(0)}(v)\right\}, \tag{E.1}$$

where

$$L^{(0)} = \ln[1+Y^{(0)}] \tag{E.2}$$

and

$$\sigma(u) = \frac{2\alpha\cosh u}{\sinh^2 u + \alpha^2}. \tag{E.3}$$

This TBA corresponds to the S-matrix

$$S(\theta) = \frac{\sinh\theta - i\alpha}{\sinh\theta + i\alpha}. \tag{E.4}$$

We will use the parameter α as our expansion parameter. The solution of (E.1) can be used to calculate the ground state energy, which is given by

$$E^{(0)} = -\frac{M_{ShG}}{2\pi}\int_{-\infty}^{\infty} \mathrm{d}u\, \cosh u L^{(0)}(u). \tag{E.5}$$

Similarly, the unknown function in the 1-particle TBA is $Y^{(1)}(u,\gamma)$, which satisfies

$$Y^{(1)}(u,\gamma) = \Sigma(u-\gamma)\mathrm{e}^{-M_{ShG}L\cosh u}\exp\left\{\frac{1}{2\pi}\int_{-\infty}^{\infty}\mathrm{d}v\,\sigma(u-v)L^{(1)}(v,\gamma)\right\}, \tag{E.6}$$

where

$$L^{(1)} = \ln[1+Y^{(1)}] \tag{E.7}$$

and

$$\Sigma(u) = \frac{\cosh u-\alpha}{\cosh u+\alpha}. \tag{E.8}$$

Let us introduce

$$D(\gamma) = M_{ShG}L\sinh\gamma - \frac{1}{2\pi}\int_{-\infty}^{\infty}\mathrm{d}u\,\tilde{\sigma}(u-\gamma)L^{(1)}(u,\gamma), \tag{E.9}$$

where

$$\tilde{\sigma}(u) = \frac{2\alpha\sinh u}{\cosh^2 u-\alpha^2}. \tag{E.10}$$

The exact rapidity β is defined to be the solution of the exact Bethe-Yang equation

$$D(\beta) = \frac{2\pi}{L}n = M_{ShG}L\sinh\theta. \tag{E.11}$$

We have to solve the coupled system (E.6) and (E.11) to calculate the energy of the first excited state with momentum

$$q = M_{ShG}\sinh\theta. \tag{E.12}$$

It is given by

$$E^{(1)} = M_{ShG}\cosh\beta - \frac{M_{ShG}}{2\pi}\int_{-\infty}^{\infty}\mathrm{d}u\,\cosh u L^{(1)}(u,\beta). \tag{E.13}$$

Finally the 1-particle spectrum is given by

$$E(q) = E^{(1)}(q) - E^{(0)} = E_0(q) + \alpha E_1(q) + \alpha^2 E_2(q) + \dots \tag{E.14}$$

and the density of states by

$$R(q) = D'(\beta) = R_0(q) + \alpha R_1(q) + \alpha^2 R_2(q) + \dots \tag{E.15}$$

We can now perturbatively solve the TBA equations and after a long computation we find that the expansion coefficients can be expressed in terms of the following integrals:

$$f_k(q) = \frac{1}{\pi}\int_{-\infty}^{\infty}\mathrm{d}u\,\frac{1}{\mathrm{e}^{M_{ShG}L\cosh u}-1}\,\frac{1}{\cosh^k w}, \tag{E.16}$$

$$g_k(q) = \frac{1}{\pi}\int_{-\infty}^{\infty} \mathrm{d}u\, \frac{1}{\mathrm{e}^{M_{ShG}L\cosh u}-1}\,\frac{\sinh w}{\cosh^k w}, \tag{E.17}$$

$$\xi_1(q) = \frac{1}{\pi}\int_{-\infty}^{\infty} \mathrm{d}u\, \frac{\mathrm{e}^{M_{ShG}L\cosh u}}{(\mathrm{e}^{M_{ShG}L\cosh u}-1)^2}\,\frac{1}{\cosh w}, \tag{E.18}$$

where

$$w = u - \theta. \tag{E.19}$$

We will also use

$$\rho = 2f_0, \tag{E.20}$$

which has been introduced in the bulk of the thesis.

The expansion coefficients are

$$E_0(q) = M_{ShG}\cosh\theta, \qquad E_1(q) = \frac{M_{ShG}\rho}{2\cosh\theta}, \tag{E.21}$$

$$E_2(q) = M_{ShG}\left\{-\left(\frac{1}{\cosh\theta}+\frac{M_{ShG}L\rho}{2}\right)\xi_1 + (1+\tanh^2\theta)\frac{\rho^2}{8\cosh\theta} - \frac{\rho f_2}{2\cosh\theta}\right\} \tag{E.22}$$

and

$$R_0(q) = M_{ShG}L\cosh\theta, \qquad R_1(q) = M_{ShG}L\left\{\frac{\rho}{2\cosh\theta} - \cosh\theta f_2\right\}, \tag{E.23}$$

$$R_2(q) = 4f_2 - 6f_4 - 2\tanh\theta g_3 + M_{ShG}L\left\{\left(\frac{1}{\cosh\theta}-\frac{1}{2\cosh^3\theta}\right)\frac{\rho^2}{4} + \cosh\theta f_2^2 - \frac{\rho f_2}{\cosh\theta}\right\}. \tag{E.24}$$

In the Lüscher approximation these coefficients agree with those we get from the α-expansion of the formulas (4.5) and (4.6):

$$\overline{E}_1(q) = \frac{M_{ShG}\bar\rho}{2\cosh\theta} = \frac{M_{ShG}}{\pi\cosh\theta}\int_{-\infty}^{\infty}\mathrm{d}u\,\mathrm{e}^{-M_{ShG}L\cosh u}, \tag{E.25}$$

$$\overline{E}_2(q) = -\frac{M_{ShG}\bar\xi_1}{\cosh\theta} = -\frac{M_{ShG}}{\pi\cosh\theta}\int_{-\infty}^{\infty}\mathrm{d}u\,\mathrm{e}^{-M_{ShG}L\cosh u}\frac{1}{\cosh w}, \tag{E.26}$$

$$\begin{aligned}\overline{R}_1(q) &= M_{ShG}L\left\{\frac{\bar\rho}{2\cosh\theta} - \cosh\theta\bar f_2\right\}\\ &= -\frac{M_{ShG}L}{\pi}\int_{-\infty}^{\infty}\mathrm{d}u\,\mathrm{e}^{-M_{ShG}L\cosh u}\sinh u\left[\tanh\theta\frac{1}{\cosh w} - \frac{\sinh w}{\cosh^2 w}\right],\end{aligned} \tag{E.27}$$

$$\begin{aligned}\overline{R}_2(q) &= 4\bar f_2 - 6\bar f_4 - 2\tanh\theta\bar g_3\\ &= \frac{M_{ShG}L}{\pi}\int_{-\infty}^{\infty}\mathrm{d}u\,\mathrm{e}^{-M_{ShG}L\cosh u}\sinh u\left[\tanh\theta\frac{1}{\cosh^2 w} - \frac{2\sinh w}{\cosh^3 w}\right].\end{aligned} \tag{E.28}$$

We always use an overline notation to indicate the Lüscher approximation of the same quantity.

Appendix F

Details of the perturbative calculation of the finite volume $0-1$ form factor

In this appendix we explain how we turned the double sums in the Hamiltonian perturbation theory to integrals and how we performed their large volume expansions.

F.1 The double sum in the energy correction

In this part we provide an integral representation for the double sum

$$\sum_{k_1\in\mathbb{Z}}\sum_{k_2\neq n_q} D_1\left(k_1,k_2\right) \tag{F.1}$$

with

$$\begin{aligned} D_1(k_1,k_2) = \frac{1}{\omega_{k_1}\omega_{k_2}\omega_{k_1+k_2-n_q}}\Bigg(&\frac{1}{\omega_{k_1}+\omega_{k_2}+\omega_{k_1+k_2-n_q}+\omega_{n_q}} \\ &+\frac{1}{\omega_{k_1}+\omega_{k_2}+\omega_{k_1+k_2-n_q}-\omega_{n_q}}\Bigg) \end{aligned} \tag{F.2}$$

We start by applying the residue method to the k_1 variable. The analytically continued function $D_1\left(z,k_2\right)$ contains two pairs of branch cuts on the z plane, starting from $\pm im$ and $q-\frac{2\pi k_2}{L}\pm im$, and going away from the real axis towards complex infinity in the imaginary direction. The integrals coming from the cuts below the real axis can be combined nicely to those above the real axis after a change of integration variable. Introducing $\kappa_2=2\pi k_2 L^{-1}$, the resulting integral can be written as

$$\begin{aligned} \sum_{k_1\in\mathbb{Z}}\sum_{k_2\neq n_q} D_1\left(k_1,k_2\right) \;=\; &\sum_{k_2\neq n_q}\int_1^\infty du\, im\frac{L}{2\pi}\coth\left(\frac{mLu}{2}\right)\left(\Theta_{q,m}\left(\kappa_2-q,u\right)+\Delta_{q,m}\left(\kappa_2,u\right)\right. \\ &\left.+\Theta_{q,m}\left(\kappa_2-q,-u\right)+\Delta_{q,m}\left(\kappa_2,-u\right)\right) \end{aligned} \tag{F.3}$$

where

$$\Theta_{q,m}(\kappa,u)=\frac{\kappa(m+iqu)-mq(u^2-1)}{\kappa m^2(\kappa+q+imu)(iq+mu)\sqrt{(u^2-1)\left(m^2+(\kappa+imu)^2\right)}} \tag{F.4}$$

and

$$\Delta_{q,m}(\kappa,u)=-\frac{\kappa qu+m^2u+imq-i\kappa m}{m^2(\kappa-q)(q-imu)(\kappa+imu)\sqrt{(u^2-1)(m^2+\kappa^2)}} \tag{F.5}$$

We now turn the remaining summation to integration.

We note that in (F.3) both $\Theta_{q,m}$ and $\Delta_{q,m}$ having $+u$ argument are the contributions of the branch cuts starting from $+im$ and $-im+q-\kappa_2$, whereas the terms of $-u$ argument correspond to the other two cuts. Interchanging the k_2 sum with the integral, the remaining sums to be evaluated have the form

$$\begin{aligned}
S_\Theta &= \sum_{k_2\neq n_q}\left[\Theta_{q,m}(\kappa_2-q,u)+\Theta_{q,m}(\kappa_2-q,-u)\right]\\
&= \sum_{k_2\neq 0}\left[\Theta_{q,m}(\kappa_2,u)+\Theta_{q,m}(\kappa_2,-u)\right]\\
&= \sum_{k_2\neq 0}\left[\Theta_{q,m}(\kappa_2,u)+\Theta_{q,m}(-\kappa_2,-u)\right]\\
&= \sum_{k_2\neq 0}\frac{2u(m^2+q^2)(\kappa_2+imu)}{m^2(q^2+m^2u^2)\left[(\kappa_2+imu)^2-q^2\right]\sqrt{(u^2-1)\left[m^2+(\kappa_2+imu)^2\right]}}
\end{aligned} \tag{F.6}$$

and

$$\begin{aligned}
S_\Delta &= \sum_{k_2\neq n_q}\left[\Delta_{q,m}(\kappa_2,u)+\Delta_{q,m}(\kappa_2,-u)\right]\\
&= -\sum_{k_2\neq n_q}\frac{2i\kappa_2q\sqrt{u^2-1}}{m\omega_{k_2}(\kappa_2^2+m^2u^2)(q^2+m^2u^2)}\\
&= \frac{2iq^2\sqrt{u^2-1}}{m\omega_{n_q}(q^2+m^2u^2)^2}
\end{aligned} \tag{F.7}$$

where in the last step we used the antisymmetry of the summand.

We now proceed by obtaining an integral representation of the sum S_Θ. Analytically continuing the summand of (F.6) into the complex κ_2 plane, we find a pair of branch cuts and two single poles. However, this time the branch points of the cuts lie at $im(\pm1-u)$, and since $u>1$, the upper cut intersects the real axis. The $k_2=n_q$ terms of the double sum in (4.69) were separated for precisely this reason. Now an

integral representation can be achieved by writing S_Θ as a sum of two contour integrals

$$S_\Theta = \frac{L}{2\pi}\left[\int\limits_{C_1} dz \frac{e^{iLz}}{e^{iLz}-1} f_\Theta(z) + \int\limits_{C_2} dz \frac{e^{iLz}}{e^{iLz}-1} f_\Theta(z)\right] \tag{F.8}$$

with

$$f_\Theta(z) = \frac{2u\left(m^2+q^2\right)(z+imu)}{m^2(z-q+imu)(z+q+imu)\left(q^2+m^2u^2\right)\sqrt{\left(u^2-1\right)\left[m^2+(z+imu)^2\right]}}. \tag{F.9}$$

The closed contours C_1 and C_2 are chosen such that C_1 goes from $-\infty - i\epsilon$ to $-2\pi L^{-1} - i\epsilon$ just below the real axis, then from $-2\pi L^{-1} + i\epsilon$ back to $-\infty + i\epsilon$ just above the real axis, while C_2 is the mirror image of C_1 with respect to the imaginary axis except that it is also directed counterclockwise. Now both contours can be blown up such that they are tightened to the cuts. As a result of the deformation, the poles of f_Θ at $z = \pm q - imu$ become encircled in the negative direction which results in additional residual terms. After the variable changes $u \to \cosh u$, $v \to \cosh v$, and extending the intagration domain over the real line by symmetrization[1], we get an integral representation of S_Θ as

$$S_\Theta = \frac{2L}{im^2}\frac{e^{mLu}}{e^{mLu}-1}\frac{\sqrt{m^2+q^2}u}{\left(q^2+m^2u^2\right)\sqrt{u^2-1}} + \frac{L}{i\pi m}\int\limits_{-\infty}^{\infty} dv\left(\lambda(u,v)\, s(u,v) + \mathrm{sing}_\Theta(u,v)\right) \tag{F.10}$$

where

$$\lambda(u,v) = \frac{e^{mL\cosh u}}{e^{mL\cosh v} - e^{mL\cosh u}} - \frac{e^{mL(\cosh u+\cosh v)}}{e^{mL(\cosh u+\cosh v)}-1}, \tag{F.11}$$

$$s(u,v) = \frac{\left(m^2+q^2\right)\cosh u\cosh v}{\left(q^2+m^2\cosh^2 u\right)\left(q^2+m^2\cosh^2 v\right)}, \tag{F.12}$$

$$\mathrm{sing}_\Theta(u,v) = \frac{2}{mL}\frac{1}{u^2-v^2}\frac{s(u,u)\,u}{\sinh u} \tag{F.13}$$

The term of (F.13) comes from the neighbourhood of the branch-overlapped pole. Note that both $\lambda(u,v)$ and $\mathrm{sing}_\Theta(u,v)$ are singular along the lines $u = \pm v$; their sum is, however, finite everywhere.

At this stage, we can represent the original double sum as a formula containing the

[1]The region around the branch-overlapped pole needs special treatment.

following double integral

$$\sum_{k_1,k_2\in\mathbb{Z}} D_1(k_1,k_2) = L^2 \int_{-\infty}^{\infty}\frac{du}{2\pi}\int_{-\infty}^{\infty}\frac{dv}{2\pi}\coth\left(\frac{mL}{2}\cosh u\right)\left(\lambda(u,v)\,s(u,v)+\mathrm{sing}_\Theta(u,v)\right) + (\text{other terms}) \tag{F.14}$$

Since the double integral is absolutely convergent, we can perform a symmetrization of the integrand as

$$\int_{-\infty}^{\infty}\int_{-\infty}^{\infty} dudv\, f(u,v) = \frac{1}{2}\int_{-\infty}^{\infty}\int_{-\infty}^{\infty} dudv\ \left(f(u,v)+f(v,u)\right) \tag{F.15}$$

which leaves the value of the integral unchanged. Upon this transformation, the first term of (F.14) becomes

$$L^2\int_{-\infty}^{\infty}\frac{du}{2\pi}\int_{-\infty}^{\infty}\frac{dv}{2\pi}\frac{1+e^{mL\cosh u}+e^{mL\cosh v}-3e^{mL(\cosh u+\cosh v)}}{2\left(e^{mL\cosh u}-1\right)\left(e^{mL\cosh v}-1\right)}s(u,v) \tag{F.16}$$

which can be further simplified as

$$L^2\int_{-\infty}^{\infty}\frac{du}{2\pi}\int_{-\infty}^{\infty}\frac{dv}{2\pi}\frac{1+e^{mL\cosh u}+e^{mL\cosh v}-3e^{mL(\cosh u+\cosh v)}}{2\left(e^{mL\cosh u}-1\right)\left(e^{mL\cosh v}-1\right)}s(u,v) = -\frac{L^2}{m^2}\left(\frac{3}{8}+\int_{-\infty}^{\infty}\frac{du}{2\pi}\frac{1}{e^{mL\cosh u}-1}\frac{m\sqrt{m^2+q^2}\cosh u}{q^2+m^2\cosh^2 u}\right) \tag{F.17}$$

if we note that

$$\frac{1+e^{mL\cosh u}+e^{mL\cosh v}-3e^{mL(\cosh u+\cosh v)}}{2\left(e^{mL\cosh u}-1\right)\left(e^{mL\cosh v}-1\right)} = -\frac{3}{2}-\frac{1}{e^{mL\cosh u}-1}-\frac{1}{e^{mL\cosh v}-1} \tag{F.18}$$

We now calculate the integral of the symmetrized second term of the integrand. For brevity, we introduce the function

$$\mathrm{sing}(u,v) = \coth\left(\frac{mL}{2}\cosh u\right)\mathrm{sing}_\Theta(u,v).$$

In this notation, the symmetrized integral has the following form

$$\frac{L^2}{2}\int_{-\infty}^{\infty}\frac{du}{2\pi}\int_{-\infty}^{\infty}\frac{dv}{2\pi}\left(\mathrm{sing}(u,v)+\mathrm{sing}(v,u)\right).$$

Both terms of this integrand are divergent by themselves; their sum, however, is finite everywhere. To perform the integrations, we notice that due to the symmetry of the integrand,

$$\frac{L^2}{2}\int_{-\infty}^{\infty}\frac{du}{2\pi}\int_{-\infty}^{\infty}\frac{dv}{2\pi}\left(\mathrm{sing}\left(u,v\right)+\mathrm{sing}\left(v,u\right)\right)=\frac{4L^2}{2}\int_{0}^{\infty}\frac{du}{2\pi}\int_{-u}^{u}\frac{dv}{2\pi}\left(\mathrm{sing}\left(u,v\right)+\mathrm{sing}\left(v,u\right)\right) \tag{F.19}$$

which we regularize[2] as

$$\begin{aligned}2L^2\lim_{\epsilon\to 0}\left[\int_{\epsilon}^{\infty}\frac{du}{2\pi}\int_{-u+\epsilon}^{u-\epsilon}\frac{dv}{2\pi}\mathrm{sing}\left(u,v\right)+\int_{\epsilon}^{\infty}\frac{du}{2\pi}\int_{-u+\epsilon}^{u-\epsilon}\frac{dv}{2\pi}\mathrm{sing}\left(v,u\right)\right] &= \\ 2L^2\lim_{\epsilon\to 0}\left[\int_{\epsilon}^{\infty}\frac{du}{2\pi}\int_{-u+\epsilon}^{u-\epsilon}\frac{dv}{2\pi}\mathrm{sing}\left(u,v\right)+2\int_{0}^{\infty}\frac{du}{2\pi}\int_{u+\epsilon}^{\infty}\frac{dv}{2\pi}\mathrm{sing}\left(u,v\right)\right] &\end{aligned} \tag{F.20}$$

In the last step we made use of the identity

$$\int_{\epsilon}^{\infty}\frac{du}{2\pi}\int_{-u+\epsilon}^{u-\epsilon}\frac{dv}{2\pi}=\int_{-\infty}^{\infty}\frac{dv}{2\pi}\int_{v+\epsilon}^{\infty}\frac{du}{2\pi}, \tag{F.21}$$

and the fact that $\mathrm{sign}\left(u,v\right)$ is symmetric in v together with the freedom to switch the labeling of integration variables. Now the integrals over v in (F.20) can be performed. Combining the remaining u integrals, we obtain

$$\frac{8L}{m}\lim_{\epsilon\to 0}\left[-\int_{0}^{\epsilon}\frac{du}{\left(2\pi\right)^2}\frac{\tilde{s}\left(u\right)}{\sinh u}\mathrm{arctanh}\left(\frac{u}{u+\epsilon}\right)+\frac{1}{2}\int_{\epsilon}^{\infty}\frac{du}{\left(2\pi\right)^2}\frac{\tilde{s}\left(u\right)}{\sinh u}\ln\left(1-\frac{2\epsilon}{\epsilon+2u}\right)\right] \tag{F.22}$$

with

$$\tilde{s}\left(u\right)=s\left(u,u\right)\coth\left(\frac{mL}{2}\cosh u\right). \tag{F.23}$$

Both integrands approximate Dirac δ-like peaks centered at $u=0$ in the $\epsilon\to 0$ limit. Thus, we approximate the regular part $\tilde{s}\left(u\right)$ with its value at the top of the peaks, and

[2]This regularization comes from regularizing the contour integral around the overlapped pole and then performing the change of variables.

integrate analytically the singular part. Finally, taking the $\epsilon \to 0$ limit, we get

$$\frac{L^2}{2}\int_{-\infty}^{\infty}\frac{du}{2\pi}\int_{-\infty}^{\infty}\frac{dv}{2\pi}\left(\mathrm{sing}\left(u,v\right)+\mathrm{sing}\left(v,u\right)\right)=\frac{L}{m\left(m^2+q^2\right)\pi^2}\coth\left(\frac{mL}{2}\right)\left(\mathrm{Li}_2\left(-2\right)+\frac{1}{2}\mathrm{Li}_2\left(\frac{1}{4}\right)-\frac{\pi^2}{6}+\left(\ln\,2\right)^2\right) \tag{F.24}$$

where $\mathrm{Li}_2\left(x\right)$ is the dilogarithm function

$$\mathrm{Li}_2\left(x\right)=\int_0^{\infty}\frac{t}{e^t/x-1},\quad x\in\mathbb{C}\setminus\left\{x\in\mathbb{R}\wedge x\geq 1\right\}. \tag{F.25}$$

Using the above integral representation, the Abel identity

$$\mathrm{Li}_2\left(\frac{x}{1-y}\right)+\mathrm{Li}_2\left(\frac{y}{1-x}\right)-\mathrm{Li}_2\left(\frac{xy}{\left(1-x\right)\left(1-y\right)}\right)=\mathrm{Li}_2\left(x\right)+\mathrm{Li}_2\left(y\right)+\ln\left(1-x\right)\ln\left(1-y\right) \tag{F.26}$$

with $x=-1$ and $y=\frac{1}{2}$, and the special value

$$\mathrm{Li}_2\left(-1\right)=-\frac{\pi^2}{12}, \tag{F.27}$$

we obtain

$$\mathrm{Li}_2\left(-2\right)+\frac{1}{2}\mathrm{Li}_2\left(\frac{1}{4}\right)-\frac{\pi^2}{6}+\left(\ln\,2\right)^2=-\frac{\pi^2}{4} \tag{F.28}$$

Putting everything together, the double sum of (4.69) can be written as

$$\sum_{k_1,k_2\in\mathbb{Z}}D_1\left(k_1,k_2\right)=C_1+C_2+C_\Delta+C_r+C_{ord}+C_{sing} \tag{F.29}$$

where:

- C_1 and C_2 contains the single sums separated in (4.69). Using (4.68) and (4.70),

$$C_1 = \frac{L}{\omega_{n_q}m^2}\left(\frac{1}{2\pi}+mL\int_{-\infty}^{\infty}\frac{du}{2\pi}\frac{e^{mL\cosh u}}{\left(e^{mL\cosh u}-1\right)^2}\cosh u\right) \tag{F.30}$$

$$C_2 = \frac{L}{4\omega_{n_q}^2 m}\coth\left(\frac{mL}{2}\right)-\frac{L}{2\omega_{n_q}}\int_{-\infty}^{\infty}\frac{du}{2\pi}\frac{\coth\left(\frac{mL}{2}\cosh u\right)}{\omega_{n_q}^2+m^2\sinh^2 u} \tag{F.31}$$

- C_Δ stands for the term coming from (F.7)

$$C_\Delta = -\int_{-\infty}^{\infty} \frac{du}{2\pi} \frac{L}{\omega_{n_q}} \coth\left(\frac{mL\cosh u}{2}\right) \frac{q^2 \sinh^2 u}{\left(q^2 + m^2 \cosh^2 u\right)^2} \tag{F.32}$$

- C_r contains the residual terms emerging from the contour deformation of the integral representation of S_Θ appearing in (F.10)

$$C_r = \int_{-\infty}^{\infty} \frac{du}{2\pi} \frac{L^2}{m} \coth\left(\frac{mL\cosh u}{2}\right) \frac{e^{mL\cosh u}}{e^{mL\cosh u} - 1} \frac{\sqrt{m^2+q^2}\cosh u}{\left(q^2 + m^2\cosh^2 u\right)} \tag{F.33}$$

- C_{ord} is the symmetrized double integral contribution (F.17)

$$C_{ord} = -\frac{L^2}{m^2}\left(\frac{3}{8} + \int_{-\infty}^{\infty} \frac{du}{2\pi} \frac{1}{e^{mL\cosh u} - 1} \frac{m\sqrt{m^2+q^2}\cosh u}{q^2 + m^2\cosh^2 u}\right) \tag{F.34}$$

- Finally, C_{sing} is the symmetrized singular contribution (F.24)

$$C_{sing} = -\frac{L}{4m\left(m^2+q^2\right)} \coth\left(\frac{mL}{2}\right). \tag{F.35}$$

Combining these terms, significant simplifiactions can be achieved. First of all, notice that C_{sing} is cancelled by a similar term appearing in C_2. As a next step, we combine C_Δ and the integral part of C_2, and perform integration by parts. The resulting boundary term cancels the explicit term appearing in C_1. C_r contains an infinite-volume term that can be separated and integrated analytically. Then, the remaining part of the integral in C_r, the integral part of C_{ord}, the integral appearing in C_1 and the result of the previous integration by parts can be combined beautifully together and lead to the following nice representation of the full double sum:

$$\sum_{k_1,k_2} D_1\left(k_1,k_2\right) = \frac{L^2}{m^2}\left(\frac{1}{8} + 3\int_{-\infty}^{\infty} \frac{du}{2\pi} \frac{e^{mL\cosh u}}{\left(e^{mL\cosh u}-1\right)^2} \frac{1}{\cosh\left(u-\theta\right)}\right) \tag{F.36}$$

where we introduced θ as the rapidity variable $q = m\sinh\theta$.

F.2 Expansion of the form factor

We first provide an integral representation of the double sum $\sum_{k_1,k_2} D_2\left(k_1,k_2\right)$, we then calculate the large volume expansion of the full form factor $\langle 0\left(b\right)|\varphi|\, q\left(b\right)\rangle$.

The transformation of

$$\sum_{k_1,k_2} D_2\left(k_1,k_2\right) \tag{F.37}$$

with

$$D_2\left(k_1,k_2\right) = \frac{1}{\omega_{k_1}\omega_{k_2}\omega_{k_1+k_2-n_q}}\left[\left(\frac{1}{\omega_{k_1}+\omega_{k_2}+\omega_{k_1+k_2-n_q}+\omega_{n_q}}\right)^2 - \left(\frac{1}{\omega_{k_1}+\omega_{k_2}+\omega_{k_1+k_2-n_q}-\omega_{n_q}}\right)^2\right] \tag{F.38}$$

can be started in parallel to the steps done in the case of $D_1\left(k_1,k_2\right)$. We first separate the $k_2 = n_q$ terms analogously to (4.69)

$$\sum_{k_1,k_2\in\mathbb{Z}} D_2\left(k_1,k_2\right) = \sum_{k_1\in\mathbb{Z}}\sum_{k_2\neq n_q} D_2\left(k_1,k_2\right) - \frac{1}{4\omega_{n_q}}\sum_{k_1\in\mathbb{Z}}\frac{1}{\omega_{k_1}^4} + \frac{1}{4\omega_{n_q}}\sum_{k_1\in\mathbb{Z}}\frac{1}{\omega_{k_1}^2}\frac{1}{\left(\omega_{k_1}+\omega_{n_q}\right)^2} \tag{F.39}$$

These separated terms can be easily calculated using the derivative of (4.70) with respect to A and the formula

$$\sum_{k\in\mathbb{Z}}\frac{1}{\omega_k^4} = \frac{2L\coth\left(\frac{mL}{2}\right)+mL^2\mathrm{csch}^2\left(\frac{mL}{2}\right)}{8m^3}. \tag{F.40}$$

Now we turn the sum over k_1 into an integral. This can be done in a straightforward manner. Using the variable $\kappa_2 = 2\pi k_2 L^{-1}$, we get

$$\sum_{k_1\in\mathbb{Z}}\sum_{k_2\neq n_q} D_2\left(k_1,k_2\right) = \sum_{k_2\neq n_q}\frac{L}{2\pi}\int_{-\infty}^{\infty} du\coth\left(\frac{mL}{2}\cosh u\right)\left(\Xi\left(k_2,\omega_{n_q},q\right)\right. \\ \left.+\Xi\left(k_2,\omega_{n_q},-q\right)-\Xi\left(k_2,-\omega_{n_q},q\right)-\Xi\left(k_2,-\omega_{n_q},-q\right)\right) \tag{F.41}$$

with

$$\Xi\left(k_2,A,q\right) = \frac{\left(\sqrt{m^2+\left(q-\kappa_2\right)^2}+\sqrt{m^2+\left(\kappa_2+im\cosh u\right)^2}-im\sinh u+A\right)^{-2}}{\sqrt{m^2+\left(q-\kappa_2\right)^2}\sqrt{m^2+\left(\kappa_2+im\cosh u\right)^2}}. \tag{F.42}$$

By means of equivalent transformations including a shift of the summation variable $\kappa_2 = \tilde{\kappa}_2 + q$, symmetrization of the integrand and algebraic manipulations, (F.41) simplifies miraculously to a sum of two terms, plus the same sum with the sign of q

switched, each term containing only a single pair of branch cuts:

$$\sum_{\substack{k_1\in\mathbb{Z}\\ k_2\neq n_q}} D_2(k_1,k_2) = -\frac{L\omega_{n_q}}{16m^2}\sum_{k_2\neq 0}\int_{-\infty}^{\infty}\frac{du}{2\pi}\Bigg[\frac{\coth\left(\frac{mL}{2}\cosh u\right)}{\kappa_2^2(\kappa_2-q+im\cosh u)^2(q+im\cosh u)^2} \times\Big(\mathcal{G}(\kappa_2-q,q)+\mathcal{G}(-\kappa_2-im\cosh u,q)\Big)+(q\to -q)\Bigg] \tag{F.43}$$

where

$$\begin{aligned}\mathcal{G}(x,q) &= \frac{4m^2(x+q)^2-2imP_1(x,q)\cosh u-2P_2(x,q)\left[2(x+q)\cosh 2u+im\cosh 3u\right]}{\sqrt{m^2+x^2}}\\ P_1(x,q) &= 4x^3+6x^2q+x\left(m^2+4q^2\right)-m^2q\\ P_2(x,q) &= 2x^2q-xm^2+m^2q\end{aligned}$$

Now we proceed to transform the remaining sum (over k_2) in these terms.

Let us first examine the sum containing $\mathcal{G}(\kappa_2-q)$. The arising complex function contains the usual set of poles on the real line and a pair of branch cuts starting from $z=\pm im+q$ to complex infinity. It also has one pole of order 3 at $z=0$ and another of order 2 at $z=q-im\cosh u$. The latter is overlapped by the lower branch cut. After the deformation of the contour, the pole of order 3 is encircled in the clockwise direction. Other finite terms come from the overlapped second-order pole which cancel the divergences of the branch cut integral. We obtain

$$-\frac{L\omega_{n_q}}{16m^2}\sum_{k_2\neq 0}\int_{-\infty}^{\infty}\frac{du}{2\pi}\frac{\coth\left(\frac{mL}{2}\cosh u\right)\mathcal{G}(\kappa_2-q,q)}{\kappa_2^2(\kappa_2-q+im\cosh u)^2(q+im\cosh u)^2} = I_1^+(q)+I_1^-(q)+R_1(q) \tag{F.44}$$

where

$$I_1^-(q) = -\frac{L^2\omega_{n_q}}{8m^2}\int_{-\infty}^{\infty}\frac{du}{2\pi}\int\frac{dv}{2\pi}\Bigg[\coth\Big(\frac{mL}{2}\cosh u\Big)\frac{e^{mL\cosh v}}{e^{mL\cosh v}-1}\frac{G(\cosh u,\cosh v,q)}{(\cosh u-\cosh v)^2} +\mathrm{sing}_1(u,v,q)\Bigg] \tag{F.45}$$

$$I_1^+(q) = -\frac{L^2\omega_{n_q}}{8m^2}\int_{-\infty}^{\infty}\frac{du}{2\pi}\int\frac{dv}{2\pi}\frac{\coth\left(\frac{mL}{2}\cosh u\right)}{e^{mL\cosh v}-1}\frac{G(\cosh u,-\cosh v,q)}{(\cosh u+\cosh v)^2} \tag{F.46}$$

$$R_1(q) = \frac{L}{192m^2}\int_{-\infty}^{\infty}\frac{du}{2\pi}\frac{\coth\left(\frac{mL}{2}\cosh u\right)P_{R1}(\cosh u,q)}{(q-im\cosh u)^4(q+im\cosh u)^2} \tag{F.47}$$

with

$$\begin{aligned} G(x,y,q) &= \frac{-4}{(q+imx)^2(q-imy)^2}\left[m^2xy\left(-1+x^2-xy+y^2\right)+q^2\left(1-xy-y^2+x^2\left(-1+2y^2\right)\right)\right. \\ &\quad \left.+imq\left(x-y+y^3-2x^2y^3+x^3\left(-1+2y^2\right)\right)\right] \end{aligned} \tag{F.48}$$

$$\begin{aligned} \mathrm{sing}_1(u,v,q) = &-2\coth\left(\frac{mL}{2}\cosh u\right)\frac{e^{mL\cosh u}}{e^{mL\cosh u}-1}\left\{\frac{u^2+v^2}{(u^2-v^2)^2}\frac{G(\cosh u,\cosh u,q)}{\sinh^2 u}\right. \\ &+\frac{u}{\sinh u}\frac{1}{u^2-v^2}\left[\left(\frac{mL}{e^{mL\cosh u}-1}+\frac{\cosh u}{\sinh^2 u}\right)G(\cosh u,\cosh u,q)\right. \\ &\left.\left.-\frac{\partial G(\cosh u,y,q)}{\partial y}\Big|_{y=\cosh u}\right]\right\} \end{aligned} \tag{F.49}$$

and $P_{R1}(x,q)$ is some complicated polynomial of x,q,L and m.

We can immediately calculate the infinite volume limit and first Lüscher correction of (F.44) and its opposite momentum pair. For the infinite volume limit, we can analytically take both integrals in (F.45) and (F.46). For the first Lüscher correction, one integral can be done analytically, and we are led to a formula containing only a single integral, as expected. We note that higher Lüscher corrections seem to be much harder to get in the form of explicit single-integral formulas. In the following, we use the rapidity variable $q = m\cosh\theta$.

The term $I_1^+(q) + I_1^+(-q)$ does not contribute to the infinite volume limit, and gives a first order Lüscher contribution

$$\begin{aligned} \widetilde{I_1^+} &= \frac{L^2}{\pi m^3}\int_{-\infty}^{\infty}\frac{du}{2\pi}\frac{e^{-mL\cosh u}}{(\cosh 2\theta+\cosh 2u)^3}\Big[-\cosh\theta\Big((3+\cosh 4\theta)\cosh 2u+\cosh 2\theta(3+\cosh 4u)\Big)\\ &\quad +\pi\cosh u(-3+\cosh 4\theta-2\cosh 2\theta\cosh 2u)\sinh^2 u\\ &\quad -u\cosh\theta(-3+\cosh 4\theta-2\cosh 2\theta\cosh 2u)\sinh 2u\\ &\quad -\theta\cosh\theta(-3+\cosh 4u-2\cosh 2\theta\cosh 2u)\sinh 2\theta\Big] \end{aligned} \tag{F.50}$$

The term $I_1^-(q)+I_1^-(-q)$ has the infinite volume limit

$$I_1^\infty=\frac{L^2\left(\pi^2-4\right)\cosh\theta}{8\pi^2m^3} \tag{F.51}$$

and admits a first Lüscher correction

$$\begin{aligned}\widetilde{I_1^-} \;=\; & \frac{3L^2}{\pi m^3}\int_{-\infty}^{\infty}\frac{du}{2\pi}\frac{e^{-mL\cosh u}}{\left(\cosh 2\theta+\cosh 2u\right)^3}\Big[-\cosh\theta\Big(\left(3+\cosh 4\theta\right)\cosh 2u+\cosh 2\theta\left(3+\cosh 4u\right)\Big)\\ & -\pi\cosh u\left(-3+\cosh 4\theta-2\cosh 2\theta\cosh 2u\right)\sinh^2 u\\ & -u\cosh\theta\left(-3+\cosh 4\theta-2\cosh 2\theta\cosh 2u\right)\sinh 2u\\ & -\theta\cosh\theta\left(-3+\cosh 4u-2\cosh 2\theta\cosh 2u\right)\sinh 2\theta\Big]\end{aligned} \tag{F.52}$$

The residual part $R_1(q)+R_1(-q)$ contributes to the infinite volume limit with

$$R_1^\infty=-\frac{L^2\cosh\theta}{8m^3}+\frac{L\left(-1+2\theta\coth 2\theta\right)}{m^4\pi\sinh^2 2\theta} \tag{F.53}$$

while its first Lüscher correction is

$$\begin{aligned}\widetilde{R_1}=\; & -\frac{L}{m^4}\int_{-\infty}^{\infty}\frac{du}{2\pi}\frac{e^{-mL\cosh u}}{\left(\cosh 2u+\cosh 2\theta\right)^4}\Big[-16+2\cosh 4\theta+\cosh 6u\cosh 2\theta\\ & +\cosh 4u(2-4\cosh 4\theta)+\cosh 2u\left(-18\cosh 2\theta+\cosh 6\theta\right)\Big]\\ & -\frac{L^2}{m^3}\int_{-\infty}^{\infty}\frac{du}{2\pi}\frac{e^{-mL\cosh u}}{\left(\cosh 2u+\cosh 2\theta\right)^4}2\cosh u\sinh^2 u\\ & \times\Big[4\cosh 2u+\cosh 2\theta(4+\cosh 4u-\cosh 4\theta)\Big]\end{aligned} \tag{F.54}$$

To deal with the other sums of (F.43) containing $\mathcal{G}(-\kappa_2-im\cosh u,q)$, it is expedient to desingularize the summand with a small auxiliary parameter a, in the following way:

$$\begin{aligned}& -\frac{L\omega_{n_q}}{16m^2}\sum_{k_2\neq 0}\int_{-\infty}^{\infty}\frac{du}{2\pi}\frac{\coth\left(\frac{mL}{2}\cosh u\right)\mathcal{G}\left(-\kappa_2-im\cosh u,q\right)}{\left(\kappa_2-ma\right)\left(\kappa_2+ma\right)\left(\kappa_2-q+im\cosh u\right)^2\left(q+im\cosh u\right)^2}\\ =\;& I_{2a}^+(q)+I_{2a}^-(q)+R_{2a}(q)\end{aligned} \tag{F.55}$$

Here $I_{2a}^+(q)$ contains the upper branch cut integral surrounding a single pole, similar to the one arising in the computation of $D_1(k_1,k_2)$, plus the sum of residues $r_{2a}(u,v,q)$ of regularized poles at $z=\pm ma$. $I_{2a}^-(q)$ denotes the lower, regular branch cut integral, while $R_{2a}(q)$ is the residual term coming from the pole at $z=q-im\cosh u$. The

limit $a \to 0$ can immediately be taken for $I_{2a}^{-}(q)$ and $R_{2a}(q)$, and the corresponding Lüscher- and infinite volume corrections are easily obtained (after the final momentum-combination) as

$$I_2^{-,\infty} = -\frac{L^2\left(4+\pi^2\right)\cosh\theta}{8m^3\pi^2} \tag{F.56}$$

$$\widetilde{I_2^{-}} = 2\widetilde{I_1^{+}} \tag{F.57}$$

$$R_2^{\infty} = \frac{L^2\cosh\theta}{4m^3} \tag{F.58}$$

$$\begin{aligned}\widetilde{R_2} = &\frac{6L^2}{m^3}\int\limits_{-\infty}^{\infty}\frac{du}{2\pi}\frac{e^{-mL\cosh u}}{\left(\cosh 2u+\cosh 2\theta\right)^3}\cosh u\sinh^2 u \\ &\times\left[3+\cosh\left(2\left(u-\theta\right)\right)-\cosh 4\theta+\cosh\left(2\left(u+\theta\right)\right)\right].\end{aligned} \tag{F.59}$$

Extracting the finite volume corrections of $I_{2a}^{+}(q)$ is a harder task. The form of the term is

$$\begin{aligned}I_{2a}^{+}(q) = &\frac{L^2\omega_{n_q}}{8m^2}\int\limits_{-\infty}^{\infty}\frac{du}{2\pi}\int\limits_{-\infty}^{\infty}\frac{dv}{2\pi}\left[\coth\left(\frac{mL}{2}\cosh u\right)\frac{e^{mL\cosh u}}{e^{mL\cosh u}-e^{mL\cosh v}}\right. \\ &\left.\times\frac{G\left(\cosh u,\cosh v,q\right)}{a^2+\left(\cosh u-\cosh v\right)^2}+\mathrm{sing}_{2a}\left(u,v,q\right)\right]+r_{2a}(q)\end{aligned} \tag{F.60}$$

with

$$\mathrm{sing}_{2a}\left(u,v,q\right) = -\frac{2}{a^2mL}\coth\left(\frac{mL}{2}\cosh u\right)\frac{u}{\sinh u}\frac{G\left(\cosh u,\cosh u,q\right)}{u^2-v^2} \tag{F.61}$$

To obtain the first Lüscher correction, we apply the symmetrization transformation (F.15) to the double integral appearing in (F.60). The form of the resulting integral is analogous to what we already saw in the case of the one-particle energy. In contrast to that calculation, now the part involving the function $\mathrm{sing}_{2a}\left(u,v,q\right)$ does not contribute to the value of the integral, since a factor $\sinh^2 u$ coming from $G\left(\cosh u,\cosh u\right)$ assures that the regular part of the integrand at $u=0$ is zero. The symmetrization removes the singularity of the integrand, and one can notice that there is no first order Lüscher term in the resulting integral. This means that any first order Lüscher correction of $I_{2a}^{+}(q)$ must come solely from the residual term $r_{2a}(q)$. The complication is that both $r_{2a}(q)$ and the double integral part of $I_{2a}^{+}(q)$ are divergent in the $a \to 0$ limit, even after symmetrization. In the following, we will outline the circumvention of this problem.

In the case of the double integral part, the root of the problem is that even though

the series expansion starts with $\mathcal{O}(a^0)$, the integrand becomes divergent at $v \to \pm u$. At this point, it is convenient to reintroduce the variables $x = \cosh u$, $y = \cosh v$. In terms of these, we can write

$$I_{2a}^{+} - r_{2a}(q) = \int_1^\infty dx \int_1^\infty dy \frac{f(x,y)}{a^2 + (x-y)^2} \tag{F.62}$$

and we separate this integral as

$$\int_1^\infty dx \int_1^\infty dy \frac{f(x,y)}{a^2 + (x-y)^2} = J_1 + J_2 \tag{F.63}$$

with

$$J_1 = \int_1^\infty dx \int_1^\infty dy \frac{1}{a^2 + (x-y)^2} \left(f(x,y) - f(x,x) - (y-x) \frac{\partial f}{\partial y}(x, y=x) \right) \tag{F.64}$$

$$J_2 = \int_1^\infty dx \int_1^\infty dy \frac{1}{a^2 + (x-y)^2} \left(f(x,x) + (y-x) \frac{\partial f}{\partial y}(x, y=x) \right) \tag{F.65}$$

Now the integrand of J_1 remains regular after the $a \to 0$ limit and the related integrals can be performed analytically. On the other hand, J_2 can be converted further by returning to the integration measure $\int_{-\infty}^{\infty} dv$, and shifting the contour corresponding to a change of variables $v = \tilde{v} - i\pi$. Upon shifting the contour, we have to encircle another pair of poles appearing at $z = -\text{acosh}(-ia + x)$ and $z = \text{acosh}(ia + x)$, respectively. We will call their contribution $r_{3a}(q)$. Aside from the residual terms, the shifted integrals are again finite at $a \to 0$ and can be evaluated analytically. After momentum combination, these integrals yield the simple infinite-volume contributions

$$J_1 = -\frac{L^2 \cosh\theta}{16 m^3} \tag{F.66}$$

$$J_2 - r_{3a}(q) = \frac{L^2 \cosh\theta}{4\pi^2 m^3} \tag{F.67}$$

All that remains to be done is the evaluation of the $a \to 0$ limit of the residual contribution $r_{2a}(q) + r_{3a}(q)$. These terms can be expressed in terms of the integrals

$$\mathcal{J}_k(a,q) = \int_1^\infty dy\, j_k(a,q,y) \tag{F.68}$$

$$j_k(a,q,y) = \frac{(y-1)^k}{q^2 + m^2 y^2} \frac{1}{\sqrt{1 + a^2 + 2iay - y^2}} \frac{1}{\sqrt{y^2 - 1}} \tag{F.69}$$

as follows:

$$\begin{aligned} r_{2a}(q)+r_{3a}(q) &= \int_1^\infty dy\Bigg[\frac{1}{a^2}\Big(\xi_{22}(q)\,\Re\mathrm{e}\left[j_2(a,q,y)\right]+\xi_{21}(q)\,\Re\mathrm{e}\left[j_1(a,q,y)\right]\Big) \\ &\quad +\frac{1}{a}\Big(\xi_{11}(q)\,\Im\mathrm{m}\left[j_1(a,q,y)\right]+\xi_{10}(q)\,\Im\mathrm{m}\left[j_0(a,q,y)\right]\Big) \\ &\quad +\xi_0(q)\,\Re\mathrm{e}\left[j_0(a,q,y)\right]\Bigg]+\mathcal{O}(a) \end{aligned} \tag{F.70}$$

Next, we can separate these integrals analogously to (F.63)-(F.65) into a part which can be expanded in a up to $\mathcal{O}(a^0)$ preserving finiteness and another part that needs to be calculated explicitely in the regularization. Fortunately the indefinite integrals $\int dy\, j_k(a,q,y)$ can be expressed for $k=0,1,2$ in terms of elliptic integrals:

$$\begin{aligned} \int dy\, j_0(a,q,y) &= \frac{2}{qm^2\cosh^2\theta\sqrt{4+a^2}}\{qF(c_2(a)\mid c_3(a)) \\ &\quad +im\left[\Pi(c_1(a,q),c_2(a)\mid c_3(a))-\Pi(c_1(a,-q),c_2(a)\mid c_3(a))\right]\} \end{aligned} \tag{F.71}$$

$$\begin{aligned} \int dy\, j_1(a,q,y) &= -\frac{2}{qm^2\cosh^2\theta\sqrt{4+a^2}}\left[(im+q)\,\Pi(c_1(a,q),c_2(a)\mid c_3(a))\right. \\ &\quad \left.+(-im+q)\,\Pi(c_1(a,-q),c_2(a)\mid c_3(a))\right] \end{aligned} \tag{F.72}$$

$$\begin{aligned} \int dy\, j_2(a,q,y) &= \frac{2i}{qm^3\cosh^2\theta\sqrt{4+a^2}}\left[(m-iq)^2\,\Pi(c_1(a,q),c_2(a)\mid c_3(a))\right. \\ &\quad \left.-(m+iq)^2\,\Pi(c_1(a,-q),c_2(a)\mid c_3(a))\right] \end{aligned} \tag{F.73}$$

These formulas enable us to calculate the definite integrals (F.68) by taking the appropriate limits. In taking these limits, sometimes it is useful to use the identity

$$\Pi\left(n,i\sinh^{-1}(\tan z)\mid 1-m\right)=\frac{i}{1-n}\left[F(z\mid m)-n\Pi(1-n,z\mid m)\right] \tag{F.74}$$

It should be noted, however, that Newton-Leibniz formula assumes the starting and ending point of the integration lie on the same Riemann sheet of the function. Any possible branch cuts crossed along the line of integration need to be taken care of by hand. In the above formulas,

$$c_1(a,q) = -\frac{a(m-iq)}{(2i+a)(m+iq)} \tag{F.75}$$

$$c_2(a) = \sin^{-1}\left(\sqrt{\frac{(2i+a)(1+y)}{a(-1+y)}}\right) \tag{F.76}$$

$$c_3(a) = \frac{a^2}{4+a^2} \tag{F.77}$$

One then needs to make a series expansion of the $\mathcal{J}_k$ in a, which can be performed by a lengthy calculation. This yields

$$\begin{aligned}
\Re e\mathcal{J}_0 &= \frac{\pi}{4m^2\cosh^2\theta} + \frac{a\left(1+\ln\left(\frac{a}{2\cosh^2\theta}\right)\right)}{2m^2\cosh^4\theta} - \frac{a^2\pi\left(21-2\sinh^2\theta+\sinh^4\theta\right)}{64m^2\cosh^6\theta} + \mathcal{O}\left(a^3\right) \\
\Re e\mathcal{J}_1 &= -\frac{a\left[4\sinh\theta\tan^{-1}\left(\sinh\theta\right)+\sinh^2\theta\ln\left(\frac{a}{8}\right)+\ln\left(\frac{2a}{\cosh^4\theta}\right)\right]}{4m^2\cosh^4\theta} + \frac{a^2\pi\left(12+\cosh^2\theta\right)}{64m^2\cosh^4\theta} \\
&\quad +\mathcal{O}\left(a^3\right) \\
\Re e\mathcal{J}_2 &= -\frac{a\left[\cosh^2\theta-4\sinh\theta\tan^{-1}\left(\sinh\theta\right)+2\left(1-\sinh^2\theta\right)\ln\left(\frac{\cosh\theta}{2}\right)\right]}{2m^2\cosh^4\theta} - \frac{a^2 3\pi}{32m^2\cosh^2\theta} \\
&\quad +\mathcal{O}\left(a^3\right)
\end{aligned} \tag{F.78}$$

$$\begin{aligned}
\Im m\mathcal{J}_0 &= \frac{2\tan^{-1}\left(\sinh\theta\right)+\sinh\theta\ln\left(\frac{a}{8}\right)}{2m^2\sinh\theta\cosh^2\theta} - \frac{a\pi}{4m^2\cosh^4\theta} + \mathcal{O}\left(a^2\right) \\
\Im m\mathcal{J}_1 &= -\frac{\tan^{-1}\left(\sinh\theta\right)+\sinh\theta\ln\left(\frac{\cosh\theta}{2}\right)}{m^2\sinh\theta\cosh^2\theta} + \frac{a\pi}{8m^2\cosh^2\theta} + \mathcal{O}\left(a^2\right)
\end{aligned} \tag{F.79}$$

The expanded part of (F.70) can be integrated analytically (surprisingly, even the terms containing the Lüscher correction $e^{-mL\cosh u}$ possess explicit integral formulas in terms of exponential integrals). As a result, all singular terms cancel, and we arrive at

$$r_{2a}\left(q\right)+r_{3a}\left(q\right) = -\frac{L\left(1-\sinh^2\theta\right)}{16m^4\cosh^3\theta} + \frac{e^{-mL}L\left(-1+\sinh^2\theta+Lm\cosh^2\theta\right)}{8m^4\cosh^3\theta} \tag{F.80}$$

At this point, we are in the position to collect all contributions of the form factor (4.84). First of all, up to first Lüscher order, the explicit terms in N_0 do not contribute. The sum $\sum_k S_1\left(k\right)$ can be transformed using (4.68), (4.70) and (4.86). Since the sum is multiplied by $\bar{\rho}$, we only need to consider its infinite volume part, leading to terms of first Lüscher order. After some cancellations, we find

$$\sum_{k\in\mathbb{Z}} S_1\left(k\right) = \frac{2L}{m^4\pi\cosh^2\theta} + \mathcal{O}\left(e^{-mL}\right) \tag{F.81}$$

According to (4.71), the double sum $\sum_{k_1,k_2} D_1\left(k_1,k_2\right)$ admits the Lüscher expansion

$$\sum_{k_1,k_2} D_1\left(k_1,k_2\right) = \frac{L^2}{8m^2} + \frac{3L^2}{m^2}\int_{-\infty}^{\infty}\frac{du}{2\pi}\frac{e^{-mL\cosh u}}{\cosh\left(u-\theta\right)} + \mathcal{O}\left(e^{-2mL}\right) \tag{F.82}$$

To deal with the nontrivial sum $\sum_{k_1,k_2} D_2\left(k_1,k_2\right)$, we first collect the explicit terms (i.e. those that can be expressed without integrals) appearing in the expansion. These terms come from the following places:

- The single sums separated in (F.39) as well as the regularized residual term $r_{2a}\left(q\right)+r_{3a}\left(q\right)$ of (F.80) contain explicit terms proportional to L, Le^{-mL} and L^2e^{-mL}.

- The residual term R_1^{∞} defined in (F.53) contains terms proportional to L and L^2.
- The terms coming from the quantities I_1^{∞}, $I_2^{-,\infty}$, R_2^{∞}, J_1, $J_2 - r_{3a}(q)$ (appearing in (F.51), (F.56), (F.58), (F.66) and (F.67), respectively) only contain terms proportional to L^2.

The above terms combine nicely so that all explicit contributions proportional to L, Le^{-mL} and L^2e^{-mL} cancel. All other terms sum up to

$$\sum_{k_1,k_2} D_2(k_1,k_2) = \frac{3L^2}{m^3}\left(\frac{1}{48} - \frac{1}{4\pi^2}\right)\cosh\theta + \mathcal{O}\left(e^{-mL}\right) \tag{F.83}$$

We now proceed to combine the various integral contributions into a more transparent form. First, $\widetilde{I_1^-}$, $\widetilde{I_1^+}$ and $\widetilde{I_2^-}$ of (F.52), (F.50) and (F.57) can be combined, and after trigonometric manipulations and the exploitation of the symmetry of the integration domain, we find

$$\widetilde{I_1^+} + \widetilde{I_1^-} + \widetilde{I_2^-} = \frac{3L^2\cosh\theta}{m^3\pi^2}\int_{-\infty}^{\infty} du\left(\frac{w\sinh w}{\cosh^3 w} - \frac{1}{\cosh^2 w}\right)e^{-mL\cosh u} \tag{F.84}$$

where

$$w = u - \theta. \tag{F.85}$$

The integrand of the residual term $\widetilde{R_1}$ of (F.54) contains a part proportional in $Le^{-mL\cosh u}$. This term can be combined with a similar integrand coming from the first Lüscher correction $\widetilde{Z}$ of the separated single sum $\sum_{k_1\in\mathbb{Z}} \frac{1}{\omega_{k_1}^2}\frac{1}{\left(\omega_{k_1}+\omega_{n_q}\right)^2}$. These can be integrated by parts, yielding an integrand that is proportional to $L^2e^{-mL\cosh u}$. This resulting integrand can be combined with the remaining part of $\widetilde{R_1}$ and also with $\widetilde{R_2}$ appearing in (F.59), and the result can be transformed using both trigonometric identities and the symmetry of the integration domain, to the following form

$$\widetilde{R_1} + \widetilde{R_2} + \widetilde{Z} = \frac{3L^2}{2\pi m^3}\int_{-\infty}^{\infty} du\left(\frac{\cosh u}{\cosh^2 w} - \frac{\cosh\theta}{\cosh^3 w}\right)e^{-mL\cosh u} \tag{F.86}$$

Using the above formulas, we can express the form factor as a function of the S-matrix parameter α

$$\begin{aligned}\langle 0(b)|\varphi|q(b)\rangle \;=\; & \frac{1}{\sqrt{2Lm\cosh\theta}}\Bigg\{1 - \alpha\int\frac{du}{2\pi}\left[\frac{e^{-mL\cosh u}}{\cosh^2\theta}\right] + \alpha^2\left(\frac{1}{48} + \frac{1}{24\cosh^2\theta} - \frac{1}{4\pi^2}\right) \\ & + \alpha^2\int_{-\infty}^{\infty}\frac{du}{2\pi}e^{-mL\cosh u}\left[\frac{\sinh u\sinh\theta}{\cosh^2\theta\cosh^2 w} + \frac{2}{\cosh^2\theta\cosh w} - \frac{1}{\cosh^3 w}\right.\end{aligned}$$

$$+\frac{2}{\pi}\left(\frac{w\sinh w}{\cosh^3 w}-\frac{1}{\cosh^2 w}\right)\Bigg]\Bigg\} \tag{F.87}$$

Appendix G

Reverse communication protocols and chiral factorisation

There are several iterative numerical methods (Lánczos, Arnoldi, Jacobi-Davidson, etc.) to obtain the smallest eigenvalues (and the corresponding eigenvectors) of a Hamiltonian. A common feature of these algorithms is that they do not need all of the Hamiltonian's matrix elements to be stored in memory. What they do require is a routine by which arbitrary vectors are acted upon by the Hamiltonian matrix. We will describe in this section how the tensor product nature of the Hilbert space for the sinh-Gordon model makes this matrix-vector multiplication remarkably efficient.

G.1 Separating zero and oscillator modes

As a demonstration of the numerical efficiency that can be obtained, we begin by factorizing the Hilbert space into (merely) two pieces,

$$\mathcal{H} = \mathcal{H}_{ZM} \otimes \mathcal{H}_{\rm osc}, \tag{G.1}$$

one encompassing the zero mode $\mathcal{H}_{ZM}$ and one the oscillator modes, $\mathcal{H}_{\rm osc} = \mathcal{H}_L \otimes \mathcal{H}_R$. Let $N = \dim\mathcal{H}$, $N_{ZM} = \dim\mathcal{H}_{ZM}$, $N_{osc} = \dim\mathcal{H}_{osc}$ be the sizes of these various Hilbert spaces.

We want to compute the action of our Hamiltonian upon a vector $|v\rangle$. Normally this would require N^2 multiplications. We show that this can be reduced by a factor of N_{ZM}. To do so, we write $|v\rangle$ in terms of our tensored Hilbert space:

$$|v\rangle = \sum_J v_J |j\rangle \equiv \sum_{j_0,\tilde{j}} v_{j_0\tilde{j}} |j_0\rangle \otimes |\tilde{j}\rangle. \tag{G.2}$$

with $|j_0\rangle$ a basis vector for $\mathcal{H}_{ZM}$ and $|\tilde{j}\rangle$ a basis vector of $\mathcal{H}_{osc}$. The Hamiltonian

consists of a sum of matrices Φ whose matrix elements respect the tensor product structure:

$$\Phi_{IJ} = (\Phi^0)_{i_0 j_0}(\tilde{\Phi})_{\tilde{k}\tilde{l}}, \tag{G.3}$$

where $\Phi^0/\tilde{\Phi}$ act in $\mathcal{H}_0/\mathcal{H}_{osc}$. Applying Φ to $|v\rangle$ then leads to the need to evaluate:

$$\sum_{J=1}^{N} \Phi_{IJ} v_J = \sum_{j_0=1}^{N_{ZM}} \sum_{\tilde{j}=1}^{N_{osc}} (\Phi^0)_{i_0 j_0}(\tilde{\Phi})_{\tilde{i}\tilde{j}} v_{j_0 \tilde{j}}. \tag{G.4}$$

To do so we first perform the matrix-vector multiplication involving the oscillator modes:

$$W_{j_0 \tilde{i}} = \sum_{\tilde{j}=1}^{N_{osc}} (\tilde{\Phi})_{\tilde{i}\tilde{j}} v_{j_0 \tilde{j}}. \tag{G.5}$$

This involves $N_{ZM} N_{osc}^2$ multiplications. We now follow this by the matrix-vector product over the zero mode space:

$$U_{i_0 \tilde{i}} = \sum_{j_0=1}^{N_{ZM}} (\Phi_0)_{i_0 j_0} W_{j_0 \tilde{i}}. \tag{G.6}$$

This involves another $N_{ZM}^2 N_{osc}$ multiplications. If we write $|u\rangle = \Phi|v\rangle$, its components, u_I are defined as

$$u_I \equiv u_{i_0 \tilde{i}} = U_{i_0 \tilde{i}}. \tag{G.7}$$

As is typical in our computations, $N_{ZM} \ll N_{osc}$, we see that we have reduced the total number of multiplications by an approximate factor of N_{ZM}. The above algorithm is a variant of the *Shuffle Algorithm* where 'shuffle' refers to the reshuffling of elements of the vector $|v\rangle$ into a multi-index tensor $v_{j_0 \tilde{j}}$.

G.2 Exploiting the structure of $\mathcal{H}_{osc}$

The above multiplication algorithm can be further optimized by taking into account the chiral structure of the oscillator Hilbert space. Here we will account for momentum conservation. Up to a chiral cutoff N_c, the oscillator Hilbert space in the momentum zero sector takes the form:

$$(\mathcal{H}_L^{(0)} \otimes \mathcal{H}_R^{(0)}) \oplus (\mathcal{H}_L^{(1)} \otimes \mathcal{H}_R^{(1)}) \oplus \cdots \oplus (\mathcal{H}_L^{(N_c)} \otimes \mathcal{H}_R^{(N_c)}). \tag{G.8}$$

Here $\mathcal{H}_{L,R}^{(m)}$ is the Hilbert space of all states in the oscillator space of level m (i.e. the state $a_{n_1}^\dagger \cdots a_{n_k}^\dagger |0\rangle \in \mathcal{H}_R$ belongs to $\mathcal{H}_R^{(m)}$ if $\sum n_l = m$). The dimensionality of $\mathcal{H}_{L,R}^{(i)}$ is

$$\dim \mathcal{H}_{L/R}^{(i)} = \mathcal{P}(i) \tag{G.9}$$

where $\mathcal{P}(i)$ denotes the number of integer partitions of i with $\mathcal{P}(0) = 1$. The dimension of the chiral/anti-chiral Hilbert space is

$$N_{L/R} = \sum_{j=0}^{N_c} \mathcal{P}(j), \tag{G.10}$$

while the dimension of the oscillator Hilbert space (of zero momentum states) is

$$N_{osc} = \sum_{j=0}^{N_c} \mathcal{P}(j)^2. \tag{G.11}$$

We can proceed just as in the previous section. We write the vector $|v\rangle$ that we want to multiply as

$$|v\rangle = \sum_{j_0=1}^{N_{ZM}} \sum_{k=0}^{N_c} \sum_{n_k,\bar{n}_k=1}^{\mathcal{P}(k)} v^{(k)}_{j_0 n_k \bar{n}_k} |j_0\rangle_0 \otimes |k, n_k\rangle_L \otimes |k, \bar{n}_k\rangle_R \tag{G.12}$$

where the same level index k appearing in the left/right chiral vectors encodes momentum conservation. The matrix Φ representing one of the terms in the Hamiltonian is

$$\begin{aligned}\Phi = \sum_{i_0,j_0=1}^{N_{ZM}} \sum_{i,j=0}^{N_c} \sum_{n_i,\bar{n}_i=1}^{\mathcal{P}(i)} \sum_{n_j,\bar{n}_j=1}^{\mathcal{P}(j)} (\Phi_0)_{i_0 j_0} \left(\Phi_L^{(i,j)}\right)_{n_i,n_j} \left(\Phi_R^{(i,j)}\right)_{\bar{n}_i,\bar{n}_j} \\ \times |i_0\rangle_0\langle j_0|_0 \otimes |i, n_i\rangle_L\langle j, n_j|_L \otimes |i, \bar{n}_i\rangle_R\langle j, \bar{n}_j|_R.\end{aligned} \tag{G.13}$$

Applying Φ to $|v\rangle$ yields

$$\Phi_{IJ} v_J = \sum_{j_0=1}^{N_{ZM}} \sum_{j=0}^{N_c} \sum_{n_j,\bar{n}_j=1}^{\mathcal{P}(j)} (\Phi_0)_{i_0 j_0} \left(\Phi_L^{(i,j)}\right)_{n_i,n_j} \left(\Phi_R^{(i,j)}\right)_{\bar{n}_i,\bar{n}_j} v^{(j)}_{j_0 n_j \bar{n}_j}. \tag{G.14}$$

We now determine the number of multiplications necessary to evaluate this expression. The first step is to evaluate the action of Φ_R. This costs $N_{osc} N_L N_{ZM}$ multiplications. Similarly the application of the Φ_L matrix involves $N_{osc} N_R N_{ZM}$ multiplications. Finally the action of Φ_0 costs $N_L N_R N_{ZM}^2$ multiplications. The total number of required multiplications is thus

$$N_{osc}(N_L + N_R) N_{ZM} + N_L N_R N_{ZM}^2. \tag{G.15}$$

For larger values of N_c, the number of needed multiplications can be several hundred times smaller than using the naive matrix-vector multiplication involving $(N_{osc} N_{ZM})^2$ multiplications.

Summary and abstracts

Summary

A large part of our current understanding about the nature of our Universe is framed in the language of quantum field theories (QFTs). On the one hand, they provide the general framework in which we describe at least three of the four known fundamental interactions of Nature: electromagnetic, weak, and strong interactions. On the other hand, they are frequently used in effective models appearing in particle, solid-state and statistical physics.

Due to their extraordinary phenomenological richness, QFTs are not expected to be exactly solvable, except for a number of special cases. The typical observables of a QFT (with massive excitations) are the mass spectrum, the scattering matrix, matrix elements of local operators (i.e., form factors), and the correlation functions of these operators.

In most applications, the concrete physical system under examination has a finite size. Scattering experiments are performed in a finite accelerator/detector; solid-state systems are analysed in laboratories, even the lattice simulations of gauge theories are performed on finite lattices. The understanding of finite size effects is therefore unavoidable, and it is natural to extend the concept of solvability to include finite volume physical quantities. Fortunately, there are profound reasons to believe that finite-size corrections can be formulated purely in terms of the infinite volume characteristics of the theory [4–7].

The set of two-dimensional integrable models is an adequate testing ground to study finite-size effects. In particular, the finite size energy spectrum can be calculated systematically in integrable theories. The most striking finite-size corrections are polynomial in the inverse volume and originate from momentum quantisation [5] There are also exponentially small corrections related to virtual processes. If bound states are present, the leading exponential corrections for bound states (called μ-terms) are related to the fact that in a finite volume bound states can virtually decay into their constituents. The next exponential corrections (F-terms) are caused by the polarisation of the non-trivial finite volume vacuum [4].

In this thesis, we extensively study a particularly important example of integrable

field theories: the sinh-Gordon model (ShG) [89, 93–95]. We are going to take as a starting point the Lagrangian formulation of the model given by

$$\mathcal{L}_{\mathrm{ShG}} = \frac{1}{16\pi} (\partial_\nu \varphi)^2 - 2\mu \cosh(b\varphi) \tag{G.16}$$

Here $\varphi(x,t)$ is a real noncompact scalar field, μ is some dimensionful mass scale, and b is a dimensionless coupling constant. The spectrum of the model is exceedingly simple, consisting of a single massive particle of mass M_{ShG}. ShG is thus the simplest of interacting integrable field theories.

One of the most striking but mysterious aspects of the ShG model is its weak-strong duality:

$$b \leftrightarrow b^{-1}. \tag{G.17}$$

In the presence of such symmetry, the self-dual point $b = 1$ becomes a unique instance of the ShG model, for it divides the weak-coupling regime, $b < 1$, from the strong-coupling regime, $b > 1$. It is important to underline that this duality is not at all manifest in the Lagrangian of the theory but is apparent in its S-matrix formulation.

The primary aim of the thesis can be summarized in the following two points:

- Provide a formula for the leading finite volume corrections to nondiagonal form factors in diagonally scattering theories due to vacuum polarisation (the F-terms). These provide the leading exponential corrections in theories without bound states, in particular in the sinh-Gordon model. We will develop analytical and numerical methods to verify this formula.

- Establish numerical truncated spectrum methods (TSM) [107–109, 112–115, 118, 126] to study the sinh-Gordon model and related theories. Apart from being related to the previous point, this is also useful to gain a better understanding on the nature of self-duality.

My results related to the above directions can be structured into the following five thesis points.

Thesis points

1. Coupling expansion of finite volume form factors and mass gap

I developed Hamiltonian perturbation theory in the coupling b to systematically study the finite volume spectrum and matrix elements of the sinh-Gordon model. This result is published in [127] and is presented in Section 4.3. I obtained volume-exact expansions

in b, which are presented for the mass gap in eq. (4.65) and for the $0-1$ form factor of the elementary field φ in eq. (4.84). I then implemented a contour integration technique to obtain the leading large volume corrections, which I then compared to excited state thermodynamic Bethe Ansatz (TBA) in Section 4.3.3.3 and to our new F-term for the $0-1$ form factor in Section 4.3.4.3.

2. TSM for the sinh-Gordon model and numerical confirmation of the F-term

I developed the zero-mode separated truncated spectrum approach for sinh-Gordon theory. I present two implementations of comparable precision, starting from either the massless or the massive boson. The method is published in [128], wherein I also found that in the small-coupling regime $b \ll 1$, the numerics is very accurate and I used it to verify our general conjecture for the F-term. The TSM method is discussed in more detail in our subsequent paper [151]. The massless zero-mode TSM method is discussed in Section 3.2, while the version based on the Fock space of the massive boson is outlined in Section 3.4. The exact relation between the free boson mass m and the chiral coupling μ_{ShG}, connecting the two schemes, is given in eq. (3.49). The numerical checks of the F-term in the small-coupling regime are presented in Section 4.5.

3. Understanding the mysterious power-law cutoff dependence of TSM numerics

In the larger-b domain, cutoff effects become stronger. I pointed out that the conventional renormalisation group improvements of TSM (expanded in μ_{ShG}) become singular for arbitrary $b > 0$, if we include high enough orders. This argument is presented in Section 3.3.4 and elaborated in more detail in Appendix D. I found that a power-law extrapolation robustly improves TSM results both for energy eigenvalues as well as operator expectation values, as discussed in Section 3.3. To understand this surprising behaviour, I derived the leading asymptotic of the perturbative series for the ground state energy in eq. (3.82). I was able to show under fairly general assumptions that the asymptotic behavior of the resummed series indeed obeys a power-law in Section 3.6.2. This explains, at least partially, the observed power-law dependence of the cutoff. This is published in [151].

4. Reproduction of the UV reflection quantization and the absence of dual terms in the Hamiltonian

Focusing on the ultraviolet behavior on the spectrum, I determined that the normal ordered Hamiltonian derived in Section 3.2 reproduces the reflection quantization results, thus being consistent with self-duality. No extra (dual) potential terms are needed to be added. I check the validity of reflection quantization analytically, starting from the Hamiltonian, beyond the semi-classic approximation in Section 3.5.3. It is possible to reproduce the UV limit of TBA up to an error of $O(b^{12})$. In turn, by using partial information on the structure of UV behavior, and fitting the infrared quantities to the corresponding expansion of TBA, it is possible to obtain a significantly better estimate to the S-matrix parameter B and the mass gap. These numerical results are presented in Section 3.5.4. Through the connection to Liouville field theory, this result indicates that a dual term is not needed into the Lagrangian definition of Liouville field theory, either (as anticipated in Section 2.2). This calculation is reported in [151].

5. Form factor TSM and the fundamental domain of the Lagrangian theory

Conventional TSM methods fail when the the self-dual point $b = 1$ is approached. The vacuum expectation value (VEV) formula of vertex operators $e^{\alpha\varphi}$ has zeroes at the Seiberg bounds $\alpha = \pm\frac{Q}{2}$ and its analytical continuation becomes negative beyond that. From the TSM point of view, negative VEVs are nonsense because of the positive definiteness of the operator. TSM results for vertex operator VEVs become instable near the Seiberg bounds and blow up beyond it, as shown on Figure 3.9. To understand these phenomena better, I developed the form factor TSM method, making use of the basis of sinh-Gordon eigenstates at a different coupling. This is reported in Section 3.7. Contrary to intuition, as the basis theory (of coupling b_0) approaches the target theory (coupling b_1), the cutoff dependence of TSM worsens. However, the setup of the method reinforces that lagrangian Sinh-Gordon theory may be well-defined (only) below the self-dual point, its operator content satisfying the Seiberg bounds. These arguments have been reported in [151].

The dissertation is based on the following publications and manuscripts

*Authors are listed in alphabetical order.

1. Z. Bajnok, J. Balog, M. Lajer, C. Wu, *Field theoretical derivation of Lüscher's formula and calculation of finite volume form factors.* Journal of High Energy Physics 2018 (7) (Jul 2018).
doi:10.1007/jhep07(2018)174.

2. Z. Bajnok, M. Lajer, B. Szepfalvi, I. Vona, *Leading exponential finite size corrections for non-diagonal form factors*, Journal of High Energy Physics 2019 (7) (Jul 2019).
doi:10.1007/jhep07(2019)173.

3. R. Konik, M. Lajer, G. Mussardo, *Approaching the self-dual point of the sinh-Gordon model* (2020). arXiv:2007.00154.

Other publication of the author not part of the present thesis

*Authors are listed in alphabetical order.

1. Z. Bajnok, M. Lajer, *Truncated Hilbert Space Approach to the 2d ϕ^4 theory*, JHEP 10 (2016) 050 (2016). doi:10.1007/JHEP10(2016)050.

Magyar nyelvű összefoglaló és tézispontok

Bevezetés

Az Univerzum természetével kapcsolatos jelenlegi tudásunk nagy része a kvantumtérelméletek (QFT) nyelvén fogalmazható meg. Egyfelől ezek biztosítják azokat a fogalmi kereteket, melyek segítségével a Természet négy alapvető kölcsönhatása közül legalább hármat le tudunk írni: az elektromágneses, a gyenge és az erős kölcsönhatást. Másrészt effektív modellekként gyakran előfordulnak a részecske, szilárdtest- és statisztikus fizika különböző területein.

Már a rendkívüli fenomenológiai gazdagságuk alapján is gyanítható, hogy a QFT-k általában nem oldhatók meg egzaktul, kivéve esetleg néhány speciális esetet. A (tömeges gerjesztéseket tartalmazó) QFT-k legfontosabb megfigyelhető mennyiségei a tömegspektrum, a szórásmátrix, a lokális operátorok mátrixelemei (alakfaktorok) és ezen operátorok korrelációs függvényei.

Az alkalmazások legnagyobb részében a ténylegesen vizsgált fizikai rendszernek korlátos a mérete. A szórási kísérletek véges gyorsítóban/detektorban zajlanak, a szilárdtest-fizikai rendszereket véges térfogatú minták segítségével vizsgálják, de a rácstérelméleti szimulációkat is véges rácsokon végzik. A véges méretből adódó effektusok megértése így elkerülhetetlen, és természetes kiterjeszteni a "megoldhatóság" koncepcióját, hogy az magába foglalja a véges térfogati mennyiségek meghatározását is. Szerencsére jó okunk van feltételezni, hogy a végesméret-korrekciók kifejezhetők tisztán a végtelen térfogati mennyiségek függvényében. [4–7]

A kétdimenziós integrálható QFT modellek halmaza ideális vizsgálati terepet nyújt a végesméret-effektusok feltérképezéséhez. Az integrálható elméletekben többek közt hatékony módszerek állnak rendelkezésre az egzakt véges térfogati energiaspektrum szisztematikus kiszámítására. A legjelentősebb véges térfogati korrekciók polinomiálisak az inverz térfogatban és az impulzus perfemfeltételekkel konzisztens kvantálásából származnak. [5] Ezen kívül a virtuális részecskék következtében megjelennek exponenciálisan kicsi korrekciók is. Ha kötött állapotok is jelen vannak, akkor az ezekhez tartozó vezető exponenciális korrekciók (az ún. μ-tagok) abból erednek, hogy a kötött állapot

virtuálisan alkotórészeire bomolhat. A következő korrekciók (F-tagok) a nemtriviális véges térfogati vákuum polarizációjából származnak [4].

A jelen disszertációban az integrálható térelméletek egy fontos példányát, a sinh-Gordon modellt (ShG) [89,93–95] tesszük alapos vizsgálat tárgyává. A modell Lagrange-i megfogalmazását vesszük alapul, ami a

$$\mathcal{L}_{\mathrm{ShG}} = \frac{1}{16\pi} \left(\partial_\nu \varphi\right)^2 - 2\mu \cosh\left(b\varphi\right) \tag{G.18}$$

Lagrange-sűrűségből indul ki. Itt $\varphi\left(x,t\right)$ egy valós (nem kompakt) skalármező, μ egy dimenziós paraméter, ami rögzíti a tömegskálát, b pedig egy dimenziótlan csatolási állandó. A modell spektruma rendkívül egyszerű, egyetlen M_{ShG} tömegű részecsketípust tartalmaz, ami egyben a mező elemi gerjesztése. Így az ShG a legegyszerűbb kölcsönható integrálható kvantumtérelméletnek tekinthető.

Az ShG modell egyik legszembetűnőbb, ugyanakkor rejtélyes tulajdonsága a

$$b \leftrightarrow b^{-1}. \tag{G.19}$$

erős-gyenge dualitás jelenléte az S-mátrixban. Ezen szimmetria jelenlétében a $b = 1$ önduális pont egy különleges esetté nemesül, amely elválasztja a gyengén kölcsönható ($b < 1$) és az erősen kölcsönható ($b > 1$) tartományt. Fontos megjegyezni, hogy ez a dualitás egyáltalán nem jelenik meg a modell Lagrange-függvényében, viszont szembetűnő jellemzője az S-mátrixnak.

A jelen disszertáció célja az alábbi két pontban foglalható össze:

- Megadni egy formulát a nemdiagonális alakfaktorok vezető rendű, vákuumpolarizációból származó végesméret-korrekcióira (az F-tagokra) diagonális szórásmátrixú elméletekben. Ezek a tagok adják meg a kötött állapotoktól mentes elméletekben (így a sinh-Gordon modellben) a vezető rendű exponenciális korrekciókat. Analitikus és numerikus módszereket kifejleszteni a formula igazolására.

- Továbbfejleszteni a numerikus csonkított állapottér-módszert (TSM) [107–109, 112–115, 118, 126] a sinh-Gordon modellre és hasonló elméletekre. Az előző ponthoz való kapcsolódáson kívül ez a módszer hasznos az öndualitás természetének jobb megértése szempontjából is.

A fenti irányokban elért eredményeimet a következő öt tézispontban foglaltam össze.

Tézispontok

1. Véges térfogati alaktényezők és a tömeg csatolás szerinti kifejtése

Sikeresen alkalmaztam a Hamilton-i perturbációszámítást a sinh-Gordon modellben, a b csatolás szerint, a véges térfogati spektrum és mátrixelemek szisztematikus tanulmányozásához. Ez az eredmény a [127] cikkben jelent meg, és a 4.3. szakaszban kerül bemutatásra. A b-beli kifejtés eredménye térfogatban egzakt. Az eredményt az első energiakülönbségre a (4.65) egyenlet, a fundamentális φ mező $0-1$ form faktorára pedig a (4.84) egyenlet tartalmazza. Ezután a kontúr-integrál technikát használtam, hogy megkapjam a vezető nagy térfogati korrekciókat. Ezeket a gerjesztett állapoti TBA eredményéhez (4.3.3.3. szakasz), valamint az új, F-tagra vonatkozó kifejezésünkhöz (4.3.4.3. szakasz) hasonlítottam.

2. Csonkolt állapottér módszer a sinh-Gordon modellre és az F-tagok numerikus alátámasztása

Kidolgoztam a zérómódus-leválasztott csonkított állapottér módszert a sinh-Gordon modellre. Két hasonló pontosságú implementációt mutatok be, melyek rendre a tömeges és a tömegtelen bozon bázisát veszik alapul. A módszert a [128] cikkben publikáltuk, ahol még az is kiderült, hogy $b \ll 1$-re a numerika nagyon precíz. Ezt használtam arra, hogy megerősítsem az F-tagra vonatkozó általános formulánk érvényességét. A TSM módszert tovább vizsgáljuk a [151] cikkben. A tömegtelen zérómódus-TSM módszert a 3.2 szakaszban diszkutálom, míg a tömeges bozon Fock-terén alapuló verzió a 3.4 szakaszban kerül bemutatásra. Az m szabad bozon tömeg és a μ_{ShG} királis csatolás közötti egzakt reláció, ami a két sémát összekapcsolja, a (3.49) egyenletben található. Az F-tag numerikus ellenőrzése a kis csatolású tartományban a 4.5 alfejezetben kerül tárgyalásra.

3.A csonkolt állapottér módszer rejtélyes hatványszerű levágásfüggésének megértése

Nagyobb b-k tartományában a levágási effektusok erősödnek. Rámutatok, hogy a TSM hagyományos RG javításai (melyek a μ_{ShG} csatolási állandóban kerülnek kifejtésre) szingulárissá válnak minden $b > 0$-ra, ha kellően sok rendet megtartunk. Ez az érv a 3.3.4 szakaszban jelenik meg, további részletek pedig a D appendixben találhatók. Azt találtam, hogy egy hatványfüggvény-illesztés robusztus módon javítja a TSM eredményeket mind az energiaszintek, mind a vákuum várható értékek esetén. Ez a 3.3 szakaszban kerül részletezésre. Hogy megértsük ezt a meglepő viselkedést, meghatároztam

az alapállapoti energia perturbatív sorának legszingulárisabb részét a (3.82) egyenletben. A 3.6.2 szakaszban viszonylag általános feltételek mellett sikerült megmutatni, hogy az újraösszegzatt sor tényleg hatványfüggvény szerint tarthat az aszimptotikus értékéhez. Ez legalábbis részben megmagyarázza a ténylegesen megfigyelt hatványszerű levágásfüggést. Ezt a [151] cikkben jelentettük meg.

4. Ultraibolya reflexiós kvantálás és a duális tagok hiánya a Hamilton-operátorban

A spektrum ultraibolya viselkedése alapján megállapítottam, hogy a 3.2 szakaszban levezetett, normálrendezett Hamilton-operátor helyesen reprodukálja a reflexiós kvantálás eredményét, és így konzisztens az öndualisással. Nincs szükség extra tagok jelenlétére. A reflexiós kvantálás érvényességét analitikusan is ellenőrzöm a 3.5.3 szakaszban, továbblépve a szemiklasszikus közelítésen. Ennek segítségével $O(b^{12})$ hiba mellett sikerült reprodukálni a TBA UV limeszét. Emellett, részleges információkat felhasználva az UV viselkedés szerkezetéről, és illesztve az infravörös mennyiségeket a TBA megfelelő kifejtésében, lehetővé vált jóval pontosabban meghatározni az S-mátrix B paraméterét és a részecske tömeget. Ezeket a numerikus eredményeket a 3.5.4 szakaszban mutatom be. A Liouville térelmélettel való kapcsolat révén ez az eredmény azt is indikálja, hogy a Liouville modellben sincs szükség explicit duális tagok hozzáadására (ahogy az a 2.2 szakaszban felvetődik). A fenti számítások a [151] cikkben kerülnek bemutatásra.

5. Alaktényező TSM és a Lagrange-i elmélet fundamentális tartománya

A hagyományos TSM módszerek kudarcot vallanak a $b = 1$ pont közelében. Az $e^{\alpha\varphi}$ operátor vákuum várható értékének zérusa van az $\alpha = \pm\frac{Q}{2}$ Seiberg-határoknál, és az analitikus elfolytatása negatívvá válik azokon túl. A TSM szemszögéből a negatív VEV-ek értelmetlenek az operátor pozitív definit volta miatt. A TSM eredmények instabillá válnak a Seiberg-határok közelében, és divergálnak azon túl, a 3.9 ábrán látható módon. Ezen jelenségek alaposabb megértése érdekében kidolgoztam az alakfaktor-alapú csonkított állapottér módszert, ami a sinh-Gordon különböző b csatolási állandójához tartozó sajátállapotait veszi alapul. Ez a 3.7 alfejezetben kerül részletezésre. A várakozással szemben, a bázis elmélet (b_0 csatolás) csatolását a target elmélethez (b_1 csatolás) közelítve, a TSM levágásfüggése romlik. Azonban a módszer rávilágít arra, hogy a lagrange-i sinh-Gordon modell talán csak az önduális pont alatt értelmes, az operátor-tartalma pedig kielégíti a Seiberg-korlátokat. Ezek az érvek a [151] cikkben kerülnek tárgyalásra.

A disszertáció az alábbi publikációkon és kéziraton alapul:

*A szerzők névsor szerint kerültek feltüntetésre.

1. Z. Bajnok, J. Balog, M. Lajer, C. Wu, *Field theoretical derivation of Lüscher's formula and calculation of finite volume form factors.* Journal of High Energy Physics 2018 (7) (Jul 2018).
doi:10.1007/jhep07(2018)174.

2. Z. Bajnok, M. Lajer, B. Szepfalvi, I. Vona, *Leading exponential finite size corrections for non-diagonal form factors*, Journal of High Energy Physics 2019 (7) (Jul 2019).
doi:10.1007/jhep07(2019)173.

3. R. Konik, M. Lajer, G. Mussardo, *Approaching the self-dual point of the sinh-Gordon model* (2020). arXiv:2007.00154.

A szerző további publikációja, mely nem része a disszertációnak:

*A szerzők névsor szerint kerültek feltüntetésre.

1. Z. Bajnok, M. Lajer, *Truncated Hilbert Space Approach to the 2d ϕ^4 theory*, JHEP 10 (2016) 050 (2016). doi:10.1007/JHEP10(2016)050.

Bibliography

[1] A. M. Polyakov, Conformal symmetry of critical fluctuations, JETP Lett. 12 (1970) 381–383 (1970).

[2] K. G. Wilson, The renormalization group: Critical phenomena and the kondo problem, Rev. Mod. Phys. 47 (1975) 773–840 (Oct 1975). doi:10.1103/RevModPhys.47.773.
URL https://link.aps.org/doi/10.1103/RevModPhys.47.773

[3] T. R. Klassen, E. Melzer, Rg flows in the d-series of minimal cfts, Nuclear Physics B 400 (1-3) (1993) 547–573 (Jul 1993). doi:10.1016/0550-3213(93)90415-l.
URL http://dx.doi.org/10.1016/0550-3213(93)90415-L

[4] M. Lüscher, Volume Dependence of the Energy Spectrum in Massive Quantum Field Theories. 1. Stable Particle States, Commun. Math. Phys. 104 (1986) 177 (1986). doi:10.1007/BF01211589.

[5] M. Lüscher, Volume Dependence of the Energy Spectrum in Massive Quantum Field Theories. 2. Scattering States, Commun. Math. Phys. 105 (1986) 153–188 (1986). doi:10.1007/BF01211097.

[6] B. Pozsgay, G. Takács, Form-factors in finite volume I: Form-factor bootstrap and truncated conformal space, Nucl. Phys. B788 (2008) 167–208 (2008). arXiv:0706.1445, doi:10.1016/j.nuclphysb.2007.06.027.

[7] B. Pozsgay, G. Takács, Form factors in finite volume. II. Disconnected terms and finite temperature correlators, Nucl. Phys. B788 (2008) 209–251 (2008). arXiv:0706.3605, doi:10.1016/j.nuclphysb.2007.07.008.

[8] S. Weinberg, The Quantum Theory of Fields, Vol. 1, Cambridge University Press, 1995 (1995). doi:10.1017/CBO9781139644167.

[9] J. Leinaas, J. Myrheim, On the theory of identical particles, Nuovo Cim. B 37 (1977) 1–23 (1977). doi:10.1007/BF02727953.

[10] F. Wilczek, Quantum mechanics of fractional-spin particles, Phys. Rev. Lett. 49 (1982) 957–959 (Oct 1982). doi:10.1103/PhysRevLett.49.957.
URL https://link.aps.org/doi/10.1103/PhysRevLett.49.957

[11] M. Girardeau, Relationship between systems of impenetrable bosons and fermions in one dimension, Journal of Mathematical Physics 1 (6) (1960) 516–523 (1960). arXiv:https://doi.org/10.1063/1.1703687, doi:10.1063/1.1703687.
URL https://doi.org/10.1063/1.1703687

[12] S. R. Coleman, The Quantum Sine-Gordon Equation as the Massive Thirring Model, Phys. Rev. D 11 (1975) 2088 (1975). doi:10.1103/PhysRevD.11.2088.

[13] S. Coleman, R. Jackiw, L. Susskind, Charge shielding and quark confinement in the massive schwinger model, Annals of Physics 93 (1) (1975) 267 – 275 (1975). doi:https://doi.org/10.1016/0003-4916(75)90212-2.
URL http://www.sciencedirect.com/science/article/pii/0003491675902122

[14] E. Witten, Nonabelian bosonization in two dimensions, Comm. Math. Phys. 92 (4) (1984) 455–472 (1984).
URL https://projecteuclid.org:443/euclid.cmp/1103940923

[15] T. R. Klassen, E. Melzer, Sine-Gordon not equal to massive Thirring, and related heresies, Int. J. Mod. Phys. A 8 (1993) 4131–4174 (1993). arXiv:hep-th/9206114, doi:10.1142/S0217751X93001703.

[16] G. Mussardo, Statistical field theory, Oxford Univ. Press, New York, NY, 2010 (2010).

[17] L. Samaj, Z. Bajnok, Introduction to the Statistical Physics of Integrable Many-body Systems, Cambridge University Press (2013).

[18] F. H. Essler, R. M. Konik, Applications of massive integrable quantum field theories to problems in condensed matter physics (2004) 684–830 (12 2004). arXiv:cond-mat/0412421, doi:10.1142/9789812775344_0020.

[19] H. Bethe, Zur Theorie der Metalle, Zeitschrift fur Physik 71 (3-4) (1931) 205–226 (Mar. 1931). doi:10.1007/BF01341708.

[20] L. Onsager, Crystal statistics. i. a two-dimensional model with an order-disorder transition, Phys. Rev. 65 (1944) 117–149 (Feb 1944). doi:10.1103/PhysRev.65.117.
URL https://link.aps.org/doi/10.1103/PhysRev.65.117

[21] S.-i. Tomonaga, Remarks on Bloch's Method of Sound Waves applied to Many-Fermion Problems, Progress of Theoretical Physics 5 (4) (1950) 544–569 (07 1950). arXiv:https://academic.oup.com/ptp/article-pdf/5/4/544/5430161/5-4-544.pdf, doi:10.1143/ptp/5.4.544.
URL https://doi.org/10.1143/ptp/5.4.544

[22] J. M. Luttinger, An exactly soluble model of a many-fermion system, Journal of Mathematical Physics 4 (9) (1963) 1154–1162 (1963). arXiv:https://doi.org/10.1063/1.1704046, doi:10.1063/1.1704046.
URL https://doi.org/10.1063/1.1704046

[23] D. C. Mattis, E. H. Lieb, Exact solution of a many-fermion system and its associated boson field, Journal of Mathematical Physics 6 (2) (1965) 304–312 (1965). arXiv:https://doi.org/10.1063/1.1704281, doi:10.1063/1.1704281.
URL https://doi.org/10.1063/1.1704281

[24] F. Haldane, Luttinger liquid theory of one-dimensional quantum fluids. I. Properties of the Luttinger model and their extension to the general 1D interacting spinless Fermi gas, J. Phys. C 14 (1981) 2585–2609 (1981). doi:10.1088/0022-3719/14/19/010.

[25] E. H. Lieb, F. Y. Wu, Absence of mott transition in an exact solution of the short-range, one-band model in one dimension, Phys. Rev. Lett. 20 (1968) 1445–1448 (Jun 1968). doi:10.1103/PhysRevLett.20.1445.
URL https://link.aps.org/doi/10.1103/PhysRevLett.20.1445

[26] F. H. L. Essler, H. Frahm, F. G ohmann, A. Kl umper, V. E. Korepin, The One-Dimensional Hubbard Model, Cambridge University Press, 2005 (2005). doi:10.1017/CBO9780511534843.

[27] E. H. Lieb, W. Liniger, Exact analysis of an interacting bose gas. i. the general solution and the ground state, Phys. Rev. 130 (1963) 1605–1616 (May 1963). doi:10.1103/PhysRev.130.1605.
URL https://link.aps.org/doi/10.1103/PhysRev.130.1605

[28] E. H. Lieb, Exact analysis of an interacting bose gas. ii. the excitation spectrum, Phys. Rev. 130 (1963) 1616–1624 (May 1963). doi:10.1103/PhysRev.130.1616.
URL https://link.aps.org/doi/10.1103/PhysRev.130.1616

[29] H. Moritz, T. Stöferle, M. Köhl, T. Esslinger, Exciting collective oscillations in a trapped 1d gas, Phys. Rev. Lett. 91 (2003) 250402 (Dec 2003). doi:10.1103/PhysRevLett.91.250402.
URL https://link.aps.org/doi/10.1103/PhysRevLett.91.250402

[30] J. Maldacena, International Journal of Theoretical Physics 38 (4) (1999) 1113–1133 (1999). doi:10.1023/a:1026654312961, [link].
URL http://dx.doi.org/10.1023/A:1026654312961

[31] E. Witten, Anti-de Sitter space and holography, Adv. Theor. Math. Phys. 2 (1998) 253–291 (1998). arXiv:hep-th/9802150, doi:10.4310/ATMP.1998.v2.n2.a2.

[32] S. Gubser, I. Klebanov, A. Polyakov, Gauge theory correlators from non-critical string theory, Physics Letters B 428 (1-2) (1998) 105–114 (May 1998). doi:10.1016/s0370-2693(98)00377-3.
URL http://dx.doi.org/10.1016/S0370-2693(98)00377-3

[33] L. Lipatov, Asymptotic behavior of multicolor QCD at high energies in connection with exactly solvable spin models, JETP Lett. 59 (1994) 596–599 (1994). arXiv:hep-th/9311037.

[34] L. Faddeev, G. Korchemsky, High energy qcd as a completely integrable model, Physics Letters B 342 (1-4) (1995) 311–322 (Jan 1995). doi:10.1016/0370-2693(94)01363-h.
URL http://dx.doi.org/10.1016/0370-2693(94)01363-H

[35] N. Beisert, The dilatation operator of n=4 super yang–mills theory and integrability, Physics Reports 405 (1-3) (2004) 1–202 (Dec 2004). doi:10.1016/j.physrep.2004.09.007.
URL http://dx.doi.org/10.1016/j.physrep.2004.09.007

[36] A. A. Tseytlin, Semiclassical strings and ads/cft (2004). arXiv:hep-th/0409296.

[37] J. Plefka, Spinning strings and integrable spin chains in the ads/cft correspondence, Living Reviews in Relativity 8 (1) (Nov 2005). doi:10.12942/lrr-2005-9.
URL http://dx.doi.org/10.12942/lrr-2005-9

[38] Z. Bajnok, R. A. Janik, Four-loop perturbative Konishi from strings and finite size effects for multiparticle states, Nucl. Phys. B 807 (2009) 625–650 (2009). arXiv:0807.0399, doi:10.1016/j.nuclphysb.2008.08.020.

[39] N. Gromov, V. Kazakov, P. Vieira, Exact spectrum of anomalous dimensions of planarn=4supersymmetric yang-mills theory, Physical Review Letters 103 (13) (Sep 2009). doi:10.1103/physrevlett.103.131601.
URL http://dx.doi.org/10.1103/PhysRevLett.103.131601

[40] N. Gromov, V. Kazakov, S. Leurent, D. Volin, Solving the ads/cft y-system, Journal of High Energy Physics 2012 (7) (Jul 2012). doi:10.1007/jhep07(2012)023.
URL http://dx.doi.org/10.1007/JHEP07(2012)023

[41] N. Beisert, et al., Review of AdS/CFT Integrability: An Overview, Lett. Math. Phys. 99 (2012) 3–32 (2012). arXiv:1012.3982, doi:10.1007/s11005-011-0529-2.

[42] A. Belavin, A. Polyakov, A. Zamolodchikov, Infinite conformal symmetry in two-dimensional quantum field theory, Nuclear Physics B 241 (2) (1984) 333 – 380 (1984). doi:https://doi.org/10.1016/0550-3213(84)90052-X.
URL http://www.sciencedirect.com/science/article/pii/055032138490052X

[43] S. Coleman, J. Mandula, All possible symmetries of the s matrix, Phys. Rev. 159 (1967) 1251–1256 (Jul 1967). doi:10.1103/PhysRev.159.1251.
URL https://link.aps.org/doi/10.1103/PhysRev.159.1251

[44] A. B. Zamolodchikov, Note: Exact two-particle s-matrix of quantum sine-gordon solitons, Comm. Math. Phys. 55 (2) (1977) 183–186 (1977).
URL https://projecteuclid.org:443/euclid.cmp/1103900986

[45] M. Karowski, H. Thun, T. Truong, P. Weisz, On the Uniqueness of a Purely Elastic s Matrix in (1+1)-Dimensions, Phys. Lett. B 67 (1977) 321–322 (1977). doi:10.1016/0370-2693(77)90382-3.

[46] R. Shankar, E. Witten, s matrix of the supersymmetric nonlinear σ model, Phys. Rev. D 17 (1978) 2134–2143 (Apr 1978). doi:10.1103/PhysRevD.17.2134.
URL https://link.aps.org/doi/10.1103/PhysRevD.17.2134

[47] G. Anderson, G. W. Moore, Rationality in Conformal Field Theory, Commun. Math. Phys. 117 (1988) 441 (1988). doi:10.1007/BF01223375.

[48] V. Knizhnik, A. Zamolodchikov, Current Algebra and Wess-Zumino Model in Two-Dimensions, Nucl. Phys. B 247 (1984) 83–103 (1984). doi:10.1016/0550-3213(84)90374-2.

[49] P. Goodard, A. Kent, D. Olive, Virasoro algebras and coset space models, Physics Letters B 152 (1) (1985) 88 – 92 (1985). doi:https://doi.org/10.1016/0370-2693(85)91145-1.
URL http://www.sciencedirect.com/science/article/pii/0370269385911451

[50] H. R. Hampapura, S. Mukhi, On 2d conformal field theories with two characters, Journal of High Energy Physics 2016 (1) (Jan 2016). doi:10.1007/jhep01(2016)005.
URL http://dx.doi.org/10.1007/JHEP01(2016)005

[51] M. R. Gaberdiel, H. R. Hampapura, S. Mukhi, Cosets of meromorphic cfts and modular differential equations, Journal of High Energy Physics 2016 (4) (2016) 1–13 (Apr 2016). doi:10.1007/jhep04(2016)156.
URL http://dx.doi.org/10.1007/JHEP04(2016)156

[52] H. R. Hampapura, S. Mukhi, Two-dimensional RCFT's without Kac-Moody symmetry, JHEP 07 (2016) 138 (2016). arXiv:1605.03314, doi:10.1007/JHEP07(2016)138.

[53] K. Gawedzki, Noncompact WZW conformal field theories, in: NATO Advanced Study Institute: New Symmetry Principles in Quantum Field Theory, 1991, pp. 0247–274 (10 1991). arXiv:hep-th/9110076.

[54] P. Forgács, A. Wipf, J. Balog, L. Fehér, L. O'Raifeartaigh, Liouville and toda theories as conformally reduced wznw theories, Physics Letters B 227 (2) (1989) 214 – 220 (1989). doi:https://doi.org/10.1016/S0370-2693(89)80025-5.
URL http://www.sciencedirect.com/science/article/pii/S0370269389800255

[55] J. Balog, L. Fehér, L. O'Raifeartaigh, P. Forgács, A. Wipf, Toda theory and w-algebra from a gauged wznw point of view, Annals of Physics 203 (1) (1990) 76 – 136 (1990). doi:https://doi.org/10.1016/0003-4916(90)90029-N.
URL http://www.sciencedirect.com/science/article/pii/000349169090029N

[56] A. Bilal, J.-L. Gervais, Systematic approach to conformal systems with extended virasoro symmetries, Physics Letters B 206 (3) (1988) 412 – 420 (1988). doi:https://doi.org/10.1016/0370-2693(88)91602-4.
URL http://www.sciencedirect.com/science/article/pii/0370269388916024

[57] A. Bilal, J.-L. Gervais, Extended C=Infinity Conformal Systems from Classical Toda Field Theories, Nucl. Phys. B 314 (1989) 646–686 (1989). doi:10.1016/0550-3213(89)90412-4.

[58] A. Bilal, J.-L. Gervais, Systematic construction of conformal theories with higher-spin virasoro symmetries, Nuclear Physics B 318 (3) (1989) 579 – 630 (1989). doi:https://doi.org/10.1016/0550-3213(89)90633-0.

URL http://www.sciencedirect.com/science/article/pii/0550321389906330

[59] J. Maldacena, H. Ooguri, Strings in ads3 and the sl(2,r) wzw model. i: The spectrum, Journal of Mathematical Physics 42 (7) (2001) 2929–2960 (Jul 2001). doi:10.1063/1.1377273.
URL http://dx.doi.org/10.1063/1.1377273

[60] J. M. Maldacena, H. Ooguri, J. Son, Strings in AdS(3) and the SL(2,R) WZW model. Part 2. Euclidean black hole, J. Math. Phys. 42 (2001) 2961–2977 (2001). arXiv:hep-th/0005183, doi:10.1063/1.1377039.

[61] J. Maldacena, H. Ooguri, Strings in ads3 and the sl(2,r) wzw model. iii. correlation functions, Physical Review D 65 (10) (May 2002). doi:10.1103/physrevd.65.106006.
URL http://dx.doi.org/10.1103/PhysRevD.65.106006

[62] L. Eberhardt, M. R. Gaberdiel, R. Gopakumar, Deriving the ads3/cft2 correspondence, Journal of High Energy Physics 2020 (2) (Feb 2020). doi:10.1007/jhep02(2020)136.
URL http://dx.doi.org/10.1007/JHEP02(2020)136

[63] A. Polyakov, Quantum geometry of fermionic strings, Physics Letters B 103 (3) (1981) 211 – 213 (1981). doi:https://doi.org/10.1016/0370-2693(81)90744-9.
URL http://www.sciencedirect.com/science/article/pii/0370269381907449

[64] T. L. Curtright, C. B. Thorn, Conformally invariant quantization of the liouville theory, Phys. Rev. Lett. 48 (1982) 1309–1313 (May 1982). doi:10.1103/PhysRevLett.48.1309.
URL https://link.aps.org/doi/10.1103/PhysRevLett.48.1309

[65] P. Ginsparg, G. Moore, Lectures on 2d gravity and 2d string theory (tasi 1992) (1993). arXiv:hep-th/9304011.

[66] Y. Nakayama, Liouville field theory: A Decade after the revolution, Other thesis (2004). arXiv:hep-th/0402009, doi:10.1142/S0217751X04019500.

[67] J. Teschner, Liouville theory revisited, Classical and Quantum Gravity 18 (23) (2001) R153–R222 (Nov 2001). doi:10.1088/0264-9381/18/23/201.
URL http://dx.doi.org/10.1088/0264-9381/18/23/201

[68] H. Dorn, H.-J. Otto, Two- and three-point functions in liouville theory, Nuclear Physics B 429 (2) (1994) 375–388 (Oct 1994). doi:10.1016/0550-3213(94)00352-1.
URL http://dx.doi.org/10.1016/0550-3213(94)00352-1

[69] A. B. Zamolodchikov, A. B. Zamolodchikov, Structure constants and conformal bootstrap in Liouville field theory, Nucl. Phys. B477 (1996) 577–605 (1996). arXiv:hep-th/9506136, doi:10.1016/0550-3213(96)00351-3.

[70] A. B. Zamolodchikov, A. B. Zamolodchikov, Factorized s Matrices in Two-Dimensions as the Exact Solutions of Certain Relativistic Quantum Field Models, Annals Phys. 120 (1979) 253–291 (1979). doi:10.1016/0003-4916(79)90391-9.

[71] F. Smirnov, Form-factors in completely integrable models of quantum field theory, Adv.Ser.Math.Phys. 14 (1992) 1–208 (1992).

[72] P. Dorey, Exact S matrices (1996) 85–125 (1996). arXiv:hep-th/9810026.

[73] H. Babujian, M. Karowski, Towards the construction of Wightman functions of integrable quantum field theories, Int. J. Mod. Phys. A19S2 (2004) 34–49 (2004). arXiv:hep-th/0301088, doi:10.1142/S0217751X04020294.

[74] C.-N. Yang, C. Yang, Thermodynamics of one-dimensional system of bosons with repulsive delta function interaction, J. Math. Phys. 10 (1969) 1115–1122 (1969). doi:10.1063/1.1664947.

[75] A. B. Zamolodchikov, Thermodynamic Bethe Ansatz in Relativistic Models. Scaling Three State Potts and Lee-yang Models, Nucl. Phys. B342 (1990) 695–720 (1990). doi:10.1016/0550-3213(90)90333-9.

[76] D. Bombardelli, A next-to-leading Luescher formula, JHEP 01 (2014) 037 (2014). arXiv:1309.4083, doi:10.1007/JHEP01(2014)037.

[77] T. R. Klassen, E. Melzer, On the relation between scattering amplitudes and finite size mass corrections in QFT, Nucl. Phys. B362 (1991) 329–388 (1991). doi:10.1016/0550-3213(91)90566-G.

[78] R. A. Janik, T. Lukowski, Wrapping interactions at strong coupling: The Giant magnon, Phys. Rev. D76 (2007) 126008 (2007). arXiv:0708.2208, doi:10.1103/PhysRevD.76.126008.

[79] C. Ahn, Z. Bajnok, D. Bombardelli, R. I. Nepomechie, TBA, NLO Lüscher correction, and double wrapping in twisted AdS/CFT, JHEP 12 (2011) 059 (2011). arXiv:1108.4914, doi:10.1007/JHEP12(2011)059.

[80] P. Dorey, R. Tateo, Excited states by analytic continuation of TBA equations, Nucl. Phys. B482 (1996) 639–659 (1996). arXiv:hep-th/9607167, doi:10.1016/S0550-3213(96)00516-0.

[81] Z. Bajnok, Review of AdS/CFT Integrability, Chapter III.6: Thermodynamic Bethe Ansatz, Lett. Math. Phys. 99 (2012) 299–320 (2012). arXiv:1012.3995, doi:10.1007/s11005-011-0512-y.

[82] H. Saleur, A Comment on finite temperature correlations in integrable QFT, Nucl. Phys. B567 (2000) 602–610 (2000). arXiv:hep-th/9909019, doi:10.1016/S0550-3213(99)00665-3.

[83] Z. Bajnok, C. Wu, Diagonal form factors from non-diagonal ones (2017). arXiv:1707.08027.

[84] A. Leclair, G. Mussardo, Finite temperature correlation functions in integrable QFT, Nucl. Phys. B552 (1999) 624–642 (1999). arXiv:hep-th/9902075, doi:10.1016/S0550-3213(99)00280-1.

[85] B. Pozsgay, Mean values of local operators in highly excited Bethe states, J. Stat. Mech. 1101 (2011) P01011 (2011). arXiv:1009.4662, doi:10.1088/1742-5468/2011/01/P01011.

[86] B. Pozsgay, Form factor approach to diagonal finite volume matrix elements in Integrable QFT, JHEP 07 (2013) 157 (2013). arXiv:1305.3373, doi:10.1007/JHEP07(2013)157.

[87] B. Pozsgay, I. M. Szécsényi, G. Takács, Exact finite volume expectation values of local operators in excited states, JHEP 04 (2015) 023 (2015). arXiv:1412.8436, doi:10.1007/JHEP04(2015)023.

[88] B. Pozsgay, Lüscher's mu-term and finite volume bootstrap principle for scattering states and form factors, Nucl. Phys. B802 (2008) 435–457 (2008). arXiv:0803.4445, doi:10.1016/j.nuclphysb.2008.04.021.

[89] A. E. Arinshtein, V. A. Fateev, A. B. Zamolodchikov, Quantum s Matrix of the (1+1)-Dimensional Todd Chain, Phys. Lett. 87B (1979) 389–392 (1979). doi:10.1016/0370-2693(79)90561-6.

[90] A. Fring, G. Mussardo, P. Simonetti, Form-factors for integrable Lagrangian field theories, the sinh-Gordon theory, Nucl. Phys. B 393 (1993) 413–441 (1993). arXiv:hep-th/9211053, doi:10.1016/0550-3213(93)90252-K.

[91] A. Koubek, G. Mussardo, On the operator content of the sinh-Gordon model, Phys. Lett. B 311 (1993) 193–201 (1993). arXiv:hep-th/9306044, doi:10.1016/0370-2693(93)90554-U.

[92] V. Fateev, S. L. Lukyanov, A. B. Zamolodchikov, A. B. Zamolodchikov, Expectation values of local fields in Bullough-Dodd model and integrable perturbed conformal field theories, Nucl. Phys. B 516 (1998) 652–674 (1998). arXiv:hep-th/9709034, doi:10.1016/S0550-3213(98)00002-9.

[93] A. B. Zamolodchikov, Mass scale in the sine-Gordon model and its reductions, Int. J. Mod. Phys. A 10 (1995) 1125–1150 (1995). doi:10.1142/S0217751X9500053X.

[94] A. B. Zamolodchikov, On the thermodynamic Bethe ansatz equation in sinh-Gordon model, J. Phys. A39 (2006) 12863–12887 (2006). arXiv:hep-th/0005181, doi:10.1088/0305-4470/39/41/S09.

[95] J. Teschner, On the spectrum of the Sinh-Gordon model in finite volume, Nucl. Phys. B799 (2008) 403–429 (2008). arXiv:hep-th/0702214, doi:10.1016/j.nuclphysb.2008.01.021.

[96] S. L. Lukyanov, Finite temperature expectation values of local fields in the sinh-Gordon model, Nucl. Phys. B 612 (2001) 391–412 (2001). arXiv:hep-th/0005027, doi:10.1016/S0550-3213(01)00365-0.

[97] S. Negro, F. Smirnov, On one-point functions for sinh-Gordon model at finite temperature, Nucl. Phys. B 875 (2013) 166–185 (2013). arXiv:1306.1476, doi:10.1016/j.nuclphysb.2013.06.023.

[98] A. B. Zamolodchikov, Resonance factorized scattering and roaming trajectories, J. Phys. A 39 (2006) 12847–12862 (2006). doi:10.1088/0305-4470/39/41/S08.

[99] C. Ahn, G. Delfino, G. Mussardo, Mapping between the sinh-Gordon and Ising models, Phys. Lett. B 317 (1993) 573–580 (1993). arXiv:hep-th/9306103, doi:10.1016/0370-2693(93)91375-W.

[100] A. Larsen, N. G. Sanchez, Sinh-Gordon, cosh-Gordon and Liouville equations for strings and multistrings in constant curvature space-times, Phys. Rev. D 54 (1996) 2801–2807 (1996). arXiv:hep-th/9603049, doi:10.1103/PhysRevD.54.2801.

[101] M. Kormos, G. Mussardo, A. Trombettoni, 1D Lieb-Liniger Bose Gas as Non-Relativistic Limit of the Sinh-Gordon Model, Phys. Rev. A 81 (2010) 043606 (2010). arXiv:0912.3502, doi:10.1103/PhysRevA.81.043606.

[102] A. Bastianello, L. Piroli, From the sinh-Gordon field theory to the one-dimensional Bose gas: exact local correlations and full counting statistics, J. Stat. Mech. 1811 (11) (2018) 113104 (2018). arXiv:1807.06869, doi:10.1088/1742-5468/aaeb48.

[103] A. De Luca, G. Mussardo, Equilibration Properties of Classical Integrable Field Theories, J. Stat. Mech. 1606 (6) (2016) 064011 (2016). arXiv:1603.08628, doi:10.1088/1742-5468/2016/06/064011.

[104] G. D. V. Del Vecchio, A. Bastianello, A. De Luca, G. Mussardo, Exact out-of-equilibrium steady states in the semiclassical limit of the interacting Bose gas (2 2020). arXiv:2002.01423.

[105] A. G. Bytsko, J. Teschner, Quantization of models with non-compact quantum group symmetry: Modular XXZ magnet and lattice sinh-Gordon model, J. Phys. A 39 (2006) 12927–12981 (2006). arXiv:hep-th/0602093, doi:10.1088/0305-4470/39/41/S11.

[106] G. Mussardo, Statistical Field Theory, Oxford Graduate Texts, Oxford University Press, 2020 (2020).

[107] V. P. Yurov, A. B. Zamolodchikov, Truncated conformal space approach to the scaling Lee-Yang model, Int. J. Mod. Phys. A5 (1990) 3221–3246 (1990). doi:10.1142/S0217751X9000218X.

[108] V. Yurov, A. Zamolodchikov, Truncated fermionic space approach to the critical 2d ising model with magnetic field, International Journal of Modern Physics A 06 (25) (1991) 4557–4578 (1991). doi:10.1142/S0217751X91002161.

[109] M. Lässig, G. Mussardo, J. L. Cardy, The scaling region of the tricritical ising model in two dimensions, Nuclear Physics B 348 (3) (1991) 591 – 618 (1991). doi:https://doi.org/10.1016/0550-3213(91)90206-D.
URL http://www.sciencedirect.com/science/article/pii/055032139190206D

[110] R. M. Konik, Y. Adamov, Numerical renormalization group for continuum one-dimensional systems, Phys. Rev. Lett. 98 (2007) 147205 (Apr 2007). doi:10.1103/PhysRevLett.98.147205.
URL https://link.aps.org/doi/10.1103/PhysRevLett.98.147205

[111] A. J. A. James, R. M. Konik, P. Lecheminant, N. J. Robinson, A. M. Tsvelik, Non-perturbative methodologies for low-dimensional strongly-correlated systems: From non-Abelian bosonization to truncated spectrum methods, Reports on

Progress in Physics 81 (4) (2018) 046002 (Apr 2018). doi:10.1088/1361-6633/aa91ea.

[112] A. Coser, M. Beria, G. P. Brandino, R. M. Konik, G. Mussardo, Truncated Conformal Space Approach for 2D Landau-Ginzburg Theories, J. Stat. Mech. 1412 (2014) P12010 (2014). arXiv:1409.1494, doi:10.1088/1742-5468/2014/12/P12010.

[113] Z. Bajnok, M. Lájer, Truncated Hilbert space approach to the 2d ϕ^4 theory, JHEP 10 (2016) 050 (2016). arXiv:1512.06901, doi:10.1007/JHEP10(2016)050.

[114] S. Rychkov, L. G. Vitale, Hamiltonian truncation study of the φ^4 theory in two dimensions, Phys. Rev. D 91 (2015) 085011 (2015). arXiv:1412.3460, doi:10.1103/PhysRevD.91.085011.

[115] S. Rychkov, L. G. Vitale, Hamiltonian truncation study of the ϕ^4 theory in two dimensions. II. The $\mathbb{Z}_2$ -broken phase and the Chang duality, Phys. Rev. D93 (6) (2016) 065014 (2016). arXiv:1512.00493, doi:10.1103/PhysRevD.93.065014.

[116] J. Elias-Miró, S. Rychkov, L. G. Vitale, Nlo renormalization in the hamiltonian truncation, Phys. Rev. D 96 (2017) 065024 (Sep 2017). doi:10.1103/PhysRevD.96.065024.
URL https://link.aps.org/doi/10.1103/PhysRevD.96.065024

[117] J. Elias-Miró, S. Rychkov, L. G. Vitale, High-precision calculations in strongly coupled quantum field theory with next-to-leading-order renormalized hamiltonian truncation, Journal of High Energy Physics 2017 (10) (2017) 213 (Oct 2017). doi:10.1007/JHEP10(2017)213.
URL https://doi.org/10.1007/JHEP10(2017)213

[118] M. Lässig, M. J. Martins, Finite-size effects in theories with factorizable s-matrices, Nuclear Physics B 354 (2) (1991) 666 – 688 (1991). doi:https://doi.org/10.1016/0550-3213(91)90371-4.
URL http://www.sciencedirect.com/science/article/pii/0550321391903714

[119] R. M. Konik, Exciton Hierarchies in Gapped Carbon Nanotubes, Phys. Rev. Lett. 106 (2011) 136805 (Mar 2011). doi:10.1103/PhysRevLett.106.136805.

[120] R. M. Konik, M. Y. Sfeir, J. A. Misewich, Predicting excitonic gaps of semiconducting single-walled carbon nanotubes from a field theoretic analysis, Phys. Rev. B 91 (2015) 075417 (Feb 2015). doi:10.1103/PhysRevB.91.075417.

[121] M. Beria, G. Brandino, L. Lepori, R. Konik, G. Sierra, Truncated conformal space approach for perturbed wess-zumino-witten $su(2)_k$ models, Nuclear Physics B 877 (2) (2013) 457 – 483 (2013). doi:https://doi.org/10.1016/j.nuclphysb.2013.10.005.

[122] R. Konik, T. Pálmai, G. Takács, A. Tsvelik, Studying the perturbed wess-zumino-novikov-witten $su(2)_k$ theory using the truncated conformal spectrum approach, Nuclear Physics B 899 (2015) 547 – 569 (2015). doi:https://doi.org/10.1016/j.nuclphysb.2015.08.016.

[123] P. Azaria, R. M. Konik, P. Lecheminant, T. Pálmai, G. Takács, A. M. Tsvelik, Particle formation and ordering in strongly correlated fermionic systems: Solving a model of quantum chromodynamics, Phys. Rev. D 94 (2016) 045003 (Aug 2016). doi:10.1103/PhysRevD.94.045003.

[124] G. Feverati, K. Graham, P. A. Pearce, G. Z. Toth, G. Watts, A renormalisation group for tcsa (2006). arXiv:hep-th/0612203.

[125] P. Giokas, G. Watts, The renormalisation group for the truncated conformal space approach on the cylinder (2011). arXiv:1106.2448.

[126] M. Lencsés, G. Takács, Excited state TBA and renormalized TCSA in the scaling Potts model, JHEP 09 (2014) 052 (2014). arXiv:1405.3157, doi:10.1007/JHEP09(2014)052.

[127] Z. Bajnok, J. Balog, M. Lájer, C. Wu, Field theoretical derivation of lüscher′s formula and calculation of finite volume form factors, Journal of High Energy Physics 2018 (7) (Jul 2018). doi:10.1007/jhep07(2018)174.

[128] Z. Bajnok, M. Lájer, B. Szépfalvi, I. Vona, Leading exponential finite size corrections for non-diagonal form factors, Journal of High Energy Physics 2019 (7) (Jul 2019). doi:10.1007/jhep07(2019)173.

[129] B. Pozsgay, I. M. Szécsényi, LeClair-Mussardo series for two-point functions in Integrable QFT, JHEP 05 (2018) 170 (2018). arXiv:1802.05890, doi:10.1007/JHEP05(2018)170.

[130] A. Cortés Cubero, M. Panfil, Thermodynamic bootstrap program for integrable QFT's: Form factors and correlation functions at finite energy density (2018). arXiv:1809.02044.

[131] P. Di Francesco, P. Mathieu, D. Senechal, Conformal Field Theory, Graduate Texts in Contemporary Physics, Springer-Verlag, New York, 1997 (1997). doi:10.1007/978-1-4612-2256-9.

[132] J. Liouville, Sur l'équation aux différences partielles $\frac{d^2 \log \lambda}{dudv} \pm \frac{\lambda}{2a^2} = 0$., Journal de mathématiques pures et appliquées (1853) 71–72 (1853).

[133] V. Dotsenko, V. Fateev, Conformal Algebra and Multipoint Correlation Functions in Two-Dimensional Statistical Models, Nucl. Phys. B 240 (1984) 312 (1984). doi:10.1016/0550-3213(84)90269-4.

[134] J.-L. Gervais, A. Neveu, Nonstandard Two-dimensional Critical Statistical Models From Liouville Theory, Nucl. Phys. B 257 (1985) 59 (1985). doi:10.1016/0550-3213(85)90336-0.

[135] N. Seiberg, Notes on quantum Liouville theory and quantum gravity, Prog. Theor. Phys. Suppl. 102 (1990) 319–349 (1990). doi:10.1143/PTPS.102.319.

[136] V. Dotsenko, V. Fateev, Four Point Correlation Functions and the Operator Algebra in the Two-Dimensional Conformal Invariant Theories with the Central Charge c $<$ 1, Nucl. Phys. B 251 (1985) 691–734 (1985). doi:10.1016/S0550-3213(85)80004-3.

[137] J. Teschner, A Lecture on the Liouville vertex operators, Int. J. Mod. Phys. A 19S2 (2004) 436–458 (2004). arXiv:hep-th/0303150, doi:10.1142/S0217751X04020567.

[138] A. Kupiainen, R. Rhodes, V. Vargas, Integrability of liouville theory: proof of the dozz formula, Annals of Mathematics 191 (1) (2020) 81–166 (2020).
URL https://www.jstor.org/stable/10.4007/annals.2020.191.1.2

[139] D. J. Amit, Y. Y. Goldschmidt, G. Grinstein, Renormalization Group Analysis of the Phase Transition in the 2D Coulomb Gas, Sine-Gordon Theory and xy Model, J. Phys. A 13 (1980) 585 (1980). doi:10.1088/0305-4470/13/2/024.

[140] S. L. Lukyanov, A. B. Zamolodchikov, Exact expectation values of local fields in quantum sine-Gordon model, Nucl. Phys. B493 (1997) 571–587 (1997). arXiv:hep-th/9611238, doi:10.1016/S0550-3213(97)00123-5.

[141] M. Lashkevich, Resonances in sinh- and sine-Gordon Models and Higher Equations of Motion in Liouville Theory, J. Phys. A 45 (2012) 455403 (2012). arXiv:1111.2547, doi:10.1088/1751-8113/45/45/455403.

[142] S. L. Lukyanov, Form-factors of exponential fields in the Sine-Gordon model, Mod. Phys. Lett. A 12 (1997) 2543–2550 (1997). arXiv:hep-th/9703190, doi:10.1142/S0217732397002673.

[143] M. Lashkevich, Y. Pugai, Form factors in sinh- and sine-Gordon models, deformed Virasoro algebra, Macdonald polynomials and resonance identities, Nucl. Phys. B 877 (2013) 538–573 (2013). arXiv:1307.0243, doi:10.1016/j.nuclphysb.2013.10.013.

[144] Z. Bajnok, F. Smirnov, Diagonal finite volume matrix elements in the sinh-Gordon model, Nucl. Phys. B 945 (2019) 114664 (2019). arXiv:1903.06990, doi:10.1016/j.nuclphysb.2019.114664.

[145] M. Hogervorst, S. Rychkov, B. C. van Rees, Truncated conformal space approach in d dimensions: A cheap alternative to lattice field theory?, Phys. Rev. D 91 (2015) 025005 (Jan 2015). doi:10.1103/PhysRevD.91.025005.
URL https://link.aps.org/doi/10.1103/PhysRevD.91.025005

[146] A. Stathopoulos, J. R. McCombs, PRIMME: PReconditioned Iterative Multi-Method Eigensolver: Methods and software description, ACM Transactions on Mathematical Software 37 (2) (2010) 21:1–21:30 (2010).

[147] L. Wu, E. Romero, A. Stathopoulos, Primme_svds: A high-performance preconditioned SVD solver for accurate large-scale computations, SIAM Journal on Scientific Computing 39 (5) (2017) S248–S271 (2017). doi:10.1137/16M1082214.

[148] C. Ahn, C. Kim, C. Rim, Hidden relation between reflection amplitudes and thermodynamic bethe ansatz, Nuclear Physics B 556 (3) (1999) 505 – 529 (1999). doi:https://doi.org/10.1016/S0550-3213(99)00405-8.

[149] G. Hardy, Divergent Series, Clarendon Press, 1949 (1949).
URL https://books.google.com/books?id=ge5QAAAAMAAJ

[150] V. Grecchi, M. Maioli, Borel summability beyond the factorial growth, Annales de l'I.H.P. Physique théorique 41 (1) (1984) 37–47 (1984).
URL http://eudml.org/doc/76249

[151] R. Konik, M. Lájer, G. Mussardo, Approaching the self-dual point of the sinh-gordon model (2020). arXiv:2007.00154.

[152] T. R. Klassen, E. Melzer, Spectral flow between conformal field theories in 1 + 1 dimensions, Nuclear Physics B 370 (3) (1992) 511 – 550 (1992). doi:https://doi.org/10.1016/0550-3213(92)90422-8.

[153] P. Dorey, A. Pocklington, R. Tateo, G. Watts, Tba and tcsa with boundaries and excited states, Nuclear Physics B 525 (3) (1998) 641 – 663 (1998). doi:https://doi.org/10.1016/S0550-3213(98)00339-3.

[154] M. Kormos, I. Runkel, G. M. Watts, Defect flows in minimal models, Journal of High Energy Physics 2009 (11) (2009) 057–057 (nov 2009). doi:10.1088/1126-6708/2009/11/057.

[155] G. Delfino, G. Mussardo, P. Simonetti, Nonintegrable quantum field theories as perturbations of certain integrable models, Nucl. Phys. B 473 (1996) 469–508 (1996). arXiv:hep-th/9603011, doi:10.1016/0550-3213(96)00265-9.

[156] M. Karowski, P. Weisz, Exact Form-Factors in (1+1)-Dimensional Field Theoretic Models with Soliton Behavior, Nucl. Phys. B139 (1978) 455–476 (1978). doi:10.1016/0550-3213(78)90362-0.

[157] C. Ahn, V. Fateev, C. Kim, C. Rim, B. Yang, Reflection amplitudes of ADE Toda theories and thermodynamic Bethe ansatz, Nucl. Phys. B 565 (2000) 611–628 (2000). arXiv:hep-th/9907072, doi:10.1016/S0550-3213(99)00705-1.

[158] E. Sklyanin, Exact quantization of the sinh-gordon model, Nuclear Physics B 326 (3) (1989) 719 – 736 (1989). doi:https://doi.org/10.1016/0550-3213(89)90552-X.
URL http://www.sciencedirect.com/science/article/pii/055032138990552X

[159] Z. Bajnok, R. A. Janik, String field theory vertex from integrability, JHEP 04 (2015) 042 (2015). arXiv:1501.04533, doi:10.1007/JHEP04(2015)042.

[160] S. Komatsu, Three-point functions in $\mathcal{N} = 4$ supersymmetric Yang–Mills theory, Les Houches Lect. Notes 106 (2019). arXiv:1710.03853, doi:10.1093/oso/9780198828150.003.0010.

[161] Z. Bajnok, R. A. Janik, From the octagon to the SFT vertex - gluing and multiple wrapping, JHEP 06 (2017) 058 (2017). arXiv:1704.03633, doi:10.1007/JHEP06(2017)058.

[162] B. Basso, V. Goncalves, S. Komatsu, P. Vieira, Gluing Hexagons at Three Loops, Nucl. Phys. B 907 (2016) 695–716 (2016). arXiv:1510.01683, doi:10.1016/j.nuclphysb.2016.04.020.

[163] B. Basso, S. Komatsu, P. Vieira, Structure Constants and Integrable Bootstrap in Planar N=4 SYM Theory (2015). arXiv:1505.06745.

[164] B. Eden, A. Sfondrini, Three-point functions in $\mathcal{N} = 4$ SYM: the hexagon proposal at three loops, JHEP 02 (2016) 165 (2016). arXiv:1510.01242, doi:10.1007/JHEP02(2016)165.

[165] B. Basso, V. Goncalves, S. Komatsu, Structure constants at wrapping order, JHEP 05 (2017) 124 (2017). arXiv:1702.02154, doi:10.1007/JHEP05(2017)124.

[166] A. Bytsko, J. Teschner, The integrable structure of nonrational conformal field theory, Adv. Theor. Math. Phys. 17 (4) (2013) 701–740 (08 2013).

[167] V. A. Fateev, S. L. Lukyanov, Boundary RG flow associated with the AKNS soliton hierarchy, Journal of Physics A: Mathematical and General 39 (41) (2006) 12889–12925 (sep 2006). doi:10.1088/0305-4470/39/41/s10.